## *Experimental Investigation and Evaluation of Future Active Distribution Networks*

LYONS, PADRAIG,FIONNBHARR

# Experimental Investigation and Evaluation of Future Active Distribution Networks

Pádraig Lyons

School of Engineering

Durham University

A thesis submitted in partial fulfilment of the requirements of the Council of the University of Durham for the Degree of Doctor of Philosophy (PhD)

2009

# Experimental Investigation and Evaluation of Future Active Distribution Networks

Pádraig Lyons

2009

***Abstract***

*The UK government's policy to achieve a 20% renewable energy generation target by 2020, will require significant amounts of SSEG (Small-Scale Embedded Generation) to be connected. In addition to the expected economic and environmental benefits, the anticipated growth in SSEG brings with it numerous challenges for the operation of low voltage and medium voltage distribution networks. At present, there are a number of competing active network management concepts being considered to overcome these challenges and at Durham University a concept defined as the Small Scale Energy Zone (SSEZ) has been proposed and is investigated as part of this research.*

*To further this, a bespoke active low voltage distribution network emulator known as the Experimental SSEZ has been developed by the author. Controllable emulated SSEG, controllable energy storage and controllable emulated load are incorporated into this laboratory. A transformation system has been developed to relate the operation of this system to that of low voltage distribution networks. Centralised and distributed network control systems have been developed for the Experimental SSEZ. These systems were used to evaluate, in conjunction with the relevant literature, the implementation of similar systems on future low voltage distribution networks. Both centralised and distributed control system architectures were found to have their merits. This research should therefore be useful in informing design decisions when developing and implementing active distribution network management systems on LV networks.*

# Acknowledgements

Firstly, I would like to express my gratitude to my Supervisor, Philip Taylor, for all his excellent support and advice during my time at Durham. I would also like to thank the many technicians who have lent their advice and expertise during the practical parts of this research, in particular David Jones, Paul Jarvis and Tony Collinson for their superb work developing the Experimental SSEZ laboratory. I would also like to thank Steve MacDonald and NaREC for their financial and technical assistance during my studies. I would also like to thank Professor Tavner and the staff of the School of Engineering for all their encouragement and for the opportunity to study at the department. Outside of my studies, I would like to thank all my colleagues and friends who have helped and encouraged me during my studies. Finally, I would like to thank Lorna, my parents Cormac and Sheila, my siblings Colum, Dáire and Aoife for all their love and invaluable support they have shown to me during my studies.

# Declaration

I hereby declare that this thesis is a record of work undertaken by myself, that it has not been the subject of any previous application for a degree, and that all sources of information have been duly acknowledged.

# Contents

# List of Abbreviations

| | |
|---|---|
| *AC* | Alternating Current |
| *ACCM* | Active Constrained Connection Manager |
| *ADMD* | After Diversity Maximum Demand |
| *AVC* | Automatic Voltage Controller |
| *AVPFC* | Automatic Voltage/Power Factor Control |
| *AVR* | Automatic Voltage Regulator |
| *CBA* | Cost Benifet Analysis |
| *CDA* | Consumer Demand Agent |
| *CHP* | Combined Heat and Power |
| *CSP* | Constraint Satisfaction Problem |
| *DC* | Direct Current |
| *DG* | Distributed Generation |
| *DNO* | Distribution Network Operator |
| *DSM* | Demand Side Management |
| *D-STATCOM* | Distribution - Static Synchronous Compensator |
| *EMTDC* | Electromagnetic Transients including DC |
| *ESA* | Energy Storage Agent |
| *ESU* | Energy Storage Unit |
| *EV* | Electric Vehicle |
| *FACTS* | Flexible AC Transmission Systems |
| *FG* | Firm Generation |
| *FIPA* | Foundation of Intelligent Physical Agents |
| *GA* | Generator Agent |

| | |
|---|---|
| *HV* | High Voltage |
| *IEA* | International Energy Agency |
| *IT* | Isolated or impedance-earthed neutral (Earthing System) |
| *LabVIEW* | Laboratory Virtual Instrumentation Engineering Workbench |
| *LDC* | Line Drop Compensation |
| *LV* | Low Voltage |
| *MAS* | Multi-Agent System |
| *MGCC* | MicroGrid Central Controller |
| *MV* | Medium Voltage |
| *NFG* | Non-Firm Generation |
| *NiMH* | Nickel Metal Hydride |
| *OGA* | Operational Goal Agent |
| *OLTC* | On-Load Tap Changer |
| *OLE* | Object Linking and Embedding |
| *OPC* | OLE for Process Control |
| *OPF* | Optimal Power Flow |
| *PHEV* | Plug-in Hybrid Electric Vehicle |
| *PI* | Proportional and Integral (Controller) |
| *PLC* | Power Line Carrier |
| *POI* | Point Of Interconnection |
| *PV* | Photovoltaic |
| *PVGA* | PV Generator Agent |
| *PSCAD®* | Power Systems Computer Aided Design |
| *RNFG* | Regulated Non-Firm Generation |
| *SCADA* | Supervisory Control and Data Acquisition |

| | |
|---|---|
| *SLD* | Single Line Diagram |
| *SOC* | State-of-Charge |
| *SSEG* | Small Scale Embedded Generator |
| *SSEZ* | Small Scale Energy Zone |
| *TLA* | Thermal Limit Agent |
| *TN* | Exposed conductive parts connected to the neutral (Earthing System) |
| *TT* | Earthed neutral (Earthing System) |
| *UA* | Unbalance Agent |
| *UK* | United Kindom |
| *US* | United States (of America) |
| *VA* | Voltage Agent |
| *VPP* | Virtual Power Plant |
| *VRB* | Vanadium Redox Battery |
| *WGA* | Wind turbine Generator Agent |
| *WLAN* | Wireless Local Area Network |
| *%DoD* | Percentage Depth of Discharge |
| *%VUF* | Percentage Voltage Unbalance Factor |

# Nomenclature

| | |
|---|---|
| $\overline{E}$ | sending end line-line voltage (pu) |
| $\overline{E}_A$ | phase A sending end voltages (V) |
| $f$ | is the frequency of the LV network (Hz) |
| $f_0$ | is the nominal frequency (Hz) |
| $f_{droop}$ | droop frequency. If the system frequency deviates by this much from nominal frequency the Sunny Island 4500™ will supply/feed $P_{nom}$ into the LV network (Hz) |
| $\overline{I}$ | phase load current (pu) |
| $\mathbf{I}_{\mathbf{ABC}}$ | 3 x 1 matrix of the three-phase line currents (A) |
| $\mathbf{I}_{\mathbf{N}}$ | 3 x 1 matrix of the neutral current (A) |
| $\mathbf{I}_{\mathbf{ABC}}^{\mathbf{LV}}$ | 3 x 1 matrix of the three-phase line currents of the LV distribution network under consideration (A) |
| $\mathbf{I}_{\mathbf{N}}^{\mathbf{LV}}$ | 3 x 1 matrix of the neutral current of the LV distribution network under consideration (A) |
| $\mathbf{I}_{\mathbf{ABC}}^{\mathbf{Ex}}$ | 3 x 1 matrix of the three-phase line currents of the Experimental SSEZ LV network (A) |
| $\mathbf{I}_{\mathbf{N}}^{\mathbf{Ex}}$ | 3 x 1 matrix of the neutral current of the Experimental SSEZ LV network (A) |
| $m$ | number of customers connected per phase to a network location |
| $n$ | number of feeder locations with customer connections |
| $p$ | number of radial feeders on the LV network |
| $P_{nom}$ | is the nominal power rating of the Sunny Island 4500™ (kW) |

$P_{ac}$ is the required output power of the Sunny Island 4500™ (kW)

$p_a^{LV}(t)$ real power import/export on phase A from/to the MV/LV transformer of the LV network under consideration (kVAr)

$p_a^{Ex}(t)$ real power import/export on phase A from/to the network connection emulator of the Experimental SSEZ (kW)

$P_L^{LV}$ is the maximum per-phase load of the LV network under consideration (kW)

$P_L^{Ex}$ is the maximum per-phase load of the Experimental SSEZ (kW)

$P_G^{LV}$ is the installed per-phase generation on the LV network under consideration (kW)

$P_G^{Ex}$ is the maximum per-phase generation available on the Experimental SSEZ (kW)

$q_a^{Ex}(t)$ reactive power import/export on phase A from/to the network connection emulator of the Experimental SSEZ (kW)

$q_a^{LV}(t)$ reactive power import/export on phase A from/to the MV/LV transformer of the LV network under consideration (kVAr)

$R_1$ positive sequence resistance (pu)

$R_{feeder}^{(ap)}$ apparent resistance [Ω] of the LV feeder

$R_{net}^{(ap)}$ apparent resistance [Ω] of the LV network

$R^{LV}$ apparent resistance ( $R_{net}^{(ap)}$ ) of the LV network under consideration [Ω]

$R^{Ex}$ sum of the phase and neutral resistances from the network connection emulator to the remote end node of the LV network of the Experimental SSEZ [Ω]

$\overline{V}$ receiving end line-line voltage (pu)

$V_a, V_b, V_c$ three-phase line or phase voltages (V)

$V_+, V_-, V_0$ positive ($V_+$), negative ($V_-$) and zero ($V_0$) sequence voltage component (V)

$\overline{V}_A$ phase A receiving end voltage with respect to ground (V)

$\overline{V}_{AN}$ phase A receiving end voltage with respect to neutral (V)

$V_{nom}^{Ex}$ nominal voltage of the Experimental SSEZ (V)

$V_{nom}^{LV}$ nominal voltage of the LV distribution network under consideration (V)

$X_1$ positive sequence reactance (pu)

$X_{feeder}^{(ap)}$ apparent reactance [Ω] of the LV feeder

$X_{net}^{(ap)}$ apparent reactance [Ω] of the LV network

$X^{LV}$ apparent resistance ( $X_{net}^{(ap)}$ ) of the LV network under consideration [Ω]

$X^{Ex}$ sum of the phase and neutral reactances from the network connection emulator to the remote end node of the LV network of the Experimental SSEZ [Ω]

$\overline{Z}_{AA}$ self impedance of A phase conductor (Ω)

$\overline{Z}_{AB}$ mutual impedance of A phase and B phase conductor (Ω)

$\overline{Z}_{AN}$ mutual impedance of A phase and neutral conductor (Ω)

$Z_{location}^{i\ (ap)}$ apparent impedance [Ω] of network location *i* with *m* customer connections

$Z_{customer}^{k\ (ap)}$ sum of the phase and neutral impedances between the substation and customer connection point *k* [Ω] neglecting the service connection impedances

$Z_{feeder}^{(ap)}$ apparent impedance of the LV feeder [Ω]

$Z_{service\ cable}^{max}$ the largest of the impedances of service cable connections to each customer [Ω] from the $n^{th}$ network location

$Z_{net}^{(ap)}$ apparent impedance of the LV feeder [Ω]

$Z_l$ 5 x 5 matrix used to represent the self and mutual impedances of any line impedance [Ω]

$\mathbf{Z_{ABC}}$ 3 x 3 matrix of the self and mutual impedances between phases (Ω)

$\mathbf{Z_{ABC}^{LV}}$ 3 x 3 matrix of the self and mutual impedances between phases of the LV distribution network under consideration (Ω)

$Z_{NN}^{LV}$ self impedance of neutral conductor of the LV distribution network under consideration (mΩ)

$\mathbf{Z_{ABC}^{Ex}}$ 3 x 3 matrix of the self and mutual impedances between phases of the LV distribution network of the Experimental SSEZ (mΩ)

$Z_{NN}^{Ex}$ self impedance of neutral conductor of LV distribution network of the Experimental SSEZ (mΩ)

$\theta$ angle between voltage at receiving end and load current

$\Delta\overline{V}_{AG}$ voltage drop in phase A with reference to ground (equivalent earth return plane of infinite conductivity) (V)

$\Delta\overline{V}_{AN}$ is the voltage drop on phase A with respect to neutral (V)

$\mathbf{\Delta V_{ABC}}$ 3 x 1 matrix of the voltage drops with respect to neutral (V)

$\mathbf{\Delta V_{ABC}^{LV}}$ 3 x 1 matrix of the voltage drops with respect to neutral of the LV distribution network under consideration (V)

| | |
|---|---|
| $\mathbf{\Delta V}_{\mathbf{ABC}}^{\mathbf{Ex}}$ | 3 x 1 matrix of the voltage drops with respect to neutral of the LV distribution network of the Experimental SSEZ (V) |
| $\mu_{P_L}$ | load power scaling factor for transformation system |
| $\mu_{P_G}$ | generation power scaling factor for transformation system |
| $\mu_P$ | system power scaling factor for transformation system |
| $\mu_Z$ | voltage scaling factor for transformation system |
| $\mu_{Vnom}$ | ratio of the nominal voltages of the LV distribution network and the Experimental SSEZ for transformation system |

# 1 INTRODUCTION

Political, scientific, environmental and economic pressures are all making the installation of large quantities of Small Scale Embedded Generation (SSEG) and micro-generation on distribution networks seem increasingly likely. An SSEG is defined as "a source of electrical energy rated up to and including 16 Ampere per phase, single or multiphase, 230/400 Volts ac" [1]. This corresponds to a generator with an installed capacity of approximately 3.7kW single-phase or 11.1kW three-phase. Electrical micro-generation by comparison has been defined in the United Kingdom (UK) as having an installed capacity of up to 50kW [2]. For the purposes of this research the term SSEG shall be used to describe these small-scale generators of zero or low-carbon electrical energy.

The UK government's policy to achieve a 20% renewable energy generation target by 2020, will require significant amounts of Distributed Generation (DG) to be connected to distribution networks [3]. SSEG will need to form a substantial proportion of this distributed generation and research has indicated that installed SSEG capacity in the UK could grow to as much as 8GW by 2015 [4]. Another study has suggested that SSEG technologies could supply between 30-40% of the UK's electricity demand by 2050 [5]. This future increase in the penetration of SSEG should fundamentally change the way energy is consumed or possibly generated by domestic and small commercial customers. The centralised generation paradigm of today will be complemented and possibly even superseded, by the future paradigm of domestic consumers and producers of electrical energy. They will not only be involved in consumption, but also in energy generation and energy storage.

In addition to the expected economic and environmental benefits, the anticipated growth in SSEG brings with it numerous challenges for the operation of low voltage (LV) and

medium voltage (MV) distribution networks [6-9]. In this work LV is defined as a system of voltages below 1kV AC [10] and MV below 38kV AC (Alternating Current) [11]. High voltage (HV) can be described as the higher voltages used for bulk transmission of electricity and for the purposes of this work are defined as any system of voltages above 38kV [12]. Experts within industry and academia perceive that the most appropriate way to solve these problems is with active distribution network management [13]. At present, there are a number of competing active network management techniques being considered but there is no single accepted best solution to these challenges [7, 14-20].

At Durham University, an active distribution network concept defined as the Small Scale Energy Zone (SSEZ) has been proposed and is investigated as part of this research [7-8, 14, 21-24]. To further this, an active low voltage distribution network emulator known as the Experimental SSEZ has been developed by the author [7, 23-24]. This has been utilised as an aid to the development of active network management techniques for low voltage distribution networks and in particular SSEZs. Controllable emulated SSEG, controllable energy storage and controllable emulated load are incorporated into this emulator. Emulation in this work is defined as a hardware simulation of a network component.

## 1.1 Research Objectives

The aim of the research into intelligent active energy management of SSEZs at Durham University is to develop and evaluate control strategies for future active distribution networks and SSEZs.

The work described in this thesis focuses on the experimental development and evaluation of these control strategies for future distribution networks carried out by the author. This research included Experimental SSEZ development, control technique

development and evaluation. The research program and the research goals are illustrated diagrammatically in Figure 1.1.

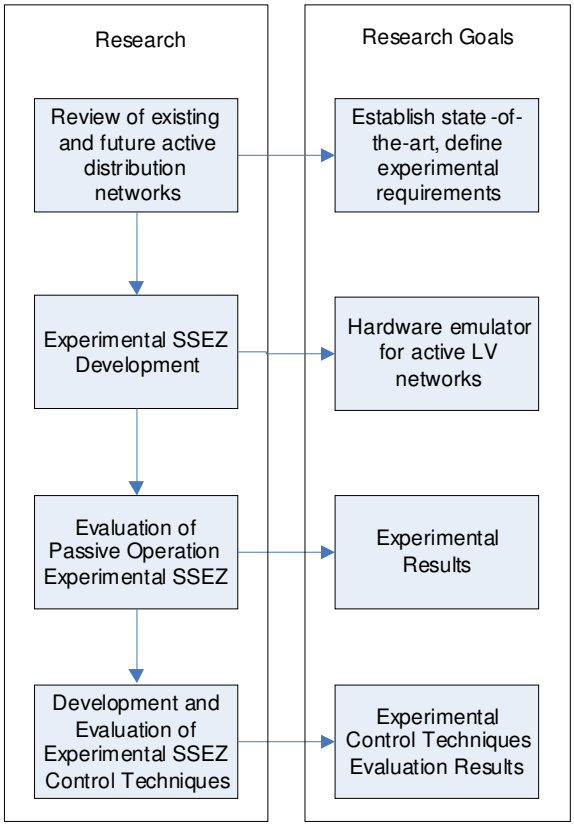


**Figure 1.1 Research program and research goals**

## 1.2 Small Scale Energy Zones (SSEZ)

The active distribution network concept known as the SSEZ seeks to solve the problems associated with embedding large amounts of SSEG into existing networks, whilst maximising their potential from an economic and environmental point of view. An SSEZ is defined as a "low voltage distribution network zone containing a significant number of controllable small scale generators, distributed energy storage units and loads" [7-8]. The structure of the SSEZ concept is illustrated diagrammatically in Figure 1.2.

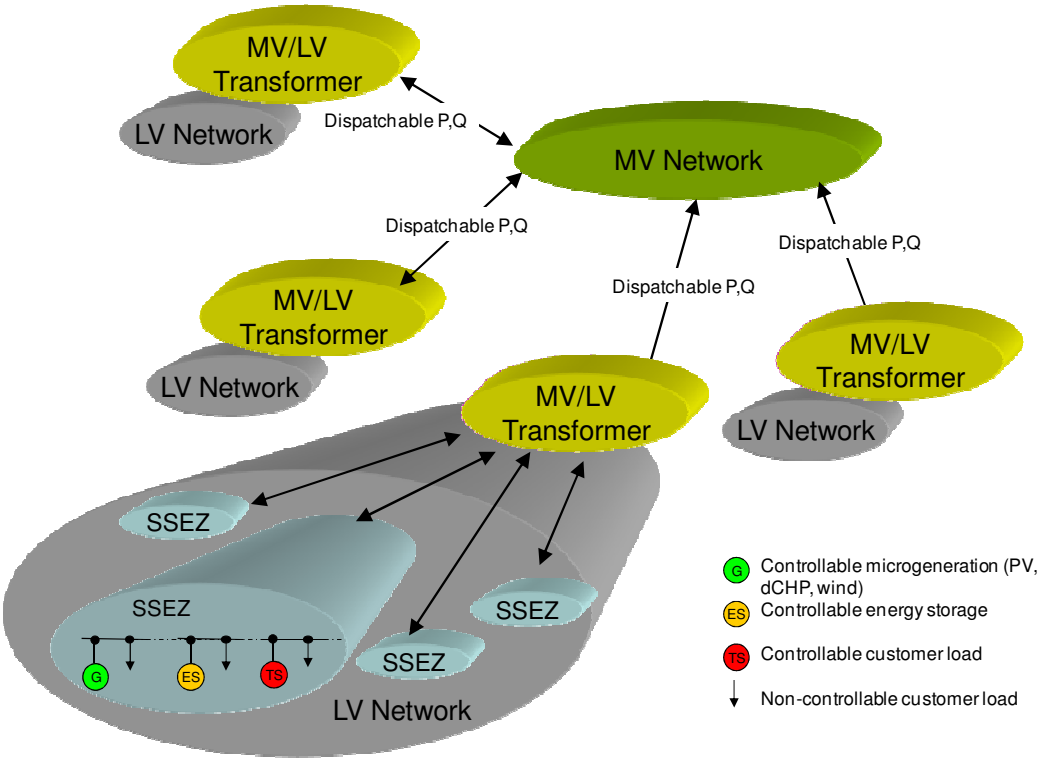


**Figure 1.2 SSEZ Concept Structure**

The aggregation of a large number of these complementary elements along with a supervisory controller has the potential to increase the value of individual SSEGs. The predictability and controllability problems associated with small scale renewable and alternative energy sources are addressed in an SSEZ utilising: -

- The availability of high concentrations of controllable energy storage and load within the SSEZ.
- The aggregation of large numbers of controllable, complementary small-scale renewable and alternative energy sources.

Moreover, it is proposed that a Virtual Power Plant (VPP) can be created if large numbers of zones are aggregated together [21]. The VPP could give Distribution Network Operators (DNOs) access to large, predictable and controllable load/generation.

## 1.3 Scope of Thesis

The second chapter of this thesis summarises the literature reviewed with regard to existing and future distribution networks and the problems associated with these systems. This is followed in chapter three by a review of control system architectures and techniques that may be employed in future distribution networks. The following chapter describes the design and development of the Experimental SSEZ. The design objectives for the system are initially presented. The design and development of the electrical systems, emulation systems and data acquisition system are subsequently detailed. Finally conclusions are drawn on the success of the system with respect to the initial design objectives.

Chapter five describes the passive operation of the Experimental SSEZ with respect to the constraints associated with large concentrations of SSEG on LV distribution networks. Voltage variation and regulation, voltage unbalance, power flow and reactive power flow impact studies are detailed. A discussion on the differences and similarities in the operation of the Experimental SSEZ and an actual LV distribution network is presented and conclusions are drawn on the validity of the Experimental SSEZ in comparison with an LV network.

In chapters six and seven the design and development of centralised and distributed control systems for the Experimental SSEZ are described. Existing distribution control and data acquisition structure is based on a centralised approach. The use of extended versions of this structure to facilitate the deployment of large numbers of SSEGs is examined. Results illustrating the development and performance of both centralised and distributed control systems are also presented in these chapters.

In chapter eight, a discussion illustrating the key findings, limitations and relevance of the research is presented. This includes an investigation into the implementation of

centralised and distributed control system architectures on LV distribution networks based on the literature reviewed and the experimental work completed in this research. Finally, in chapter nine conclusions drawn as a result of the research are detailed and future work is proposed.

# 2 LITERATURE REVIEW

## 2.1 Introduction

This research seeks to investigate the research challenges associated with the SSEZ concept. To enable this, a review of the literature relating to existing and future distribution networks with large concentrations of SSEG is presented.

The development of distribution networks from the initial small islanded systems of the late 1800s to the design and operation of the large, complex interconnected systems that exist today is initially described. Secondly, the grounds for the widespread adoption of embedded generation and in particular SSEG are described. Furthermore, the impact that these changes, to the existing generation paradigm, will have on the design and operation of distribution networks are summarised. This is followed by a description of the low voltage network constraints, where SSEZs will be implemented, that will arise from the large-scale deployment of SSEG.

The characteristics and connection issues associated with the various forms of SSEG are then described. This is followed by a description of an investigation into existing and future load in distribution networks. Energy storage, which is seen as an enabler for embedded generation and SSEG, is also likely to be part of future distribution networks and therefore a review of these technologies is also presented. Finally conclusions are drawn from this review with regard to the investigation of the SSEZ concept.

## 2.2 Distribution Networks

Electricity distribution is the penultimate stage (before retail) in the supply of electricity to customers. It includes MV overhead lines and cables, electrical substations and pole-mounted transformers, LV distribution wiring and possibly also metering systems.

The first distribution networks were installed in Europe and the United States (US) and utilised DC (Direct Current). Islanded systems were the standard design paradigm initially beginning with Manhattan's Pearl Street DC station, which was opened in 1882 by Thomas Edison [25-27]. In an islanded system the load is supplied by local generation as there is no connection to a larger electricity grid. In contrast today's power systems are large interconnected systems comprising of large generating units and AC transmission and distribution systems.

At present hundreds of generating stations, mostly sized between 100MW and 1GW, feed three-phase AC power into a national grid of HV transmission lines which interconnect multi-megawatt generators, substations, and demand centres. The grid design philosophy provides redundancy, so that if overhead lines, underground cables, transformers or generators fail, power can be found from other generators via a different route through the electricity grid. This has resulted in huge vertically integrated power systems. For example, the UK's national grid handles approximately 327TWh of energy per year, through more than 7,000km of transmission infrastructure [28].

Power on the transmission network is then routed to the distribution network via the transmission/distribution interface substations and transformers. Distribution networks are operated primarily as passive entities with power flowing from primary and secondary transformers to customers with little or no intervention from automated control systems. The primary distribution transformers are HV/MV transformers and generally feature On-Load Tap-Changers (OLTCs). Secondary distribution transformers are MV/LV and have a manual tap-change capability. In the UK for example, where the distribution network has been significantly extended during the last 50 years to accommodate the increase in demand, the structure and operation of the distribution network has remained largely unchanged [28-29].

Distribution networks are categorised as either radial or interconnected or mesh type. A radial network leaves the distribution substation and passes through the distribution network area with no connection to any other part of the network. Long overhead rural lines with isolated load connections are examples of this topology. An interconnected or mesh network is often found in more urbanised areas and each feeder that leaves the substation has a connection or connections to other feeders of the system. These points of connection between the feeders are normally left open but enable different configurations of the system.

Within these networks there may be a mixture of overhead line construction using traditional poles or towers and conductors and increasingly, underground construction with cables and indoor substations. This can be more expensive and underground distribution systems can cost between twice or four times as much as overhead systems [30].

As the distance from the substation increases the loads become smaller and typically DNOs use conductors of decreasing cross-sectional area in order to reduce network development costs. This design is known as tapering. However, this results in the specific network resistance (Ω/km) of the cable increasing. This has serious implications for the connection of distributed generators and SSEGs located close to the remote ends of the distribution network as the increased resistance will exaggerate the rise in voltage due to generated power export [31].

LV networks, where single-phase loads and SSEGs are connected between phase wires and neutral, with three-phase, four or five-wire configurations have been widely adopted and are likely to remain the standard topology in the future. A neutral wire allows the system to use a higher voltage while still supporting lower voltage single-phase appliances [32]. The neutral is often grounded at regular intervals in these systems. The

objective of grounding the neutral wire is to stabilise system voltages in order to reduce voltage unbalance and provide the return path for grounded-fault current [33]. Hence, neutral wires and system earthing are important when considering power quality and safety issues.

LV earthing systems characterise the earthing mode of the secondary winding of the MV/LV transformer and the means of earthing the frame of the load equipment [34]. Three main configurations are used for LV earthing systems: TT systems, where both the transformer neutral and the frame are earthed; TN systems, where the transformer neutral is earthed and the installation frame is connected to the neutral; and IT systems, where the transformer neutral is unearthed or earthed through a resistor, while the installation frame is earthed [35-36]. A TT earthing system which is common in the UK especially in rural areas, is used in the Experimental SSEZ described in this work. This configuration is chosen as it ensured that all devices on the Experimental SSEZ network were earthed at all times.

## 2.3 Distribution Network Evolution

### 2.3.1 Connecting SSEGs to Distribution Networks

The centralised generation network topology, described previously has a number of drawbacks [25]. This network topology makes large-scale use of Combined Heat and Power (CHP) almost impossible for example. This is because while electricity can be transmitted easily over large distances; an analogous system for transmitting low-grade heat from the place where it is generated to the points of demand does not exist [25, 37].

Furthermore, centralised generation can also have an effect on reliability. If generation is concentrated in a few large units, then the failure of one of these units will have a greater impact on the system. To protect against this, network planners use spinning reserve. This

is reserve capacity of power plant (or plants) of total capacity equal to the largest single plant in use. This reserve capacity is therefore ready to pick up the load immediately.

Transmission and distribution systems dissipate energy as heat during operation and it is estimated that the losses of the UK National Grid transmission system in 2009/2010 are 2.1% at peak demand which is approximately 58GW [38]. Due to the enormous amounts of electricity being transmitted however, this relatively small percentage represents a large loss in absolute terms, in this case approximately 1240MW. This figure varies according to network configuration and does not include distribution losses, which are more difficult to quantify, but are probably of a similar magnitude or even larger.

Electricity demand continues to grow in developed economies. For example, demand is predicted to increase by about 50% in the next 25 years in the United States (US) [25]. Existing centralised infrastructure may not be expandable to meet larger load requirements as the political, social and economic hurdles in the implementation of these changes required may be insurmountable.

It is not certain whether the required investment, to support demand growth, in distribution networks will be available. Network investment in the US for example, has been trailing demand growth for the past twenty five years. This culminated in the highly publicised power outage across the North Eastern US and Canada on August 14-15, 2003 [39]. Subsequently, critics described the US power system as “antiquated”, comparable to that of a Third World nation and in need of modernisation [40].

Investment in generating capacity has also been sporadic [25]. Many developing countries are in the process of improving their electrical infrastructure to cater for greater industrial and domestic demand. Distributed rather than centralised power system topologies may prove to be more advantageous from economic and environmental points of view.

Distributed generation systems, could present solutions to many of the disadvantages of centralised power systems. In addition, they are likely to possess inherent extra functionality and security to the system. Distributed generation is likely to make power systems more resilient to malicious attacks. In addition, the complex interdependencies that currently exist between infrastructures, if the power fails, could be reduced if other infrastructures used there own generation systems rather than the electricity grid [25]. These interdependencies were illustrated by the chaos ensuing from the North Eastern US and Canada outage where transportation, water and communications infrastructure were critically affected by the outage [39].

### 2.3.2 Low Voltage Network Constraints

The deployment of large numbers of SSEG on LV distribution networks is not without problems. A number of technical constraints exist which must be overcome if these future networks are to meet existing and future power quality requirements.

The technical constraints that are focussed on in this work are: -

1. Steady-state voltage rise and variation exceeding statutory limits.
2. Operating distribution network circuits above their thermal limits and reverse power flow.
3. Steady-state voltage unbalance moving outside statutory limits.

#### Voltage Regulation and Voltage Rise

Voltage rise has already been identified as a problem in future distribution networks with high concentrations of SSEG [7, 41]. In addition, voltage drop, a problem associated with existing networks, may become a problem. This may arise when the available distributed generation is low, the demand in the distribution network under consideration is high and the tap position of the secondary distribution transformer has been adjusted to

accommodate high penetrations of SSEG [4]. In addition, voltage regulation limits may also become a problem. Voltage regulation is the permissible voltage rise/drop between the secondary substation transformer and the remote end of the distribution network [29, 42].

In a symmetrical three-phase power system operation, the voltage rise across a line segment 1 due to generation flow can be illustrated diagrammatically as shown in Figure 2.1.

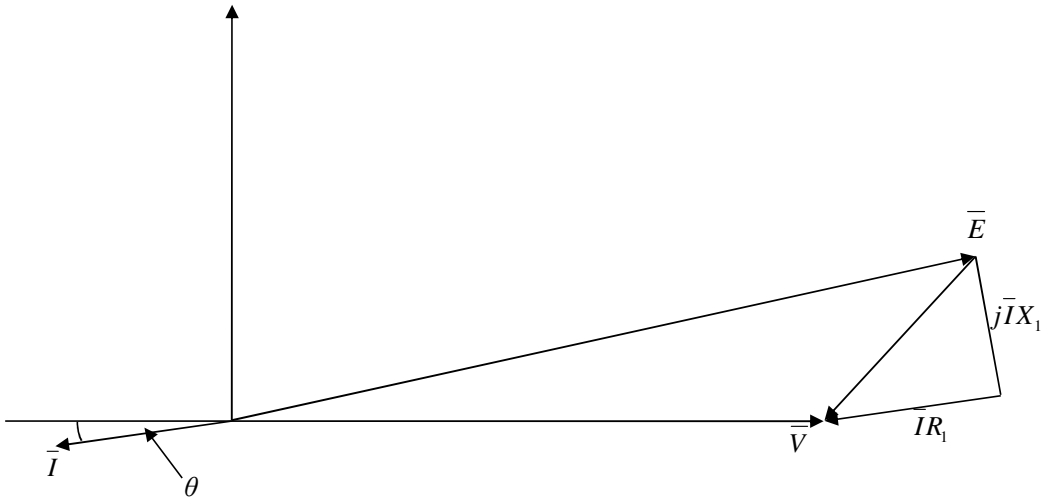


**Figure 2.1: Phasor diagram of voltage rise across line segment due to generation**

This relationship can also be described approximately in the following equation: -

$$\left|\overline{E}-\overline{V}\right| \simeq \frac{\sqrt{3}\left|\overline{I}\right|\left[R_1 \cos\theta + X_1 \sin\theta\right]}{\left|\overline{V}\right|} \qquad (2.1)$$

where: -

$\overline{E}$ sending end line-line voltage (pu)

$\overline{V}$ receiving end line-line voltage (pu)

$\overline{I}$ phase load current (pu)

$R_1$ positive sequence resistance (pu)

$X_1$ positive sequence reactance (pu)

$\theta$ phase angle between voltage at receiving end and load current (pu)

Rearranging this equation to use phase-neutral quantities and using absolute rather than per unit quantities gives approximately: -

$$\left|\Delta\overline{V}\right| \simeq \left|\overline{I}\right|\left[R_1 \cos\theta + X_1 \sin\theta\right] \tag{2.2}$$

However, when analysing four-wire LV networks under unbalanced loading/generating conditions, the voltages attributable to the return currents now flowing in the neutral conductor and earth need to be considered in addition to the voltage changes attributable to the phase currents. The proportion of current that flows in each of these two return paths is dependent on their relative impedances. In four-wire LV distribution networks the neutral of the three-phase four-wire network is often systematically earthed at regular intervals depending on the earthing configuration. Expressions have been derived which express this effect of earth resistance on the return current [43].

For the general situation, the phase-ground voltage drop along a line section *l* of a single-phase conductor in a four-wire system including the effect of self and mutual coupling between the phase and the neutral conductors and the effects of the grounding points can be written [43]: -

$$\Delta\overline{V}_{AG} = \overline{Z}_{AA}\overline{I}_A + \overline{Z}_{AB}\overline{I}_B + \overline{Z}_{AC}\overline{I}_C + \overline{Z}_{AN}\overline{I}_N \tag{2.3}$$

$$\Delta\overline{V}_{BG} = \overline{Z}_{BA}\overline{I}_A + \overline{Z}_{BB}\overline{I}_B + \overline{Z}_{BC}\overline{I}_C + \overline{Z}_{BN}\overline{I}_N \tag{2.4}$$

$$\Delta\overline{V}_{CG} = \overline{Z}_{CA}\overline{I}_A + \overline{Z}_{CB}\overline{I}_B + \overline{Z}_{CC}\overline{I}_C + \overline{Z}_{CN}\overline{I}_N \tag{2.5}$$

$$\Delta\overline{V}_{NG} = \overline{Z}_{NA}\overline{I}_A + \overline{Z}_{NB}\overline{I}_B + \overline{Z}_{NC}\overline{I}_C + \overline{Z}_{NN}\overline{I}_N \tag{2.6}$$

where: -

$\Delta\overline{V}_{AG}$ voltage drop in phase A with reference to ground (equivalent earth return plane of infinite conductivity) (V)

$\overline{Z}_{AA}$ self impedance of A phase conductor (Ω)

$\overline{Z}_{AB}$ mutual impedance of A phase and B phase conductor (Ω)

$\overline{Z}_{AN}$ mutual impedance of A phase and neutral conductor (Ω)

similarly for phase B, C and for the neutral N.

To relate all phase voltages with reference to the neutral point of the load, the primary phase voltage drops with respect to neutral can be expressed as follows [43]: -

$$\Delta\overline{V}_{AN} = \Delta\overline{V}_{AG} - \Delta\overline{V}_{NG} \tag{2.7}$$

$$\Delta\overline{V}_{AN} = \overline{I}_A(\overline{Z}_{AA} - \overline{Z}_{NA}) + \overline{I}_B(\overline{Z}_{AB} - \overline{Z}_{NB}) + \overline{I}_C(\overline{Z}_{CC} - \overline{Z}_{NC}) + \overline{I}_N(\overline{Z}_{AN} - \overline{Z}_{NN}) \tag{2.8}$$

where $\Delta\overline{V}_{AN}$ is the voltage drop on phase A with respect to neutral.

In order to simplify the analysis it can be assumed that the mutual impedances between the conductors of the network can be ignored without losing much accuracy. Therefore (2.8) simplifies to: -

$$\Delta\overline{V}_{AN} = \overline{I}_A\overline{Z}_{AA} - \overline{I}_N\overline{Z}_{NN} \tag{2.9}$$

### Voltage Unbalance

The single-phase nature of SSEGs, combined with the fact that their growth is consumer-driven and not centrally planned is likely to result in larger unbalanced voltages [8]. Voltage unbalance is a condition in which the three-phase voltages differ in amplitude or are displaced from their normal 120° phase relationship or both. The percentage Voltage Unbalance Factor (%VUF) in distribution networks in the UK [44] and Europe [42] is used to define the acceptable level of voltage unbalance in a system. A number of definitions exist but in this work it is defined as the ratio of the negative ($V_-$) to the positive ($V_+$) sequence voltage component [43].

$$\%VUF = \frac{V_-}{V_+} \times 100\% \tag{2.10}$$

where the negative ($V_-$) and positive ($V_+$) sequence components may be computed using the following equation: -

$$\begin{bmatrix} V_a \\ V_b \\ V_c \end{bmatrix} = \frac{1}{3} \begin{bmatrix} 1 & 1 & 1 \\ 1 & 1\angle 120° & 1\angle -120° \\ 1 & 1\angle -120° & 1\angle 120° \end{bmatrix} \begin{bmatrix} V_0 \\ V_+ \\ V_- \end{bmatrix} \tag{2.11}$$

where: -

$V_a$ $V_b$ $V_c$ three-phase line or phase voltages (V)

$V_+$ $V_-$ $V_0$ positive ($V_+$), negative ($V_-$) and zero ($V_0$) sequence voltage component (V)

The %VUF has a statutory limit of 1.3% in the UK, although short-term deviations (less than 1 minute) may be allowed up to 2%, which is the standard limit used for the maximum steady-state %VUF allowed in European networks [42, 44].

The primary causes for voltage unbalance in future LV networks are likely to be: -

1. Asymmetrical impedances (self and mutual) of LV distribution network.
2. SSEGs are often connected in single-phase.
3. Load is distributed unevenly across each phase of the LV network.

It should be noted however, that voltage rise limits are much more likely to be violated than percentage voltage unbalance limits in an LV network with high penetrations of SSEG.

### Thermal Limits

LV network components, such as overhead lines and underground cables, have a maximum current carrying capacity. These limits are based on the thermal heating effects of the current carried by the devices. These ratings are symmetric, that is rating of the

component is the same if it is exporting or importing power. If a component is loaded above its thermal rating for an extended period of time, it will overheat which could then lead to permanent damage. In many cases, high penetrations of SSEGs could cause an increase in the current flow in the network, resulting in system equipment operating closer to their thermal limits. However, it is possible with judicious planning that connecting SSEGs could have a beneficial effect, with no increases in current levels and even some significant reductions.

Distribution transformer specifications are primarily defined in terms of operating voltage and nominal VA rating. At low load and high SSEG penetration and output, generation may be greater than local demand resulting in the export of excess real and reactive power to the higher voltage system through distribution transformers, which could exceed the reverse power flow ratings of the transformer. Moreover, older AVCs (Automatic Voltage Controllers) which feature LDC (Line Drop Compensation) algorithms may not be able to detect the direction of the power flow and may operate erroneously when power is flowing in the reverse direction through the transformers.

Distribution transformers fitted with off-load tap changers have a symmetrical rating, as discussed earlier. For transformers fitted with OLTCs, however, reverse power flows may present a significant problem as the OLTC mechanism can impose an asymmetrical power flow limit [6, 45]. Older tap changer systems of 30 to 40 years, may not operate or may operate with a greatly reduced VA rating when power flows in the reverse direction [46].

### 2.3.3 Future Active Distribution Networks

Future distribution networks will be required to accommodate the forecast increase in SSEG. As described in the previous section a number of technical limitations exist with

regards to large scale deployment of SSEG. These constraints can be overcome by either upgrading the distribution network infrastructure or by changing distribution networks from passive to active entities. Upgrading the distribution network infrastructure is likely to be prohibitively expensive in terms of cost and time and this is why many within industry and academia see active distribution networks as the appropriate choice [13].

These networks will need metering, data acquisition and active control techniques to implement these control schemes. Dedicated communications systems may be incorporated into new build networks or might be retrofitted onto systems using Power Line Carrier (PLC) systems, carried wirelessly or maybe using existing internet infrastructure.

The infrastructure of distribution networks themselves may see a review in their design. The mesh and radially tapered networks of today may be replaced by dynamic networks with control over normally open points to switch from mesh to radial networks as network conditions change. Tapered networks may no longer be the default design with larger cross sectional areas used at the end of LV networks to facilitate to integration of large amounts of SSEG into a distribution networks. In this case large sections of the network could be supplied with local generation reducing the requirements for large conductors closer to the distribution substations.

## 2.4 Small Scale Embedded Generators

Domestic Combined Heat and Power (dCHP) is an SSEG that is very close to being implemented in large amounts on existing distribution networks. Sterling engine type dCHPs units have been trialled in the UK and fit the requirements of customers who wish to replace their existing central heating units with dCHPs units which also supply some generation to reduce their electricity bill [47-50]. Due to their low heat energy to

electrical energy ratio, Internal Combustion Engines (ICE) units, in contrast, supply too much electrical energy when simultaneously supplying the heating requirements for a single home. This would require excess electricity to be stored or exported back to the LV network. Moreover, ICEs are also quite noisy [51-52]. Both of these technologies use a single-phase induction machine to export energy to the LV distribution network.

In contrast, fuel cells require an inverter to export power to the LV distribution network. The dominant fuel cell technologies for dCHP at present are Proton Exchange Membrane Fuel Cell (PEMFC) and Solid Oxide Fuel Cell (SOFC). SOFCs are seen as the most promising technology to be commercialised for dCHP applications [53-56]. Fuel cells, however, need to overcome reliability problems before they can be considered viable alternatives to the ICE and the Sterling engine in the near term.

Two basic competing technologies exist for small-scale wind turbine generation, the horizontal and vertical axis wind turbines. Horizontal axis wind turbines have a greater efficiency for a given "swept area" and may be the preferred option in a rural environment. The vertical axis turbine, however, presents fewer problems with noise and vibration and also is more effective in the turbulent airflows of urban environments and might therefore be more suitable in built up areas [57-61]. Curtailment of generation in small-scale wind applications is not straightforward, as a reduction in the current taken from the generator by the inverter system results in a reduction in torque produced by the generator. This has the effect of speeding up the rotation of the turbine that could lead to undesirable turbine operating conditions. Inverters such as the Windy Boy™ [62] and associated power electronics are required at small-scale wind turbine generation locations.

Photovoltaics (PV) at present are an expensive option for SSEG. The best and also most expensive commercially available panels currently have an efficiency of between 15% 19%. Research indicates, however, that the use of solar concentrators could increase ten-

fold the power obtained from photovoltaic cells [63]. Inverters such as a Sunny Boy™ [64] and associated power electronics are required at PV generation locations.

## 2.5 Domestic Load and Consumer Demand Management

### 2.5.1 Load Characterisation

The task of characterising load is difficult due to the vast array of different load types and compositions. Load compositions are dependent on the geographical area, climate and the load class. Examples of load class include commercial, light commercial, industrial and residential. In addition, these compositions are themselves subject to seasonal and daily variations.

Individual loads have different power factor and different voltage dependent characteristics. The power factor varies from 0.85 to 0.99 in residential premises and from as little as 0.8 to 0.9 in commercial premises [65-66]. A summary of the most common system loads and their characteristics follows. It is important to note that the load seen by MV/LV distribution systems will consist of an aggregate of all these specific load characteristics.

#### Motors

It is estimated that there are over 11 million motors in industry with a total capacity of 90GW, the vast majority of which are connected to the UK distribution network. Moreover, on a typical industrial site, motors consume 66% of the total electrical demand and are responsible for approximately 40% of the UK's total electricity demand [67]. Industrial users for example can contain up to 95% motor load [66]. They are considered to be constant MVA loads but this can be lost if the voltage dips below 65-70% of nominal voltage. In addition, many motors are protected by voltage sensitive contactors

or inverters which trip out the motors during undervoltage events [66]. Unbalanced voltages on distribution networks can result in large negative sequence currents in three-phase induction motors which reduces efficiency and may damage the machine itself [68].

### Air-conditioning and refrigeration

Air-conditioning and refrigeration are very similar to motor loads as the load in these systems are motors to power the compressors etc. in the refrigeration systems. They do not disconnect from the LV network using contactors and due to their low inertia slow considerably during undervoltage conditions. This can cause problems during restarting of the system as overload protection is quite slow on an LV network. A large proportion of demand is consumed by these loads. In areas of the US, for example, as much as 50% of load is refrigeration and air-conditioning [69].

### Discharge lighting

Discharge lighting may account for up to 20% in some commercial areas [69]. They exhibit a constant MVA load characteristic and extinguish often at 80% of rated voltage. Their operation changes slightly above rated voltage and exhibit a constant current characteristic.

### Incandescent lighting

The active power in an incandescent light source varies with voltage at an exponential power of 1.55 [69]. This is due to the large temperature swing that occurs in the filament when voltage changes which changes the filament resistance. Overall, artificial lighting consumes 19% of total worldwide electrical energy production [70].

#### Thermostatic loads

Thermostatic loads exhibit short term individual constant resistance characteristics but are effectively constant power when aggregated and viewed over an extended period of time. In the UK, only 9% of households use electricity for space heating [71] but this can rise to between 20 and 40% of system load in some areas [9]

#### Electronic loads and consumer appliances

Electronic loads and consumer appliances make up a very large proportion of today's household load. These loads are effectively constant power but can exhibit poor power factor due to the harmonic distortion that is a result of the switched mode power supplies that are generally used in these devices. Consumer appliances consumed about 19% of domestic electricity consumption in 2006 in comparison to 9% in 1976 [72]. Among the International Energy Agency (IEA) countries, customer appliances are the fastest growing category of domestic load with consumption increasing by 57% from 1990 to 2005 They now account for 21% of total household energy consumption which is in contrast to the share of water heating which fell to 16% in 2005 [73].

### 2.5.2 Demand Side Management

#### Introduction

Demand Side Management (DSM), also known as energy demand management or demand response is a concept that was a response from utilities to the energy crises which took place in 1973 and 1979. It is defined as the "planning and implementation of those electric utility activities designed to influence customer uses of electricity in ways that will produce desired changes in the utility's load shape" [74-75].

DSM is inextricably linked to social issues as load manipulation can have a large impact on consumers. It is important to take these into account when determining which loads may be managed without deteriorating the customer's supply quality unacceptably [75]. A summary of the DSM strategies which could be used in an active LV network control strategy is presented in the following sections.

## DSM Strategies for Active Low Voltage Networks

### *Peak Clipping*

This can also be described as the reduction of the system peak loads. Peak clipping is generally considered as the reduction of peak load by using direct load control [74, 76]. An example of this would be timers on water heaters which would shut down during diurnal peaks.

### *Valley Filling*

Valley filling describes the management of demand in order to augment off-peak load to smooth the load profile and increase the system efficiency. Adding properly priced off-peak load, under these circumstances, decreases the average cost to customers. Valley filling can be achieved in a variety of ways, the most popular being the addition of new thermal energy storage (water heating and/or space heating) or charging of electric vehicles (EVs) or plug-in hybrid vehicles (PHEVs) [74, 76].

### *Load shifting*

This is the final classical from of load management. This involves shifting load from on-peak to off-peak periods. Popular applications include use of storage water heating, storage space heating, coolness storage, electrical energy storage and customer load shifts [74, 76].

#### *Flexible Load Shape*

Once the anticipated load shape, including DSM, is forecasted the power system planner investigates the supply-side options. In this case, an additional variable in the analysis is reliability. The load shape can change if customers are presented with incentivised options with regard to the reliability of the supply. An example of this would be an interruptible or curtailable load or individual customer load constraints [74, 76]. The utility would therefore charge a less costly interruptible rate to these customers.

## 2.6 Distributed Energy Storage

The large scale deployment of SSEG may result in scenarios where the installation of energy storage may be economically and environmentally beneficial. Moreover, it appears that energy storage will connected to LV distribution network in the near term in the form of PHEVs or EVs which are receiving considerable interest from vehicle manufacturers and policy makers [77].

### 2.6.1 Benefits of energy storage

Similarly to SSEGs operating collaboratively as a VPP, as described in chapter one, once aggregated and controlled the combined energy storage capability of a large number of small scale energy stores could greatly increase the value of distributed energy storage units. Aggregated energy storage could be used by distribution network operators to provide: -

1. System regulation – smoothing out fluctuations in demand so that frequency is not affected [78-79].
2. Spinning reserve – using energy storage instead of part loaded plant for supply when there are sudden changes in demand [78-79].

3. Peak shaving/clipping – energy storage can be used to supply peak demand instead of peak power generators [78].
4. Reliability – energy storage could eliminate voltage sags and surges and provide ride through [78-79].

For consumers the following advantages exist: -

1. Load-Levelling or Load Shifting (DSM) - Energy can be stored during off peak periods and used during peak periods
2. Renewable energy - renewable energy can be stored when it is not needed for use when it is.
3. Reliability – Energy storage may provide ride though facilities for system operator improving system reliability. Energy may also provide back up during loss of supply and may facilitate "islanded" operation of an SSEZ.

### 2.6.2 Energy storage technologies for LV distribution networks

A wide range of storage technologies exist that could be used for small-scale renewable energy systems. When selecting the most appropriate technology, the most relevant considerations are cost, energy capacity, power capacity, lifetime and energy efficiency. A summary of a review of the various technologies is given in tabular form in Table 2.1.

| Energy Storage Technology | Advantages | Disadvantages |
|---|---|---|
| Lead-Acid Batteries | Low initial cost (approx. £65/kWh) Efficient (85% - 90%) | Short lifetime (3-7 years) Deep discharges shorten lifetime |
| Compressed Air | Large capacity (extra tanks are easily added to system) | High self-discharge rate (12% every 24 hours for l0kWh system) Slightly higher initial costs than lead-acid batteries |
| Flywheel | High specific power (can supply 25kW — 50kW) High efficiency (90%) | Very high self-discharge rate (20% every hour) Unable to store more than 1kWh |
| NiMH Batteries | Reliable Long lifetime | 10 times as expensive as lead-acid batteries |
| Hydrogen Fuel Cell (PEMFC) | High power density | Expensive Short lifetime |
| Supercapacitor | Long lifetime (over 20 years) | High self-discharge rate (4% - 100% in 4 hours) Low energy density values |
| Redox (all-vanadium) | Low self-discharge | Limited temperature range (5°C- 45°C) |
| Lithium Ion (Li-Ion) | High specific energy, power, lifetime | Very expensive at present |
| ZEBRA Batteries | Energy storage capacity is too large for this application (17kWh - 20kWh) | No self-discharge Short lifetime (2—5 years) |

**Table 2.1: Summary of Energy Storage Systems for LV distribution networks**

Most of the potential alternatives to lead-acid batteries are currently too expensive, such as nickel metal hydride (NiMH) batteries [80], hydrogen fuel cells in conjunction with electrolysers to produce hydrogen, supercapacitors [80] , and ZEBRA batteries [80-81]. Compressed-air systems [80] and flywheels [80] are let down by their high level of self-discharge while on standby. Some of the technologies also require more testing and development before they can properly break into the energy storage market, as is the case with the Redox energy storage system [82]. At present even with a relatively low lifetime, the lead-acid battery is the most appropriate for domestic applications, as it is low cost and efficient [80]. In addition, it has a low self-discharge when on standby. However, the possibility of the widespread deployment of PHEVs or EVs with an ability to interact with the distribution network or domestic energy management systems may enable the

use of lithium ion (Li-Ion) batteries as an energy storage medium in LV distribution networks [79, 83-84]. For PHEV applications an energy storage capacity of about 19kWh to be typical [77], however prototypes with capacities of 27.4kWh are reported for a small PHEV sport utility vehicle [79].

## 2.7 Conclusion

Existing distribution networks have evolved over the past hundred years based on a centralised control and generation paradigm. The system has a number of advantages including economies of scale and offers relatively efficient operation due to high voltage bulk transmission and reliability. Large power losses in transmission and distribution are also part of this system and the fragile, aging infrastructure is often in need of refurbishment and reinforcement.

Future distribution networks are likely to have high penetrations of SSEGs. However, a number of technical constraints were identified which could limit the penetration of SSEG on LV distribution networks. Active network management is seen by many as the appropriate choice to accommodate these high penetrations and overcome these technical constraints. Active network management techniques are likely to have control over not only of SSEGs but also over controllable load, energy storage, OLTCs or even the topology of the system.

The task of accurately modelling or emulating load in power systems is an onerous one. It is necessary to class and characterise accurately the load in the power system under consideration and also correctly select a model or a mixture of models which can represent this system. It is important when simplifying the model, for emulation of simulation purposes, to maintain the important characteristics of the actual load system.

The most likely energy storage that will be used in LV active distribution networks is the lead acid battery. Its low cost and relatively high efficiency make it the best choice in the short to medium term. Advanced battery chemistries deployed in EVs and PHEVs and fuel cells may in the long term represent a choice to replace both the lead acid battery as energy storage and dCHP for SSEG.

# 3 CONTROL SYSTEM ARCHITECTURES AND TECHNIQUES FOR DISTRIBUTION NETWORKS

## 3.1 Introduction

In order to develop a hardware platform that enables investigation of active control techniques for LV networks it is necessary to review existing and future control techniques and approaches. Evaluation criteria are initially presented which enable qualitative and quantitative assessment of control systems for LV distribution networks that is described in later chapters. Centralised and distributed control architectures are then defined and discussed as they apply to LV networks in this work. This is followed by a review of active distribution network control techniques as they apply to each of the network constraints defined previously. Finally, conclusions are drawn on the relevance of these control system architectures and techniques to LV networks and the SSEZ concept.

## 3.2 SSEZ Control System Architecture Evaluation Criteria

Control system architectures for the SSEZ will be required to ensure that the system operates within distribution network constraints described in section 2.3.2. However, control system architectures for the SSEZ are not only assessed under these operational criteria. The following sections describe the functional, qualitative and quantitative criteria that are proposed to evaluate controllers for the SSEZ concept.

### *Ensure system operates within network constraints*

Excursions from the LV distribution network constraints described in section 2.3.2 are minimised.

### *Resilience and reliability*

The failure or erroneous operation of a component or a software error can also affect the operation or may result in the complete failure of a control system of an SSEZ. The resilience to faults and the reliability of the system should therefore be considered [14].

### *Scalability*

As the addition of SSEGs or other controllable entities are likely to be incremental in nature it is desirable that the control system architecture is capable of easily integrating extra SSEG, energy storage or controllable load. An ideal system would be open and infinitely scalable so that the connection of additional devices would require minimal manual modifications. This is known as “plug and play” capability [14].

### *Communications requirements*

It is desirable that the burden on communications is minimised to reduce costs and facilitate using existing infrastructure.

### *Renewable energy output*

The operating strategy of a control system for a radial network can influence the renewable energy exported by the SSEZ. Operating strategies should seek to maximise the renewable energy consumed in or exported by an LV distribution network.

### *Economic benefit to SSEG/ES/controllable load owners*

This is a complicated criterion to assess as this depends on the way that an SSEZ would interact with the energy market and how each individual SSEG owner is compensated financially for their participation within the SSEZ. Renewable energy export and offsetting local load are the primary advantages of SSEG for individual consumers. In addition, reductions to generation or use of energy storage and controllable load also need to be incentivised. For the purpose of this research, it is proposed that each participating owner is compensated in proportion to their generation/storage/consumption capacity. This implies that the economic benefit to the owner of a controllable load of 1kW that is activated for ten minutes receives the same financial compensation that the owner of an SSEG who reduces his generation by 1kW for ten minutes. This is in addition to compensation for extra generation that is exported to the LV distribution network.

### *Cost and complexity*

The final criteria to be investigated when evaluating control system architectures is the complexity and the cost of deploying the control system. The complexity and costs associated with the control system need to be minimised if this approach to the addition of SSEG on an LV distribution network is to be preferred to infrastructural upgrade or constrained SSEG connections. Costs increase with the addition of communications infrastructure, data acquisition and controller hosting hardware. Moreover, bespoke software solutions may also be required to implement the control system architecture. Apart from initial system implementation it may also be necessary to modify the system to account for changes to the LV distribution network which is likely to further increase the overall lifetime cost of the control system.

## 3.3 Centralised and Distributed Control Architectures for LV Networks

Active control systems for power systems have been previously categorised as either centralised, distributed or decentralised. A strictly defined centralised control system would consist of a data acquisition, decision making algorithms and the control operation to take place at a single location. A distributed control system, in contrast, consists of a number of independent devices or control systems that appear to its users as a single system. In a decentralised system a problem is divided into smaller problems which are solved by a decentralised controller using local data. These decentralised controllers then interact with each other to solve the overall problem [85-86].

These categorisations for control system architectures can become ambiguous when one considers an actively managed power system with distributed generation requiring several layers of hierarchical control. For example in the case of the SSEZ concept it could be considered that the control system is essentially distributed as a number of independent devices would appear to the DNO as a single system. However, within each SSEZ the control system could be considered to utilise either a centralised, distributed or decentralised architecture. In this work, two control system architectures are considered to implement the SSEZ concept in an LV network and are categorised as centralised and distributed.

Centralised control, in this work, implies a central controller located at the secondary distribution substation which would acquire data from nodes in the LV network particularly at the network connection point. More sophisticated systems would also monitor at other nodes of the distribution network, particularly at the remote end. The central controller would then process this data and instruct LV network components to operate in a way that alleviates some network constraint or satisfies an operational goal.

These components include SSEGs, controllable load, Energy Storage Units (ESUs) or controllable normally open switches. The system topology is illustrated diagrammatically in Figure 3.1.

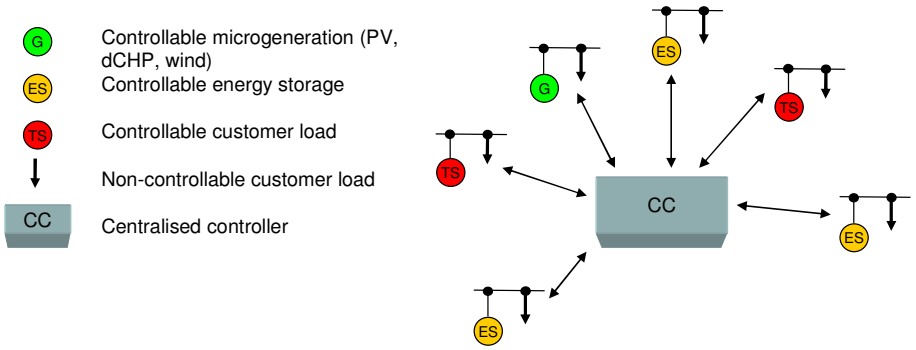


**Figure 3.1: Centralised controller topology for LV networks**

A centralised control topology can compute a global optimum distribution system operating state in contrast to a distributed controller topology whose objectives can be localised [87]. This is only possible, however, if the system has access to large numbers of distributed, high-speed measurements coupled with a detailed model of the system. This could be a problem, especially in rural areas, where high speed communications structures may be unavailable. If this infrastructure needs to be improved it could lead to high installation costs [88]. A number of other limitations exist in the extension of the current, centralised control system approach to LV networks [13-14, 93]. Existing Supervisory Control and Data Acquisition (SCADA) based centralised control systems distribution control systems were not designed to accommodate large penetrations of SSEG and at present do not extend far beyond the 11kV distribution system in the UK [13]. Furthermore, the forecast large quantities of these units and the nature of their uncontrolled and incremental connection makes the realisation of any potential centralised control system even more difficult.

A centralised control system also means that the additional connection of new SSEGs to the active distribution network would require re-programming of the central controller,

which is likely to be slow and complex, unless modular schemes are available [13]. Furthermore, if there is an error in or if there is damage to the central controller it may lead to complete failure of the active distribution network control system.

In a highly distributed control system architecture each SSEG, controllable load and ESU would have their own controller operating autonomously to react to network conditions and customer requirements as illustrated in Figure 3.2. A basic scheme would have a number of distributed controllers acting completely autonomously to control voltage. If the control requirements of the system are more complicated than this however the distributed controllers will be required to operate collaboratively. At present there are a number of competing strategies to implement the distributed control paradigm for SSEG with a variety of functionalities and implementations [7, 14-20].

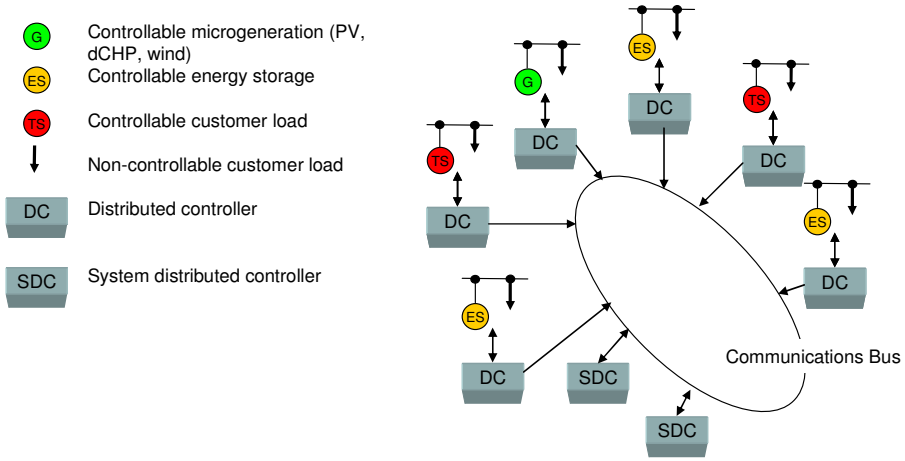


**Figure 3.2: Distributed controller topology for LV networks**

A distributed control approach offers advantages in satisfying the specific control requirements of a future active distribution network. The possibility of "plug and play" insures there are no master or central controllers which means that the system can continue functioning with the loss of any component [19, 89] but with a possible loss of functionality. A distributed control system could therefore address the scalability and reliability issues of centralised systems. In addition, communications between each

controller need not be fast or detailed as the many of the decisions are taken autonomously at each distributed controller. In particular, Multi-Agent Systems (MAS) are already being considered for this purpose [15-18, 90-91]. In the following sections the active management techniques for each of the network constraints are investigated.

## 3.4 Voltage Control Techniques

Voltage regulation and rise have been identified earlier as the likely first constraints to be violated as deployments of SSEG increase. Both centralised and distributed control systems have been developed which control voltage in distribution networks. The majority of the research into the mitigation of these constraints on distribution networks have been at MV rather than at LV level. A number of active network management techniques have been identified previously for voltage control in distribution networks with large quantities of distributed generation [92-108]: -

1. *OLTC control* - Change the position of the tapchanger of the primary distribution network transformer to lower system voltage
2. *Reactive compensation* - Increase the reactive power import to the distributed generation
3. *Generation curtailment* - Decrease the active power export from the distributed generation
4. *Load management* - Increase the load on the system
5. *Energy storage control* - This is a combination of options 2, 3 and 4 but using energy storage to reduce voltage by storing energy or importing reactive power
6. *Network reconfiguration* - Feeders are often operated in a radial configuration. If the normally open points between two adjoining feeders are closed it may reduce system voltage. However, short circuit levels are likely to increase which may

result in damage to equipment during fault conditions. Moreover, the protection systems on the LV feeders are likely to be affected and may not operate correctly.

7. *Power electronic-based distribution network management devices* - Power electronic based system and other static equipment that provide control of one or more LV distribution network parameters and can be used to control system voltage. These systems would provide analogous power quality and network configuration management to those provided at HV levels using Flexible AC Transmission Systems (FACTS).

In addition, each of these active network management techniques can also be operated in conjunction with each other.

### 3.4.1 OLTC Control

On Load Tap-Changers (OLTCs) in conjunction with Automatic Voltage Controllers (AVCs) are the existing principal method of control of voltage on distribution networks. In addition, they have also been investigated with a view to mitigating against the voltage rise issues associated with large quantities of distributed generation in distribution networks [92, 95]. An AVC relay controls the tap position of one or more transformers using their respective OLTCs. The AVC can be configured to operate in a number of ways. The simplest is the control of the voltage on the secondary side of the transformer within a dead band centred around a target voltage [92]. Line drop compensation (LDC) can also be used and this utilises a simple internal model of the distribution system to estimate the voltage at a regulation point within the distribution system [26, 95]. However, in reality in systems where there are multiple feeders the system is used to provide a voltage boost to the system under maximum load conditions. Conversely, in the presence of large penetrations of distributed generation where reverse power flows are

possible the AVC will operate to reduce the voltage under low load, high generation conditions [95-96].

A development of an AVC based LDC control system has been developed known as GenAVC™ [92, 96-98]. To improve the estimates of the voltages on the system one or more remote voltage sensing units are deployed on the distribution network. A state estimation algorithm is used to process this data and make accurate estimates of the voltage throughout the distribution network. These estimates are used to determine the operation of the AVC and thus the OLTC. These operating control algorithms were developed for use on MV distribution networks and assume balanced operation. Single-phase voltage and current measurements are therefore required only. As shown in chapter five however, large differences could exist between voltage and current flow on each of the phases on LV distribution networks.

The definition of an SSEZ does not extend to the primary distribution transformer with an OLTC so that control method is not applicable to LV network controllers at present. However, it is possible that aggregated SSEZs would be able to communicate with a supervisory controller which may have control over the Automatic Voltage Controllers (AVC) at the primary distribution station. It should be noted that all these OLTC based control systems are defined as centralised control architectures in this work as all measurements are brought back to a centralised controller.

### 3.4.2 Reactive Compensation

Another method to reduce voltages on distribution networks is to utilise the distributed generators to import reactive power [93, 99-100]. This flow of reactive power into the distributed generation has the effect of depressing the voltages on the distribution network. In [93] a centralised approach utilising optimal power flow (OPF) and cost

benefit analysis (CBA) which compares the effectiveness of generation control, reactive power control and OLTC control on an 11kV network is described. This system requires measurements throughout the distribution network with an increase in measurement nodes increasing the accuracy of the estimates of the parameters of the LV network and thus the performance of the system. A centralised strategy is also employed in [100] but in this case the measurements are taken at the point of interconnection (POI) only.

Centralised and distributed systems utilising reactive power control are proposed and simulated in [99]. In common with [93] an OPF algorithm is used as a basis for a centralised control algorithm. In contrast to [93, 100] both real and reactive power export and import are simultaneously controlled by the control system to ensure that the system is operating within the statutory voltage limits. The distributed control system proposed uses the voltage measurement signals at the terminals of each generator to control the real and reactive power flow from the generator. This control algorithm is known as Automatic Voltage/Power Factor Control (AVPFC) [31, 99].

The power factor of load on LV distribution networks tends to be between 0.8 and 1.0 lagging as detailed in section 2.5.1 and SSEG are required to export active power at a power factor of between 0.95 lagging and 0.95 leading. Therefore the voltage rise or drop in LV distribution networks is dominated by the resistive rather that the reactive part of equation (2.1).

$$\left|\overline{E}-\overline{V}\right| \simeq \frac{\sqrt{3}\left|\overline{I}\right|\left[R_1\cos\theta + X_1\sin\theta\right]}{\left|\overline{V}\right|} \qquad (2.1)$$

Moreover, in contrast to MV and HV networks the X/R ratio is small in LV networks and in particular underground cable networks, which also reduces the effect of reactive power flow on voltage rise and drop in LV distribution networks.

Therefore, reactive compensation, however, has been shown to have limited effect on voltage rise in LV distribution networks. This has also been shown in simulation [7].

### 3.4.3 Generation curtailment

Generation curtailment has been previously investigated as a method to control voltage on distribution systems [93-94, 101-102]. Similarly to reactive power control both centralised and distributed strategies have been used in conjunction with generation curtailment. In [93] the effectiveness of generation curtailment in contrast to reactive power control and OLTC control is investigated utilising a centralised control system based on an OPF algorithm.

Curtailment of generators towards the remote end of the network has a greater effect on voltage rise as generators nearer the remote end of a radial distribution network feeder have a greater impact on voltage rise than those closer to the network connection. To maximise generation therefore, in a radial distribution network, the generators at the remote end would be curtailed or shut down completely in the event of the network voltage rising above the statutory limits. If one considers, however, that an overvoltage condition may exist on an LV distribution network with a high penetration of SSEG, five times in one year, which would result in zero generation from these SSEGs during these voltage excursions. Therefore the annual energy yield from these SSEGs is lower than those located nearer the network connection. Instead of this strategy, algorithms equally or optimally sharing the duty of mitigating against overvoltage conditions using a centralised algorithm have also been investigated [101].

Active power generation is has a much higher economic value than reactive power import in distribution networks as active power generation can result in a reduction in active power consumed by load or the export of active power to the LV network [109]. Both of

these options benefit SSEG owners economically with reductions in active power imported from the grid or feed-in tariffs respectively. In contrast, there is no economic framework to incentivise SSEG owners to import reactive power. Therefore, a number of active network management techniques initially utilise reactive power control to control the voltage. If reactive power control is unable to regulate the voltage, generation curtailment is used to reduce the voltages on the system [104, 106]. Similarly, in the MAS based control framework proposed in [103] the SSEGs are initially controlled to absorb reactive power if the voltage exceeds the desired limits which is defined as the alert stage. If the voltage on the system exceeds the maximum permissible limit, which is defined as the emergency state, then the SSEGs are instructed to curtail generation.

### 3.4.4 Load management

Load management or DSM techniques described previously typically modulate the load on a distribution system during periods of maximum load, to maintain the security of the system [105]. However, an increase in load also has the effect of reducing the voltages on a distribution network. This additional functionality of DSM has been explored previously in which a centralised control system is used to control four loads [105]. Voltages on the LV network are monitored and as the voltage exceeds predefined limits, additional load units are switched in. The MAS framework described in [103] also proposes switching in controllable load in the alert stage as generation curtailment is the least preferred option in this system.

### 3.4.5 Energy storage

As energy storage almost always requires power electronic converters to interface with the distribution network, real and reactive power can controlled which can be used to regulate network voltage. Voltage regulation in a distribution network using energy

storage has been demonstrated previously [107-108]. In addition, centralised control of voltage using active management of energy storage is also possible. Any control strategy will be required to account for the limited energy capacity of any energy storage under consideration. Within the MAS framework described in [103], energy storage is switched in during the alert stage similar to the control technique for controllable load.

### 3.4.6 Power electronic-based distribution network management devices

Power electronic-based distribution distribution network management devices can provide the same functionality as reactive power control in distributed generation units except that this is independent of the generator. At present the deployment of power electronic-based distribution network management devices such as the Distribution - Static Synchronous Compensator (D-STATCOM) or Distribution Static VAr Compensators on distribution networks is limited by high costs [94, 110].

### 3.4.7 Discussion

OLTC control, network reconfiguration and power electronic-based distribution network management devices, with regard to the SSEZ concept, are associated with centralised control as all measurements and data are processed and control decisions take place at a central location. Moreover, an OLTC is usually only available at the primary substation distribution network transformer and its control will therefore lie above an SSEZ in a hierarchical control system architecture.

Network reconfiguration is also a possibility to assist in voltage control but would facilitate voltage control in a limited number of network topologies. Power electronic-based distribution network management devices were also investigated to provide

regulation of voltages in an LV distribution network but may have limited effect on networks with low X/R ratios and additionally are hampered by their high cost.

Reactive compensation has a number of advantages as it does not impact on the end customer or require extra equipment for voltage control if inverters are used to couple SSEG to the LV network. However, reactive compensation, as in the case of D-STATCOMs, may have very limited impact in LV networks where X/R ratios are low. Generator curtailment offers the possibility of voltage control in LV networks with low X/R ratios. However, these strategies result in reduced renewable energy output and reduced direct economic benefits to SSEG owners. However, this control technique could be economically incentivised if SSEG owners are compensated for this facility. Load management and energy storage also facilitate voltage regulation in networks with low X/R ratios but again these systems need to be incentivised economically as the direct economic benefits to the owners of these systems may be small. Reactive compensation, generator curtailment, load management and energy storage are compatible with both distributed and centralised control system architectures.

## 3.5 Voltage Unbalance Control Techniques

Specially designed D-STACOMS and other power electronics devices could provide the functionality to compensate for unbalanced voltages in LV distribution systems [111-114]. Use of these power electronic devices is the only option at MV level as the vast majority of generation and loading units connected at MV are three-phase. However, at LV, coordinated control of generation, controllable load or energy storage could be used to equalise the distribution of load and generation across the three phases of an LV network. The MAS framework proposed in [23-24, 103] proposed an unbalanced agent

which collaborates with other generation, consumer demand or energy storage agents in the system to mitigate against voltage unbalance.

## 3.6 Power Flow Control Techniques

A number of centralised strategies have been developed to ensure that the thermal limits of underground cables, overhead lines, transformers and switchgear are observed when large quantities of distributed generation are connected to the distribution network [13, 100, 102, 115-117]. In [100], the power flow at the Point of Interconnection (POI) is measured along with the system frequency and the rate of change of power. It was envisaged in this work that network operators would require control of these three parameters. Depending on the system requirements and network conditions one of these parameters is assigned highest priority and this determines the power command to each distributed generator. Other active management techniques for managing thermal limits include "All off inter-trip" in which case a violation of the thermal limit will result in the disconnection of all distributed generators on the feeder [13]. A more advanced system, after a thermal limit violation, initially issues a 33% reduction commands to each of the distributed generators on the system. If this fails to restore satisfactory system operation a 66% reduction signal is sent and finally a trip signal is issued [13].

Artificial intelligence techniques, OPF techniques, current tracing and Constraint Satisfaction Problem (CSP) techniques have also been investigated to solve power flow constraints [102]. Generation was classified into firm generation (FG), non-firm generation (NFG) and regulated non-firm generation (RNFG) in [115]. In this case only the RNFG is regulated to control power flow. A trim margin is proposed based on the rate of change of generation and load and when this limit is violated the RNFG is curtailed. Furthermore, if the trip margin is violated, the RNFG is disconnected completely but is

reconnected after 5 minutes. The trip margin is based on the thermal limits of the circuits. An investigation into the impact of different methods of estimating the current/thermal capacity of the network, which is a function of the meteorological conditions throughout the year, is presented [116]. A conventional static estimation of capacity is compared with seasonal, static and dynamic Active Constrained Connection Managers (ACCMs). Load management is an alternative strategy to mitigate against violation of thermal limits caused by distributed generation. A drawback to this approach is that it is easier to shed load than to increase load on a distribution network [117]. However, energy storage can be used to provide this facility [117-119].

## 3.7 Conclusions

A set of evaluation criteria for the quantitative and qualitative assessment for control systems for LV distribution networks is initially presented. Centralised and distributed control system architectures as they apply to LV distribution networks and the SSEZ concept are then defined. This was followed by a discussion on the advantages and disadvantages of the implementation of each of these control system architectures in LV distribution networks.

Both architectures are capable of mitigating the network constraints detailed in chapter two however, a number of control techniques exist to achieve this in distribution networks. Voltage variation and regulation, voltage unbalance and thermal limit control techniques were investigated with respect to LV distribution networks and the SSEZ concept.

Reactive compensation generation curtailment, load management and energy storage for voltage control were found to be compatible with both centralised and distributed control system architectures. This is in contrast to OLTC control, network reconfiguration and

Power electronic-based distribution network management devices which are more compatible with centralised control system architectures.

Specially designed power electronic-based distribution network management devices are presently used in MV networks to provide voltage unbalance control. These systems are very expensive at present and an alternative, distributed control strategy has been proposed at Durham University to mitigate this network constraint.

A wide variety of thermal limit control techniques exist which have been developed primarily for MV networks. All the techniques reviewed use a centralised control architecture where the network conditions are monitored and a generator dispatch strategy is designed by a central controller. However, energy storage and load management can also be used to reduce the power flows in overloaded areas of the system.

# 4 DESIGN AND DEVELOPMENT OF THE EXPERIMENTAL SSEZ AT DURHAM UNIVERSITY

## 4.1 Introduction

The Experimental SSEZ has been designed to enable investigation into the effect of high penetrations of SSEG on distribution networks and enable development of intelligent controllers which maximise their impact whilst maintaining satisfactory system operation. In this chapter, the experimental requirements for the investigation of the SSEZ concept are initially presented. This is followed by a summary of an investigation of the existing low voltage distribution network emulation laboratories worldwide. A detailed description of the individual components and systems of the Experimental SSEZ is then presented. The end of the chapter consists of a discussion on how the experimental requirements are satisfied by the design and implementation of the Experimental SSEZ.

## 4.2 Experimental Requirements for Investigation of SSEZ

An investigation into the requirements for a low voltage distribution network laboratory was completed as part of this research. The details of this investigation are presented in more detail in Appendix B.

It was found that emulation could be powerful tool to assist in the evaluation of control systems for the SSEZ concept due to the possibilities of constructing repeatable scenarios in an LV distribution network laboratory. This ability to recreate scenarios presents a number of advantages in the assessment of control algorithms.

The LV distribution network laboratory should be a three-phase, four-wire system with a power balancing facility. The LV network should have low X/R ratios in common with LV distribution networks and should be tapered that is the conductors should be reducing

in cross-section near the remote end of the feeder. In addition, the system should facilitate connection of accurately emulated single-phase load and generation and energy storage distributed throughout the circuit.

The data acquisition system will need to be able to measure parameters throughout the circuit and must be able to measure the network constraints described in the previous chapters. This is important to be able to assess the performance of the control algorithms. The data acquisition system is also essential for the development of the control systems as measurements of voltage, voltage unbalance and current are inputs to any control algorithm.

The control system platform should facilitate the development of both centralised and distributed control architectures. The system should be able to control generation, load and energy storage within the system and should operate fast enough that network constraints are mitigated within defined limits.

The requirements are for an ideal LV distribution network laboratory facility and these idealisations need to be considered in practice under economic or practical constraints.

## 4.3 Review of Existing Low Voltage Distribution Network Emulation Laboratories

A review of the low voltage distribution network emulation laboratories was undertaken by the author in order to inform the development of the Experimental SSEZ. European laboratories at NTUA [120-121, 164-165] in Athens, Greece, DeMoTec [120-121, 164-166] at Kassel, Germany, Labein's Experimental Centre in Bilbao, Spain [164-165, 167], and the SYSLAB at Risø, Denmark [168-169] were found to be useful for comparison. In addition, UK laboratories, NaREC's EnergyLINK Laboratory [7, 142] in Blyth,

Northumbria and the University of Manchester Microgrid/Flywheel energy storage prototype [120-121, 164-165], were also considered in this investigation.

The topology of the LV distribution network itself is crucial to establishing whether active network management algorithms are effective in managing network components to ensure that network constraints, such as voltage rise, are observed. DeMoTec, Labein and the EnergyLINK Laboratory feature three-phase multiple bus systems where load, generation or energy storage can be easily configured into various power system topologies [120-121]. This functionality is augmented by the availability of line emulators. In contrast, SYSLAB includes long LV conductor sections [107, 122]. The NTUA facility is single-phase and while it could possibly be used to evaluate voltage rise or regulation or thermal limit algorithms, it cannot evaluate unbalance algorithms as it is a single-phase system [120-121].

Actual SSEG is very useful to validate models and accurately evaluate the effect of generation on LV networks. Many SSEGs, however, are coupled to the LV network using inverters. The dynamic operation of SSEG systems may be dominated by the operation of the power electronics/inverter drives rather than the SSEGs that they are supplied by. Therefore, the differences in accuracy between emulation and actual wind generation maybe minimal if the same power electronic interfaces are used in both applications.

Real domestic load offers the advantage that it can provide accurate emulation of any load but it may not be useful in carrying out emulation of scaled down networks due to diversity. Moreover, it is necessary to carry out detailed analyses of domestic electric habits to emulate the load profile of domestic residences and considerable variations exist in typical individual domestic profiles as established in chapter two.

While it is useful to be able to evaluate all future energy storage options the most relevant form of energy storage in the short-term is lead acid battery storage and advanced battery

chemistries and possibly SOFC fuel cells in the near term. Lead-acid based energy storage is integrated into the systems at NTUA, DeMoTec and Labein. Flywheels, like those installed at DeMoTec, Labein, the EnergyLINK Laboratory and at the University of Manchester have quite large power outputs and therefore are unlikely to be installed in domestic premises but are likely to be applicable to other active distribution network concepts [89, 123-124]. In addition, their low energy capacity which is important for domestic applications, may also limit their deployment. Fuel cells have been installed only at DeMoTec. SYSLAB is the only laboratory to feature an advanced battery chemistry installation and moreover includes this as part of a PHEV system. Finally, energy storage is limited to one or two units on each network and is not distributed throughout the network.

The data acquisition system at NTUA is unlikely to be utilised for data acquisition in a future actively managed network as it is a slow system and the protocols used are proprietary. The custom systems at the EnergyLINK laboratory and at the Flywheel facility utilising LabVIEW™ and dSPACE® enable faster access to the parameters of the network is also possible. At DeMoTec the SCADA system used for data acquisition is similar in some respects used on existing distribution and transmission networks. However, the development of a functioning SCADA with supporting Remote Terminal Units (RTUs) [125] is a complex task and is costly to design and develop. The system at Labein is very flexible and provides a large number of power quality measurements including harmonics.

The dSPACE® systems, like that at the University of Manchester Microgrid, would facilitate development of control algorithms using Simulink® [126] such as will be developed for the Experimental SSEZ. The IEC 61850 protocol is used at DeMoTec, Labein and at SYSLAB is at present a standard substation automation protocol but an

extension of this protocol IEC61850-7-420 is in development. It is envisaged that this will form the communication protocol with SSEG, ESUs and controllable load [127]. These systems enable both centralised and distributed control platforms to be developed. At NTUA a central PC is used to run the agents in the system and therefore could be viewed as a centralised control platform. However, agents operating autonomously on the same PC are possible and therefore the system exhibits many of the salient properties of a distributed system. A summary of the capabilities of each of the laboratories is illustrated in tabular form in Table 4.1.

| | **NTUA** | **DeMoTec** | **Labein** | **SYSLAB** | **EnergyLINK** | **Manchester** |
|---|---|---|---|---|---|---|
| *LV Network* | Single-phase grid connected | Two bus, three-phase network, MV/LV transformers and grid emulation | Three bus three-phase network, MV/LV transformers and grid and network emulation | Network connection emulator, large three-phase network | Two bus, three-phase network, M/V/LV transformers and grid emulation | Flywheel used to provide power balance |
| *SSEG* | PV, Wind | PV, Wind, Wind emulation dCHP | PV, Wind | PV, Wind | PV, Wind | Single SSEG emulator |
| *Energy Storage* | Lead-acid battery | Fuel cells, lead acid battery and flywheel | Ultra-capacitors, lead acid battery and fly-wheel | Vanadium Resox Battery (VRB) and PHEV | Flywheel | Flywheel |
| *Load* | Household load controlled by PLC | Workshop of household load, controllable inductive, resistive | Controllable Resistive Load | Resistive load, defferable heating load and an office bulding *Flexhouse* | Domestic load simulator and controllable resistive load | Selection of household loads |
| *Data Acquisition* | RS232 and interface inverter systems | Custom system managed by proprietary SCADA system | Custom system, enables high resolution power quality measurements | Module at each node linked via high speed network (IEC61850) | LabVIEW™ and bespoke transducer systems | DSPACE® and bespoke transducer systems |
| *Control Infrastructure* | RS232 and interface inverter | Ethernet between generators, IEC61850 based system | IEC61850 based system | Module at each node linked via high speed network (IEC61850) | N/A | DSPACE® based system |

**Table 4.1: Summary of low voltage distribution network emulation laboratories**

Further details of this investigation are presented in Appendix C.

## 4.4 LV Network

The network connection emulator consists of a 30kVA synchronous machine coupled to an induction machine driven by a four-quadrant inverter drive [128] which is connected to the grid as illustrated in Figure 4.1. The grid in this chapter is the LV network of the School of Engineering at Durham University.

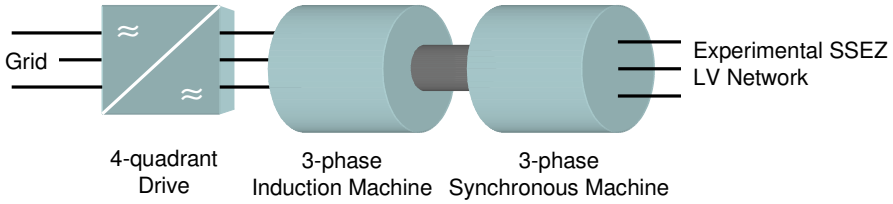


**Figure 4.1: Network connection emulator**

The four-quadrant drive enables the import and export of active power from the Experimental SSEZ. In addition, the four-quadrant drive also provides: -

1. Frequency regulation for the system. This is typically set at 50Hz.
2. Regulates inrush current to three-phase induction machine. This would be a problem if the induction machine was connected directly to the grid.

The steady-state and dynamic operation of a synchronous machine is different from that of a transformer. In particular, the positive and negative sequence impedances of transformers are similar in contrast to a synchronous machine where the negative sequence components are much smaller than the positive sequence impedances. This has consequences on the voltages observed at the terminals of the synchronous machine under unbalanced conditions as demonstrated later in chapter five. However, unlike a grid connected transformer, it is possible to easily change the system voltage by varying the automatic voltage regulator (AVR) and also vary the system frequency by changing the speed set point on the four-quadrant drive. In addition, this design of network connection emulator results in an LV network electrically isolated from the grid. A virtual power system would also be a good solution as a network connection emulator but development

costs and time constraints made this approach unviable. The final system installed in the Experimental SSEZ is shown in Figure 4.2.


**Figure 4.2: Network connection emulator installation at Durham University**

The Experimental SSEZ does not feature any sophisticated, flexible LV network emulation facilities as at DeMoTec, Labein and the EnergyLINK laboratory. However, simulation is fast and accurate in the modelling of voltage drops, unbalance etc. in LV networks. This is in marked contrast to the simulation of SSEGs, ESUs and their associated power electronics which often require computationally intensive, complicated models. Therefore, it is proposed that shortcomings in the system due to inaccuracies in network emulation can be quickly and accurately overcome using a transformation system. The development of such a system is described later in this work in Appendix H.

The LV network of the Experimental SSEZ has a tapered, radial topology and its impedances are primarily resistive, in accordance with the requirements described earlier in this chapter. The system is four-wire with a TT earthing system [34, 129-131] which is common in the UK in rural areas. The LV network topology and the placement of the nodes are illustrated diagrammatically Figure 4.3.

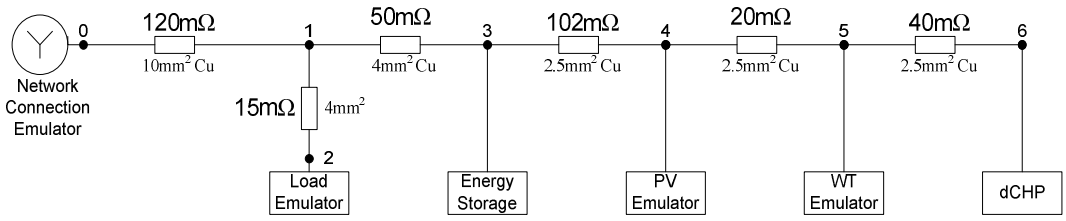


**Figure 4.3: Single line diagram of the topology of the Experimental SSEZ**

## 4.5 SSEG Emulation in the Experimental SSEZ

As identified previously, small-scale wind, PV and dCHP are seen as the most likely technologies to achieve large-scale deployment on LV networks in the near future. Thus, the Experimental SSEZ features small-scale emulators of these three technologies.

While actual generation and load are more accurate, emulation of SSEGs is more useful and flexible than using actual PV, wind turbines and dCHP. Firstly, emulation permits the user to validate distribution network simulation models quickly and easily. Secondly, it can be used to create a performance matrix to systematically test control algorithms. Finally, scenarios at the outer operating points of the system envelope can easily be implemented. For example a worst case scenario of maximum small-scale wind generation and dCHP generation could be implemented. Furthermore, domestic load will be emulated so that a number of load profiles and load compositions can be implemented in repeatable tests.

In addition, emulation is useful if aggregated cases of load and generation need to be considered. In this instance, LV network emulator can be considered to be a scaled model of a network rather than using the system as an LV network albeit on a small-scale. Aggregated PV, wind, dCHP and load profiles can then be used when implementing these models of these systems. When considering aggregated cases however it should be noted that while the generation sources and energy storage for the SSEZ are single-phase, when many SSEG and distributed energy storage units available in an SSEZ they are likely to

be distributed across all three-phases. Therefore, in these cases balanced generation may be a more accurate approximation of the operation of future LV distribution networks.

### 4.5.1 dCHP Emulator

A three-phase induction machine, 2-quadrant inverter drive, a single-phase induction machine and a capacitor is used to emulate dCHP as illustrated in Figure 4.4. The three-phase induction machine and inverter drive are used to emulate the action of the mechanical output of the dCHP unit which could be an internal or external combustion machine mentioned in chapter two.

The supervisory PC running LabVIEW™ is used to control this inverter drive via the analogue outputs of the National Instruments™ data acquisition board and the analogue inputs of the inverter drive so that the speed and torque can be varied to emulate the action and duty cycle of an actual dCHP system. When emulating a dCHP unit the torque of the three-phase induction machine is set so that the single-phase induction machine operates above synchronous speed and export energy into the three-phase LV network of the Experimental SSEZ.

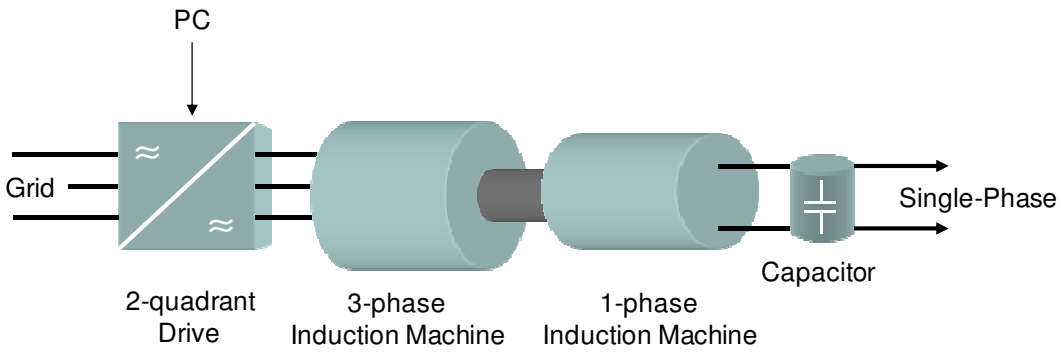


**Figure 4.4: dCHP emulation system**

In normal operation, the single-phase induction machine operates as a generator exporting real power to the Experimental SSEZ LV network as per a regular domestic dCHP installation. The capacitor is used to supply reactive power to the single-phase induction

machine during start-up and also during steady-state operation as the induction machine does not operate at unity power factor. The installed capacity of the dCHP emulation system is 1.1kW which is similar to the Whispergen [47] units which have been trialed in the UK.

### 4.5.2 PV Emulator

A three-phase autotransformer, DC machine drive, inductor and G83 compliant inverter are used to emulate small-scale PV generation as illustrated in Figure 4.5.

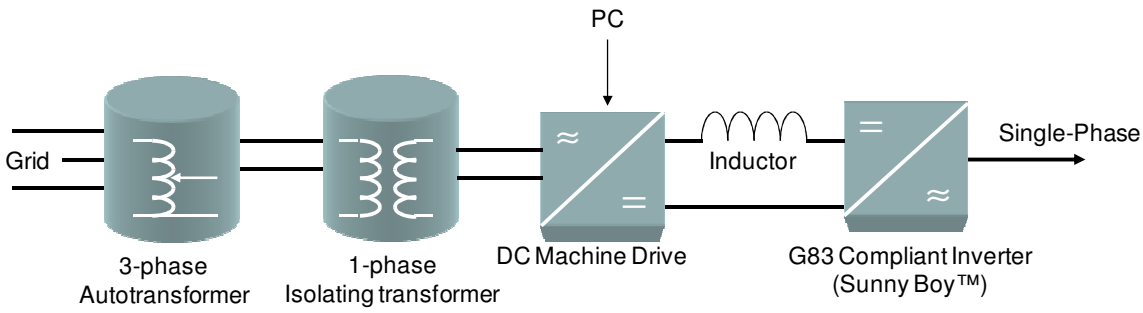


**Figure 4.5: PV generation emulation system**

A single-phase transformer is used to isolate the system from the grid. In order to limit in-rush current into the single-phase transformer on start-up, a three-phase variable autotransformer is used. The single-phase transformer supplies the DC machine drive. The DC machine drive is used to emulate the voltage and current supplied from a PV array. The DC machine drive output supplies the SMA Sunny Boy™ [64] single-phase G83 compliant [1] inverter via an inductor as the DC machine drive introduces large of amounts of harmonic distortion into the current flowing into the inverter. This device supplies synchronised, 50Hz, 230V single-phase ac voltage to the LV network. In addition, the Sunny Boy™ has a number of communications options including PLC, RS232 and RS485 serial links which can be used for monitoring and control. This control functionality is used to limit the power output from the Sunny Boy™ and therefore can also be used to emulate the power output of a PV generation system. The Sunny Boy™ is

also in use at NTUA, DeMoTec and at the EnergyLINK laboratory to couple PV arrays to their laboratory LV network emulators. The installed capacity of this system is 1.7kW which is a limitation of the Sunny Boy™ and is typical of domestic PV applications. The final installation is shown in Figure 4.6.


**Figure 4.6: PV generation emulator at Durham University**

### 4.5.3 Small-scale Wind Turbine Emulator

A three-phase induction machine and inverter drive, a three-phase axial flux synchronous machine and power electronics are used to emulate a small-scale wind turbine generation system as illustrated in Figure 4.7.

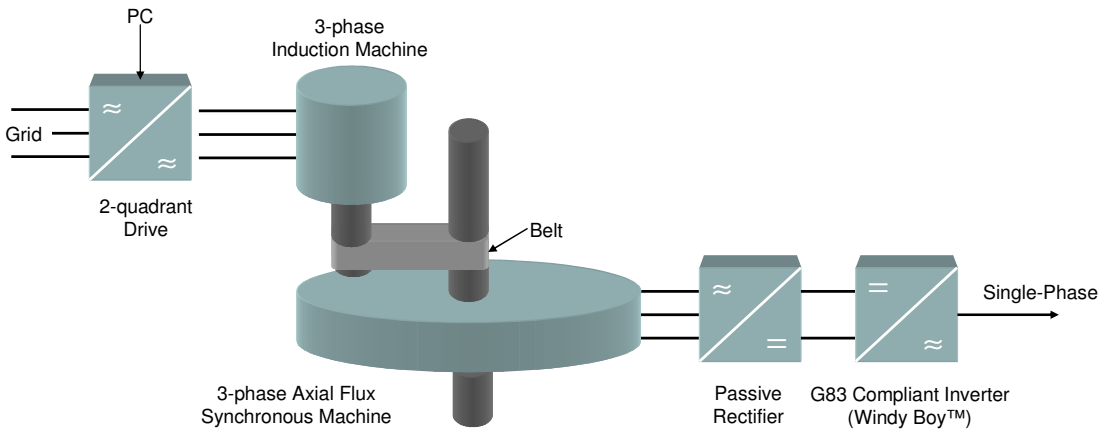


**Figure 4.7: Small-scale wind turbine emulation system**

The three-phase induction machine and inverter drive system is used to drive the three-phase axial machine via a belt drive. The three-phase axial flux machine is typical of designs that are being used in small-scale vertical axis turbines.

The supervisory PC running LabVIEW™ controls the speed or the torque of the three-phase induction motor; via the analogue voltage outputs of the National Instruments™ and the inverter drive analogue voltage inputs, so that the speed and torque can be varied to emulate actual wind turbine torque or speed characteristics.

The three-phase output of this machine is then rectified. This is used to supply a DC bus for the Windy Boy™ single-phase inverter [62]. The SMA Windy Boy™ is a G83 [1] compliant inverter for coupling of small-scale wind turbines to LV networks. As in the case of the Sunny Boy™, this system has a number of communications options including PLC, RS232 and RS485 serial links which can be used for monitoring and control. The Windy Boy™ is also in use at NTUA, DeMoTec and at the EnergyLINK laboratory to couple wind energy to their laboratory LV network emulators. This device inverts the output from the rectifier to 50Hz, 230V single-phase AC voltage which is synchronised to one of the phases of the Experimental SSEZ of the LV network. The small-scale wind turbine emulator is shown in Figure 4.8. The maximum output of the small-scale wind

turbine generator emulator is approximately 2kW which is a typical value of installed domestic generation.

**Figure 4.8: Small-scale wind turbine emulator at Durham University**

## 4.6 Experimental SSEZ Load Emulator

The load emulation system consists of a LabVIEW™ algorithm, that converts the load data to digital data, a National Instruments™ interface board and a three-phase load bank as illustrated in Figure 4.9. The load bank consists of a set of resistors controlled by solid-state relays which are controlled by the LabVIEW™/National Instruments™ control system. These solid-state relays control a set of 250W, 500W and 1000W resistors in the load bank. This results in a computer controlled load which can vary independently the demand on each of the three-phases of the system. The load on each phase can be varied in 250W steps up to a maximum of 2.75kW at nominal voltage.

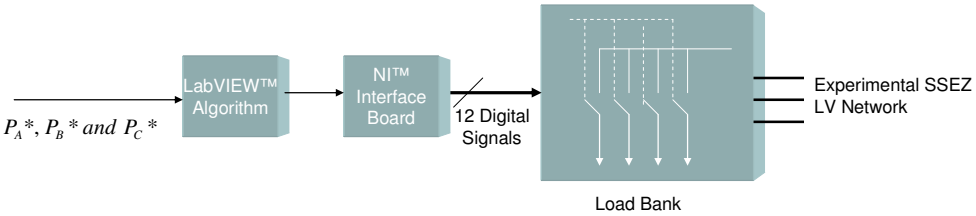


**Figure 4.9: Load emulation system**

Controlled and uncontrolled loads can be lumped together and can, in conjunction with control supplied via LabVIEW™ and the National Instruments™ system, be emulated on the same load bank. The load bank is resistive; therefore the system is capable of emulating unity power factor loads only. In addition, harmonic effects cannot be emulated by this load bank. The Experimental SSEZ load bank is shown in Figure 4.10.

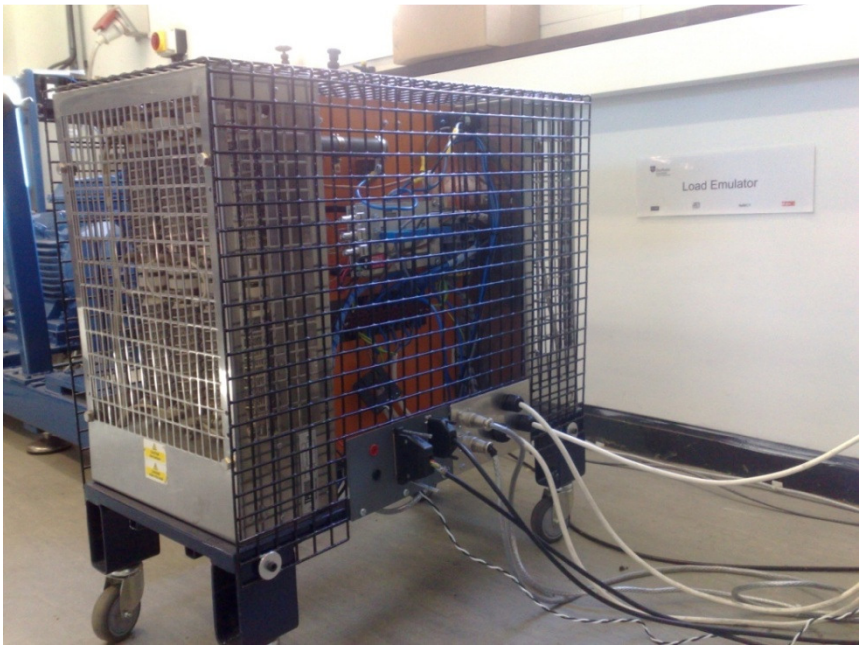


**Figure 4.10: Load emulator at Durham University**

In addition, to the load emulator it is also possible to connect household appliances to any of the phases using the power sockets located at nodes 4, 5 and 6 of the LV network of the Experimental SSEZ as illustrated in Figure 4.3.

## 4.7 Experimental SSEZ Energy Storage System

The energy storage system consists of a SMA Sunny Island 4500™ (Sunny Island 4500™) bi-directional PWM (Pulse Width Modulation) inverter, a battery bank

consisting of 4 X 110Ah batteries and a control and measurement system. The system is illustrated diagrammatically in Figure 4.11.

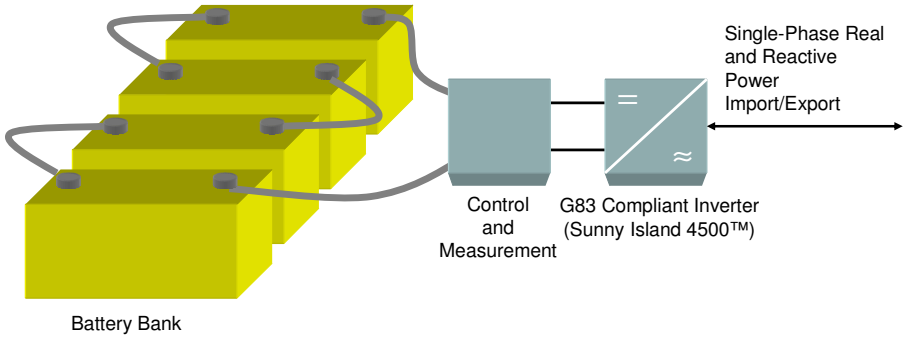


**Figure 4.11: Energy storage system**

### 4.7.1 Sunny Island 4500™

A Sunny Island 4500™ bi-directional PWM inverter is used to interface the lead-acid battery based energy storage with the Experimental SSEZ. Real-time computer control of real and reactive power flow into an LV network is possible with this unit [132]. The Sunny Island 4500™ has been developed in conjunction with the University of Kassel Institute of Electrical Engineering [133], ISET [134] and SMA and features sophisticated control systems and functionality which facilitates integration of this unit into active power systems. This unit features the ability to connect in parallel to the utility grid and also facilitates islanded operation of an LV network [132, 135].

In the Experimental SSEZ the frequency of the system is fixed using the network connection emulator. To vary the power output of the ESU the nominal frequency parameter of the Sunny Island 4500™ is changed. This regulates the power exported to and imported from the Experimental SSEZ system. Similarly, reactive power output from the Sunny Island 4500™ can be controlled by varying the value of the nominal voltage.

The Sunny Island 4500™ also features advanced State of Charge (SOC) estimation, battery state estimation and battery charge management algorithms. Communication to

the Sunny Island 4500™ is achieved using RS232 or RS485 serial connections operating under SMA's proprietary SunnyNet or SMANet protocols. Further details of the algorithms used to control the Sunny Island 4500 in the Experimental SSEZ can be found in Appendix D.

### 4.7.2 Battery Bank

The battery bank consists of four carbon-fibre lead-acid Elecsol 110 batteries [136] These batteries are rated at 110Ah. The nominal voltage for these batteries is 12V which results in an energy capacity of 5.28kWh. These batteries are reported to have three times the life of conventional lead-acid batteries and can be discharged to 80% depth of discharge (%DoD) over one thousand times. These batteries are commercially available and are the recommended lead-acid battery for installation with the Sunny Island 4500™ in the UK. The energy storage system at Durham University is shown in Figure 4.12.


**Figure 4.12: Energy storage unit installation at Durham University**

## 4.8 LabVIEW™

LabVIEW™ (Laboratory Virtual Instrumentation Engineering Workbench) [137] is a development environment for a visual programming language known as G from National Instruments™ [138]. G is dataflow language and is inherently capable of parallel execution. LabVIEW™ is an industry standard platform for data acquisition, instrument control and industrial automation on a variety of platforms.

## 4.9 Experimental SSEZ Data Acquisition System

A data acquisition and control system is required for the Experimental SSEZ to measure the impact of SSEG, ESUs etc. on the LV network, to determine whether defined operational limits are violated and to provide feedback to control systems.

It is not possible or even desirable to monitor every single electrical parameter within an LV network. It was decided to monitor the three-phase current and voltage at about six points around the LV distribution circuit (five are installed at present). This corresponds to the six nodes shown in Figure 4.3. This methodology ensures that all the power flows from each of the various SSEZ components on the system are monitored as illustrated in Figure 4.13.

Monitoring at more points than this around the LV network may have limited benefit. This is because the most difficult things to measure in the system e.g. voltages and current flow to/from SSEGs, ESUs etc. are adequately monitored and the voltages and currents at other locations on the LV network can be predicted using the theory described in section 2.3.2.

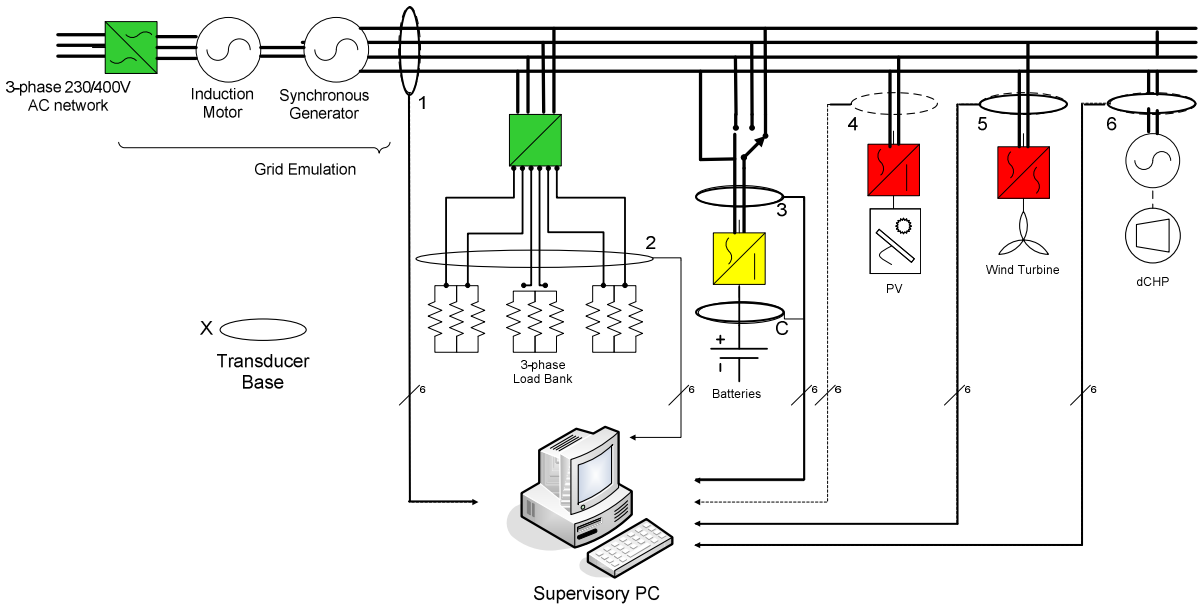


**Figure 4.13: Data Acquisition System haveing measurement nodes 1, 2, 3, 4, 5 and 6**

As in the case of the data acquisition systems at the EnergyLINK laboratory and at the University of Manchester Microgrid, a set of interface boards using transducers providing galvanic isolation were used. 1kV of electrical isolation is provided by the transducers. Each transducer system sends analogue voltage signals, which represent the instantaneous voltage and current, to a National Instruments™ interface board via shielded cables. This board is connected to the National Instruments™ data acquisition boards in the supervisory PC. In the supervisory PC the instantaneous current and voltage measurements are processed so that RMS and phase measurements of voltage and current, real and reactive power and sequence component measurements are available for system monitoring and for control system feedback with a sample rate of 1000 Samples/s per channel. This process is illustrated by the flow chart in Figure 4.14.

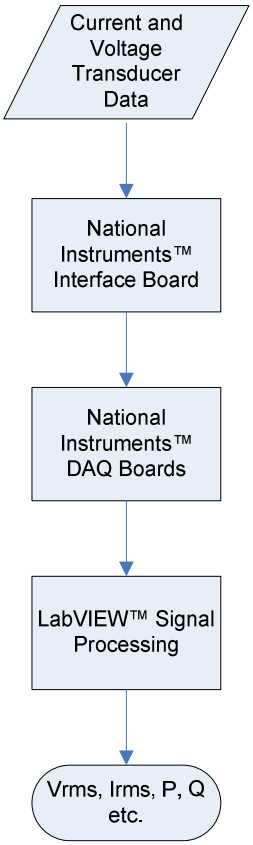


**Figure 4.14: Data acquisition system flow chart**

Elementaries of the transducer bases featuring current and voltage transducers are shown in Appendix E [139]. The outputs of the transducers are +/-10V where +/-10V would represent the rated voltage/current of a transducer base channel.

## 4.10 Experimental SSEZ Active Network Control Infrastructure

Centralised and distributed active network controllers have been implemented in the Experimental SSEZ using the graphical programming language in LabVIEW™. This flexibility is essential so that a performance evaluation of a variety of competing LV active network control systems and algorithms can take place. The Experimental SSEZ can be used to evaluate the active network control systems by emulating a variety of different distribution network operating points and/or systems and implementing control algorithms in LabVIEW™.

A sample control panel for one of the final LabVIEW™ system is shown in Figure 4.15 illustrating where system control, data acquisition and emulation functions are to be found on the panel.

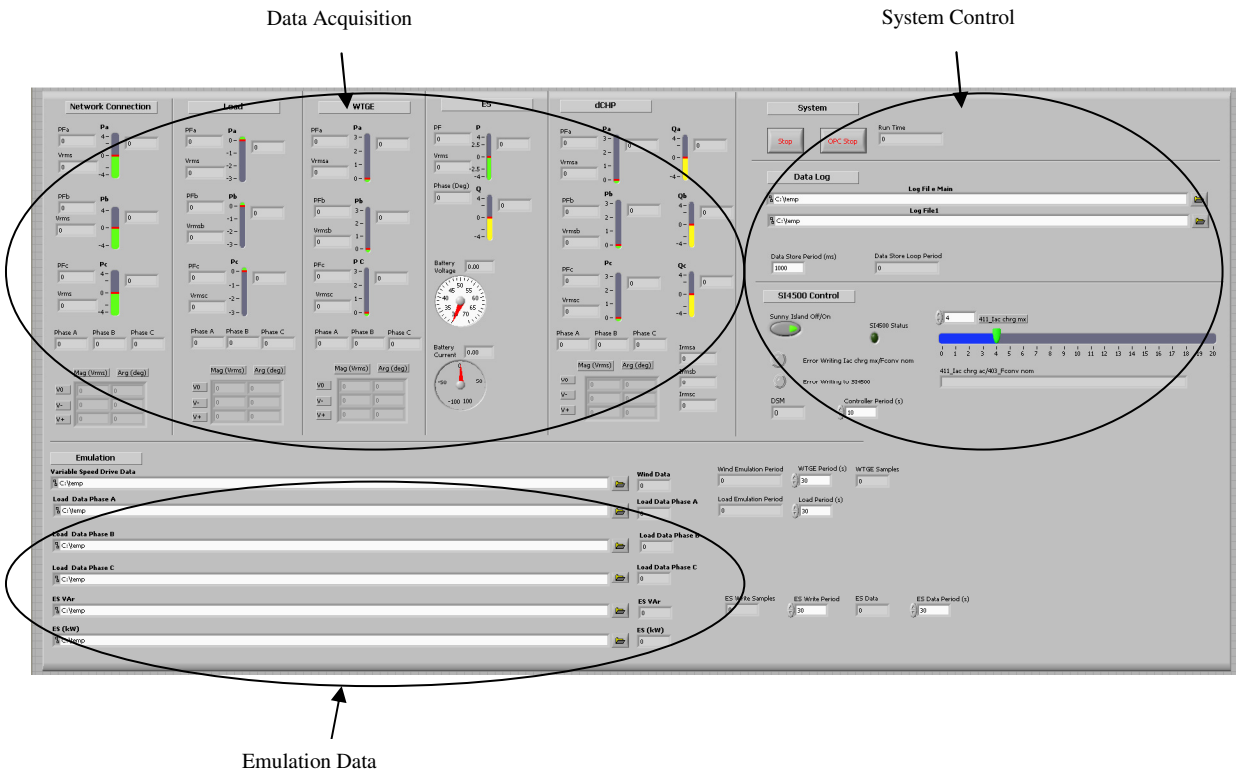


**Figure 4.15: LabVIEW™ Control Panel**

To enable the LabVIEW™ control algorithms and techniques an RS485 communications system has been installed in the Experimental SSEZ which links the supervisory PC, the Windy Boy™, the Sunny Boy™ and the Sunny Island 4500™. PLC (Power Line Carrier) communications are available as options on the Sunny Boy™ and Windy Boy™ but not on the Sunny Island 4500™. Moreover, consistent PLC communication can prove to be quite difficult in electrically noisy environments. RS232 is also an option but this would have necessitated a dedicated serial port for each device. RS485 permits a “daisy chain” structure as shown Figure 4.16. This RS485 system was successfully tested using SMA’s Sunny Data™ plant monitoring and control software.

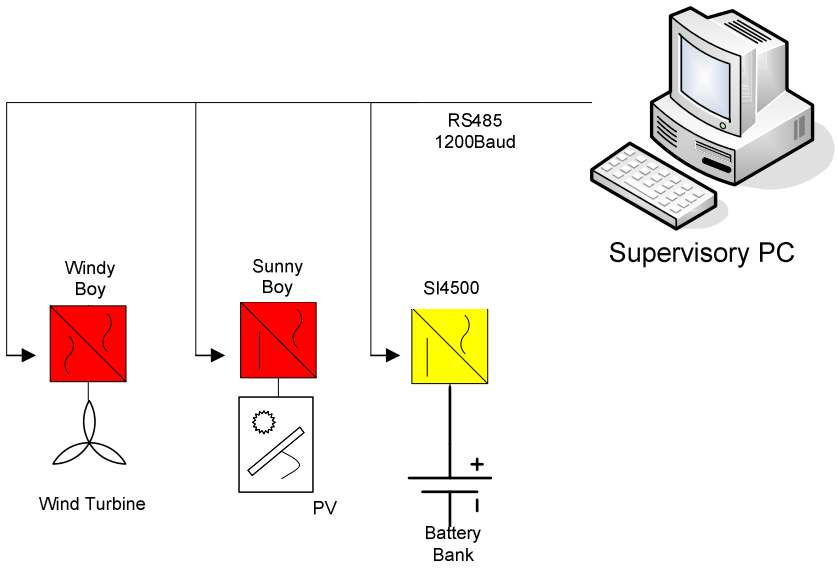


**Figure 4.16: RS485 Communication Network**

Communications between SMA inverters and LabVIEW™ have been reported previously [120]. Communication between the control algorithm, running in LabVIEW™ and the inverters is achieved using OPC [OLE for Process Control where OLE stands for Object Linking and Embedding] servers/clients, utilising the DataSocket™ I/O interface technology in LabVIEW™.

OLE is a distributed object system and protocol, developed by Microsoft®, and is typically used to link embedded objects in web documents to other programs or link embedded objects in Microsoft Office™ documents. OLE for Process Control (OPC) is the original name for an open standard specification developed in 1996 that enables communication of real-time plant data, between control devices from different manufacturers. In this instance the OPC system is used to link LabVIEW™ to the SMANet or SunnyNET proprietary SMA protocols running on the RS485 network. The operation of the communication system is illustrated in Figure 4.17.

The OPC server was supplied by SMA. The OPC server and the operation of the inverters were tested initially using Matrikon OPC Explorer™. This is also used for validating the operation of the visual programs developed in LabVIEW™.

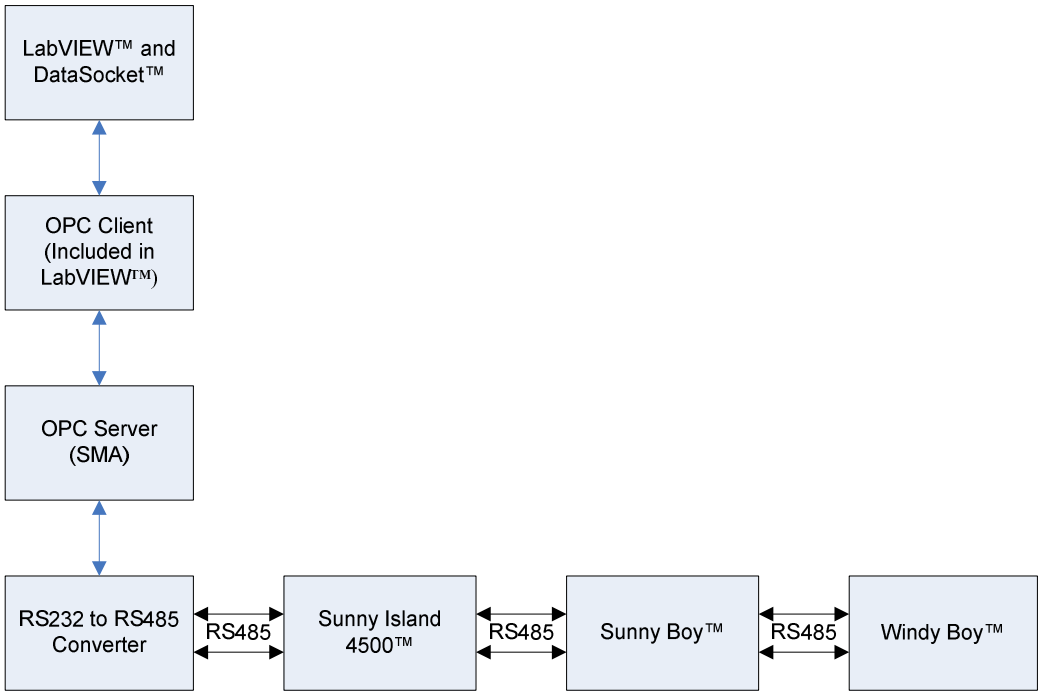


**Figure 4.17: Communication path between SMA inverters and LabVIEW™**

LabVIEW™ curtails the power output of the SSEG interface inverters (Sunny Boy™ and Windy Boy™) by writing to the *Pmax* parameters of each inverter using the OPC/RS485 communications bus. It is also possible to control both the real and reactive power import/export of the Sunny Island 4500™ as described earlier. This is achieved by varying the nominal frequency $f_0$ and the nominal voltage $V_0$ parameters using the OPC/RS485 communications bus.

The Sunny Island 4500™ is set to *Mains Droop* mode and in this mode a change in these nominal values results in a corresponding change in the real and reactive power output of the inverter as described earlier in this chapter. The power controller does not operate instantaneously. This is due to latency in the update of the parameter values of the Sunny Island 4500™ over the RS485 system. This has been documented previously [120]. This is illustrated by the response of the ESU *Pinv* to a changing (power command) *P** as shown in Figure 4.18.

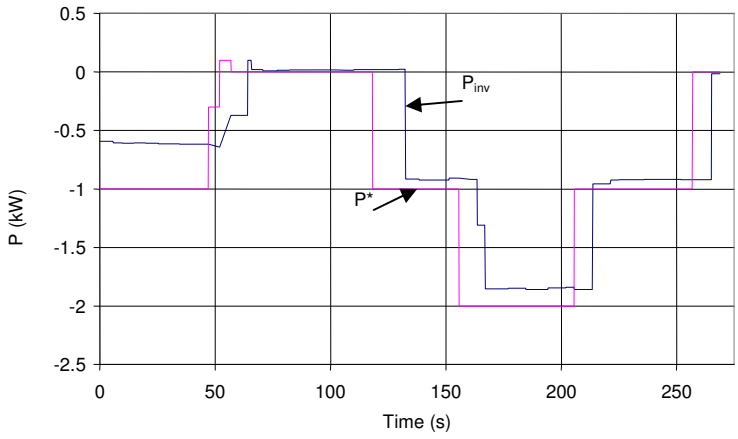


**Figure 4.18: Response of Energy Storage System *Pinv* to Step change in *P**

## 4.11 Discussion

The LV network of the Experimental SSEZ is made up of two systems: the network connection emulator and the LV network conductors. The network connection emulator provides power balance over the three-phases of the system and also provides frequency regulation. It is also possible to change both the frequency and the voltage of the of the LV network using the network connection emulator. However, the synchronous machine does not or is not capable of exhibiting the same characteristics as a distribution network transformer. However, it is proposed in Appendix H that this deficiency can be compensated for by using a transformation system.

The LV network of the Experimental SSEZ is three-phase and is of a radial, tapered design as per the experimental requirements detailed at the start of this chapter. The LV network is earthed in a TT configuration which is a common topology in the UK. The network is relatively small in comparison to an actual LV networks and to some of the larger laboratories such as DeMoTec and Labein's Experimental Centre. Moreover, there are fewer nodes for connection of SSEG and a limited flexibility in the configuration of the network. The LV network impedances of the system are given in Appendix F. A

summary of the functionality of the LV network of the Experimental SSEZ is given in tabular format in Table 4.2.

| **Variable Frequency** | **Transformer/ Transformer Emulation** | **Radial Topology** | **Three-phase System** | **Variable Impedance** | **Islanding Capability** |
|---|---|---|---|---|---|
| Yes | No, synchronous machine only | Yes, limited flexibility | Yes, single bus | Limited | No |

**Table 4.2: Experimental SSEZ LV network functionality**

Small-scale generation emulators have been installed, for the technologies which were identified as most likely for large-scale deployment in future LV networks, in the short or medium term, in the Experimental SSEZ. Emulation is used as it enables repeatable testing which is important for investigating the operation of control systems for active LV networks. All the generators are single-phase which would be the likely connection method in domestic premises. However, emulators of larger three-phase SSEGs that could be installed at small commercial premises are not part of the system. Moreover, as all the generation is single–phase, highly unbalanced conditions which are unlikely to be replicated on an LV distribution network, could result.

The dCHP emulator is based on the current commercialised technologies for dCHP which are based on external combustion Sterling or Rankine engines. It is not possible to curtail the power output of the dCHP emulator or commercial dCHP units as they are coupled to the LV network with an induction machine. It is possible, however, to switch it on and off using the supervisory computer. It is therefore considered non-dispatchable for the purposes of this investigation. Fuel cells have not been considered for installation in the system at this stage as these systems are not commercially available at present and are very costly.

The PV generator emulator and wind turbine generator emulator share much of the equipment and have similar installed capacities that would be used in a conventional

household installation. In addition, the same inverter interfaces, the Sunny Boy™ and Windy Boy™, are used at NTUA, DeMoTec and the EnergyLINK laboratory. These units are likely to be primary factor affecting the generators dynamic impact on the network. The power output of these inverters is curtailable using the active network control infrastructure. Both PV and wind are therefore considered to be dispatchable. A summary of the SSEG systems of the Experimental SSEZ is shown in tabular format in Table 4.3.

| dCHP | PV | Wind |
|---|---|---|
| Yes, single-phase emulation, dispatchable | Yes, single-phase emulation, dispatchable | Yes, single-phase emulation, non-dispatchable |

**Table 4.3: Summary of SSEG systems in the Experimental SSEZ**

The power factor of the load emulator is almost unity as the loads are resistive and do not feature an ability to introduce any inductive or harmonic components to the load. Moreover, the load is not continuously varying and instead increases in 250W steps. To introduce, inductive loads or loads with a high harmonic content it is possible to add actual demand devices to provide this. The load emulator however is controlled by the emulation system and is therefore useful in creating repeatable dynamic scenarios for the testing of active network control techniques.

| | Emulation | Actual Load |
|---|---|---|
| Computer control | Yes, controlled by LabVIEW™ | No, manually connected |
| Range | 0 to 2.75kW, 0.25 kW steps per phase | 0 to 3kW, per phase |
| Non-unity power factor | No, resistive only | Yes, by connecting inductive load |
| Distributed over LV network | No, load at one node only | Yes, can be connected to nodes 4, 5 and 6 |

**Table 4.4: Load systems functionality of the Experimental SSEZ**

Similarly to the SSEG emulators, an industry standard grid inverter is used to couple energy storage to the LV network. These inverters are also used at NTUA and DeMoTec

to investigate and develop active network control systems. The only energy storage available at the Experimental SSEZ is an advanced lead-acid battery bank which is among the required energy storage systems identified earlier.

The data acquisition system, as per the requirements in chapter four, is capable of reliably measuring and calculating the power quality quantities under investigation: voltage rise/regulation, thermal limits and voltage unbalance. The present system however does not measure harmonics but this is a possible extension of the system. Moreover, the system also provides galvanic isolation to provide safety to both the National Instruments™ DAQ systems and the operator.

| | |
|---|---|
| **Distributed measurements** | Yes, nodes 1, 2, 3 ,5 and 6 |
| **Three-phase voltage, current, P, Q measurements** | Yes |
| **Voltage and current phase measurements** | Yes |
| **Sequence components** | Yes |
| **Harmonics** | No |

**Table 4.5: Functionality of data acquisition system**

The active network control infrastructure is similar to the system installed at NTUA but based on LabVIEW™ rather that WinCC. The inherently parallel nature of LabVIEW™ or G code enables the emulation of both distributed and centralised control systems. The control structure is based on proprietary protocols which are not likely to compatible with other systems unlike the IEC61850 protocol and its extensions.

# 5 INVESTIGATION INTO THE PASSIVE OPERATION OF THE EXPERIMENTAL SSEZ

## 5.1 Introduction

As stated previously the technical problems that are focussed on in this work are: steady-state voltage rise and regulation thermal limits and steady-state voltage unbalance. This passive investigation will enable characterisation of the operation of the Experimental SSEZ under a variety of generation and load conditions. Moreover, the results of these studies will enable identification of the advantages and disadvantages of the LV network emulator which will aid development of the transformation described in Appendix H. They will also assist in understanding the impact of SSEGs on future LV networks. Finally, these studies will enable evaluation of the centralised and distributed control strategies developed on the Experimental SSEZ in chapter six and chapter seven as the operation of the Experimental SSEZ LV network is clearly understood with respect to the operation of generic and actual LV networks.

## 5.2 Input Data and System Configuration

To investigate the impact of SSEG on the LV network of the Experimental SSEZ on these constraints without any active network control systems, a systematic testing program was developed. While each test was designed individually, all the tests featured a common load profile and where applicable, small-scale wind turbine generation profile. The daily demand profile used in these studies is shown in Figure 5.1 and is based on a household load with no electric heating monitored on a Sunday in the UK [140]. The maximum demand of the load emulator of the Experimental SSEZ is 2.2kW at 225V, therefore the data which is based on [141] is scaled to preserve the load profile shape. In addition, in

order to emulate non-unity power factor loads the Sunny Island 4500™ is used to absorb reactive power. Single-phase non-unity power factor loads of power factors of 0.85, 0.9 and 0.95 can therefore be emulated. These figures for power factor are based on the data regarding LV load presented in chapter two.

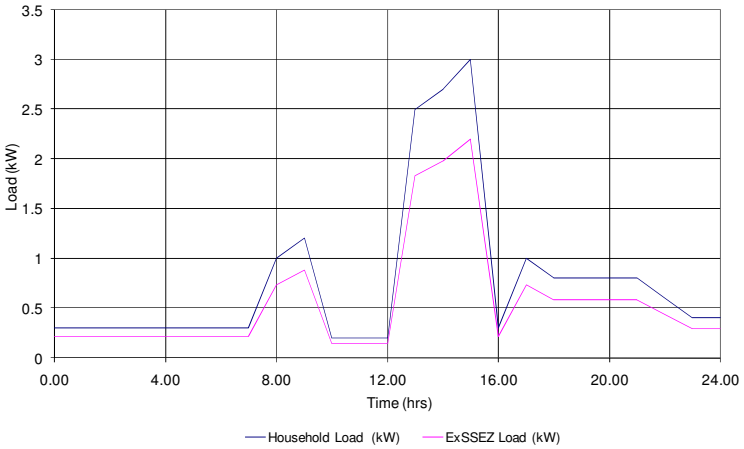


**Figure 5.1: Load profile**

Actual wind speed, turbine speed and power data over a twenty hour period, taken from small-scale wind turbines installed at NaREC's EnergyLINK laboratory [7, 142] is used to emulate a small-scale wind turbine in the Experimental SSEZ. As in the case of demand emulation, the data is processed for implementation in the Experimental SSEZ. In this case, low wind speed data is filtered out to ensure that the speed of the turbine does not result in the disconnection of the Windy Boy™ during the tests.

Disconnection is due to the fall in voltage on the DC output of the rectifier of this system. This is due to lower output voltages from the permanent magnet synchronous machine, as the machine rotates at slower speeds during periods of low wind. Disconnection should be avoided because the tests are not being run in real-time but instead at 120 times real time. This implies that 30s of runtime in the Experimental SSEZ represents one hour in real-time. Following disconnection of the Windy Boy™ it may take up to 5 minutes to

reconnect to the LV network depending on the voltage on the DC bus. Therefore, the disconnection and reconnection of the Windy Boy™ may last for a disproportionate period of time during the tests. The low wind level is chosen so that the Windy Boy™ remains connected but exports a relatively small power output ($\simeq$ 70W) during these periods. The wind speed recorded and the resultant turbine speed data implemented in the testing program is illustrated in Figure 5.2 and Figure 5.3. In addition, to the wind speed data the output power of each wind turbine generator during the study period was available and this was used to perform a first stage validation of the wind turbine emulator.

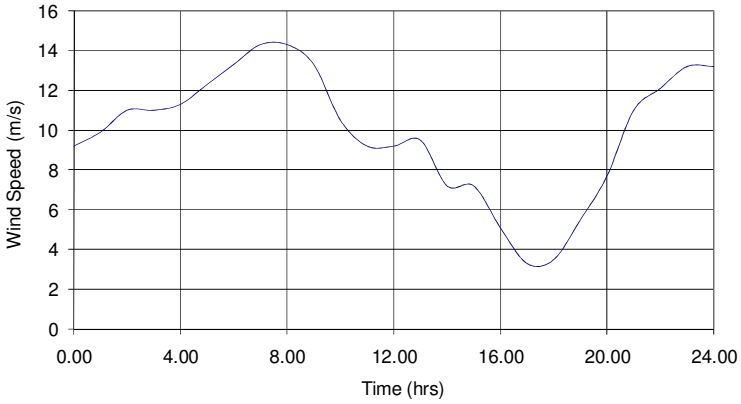


**Figure 5.2: Wind speed profile of Energy LINK Laboratory small-scale wind turbine**

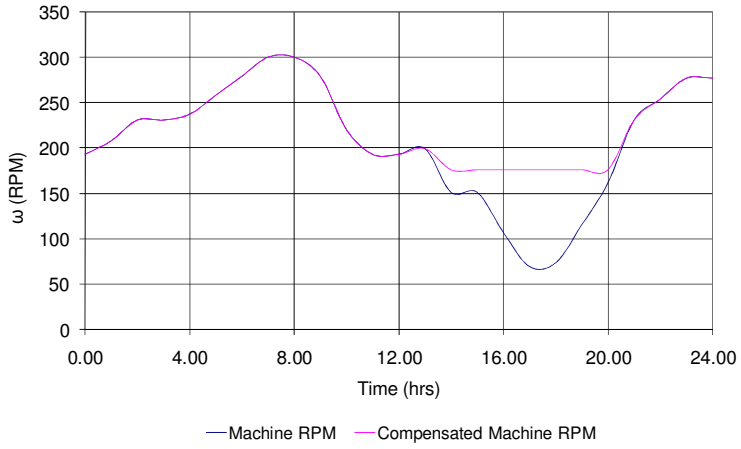


**Figure 5.3: Actual and processed (small-scale wind turbine) rotational speed**

The Experimental SSEZ was connected in two different configurations for this testing programme. The standard configuration is illustrated by means of single line diagram (SLD) in Figure 5.4 and is defined as configuration I. The Experimental SSEZ is also configured so that the load emulator is at the remote end of the network connected through an impedance of 180mΩ/phase to node 6 as illustrated by the SLD in Figure 5.5. This is known as configuration II and enables investigations into the impact of the distribution of load on the network constraints under examination.

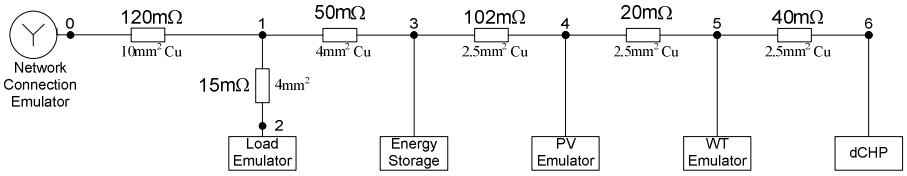


**Figure 5.4: Standard configuration of Experimental SSEZ (Configuration I)**

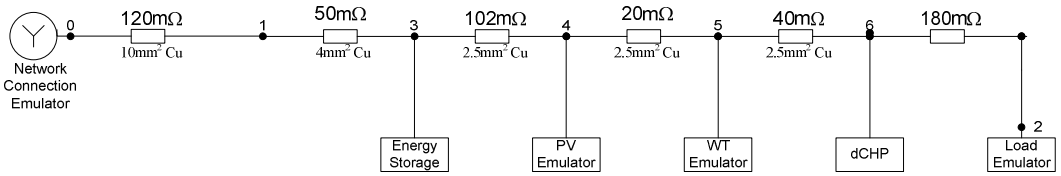


**Figure 5.5: Remote end load configuration of the Experimental SSEZ (Configuration II)**

## 5.3 Voltage Variation and Regulation

The steady-state equations in chapter two can be used to estimate the voltage change across line sections of radial network. As the LV network of the Experimental SSEZ is a real three-phase four-wire network the earlier analysis is a useful tool for understanding the operation of the Experimental SSEZ LV network. In this section, the effect of loading the LV network and also introducing single-phase generation is investigated with respect to its effect on voltage variation and regulation.

### 5.3.1 Load only

Balanced and unbalanced load scenarios are considered to investigate voltage drop on the Experimental SSEZ. In addition, the effect of the distribution of the load is also examined

by using both configurations of the Experimental SSEZ illustrated in Figure 5.4 and Figure 5.5.

### Scenario I - Balanced Load

The voltages across the system measured at node 1, node 2 and node 5 when a balanced load profile is emulated on the Experimental SSEZ are shown in Figure 5.6, Figure 5.7 and Figure 5.8. The voltages at node 1 rise as the load increases due to the operation of the AVR in the synchronous machine which compensates for the increased load and the resultant internal voltage drop within the synchronous machine. AVRs are installed for the same purpose in large-scale generators [143]. This is achieved by increasing the current in the field winding, thus ensuring that unity power factor operation of the synchronous machine is maintained. In the synchronous machine of the Experimental SSEZ the line-line voltage between phase A and phase B is measured and this parameter is used to control the field current of the machine. This characteristic is also somewhat similar to what happens on primary distribution network transformers under maximum load conditions when the OLTC will adjust to increase the voltage on the distribution network. In addition, it can be seen that the voltages on the three phases are different especially phase C which is 0.7V lower than phase A and phase B during low load conditions. This is due to asymmetries in the synchronous machine of the network connection emulator.

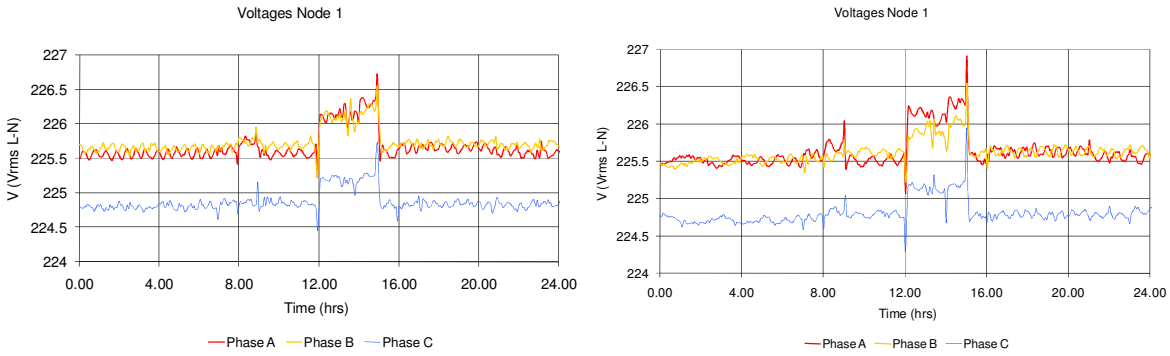


**Configuration I** **Configuration II**

**Figure 5.6: Voltages at node 1 during zero generation and balanced load tests**

The voltage drops observed in configuration II are much greater than those in configuration I of the Experimental SSEZ as illustrated by Figure 5.7. This is because of the larger impedance from the network connection emulator to the load in configuration II, as node 2 is now at the remote end of the network.

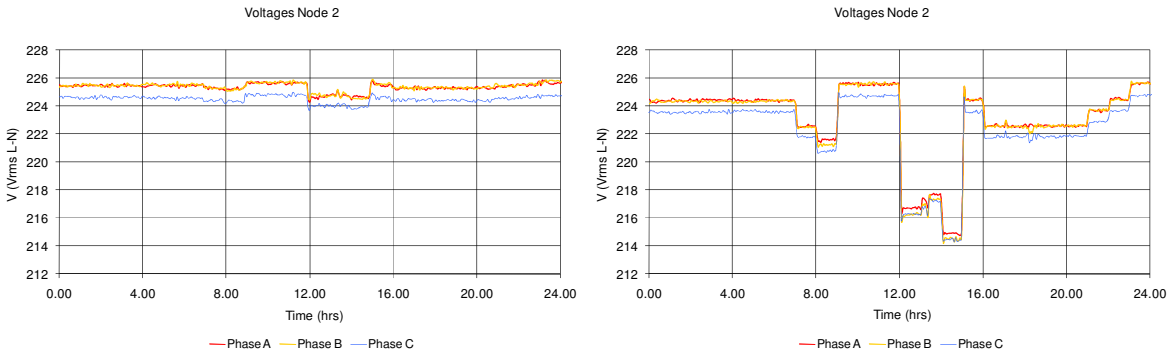


**Configuration I** **Configuration II**

**Figure 5.7: Voltages at node 2 during zero generation and balanced load tests**

The effect of the distribution of load on voltage drop is also illustrated in Figure 5.8. In addition, the system asymmetries are apparent in the traces for configuration II. It should be noted that this distribution of load is not particularly realistic as can be seen in the distribution of load in both the UK and European generic networks described in Appendix B. It can be seen that the voltage drop on phase B of the network is slightly greater than the voltage drop on phase A even though the load on both phases is equal. Measurements of the self impedances of the conductors of the Experimental SSEZ indicate that the

impedance of the phase B conductor of the Experimental SSEZ LV network is slightly larger than that of the phase A or phase C conductors.

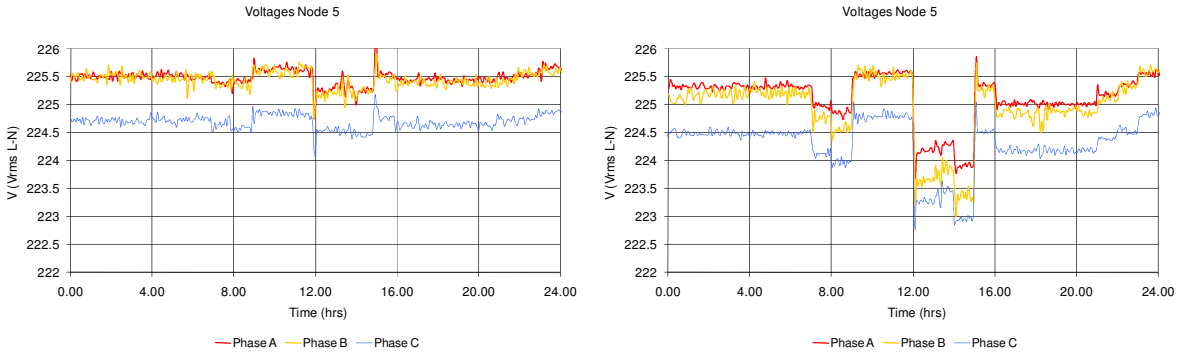


**Configuration I** **Configuration II**

**Figure 5.8: Voltages at node 5 during zero generation and balanced load test**

In the context of the Experimental SSEZ the term voltage regulation will refer to the voltage drop from the network connection emulator (node 1) which is analogous to the secondary distribution transformer and the remote end (node 5 – configuration I and node 2 configuration II). The impact of balanced load on the voltage regulation of the system is illustrated in Figure 5.9.

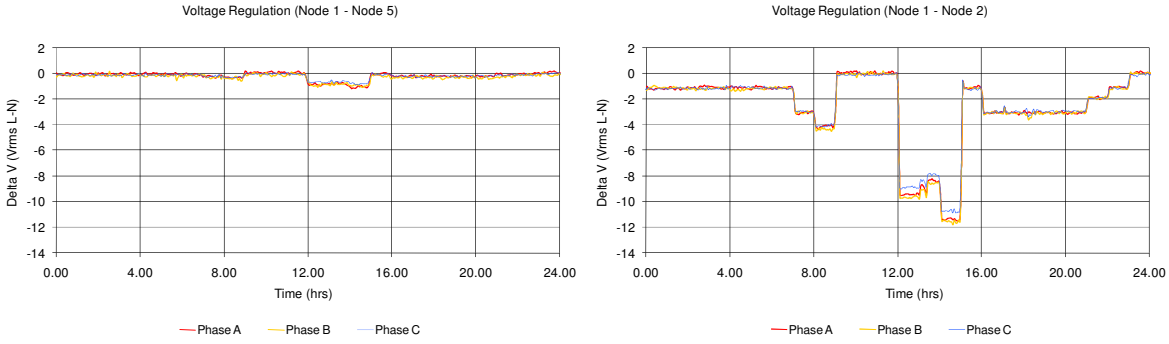


**Configuration I** **Configuration II**

**Figure 5.9: Voltage regulation during zero generation and balanced load test**

The voltage drop in configuration II is much greater than in configuration I as expected as the impedance between the network connection emulator and the remote end is greater in configuration II where node 2 is at the remote end of the LV network.

### Scenario II - Unbalanced Load (Phase A)

In this study, two unbalanced load scenarios using the two Experimental SSEZ configurations described earlier are implemented. The voltages at node 1, node 2 and node 5 are shown below in Figure 5.10, Figure 5.11 and Figure 5.12. Figure 5.10 illustrates the inconsistent voltage variations observed on the three-phases, at node 1. As in the case of the balanced load tests the AVR compensates for the increased load and consequent voltage drop within the synchronous machine as there is a decrease in the line-line voltage between phase A and phase B. However, the reaction of the AVR is not great enough because there is no corresponding voltage drop in phase B. The AVR is designed to be used under balanced conditions. Additionally, the behaviour of the network connection emulator is complicated by mutual impedances between the windings of the synchronous machine [144]. Voltages are induced in the phase B and phase C windings of the synchronous machine due to the current flow in phase A. This current flow results in changes in magnitude and phase of the phase-neutral voltages observed at the terminals of the machine. It can be seen that the voltage changes at node 1 in both configurations are almost identical as they are almost entirely a result of the currents flowing in the synchronous machine of the network connection emulator.

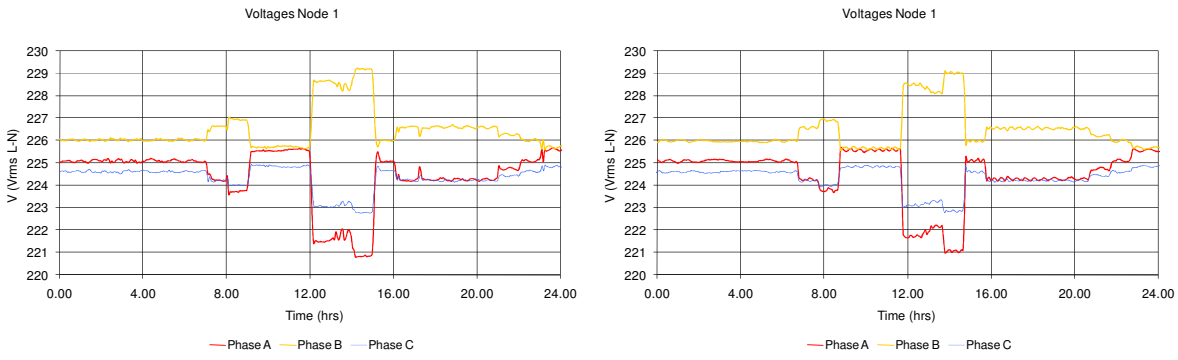


**Configuration I** **Configuration II**

**Figure 5.10: Voltages at node 1 during zero generation and unbalanced load (Phase A) tests**

The voltage drop observed at node 2 in both configurations on phase A is larger than in the balanced case as illustrated in Figure 5.11. This is due to the currents flowing through the neutral conductor which results in a neutral-ground voltage displacement. This voltage displacement results in a change in the phase–neutral voltages on all phases but the voltage change is most apparent on phase A as the neutral voltage displacement is approximately 180° out of phase with the voltage drop across the phase A conductor. As predicted by the unbalanced four-wire network analysis presented in chapter two (2.3) – (2.6) the voltage drop on phase A has a greater magnitude when the load is located at the remote end of the network.

$$\Delta\overline{V}_{AG} = \overline{Z}_{AA}\overline{I}_A + \overline{Z}_{AB}\overline{I}_B + \overline{Z}_{AC}\overline{I}_C + \overline{Z}_{AN}\overline{I}_N \quad (2.3)$$

$$\Delta\overline{V}_{BG} = \overline{Z}_{BA}\overline{I}_A + \overline{Z}_{BB}\overline{I}_B + \overline{Z}_{BC}\overline{I}_C + \overline{Z}_{BN}\overline{I}_N \quad (2.4)$$

$$\Delta\overline{V}_{CG} = \overline{Z}_{CA}\overline{I}_A + \overline{Z}_{CB}\overline{I}_B + \overline{Z}_{CC}\overline{I}_C + \overline{Z}_{CN}\overline{I}_N \quad (2.5)$$

$$\Delta\overline{V}_{NG} = \overline{Z}_{NA}\overline{I}_A + \overline{Z}_{NB}\overline{I}_B + \overline{Z}_{NC}\overline{I}_C + \overline{Z}_{NN}\overline{I}_N \quad (2.6)$$

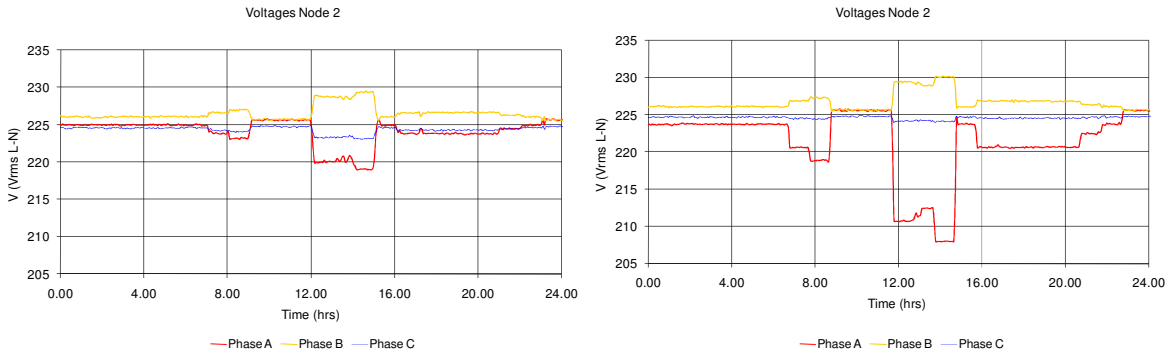


**Configuration I** **Configuration II**

**Figure 5.11: Voltages at node 2 during zero generation and unbalanced load (Phase A) tests**

Figure 5.12 illustrates the change in voltages at node 5 during the test. These results are consistent with the analysis based on the four-wire theory described earlier. The voltage drop observed at node 5 in configuration I is significantly less than that observed when the Experimental SSEZ is in configuration II.

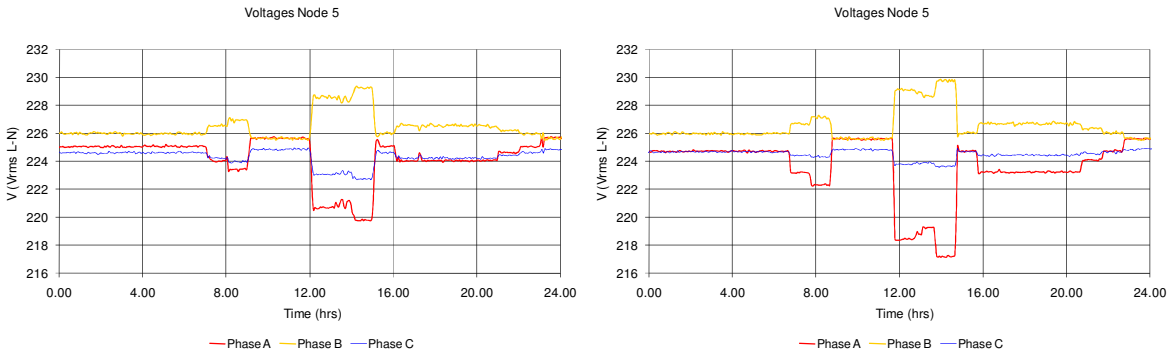


**Configuration I** **Configuration II**

**Figure 5.12: Voltages at node 5 during zero generation and unbalanced load (Phase A) tests**

The voltages measured on phase B and phase C in Figure 5.10, Figure 5.11 and Figure 5.12 during the test are relatively similar which is as expected as there is no load on these phases. However, small differences do exist and this is due to the effect of neutral voltage displacement which is due to the flow of return current along the neutral conductor. This effect is more noticeable in configuration II. The results for voltage regulation for this scenario are illustrated in Figure 5.13.

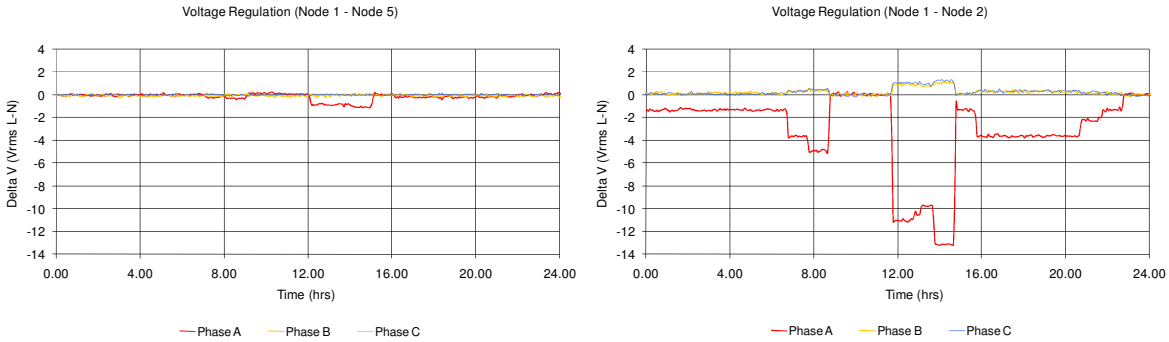


**Configuration I** **Configuration II**

**Figure 5.13: Voltage regulation during zero generation and unbalanced load (Phase A) tests**

It can be seen that the voltage drop observable on the loaded phase is much greater in configuration II rather than configuration I. However, the voltage drop in configuration II in this scenario, in comparison to scenario I, is not as great as expected. This is because of the drop in voltage at the network connection emulator terminals has reduced the voltage across the system. As the load is resistive the current imported by the load bank is lower

and therefore the voltage drop across the phase and neutral of the system is lower than expected.

### 5.3.2 Generation and Load

SSEG has the effect of supplying some of the local load and could at some periods supply all local demand resulting in the export of excess generation to the rest of the distribution network. This excess generation can result in voltage rise in LV networks. Balanced and unbalanced load profiles as per Figure 5.1 are used and unbalanced generation is considered only as the SSEG emulators are single-phase. Both configurations of the Experimental SSEZ are used to investigate the effect of the distribution of load. The daily generation profiles illustrated in Figure 5.2 and Figure 5.3 were used to emulate the generation from a small-scale wind turbine.

#### Scenario III - Balanced Loading and Unbalanced Generation (Phase A)

The phase-neutral voltage changes on each phase at node 1 are inconsistent, as in the scenario II (Unbalanced load) tests. As before, the AVR compensates for the load or generation and consequent voltage change within the synchronous machine. As previously, the behaviour is complicated by the mutual impedances between the windings of the machine [144]. As the magnitude of the current flows in the phases are unequal the resultant induced voltages due to the mutual inductances between the phases of the synchronous machine are not the same. Thus, as in the case of scenario II (Unbalanced load), the phase-neutral voltages observed at the terminals of the machine are affected. The same effects were observed in configuration I and configuration II and the voltage traces illustrating this are available in Appendix G.

The voltages measured at node 2 and node 5 when a balanced load profile and an unbalanced generation profile are emulated in the Experimental SSEZ are shown in

Figure 5.14 and Figure 5.15. As predicted by (2.3) – (2.6) the voltage drops in configuration II, in comparison to configuration I, of the Experimental SSEZ are much greater. However, when the small-scale wind turbine is exporting real power it can be seen that the phase-neutral voltage variations for each phase change, as seen in Figure 5.14. This is due to: -

1. The asymmetric current flows result in changes in the terminal voltages of the synchronous machine due to the mutual inductances between the phases of the synchronous machine.
2. The voltage rise/fall due to the flow of asymmetric current flow through the phase and neutral conductors as described in (2.3) – (2.6).

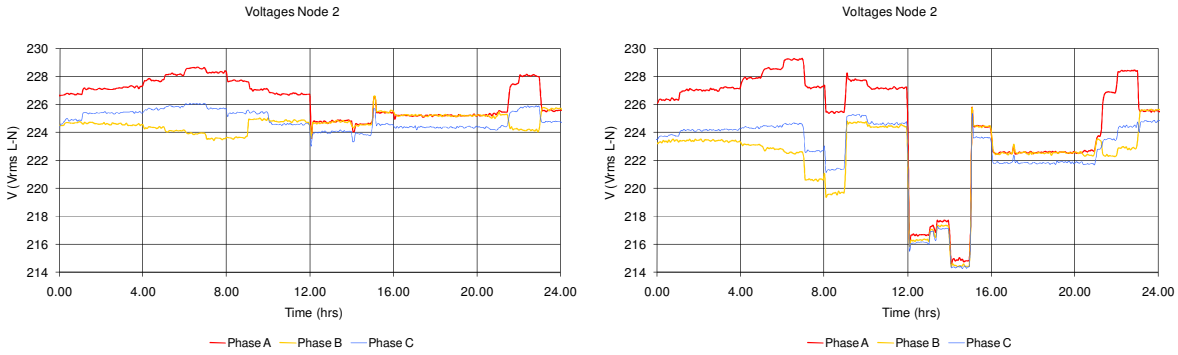


**Configuration I** **Configuration II**

**Figure 5.14: Voltages at node 2 during generation and balanced load tests**

At node 5 the voltage change due to an increase in generation from the wind turbine generator emulator is greater than at node 2 as the wind turbine generator emulator is connected at node 5. Moreover, the effect of load on the voltage at node 5 is less than at node 2 as the load is not as close electrically to node 5 in both configurations.

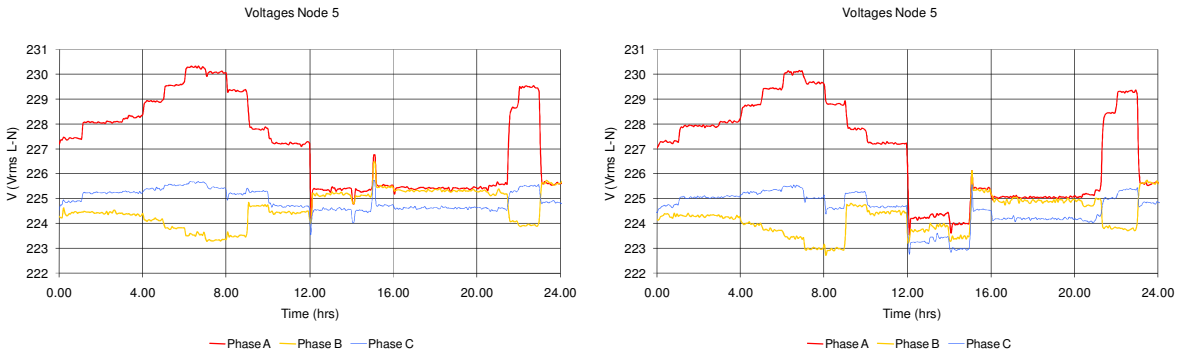


**Configuration I** **Configuration II**

**Figure 5.15: Voltages at node 5 during generation and balanced load tests**

The results for voltage regulation for this scenario are illustrated in Figure 5.16. It can be seen that the voltage drop observable on the loaded phase, during periods of low generation and high demand, is much greater in configuration II than configuration I as would be expected. The generation results in a voltage rise on phase A of the system and is the dominant effect in configuration I. However, in configuration II the effect of generation is less than the effect of load located at the remote end of the LV network.

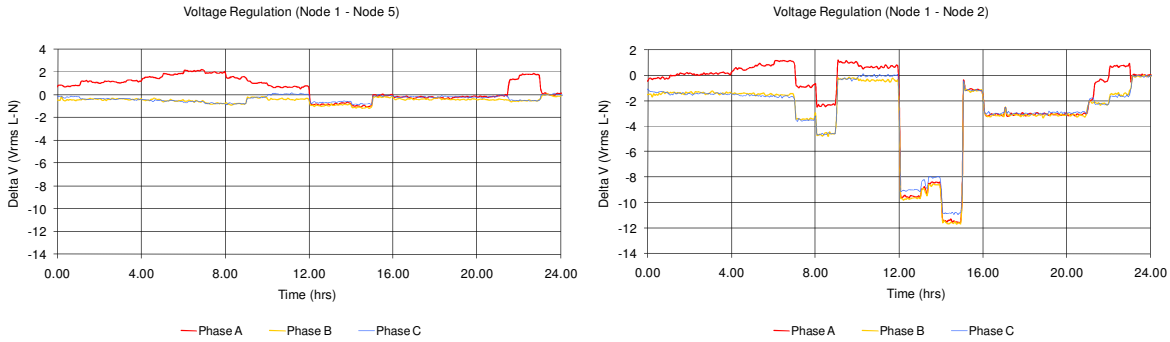


**Configuration I** **Configuration II**

**Figure 5.16: Voltage regulation during generation and balanced load tests**

## Scenario IV- Unbalanced Loading (Phase A) and Unbalanced Generation (Phase A)

As in the case of the earlier tests, it was observed that the AVR compensates for the effects of the changes in current flow on synchronous machine in order to try and

maintain unity power factor operation. As in scenario II (Unbalanced load) and scenario III (Balanced load - Generation) asymmetric current flows result in changes to the phase-neutral voltages at the terminals of the network connection emulator. The voltage traces for node 1 in both configurations are almost identical and are available in Appendix G.

The voltages measured at node 2 and node 5 of the LV network when an unbalanced load profile and an unbalanced generation profile are implemented on phase A of the Experimental SSEZ LV network, are shown in below in Figure 5.17 and Figure 5.18.

Unbalanced current flow through the neutral conductor again results in neutral-ground voltage displacements at all nodes in the LV network of the Experimental SSEZ. These voltage displacements result in changes to the phase–neutral voltages on all phases but the voltage change is most apparent on phase A as the neutral voltage displacement is approximately 180° out of phase with the voltage drop across phase A. The voltage variations observed are consistent with equations (2.3) - (2.6). In Figure 5.17, the voltage changes at node 2 for both Experimental SSEZ configurations are shown or this scenario. Voltage rise or drop is observed in both traces during the test depending on the flow of power through the LV network of the Experimental SSEZ on phase A. The changes in voltages on phase B and phase C are primarily due to the changes in voltages at the network connection emulator.

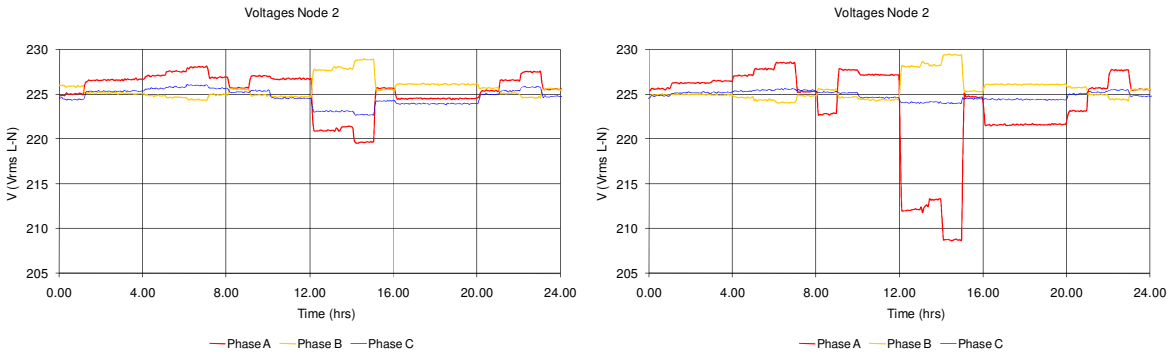


**Configuration I** **Configuration II**

**Figure 5.17: Voltages at node 2 during generation and unbalanced load (Phase A) tests**

At node 5 the voltage rise due to an increase in generation from the wind turbine generator emulator is greater than at node 2 as the wind turbine generator emulator is connected at node 5 as shown in Figure 5.18. Moreover, the effect of the load on node 5 is less than at node 2 as the load is not as close electrically to node 5 in both configurations as in scenario III (Balanced load - Generation). The voltage drop observed during this test at node 5 is much greater than in scenario III (Balanced load - Generation) as shown in Figure 5.15. This is due the current flow in the neutral conductor, during heavy load and low generation conditions, which results in a neutral voltage displacement that increases the magnitude of the phase-neutral voltage drop.

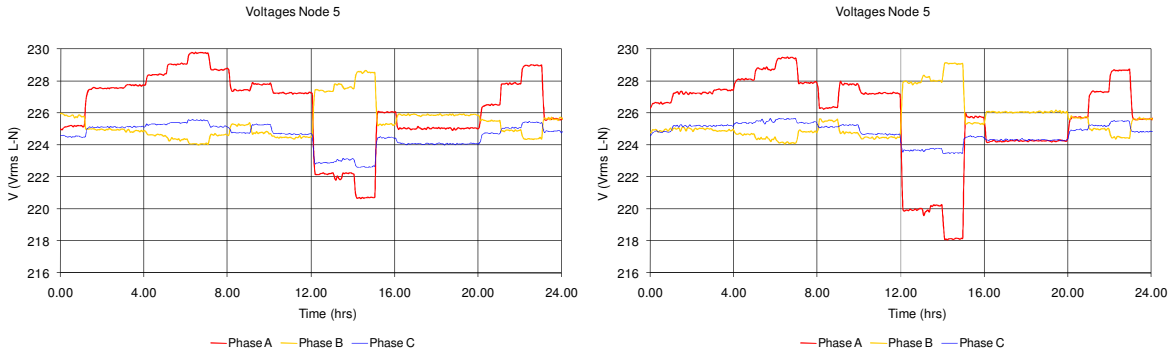


**Configuration I** **Configuration II**

**Figure 5.18: Voltages at node 5 during generation and unbalanced load (Phase A) tests**

The results for voltage regulation for this scenario are illustrated in Figure 5.19. It can be seen that the voltage drop observable on the loaded phase at maximum load is again much greater in configuration II rather than configuration I. The generation results in a voltage rise on phase A of the system and is the dominant effect in configuration I. However, in configuration II the effect of generation is less than the effect of load located at the remote end of the LV network. The voltage drop at maximum load is also greater than that measured in scenario III (Balanced load – Generation) due to current flow in the neutral conductor.

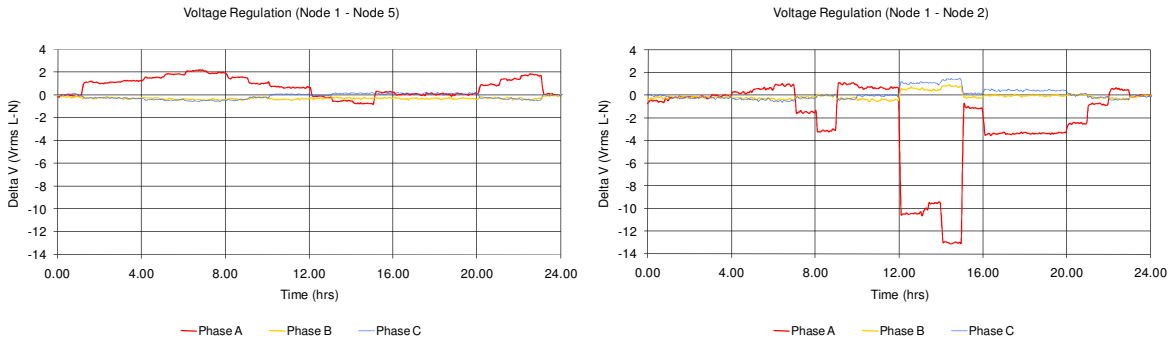


**Configuration I** **Configuration II**

**Figure 5.19: Voltages regulation during generation and unbalanced load (Phase A) tests**

### 5.3.3 Power factor

The effect of power factor on the voltage variation seen on the LV network of the Experimental SSEZ was investigated. The Sunny Island 4500™ is configured to supply reactive power and the resistive load bank is used to import real power into the Experimental SSEZ LV network.

The load profile illustrated in Figure 5.1 is used to emulate the real power demand of a household. The power factor of a household or an industrial consumer can vary from 0.85 lagging to unity depending on the application and the usage [65-66] as established in chapter two. The reactive power profiles therefore were generated by considering the load or active power profile and using this to generate reactive power profiles which would result in loads with power factors of 0.85 lagging, 0.90 lagging and 0.95 lagging.

The Sunny Island 4500™ was used to regulate the reactive power flow from the network connection emulator into the LV distribution work as described in chapter four [62].

#### Scenario V - Non-Unity Power Factor Load

Previous studies have shown that if reactive power is consumed by an LV network it has the effect of depressing the voltage on the network if the loads considered to be constant current sources [7]. As the X/R ratio of the LV network of the Experimental SSEZ is

much lower that that of an LV distribution network the reduction in voltage due to the flow of reactive power within LV network is likely to be comparatively smaller. This is illustrated in Figure 5.20. The voltages at node 3 and at node 5 are almost identical as expected as no current flows between node 3 and node 5 in this scenario. The voltage traces for node 3 are available in Appendix G. The voltages at node 1 are higher than those measured at node 3 and at node 5 as expected by [7]. The traces of the voltage at all nodes are lower at higher power factors which is also predicted by simulations of LV networks [7]. However, the effect of power factor on voltage variation has a smaller effect on the LV network of Experimental SSEZ.

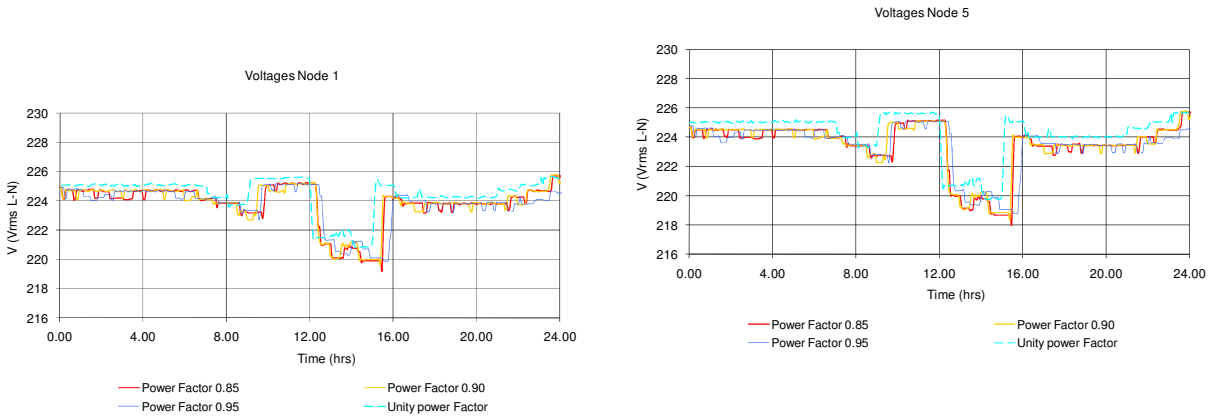


**Figure 5.20: Voltages at node 1 and node 5 during zero generation and non-unity unbalanced load (Phase A)**

The results for voltage regulation for this scenario are illustrated in Figure 5.21. It can be seen that the difference in magnitude between the traces is relatively small with the unity power factor trace having the highest voltages. It can be seen therefore that the flow of reactive power has limited effect on voltage regulation in the LV network of the Experimental SSEZ without small-scale generation on the system.

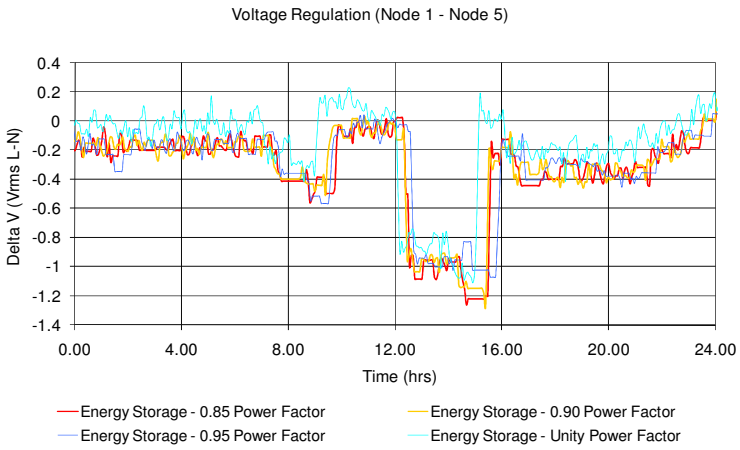


**Figure 5.21: Voltages regulation during zero generation and non-unity unbalanced load (Phase A)**

## Scenario VI - Non-Unity Power Factor Loads and Unity Power Factor Generation

The G83 standard for connection of SSEG to LV networks requires that all SSEGs generate at a power factor between 0.95 leading and 0.95 lagging. To investigate the effect of a single-phase connected SSEG on the voltages within the Experimental SSEZ under conditions when the power factor of the load is not unity, a generator profile as per Figure 5.2 was emulated. As in scenario V, the high power factor load profile, which requires the most reactive power from the network connection emulator, has the lowest voltage with the loads at unity power factor having the higher voltages. This is as expected as the wind turbine generator emulator has been found to export power at approximately unity power factor. The voltages at node 5 during periods of high generation are the highest of the three nodes as expected. As in the case of scenario V (Non-Unity Power Factor Load ) the voltages at node 3 and node 5 are almost identical during periods of minimal generation and maximum load. The export or import of reactive power by the small-scale generator has very little effect on the voltages of the LV network. This is because the flow of reactive power is much greater from the Sunny Island 4500™ than that exported or imported by the Windy Boy™.

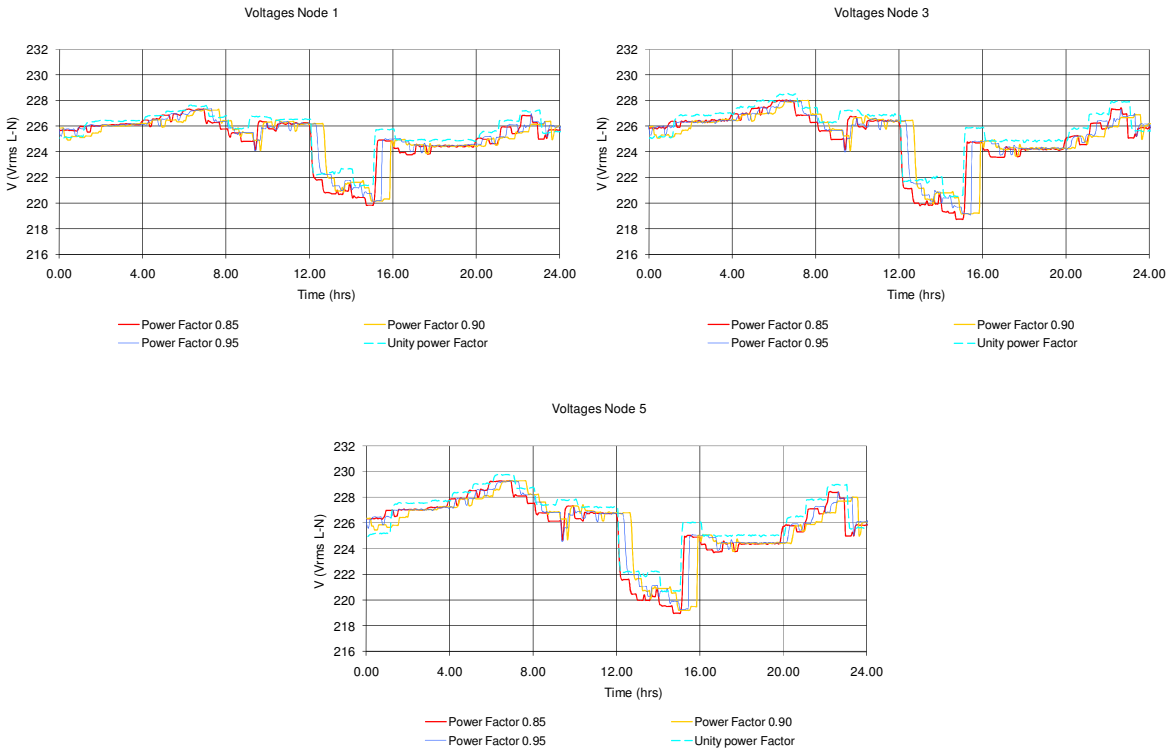


**Figure 5.22: Voltages at node 1, node 2 and node 5 during small-scale wind turbine generation and non-unity unbalanced load (Phase A)**

The results for voltage regulation for this scenario are illustrated in Figure 5.23. It can be seen that the difference in magnitude between the traces is relatively small with the unity power factor trace having the highest voltages. It can be seen therefore that the import or export of reactive power from G83 compliant inverters has limited effect on the voltage regulation in the LV network of the Experimental SSEZ.

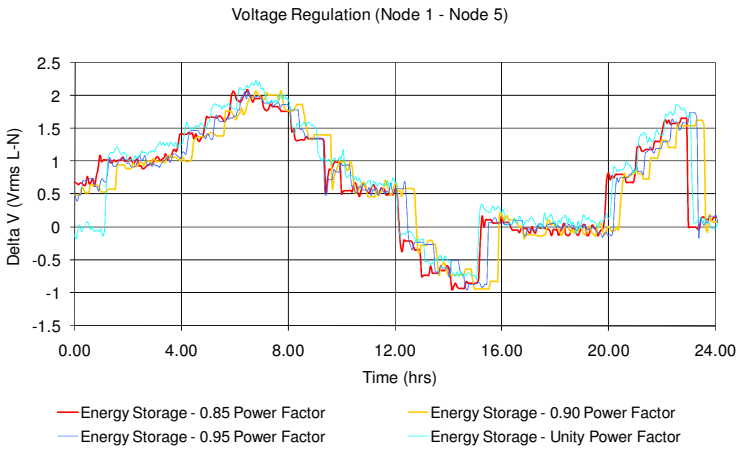


**Figure 5.23: Voltage regulation during small-scale wind turbine generation and non-unity unbalanced load (Phase A)**

## 5.4 Voltage Unbalance

### 5.4.1 Introduction

Asymmetrical impedances, the connection of SSEGs in single-phase and uneven distribution of load have been postulated in chapter two as the primary causes of voltage unbalance in future LV networks. Measurements of the self impedances of the phase conductors of the LV network of the Experimental SSEZ indicate that the LV network impedances are asymmetrical as detailed in Appendix F. Moreover, the voltages at the terminals of the network connection emulator have been determined to be asymmetrical even under zero loading and generation conditions. As it is possible to determine both the magnitude and phase of voltages on the LV network of the Experimental SSEZ, it is possible to determine the voltage sequence components by processing the instantaneous data from voltage and current transducers in LabVIEW™ in real-time. These sequence components are then used to determine the %VUF at each node as detailed in (2.10) and (2.11).

$$\%\ VUF = \frac{V_-}{V_+} \times 100 \qquad (2.10)$$

$$\begin{bmatrix} V_a \\ V_b \\ V_c \end{bmatrix} = \frac{1}{3}\begin{bmatrix} 1 & 1 & 1 \\ 1 & 1\angle 120° & 1\angle -120° \\ 1 & 1\angle -120° & 1\angle 120° \end{bmatrix}\begin{bmatrix} V_0 \\ V_+ \\ V_- \end{bmatrix} \tag{2.11}$$

A testing program was developed for voltage unbalance which is used to investigate the effect of load and SSEG on voltage balance in the Experimental SSEZ LV network.

### 5.4.2 Load only

#### Scenario I - Balanced Load

The %VUFs at the nodes of the network under balanced load conditions, emulating the same load profile as in earlier tests, are shown in Figure 5.24. The %VUF increases slightly as the balanced load of the system is increased. This effect is apparent in configuration II. The %VUF is greater at node 1 than at node 5 and node 2. This is due to the proximity of node 1 to the source of unbalance which is the network connection emulator.

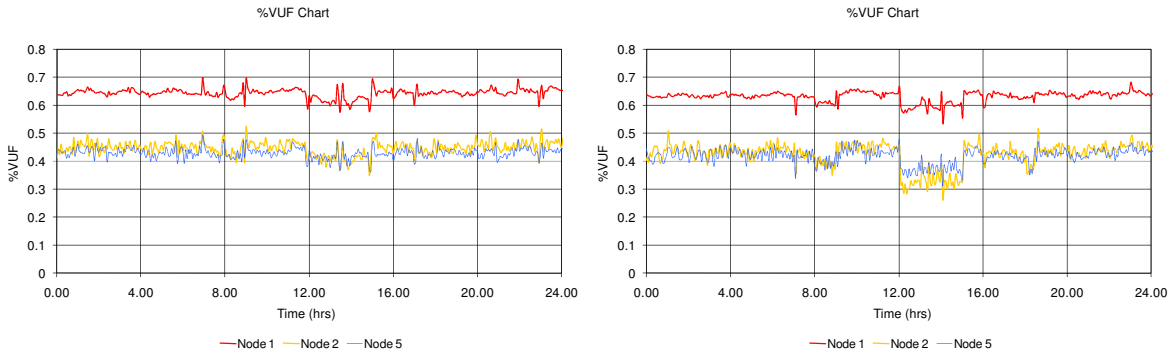


**Configuration I** **Configuration II**

**Figure 5.24: Percentage Voltage Unbalance Factors (%VUFs) under balanced load and zero generation.**

#### Scenario II - Unbalanced Loading

In section 5.3.1 the impact of single-phase load on voltage variation and regulation of the Experimental SSEZ was examined. These changes in voltages have a large impact on the

%VUF measured at each of the nodes. The impact of load on phase A of the LV network on the %VUF of the system is illustrated in Figure 5.25. It can be seen that the increase in load correlates very closely with the changes in %VUF in this scenario. In configuration I the difference in %VUF at the different nodes is small as the impedances between nodes 1 and node 2 are relatively low and as there is no current flow to node 5. In configuration II the %VUF is much greater at node 2 due to the relatively large impedances from the load emulator to the network connection emulator

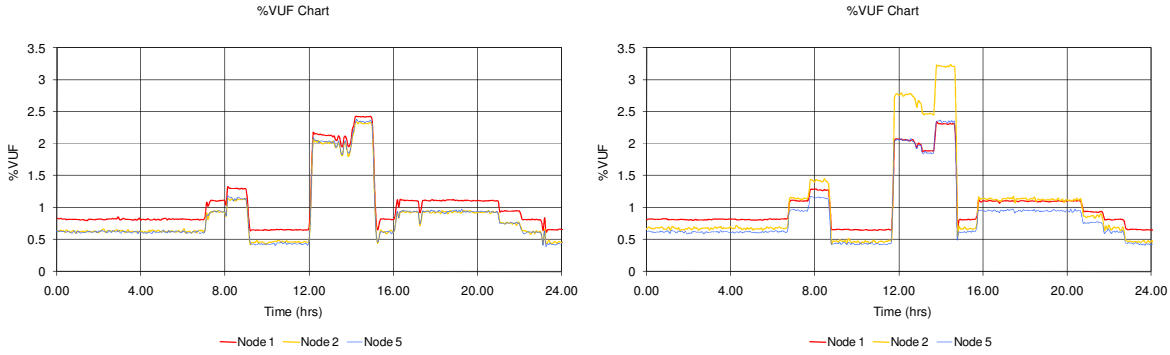


**Configuration I** **Configuration II**

**Figure 5.25: Percentage Voltage Unbalance Factors (%VUF) under unbalanced loading conditions**

### 5.4.3 Impact of Generation and Load

#### Scenario III - Balanced Load and Unbalanced Generation (Phase A)

The addition of SSEG can reduce or increase the %VUF exhibited by LV networks depending on the loading conditions of the distribution network [8]. To investigate the impact of SSEG on the Experimental SSEZ a balanced load as per Figure 5.1 and the wind generation profile as per Figure 5.2 and Figure 5.3 were emulated. The resultant %VUFs measured at node 1, node 2 and node 5 are illustrated in Figure 5.26.

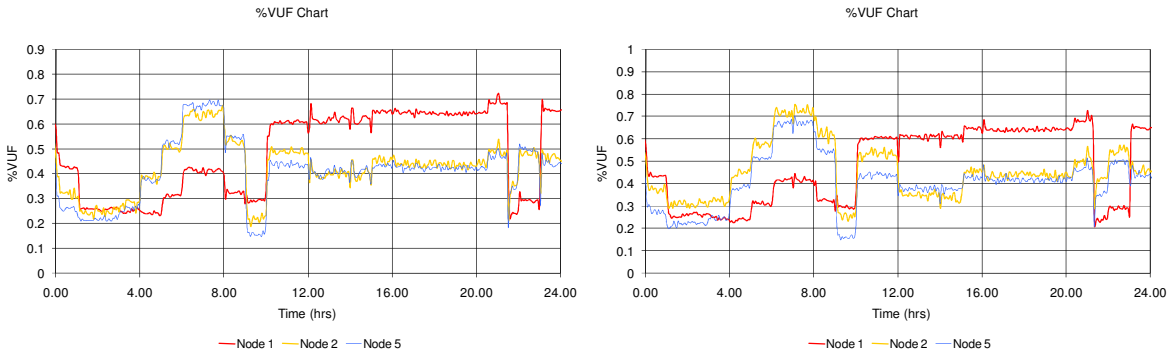


**Configuration I** **Configuration II**

**Figure 5.26: Percentage Voltage Unbalance Factors (%VUF) under balanced loading and unbalanced generation conditions (Phase A)**

The operation of the Experimental SSEZ in Figure 5.26 is not consistent with previous research in voltage unbalance in LV distribution networks because of the functionality of the network emulator in the Experimental SSEZ [8]. These studies have demonstrated that if balanced load is connected to a symmetrical distribution network an increase in the SSEG on one phase of the network resulting in asymmetrical sequence current flows will result in an increase in the %VUF. In actual LV distribution networks this is also likely to be the case as a transformer is used to used to connect to the grid unlike the Experimental SSEZ which utilises a synchronous machine. The converse was found to be true during these tests on the Experimental SSEZ. An increase in generation in this case can actually result in a decrease in %VUF. This is due to a combination of the unbalanced voltages at the terminals of the synchronous machine, the effect of voltages induced within the machine during unbalanced conditions and the effect of voltage drops or rises through the neutral and phase conductors of the LV network of the Experimental SSEZ.

At node 1, as the magnitude of the negative sequence current increases the magnitudes of the induced voltages in the synchronous machine also increases. These induced voltages result in changes in the magnitudes and the phase of the phase-neutral voltages at the terminals of the network connection emulator. This effect can be mitigated, from a

percentage voltage unbalance factor point of view, however by the phase changes on the phase-neutral voltages of the network connection emulator which in this case results in the three-phases getting closer to a balanced 120° set. Therefore, there is a net decrease in the negative sequence component of voltage ($V_-$) at this node resulting in a consequent drop in the %VUF. Further studies have shown that this effect is different on each phase of Experimental SSEZ as the resultant voltage change due to unbalanced generation results in the phase angles of the voltages moving closer to or further away from 120° between each phase. This has the effect of increasing voltage symmetry and decreasing the negative voltage sequence component ($V_-$).

At nodes 2 and 5 however, the voltage asymmetries in the LV network are dominated by the effect of the unbalanced currents flowing through the phase and neutral conductors resulting in changes to phase-neutral voltages. This is apparent in the %VUF trace for node 2 and node 5 where the %VUF, illustrated in Figure 5.26, while still influenced by the effects described above, can be seen to be closed related to the real power exported by the wind turbine generator emulator.

### Scenario IV - Unbalanced Load (Phase A) and Unbalanced Generation (Phase A)

The effect of generation on reducing %VUF of an unbalanced load is investigated in this scenario. It can be seen that during periods of high generation and low demand the %VUF drops due to the reasons outlined in the previous section. It can also be seen in periods of high demand that the %VUF increases. The voltage unbalance is greater when the LV network is in configuration II as voltage drops due to load are much greater in this configuration which has a direct impact on %VUF. This change in location has limited

effect on the voltage unbalance at nodes 1 and 5. The voltage traces illustrating these results are available in Appendix G.

#### Scenario V - Unbalanced Load (Phase B) and Unbalanced Generation (Phase A)

In this scenario, the single-phase wind turbine generator emulator exports power into phase A of the Experimental SSEZ LV network and load is connected to phase B.

The effect of increasing generation on voltage unbalance results in an increase in %VUF in comparison to scenario IV where generation and load are on the same phase of the Experimental SSEZ. This is due the effect of generation and load, on phases A and B respectively, on the magnitudes and phase angles of the voltages at the terminals of the network connection emulator as discussed in earlier in this section. Thus, the phase-neutral voltages along the radial LV network of the Experimental SSEZ are changed. In addition, the resultant neutral current flow in some areas of the network is greater than if generation and load were on the same phase resulting in a greater magnitude of neutral voltage displacement. The voltage traces illustrating these results are available in Appendix G.

### 5.4.4 Power factor

As in the case of the voltage variation and regulation study, the effect of power factor on voltage unbalance in the LV network of the Experimental SSEZ was investigated. The Sunny Island 4500™ is again controlled to supply reactive power and the resistive load bank is used to import real power into the Experimental SSEZ LV network.

## Scenario VI - Non-Unity Power Factor Unbalanced Load

In chapter four it was stated that the X/R ratio of the LV network of the Experimental SSEZ is much lower that that of an LV distribution network and thus the impact of reactive power the LV network is likely to be small. The effect of loading the LV network on phase A with varying power factors on %VUF at node 5 is illustrated in Figure 5.27. As the power factor increases the voltage unbalance at each of the nodes under investigation increases. The differences in the %VUF at nodes 1, 3 and 5 is low as the increases and decreases in the measured %VUF are due to the effect of the reactive power on the synchronous machine. The traces for node 1 and node 3 are available in Appendix G. The reactive power current, in vector addition to the active power producing current, induce changes in the voltages of the synchronous machine of the network connection emulator.

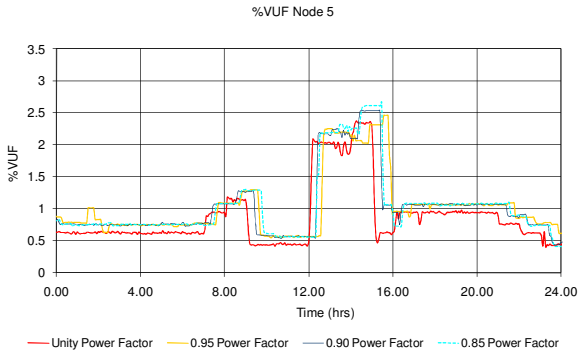


**Figure 5.27: Percentage Voltage Unbalance Factors (%VUF) at during zero generation and unbalanced load (Phase A) and varying power factor**

## Scenario VII - Non-Unity Power Factor Unbalanced Load (Phase A) and Unity Power Factor Generation (Phase A)

As in the case of the voltage variation and regulation investigation the impact of SSEG on the voltage unbalance of the LV network of the Experimental SSEZ with non-unity loads connected was investigated. In this scenario, the non-unity load and the wind turbine

generator emulator were both coupled to phase A to evaluate their combined impact on %VUF in the Experimental SSEZ. As in the load only test, scenario VI, lower power factors in these scenarios increase the voltage unbalance of the LV network. However, the effect of increased generation in as in scenario IV (Unbalanced Load (Phase A) and Unbalanced Generation (Phase A)) is to reduce %VUF. Voltage traces illustrating these results can be found in Appendix G.

### Scenario VIII - Non-Unity Power Factor Unbalanced Load (Phase B) and Unity Power Factor Generation (Phase A)

This scenario investigated the effect of load with low power factors on phase B of the system while the wind turbine generator emulator is connected to phase A on %VUFs. As in the unity power factor scenarios the generation had a large effect on the voltage unbalance within the system with the power factor of the load having a secondary effect. Similarly, to scenario V (Unbalanced Load (Phase B) and Unbalanced Generation (Phase A)) the effect of generation in this case is to increase %VUF in contrast to scenario VII (Non-Unity Power Factor Unbalanced Load (Phase A) and Unity Power Factor Generation (Phase A)) where load and generation are on the same phase. Voltage traces illustrating these results can be found in Appendix G.

## 5.5 Power Flow

It has been identified earlier that forward and reverse power flow limits of distribution network infrastructure could be a major problem in future distribution networks with high concentrations of SSEG. Power or MVA flow limits may be encountered on both the phase and neutral conductors of distribution networks. The following studies were carried out to investigate the effect of different scenarios of loading and generation on the effect of electrical power flow in both the forward and reverse directions through the network

connection emulator at node 1. In practice, current or MVA ratings are used as limits for infrastructure such as conductors or transformers. Results detailing current flows rather than power flows within the LV network of the Experimental SSEZ therefore will be presented in the following sections.

### 5.5.1 Generation and Load

#### Scenario I - Unbalanced Load (Phase A) and Unbalanced Generation (Phase A)

SSEGs can be used to supply local load and in cases where local generation is greater than demand the LV network under consideration may begin to export power to the rest of the LV distribution network. To investigate the impact of SSEG on the Experimental SSEZ a balanced load as per Figure 5.1 and the wind generation profile as per Figure 5.2 and Figure 5.3 were emulated.

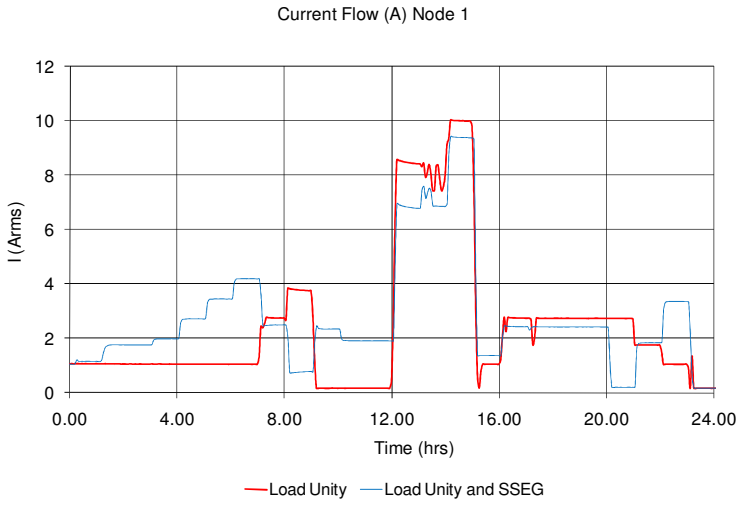


**Figure 5.28: Magnitude of current flows through node 1 with and without SSEG**

Node 1 is the node of interest as the connection to the network is likely to be the node where MVA or current limits are most likely to be exceeded [6]. It can be seen in this implementation that high levels of demand are the most likely cause of the system

violating the infrastructural thermal limits in the Experimental SSEZ. It can also be seen that both excess SSEG power export and load import both result in an increase in current.

### 5.5.2 Power Factor

#### Scenario II – Unbalanced Non-Unity Power Factor Load (Phase A)

The effect of power factor on current/MVA limits of the LV network of the Experimental SSEZ was investigated. As in the earlier studies the Sunny Island 4500™ is configured to supply the reactive power and the resistive load bank is used to import real power into the Experimental SSEZ LV network. A load profile as illustrated in Figure 5.1 with varying power factor was used and generation profiles as illustrated Figure 5.2 and Figure 5.3 were implemented.

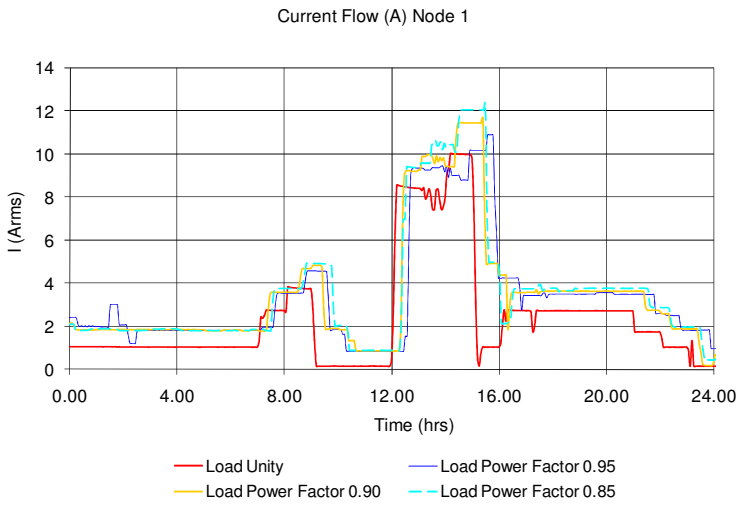


**Figure 5.29: Current flows through node 1 with varying load power factors**

There are technical difficulties in controlling exactly the reactive power flow from the Sunny Island 4500™ especially at lower reactive power levels. It can be seen however that an increasing lagging power factor increases the current flow through the network connection emulator and at a power factor of 0.85 lagging; current flow is 16% greater in comparison with the unity power factor load.

### Scenario III - Unbalanced Non-Unity Power Factor Load (Phase A) and Unbalanced Non-Unity Power Factor Generation (Phase A)

As in the case of the voltage variation and voltage unbalance investigation the impact of SSEG on the thermal limits of the LV network of the Experimental SSEZ with non-unity loads connected was investigated. In this scenario the non-unity load and the wind turbine generator emulator were both coupled to phase A.

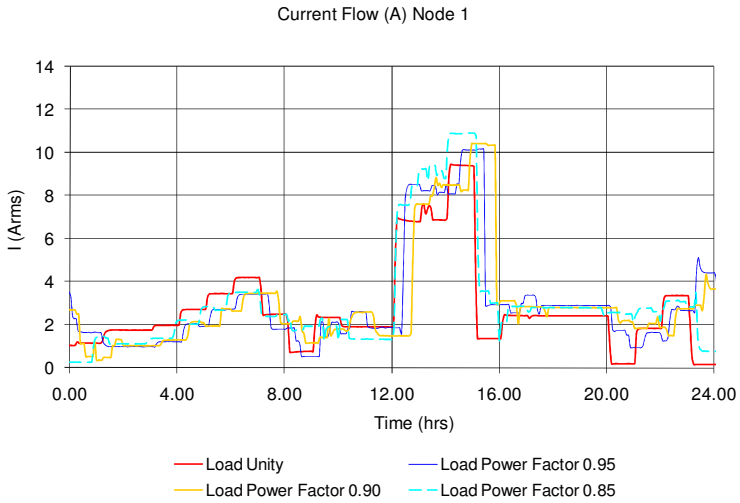


**Figure 5.30: Current flows through node 1 with varying load power factors and SSEG**

It can be seen that an increase in SSEG results in a reduction in current flows during periods of high demand as illustrated in Figure 5.30. However, unless demand is zero the current flow through node 1 can never be zero even if the real power flow from the SSEG, which tries to generate at unity power factor, is equal to the real power demand from the load. This is because the network connection emulator supplies all the reactive power to the load as the SSEG generates at almost unity power factor. The reactive power flows within the LV network of the Experimental SSEZ are illustrated in Figure 5.31.

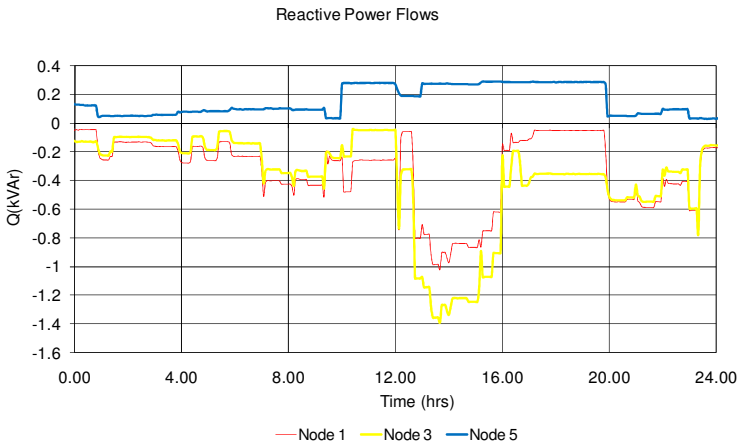


**Figure 5.31: Reactive power flows at node 1, 3 and 5- load (0.85 power factor) and SSEG**

## 5.6 Conclusion

A series of tests were carried out to investigate the operation of the LV network of the Experimental SSEZ under a variety of scenarios. Each of the network constraints identified previously were investigated on the Experimental SSEZ. Although these studies are useful in evaluating the passive operation of the Experimental SSEZ it should be noted that only one generation and load profile is investigated and therefore the testing programme cannot be considered exhaustive. For example a load profile derived from the power consumption of a household on a weekday or a Saturday could be used.

Due to asymmetries in the construction of the synchronous machine the voltages at the terminals of the network connection emulator are unbalanced. In addition, the impedances of the LV network are also unequal. Loading or generation of individual phases rather than using a balanced load was found to result in much larger voltage variations. Moreover, the effects of the mutual impedances of the network connection emulator were also found to have some impact on the voltage variations on the LV network. However, at the remote end of the LV network, the voltage variation and regulation characteristics are dominated by the effects of the voltage variation due to the phase and neutral conductors of the system. Voltage variation and regulation is also affected by the characteristics of

the load. As the load emulation of the Experimental SSEZ is resistive the current imported by the system is determined by the phase-neutral voltage. Finally, the effect of load power factor was found to have a small effect on voltage variation and regulation in the LV network with the reactive power of the SSEG having almost no effect as the X/R ratios of the Experimental SSEZ are very low.

The Experimental SSEZ LV network is unbalanced even under no load or balanced load conditions due to system asymmetries described earlier. %VUF can increase or decrease with the increase or decrease of generation depending on the deployment of the SSEG. The %VUF of the system is complicated due to the cumulative effects of real and reactive current flow in the synchronous machine on the phase and magnitude of the network connection emulator phase-neutral voltages and the voltage variation on the LV network due to the phase and neutral conductors.

Moreover, the power flows within the Experimental SSEZ were investigated and it was found that when the Experimental SSEZ is configured with loads with low power factors with SSEG, the reactive power requirements of the loads was supplied almost entirely by the network connection emulator. Finally, the results from the Experimental SSEZ LV network have demonstrated the asymmetries of a real system.

The studies in this chapter indicate how the operation of the LV network of the Experimental SSEZ is different to an actual LV network. The three primary differences are: -

1. The impedances of an actual LV network and the LV network of the Experimental SSEZ are very different both in terms of X/R ratios and the magnitude of the impedance.

2. An actual LV network would have many SSEGs deployed over a number of phases in contrast with the Experimental SSEZ has only three SSEGs available for emulation.
3. The behaviour of a secondary distribution transformer and the network connection emulator.

In Appendix H, a transformation system is described which compensates for some of these differences so that results from the Experimental SSEZ can be related to those of an actual or generic LV distribution network. The following chapter describes the design and development of centralised control systems for the Experimental SSEZ.

# 6 DESIGN AND LABORATORY IMPLEMENTATION OF A CENTRALISED CONTROL SYSTEM

## 6.1 Introduction

In chapter three, centralised and distributed control architectures for the SSEZ concept were defined. To enable a comparative evaluation of these control system architectures centralised and distributed control systems are realised in the Experimental SSEZ.

In this chapter, the design and development of centralised control systems for the Experimental SSEZ are described. A centralised control system for the purposes of this research, as defined in chapter three, implies a central control system located at the secondary distribution substation which acquires data from nodes throughout the LV network.

The criteria for evaluation of a centralised control system for the Experimental SSEZ, based on the literature reviewed in chapter three, are initially presented. The development approach, which includes a description of the incremental design method and an associated evaluation program, is then described. This is followed by a description of the design and development of the centralised control systems. This description includes results illustrating the effect of their operation on the LV network of the Experimental SSEZ. Finally, conclusions are drawn from the implementation and operation of these centralised control systems on their operation in Experimental SSEZ and the implications for their deployment on LV distribution networks.

## 6.2 Evaluation Criteria for Centralised Control Systems

To be consistent with the control system architecture evaluation criteria described in chapter three, the following criteria are used in evaluating the operation of the centralised control systems developed in the following sections: -

- Ensure system operation within network constraints
- Resilience and reliability
- Scalability
- Communications requirements
- Renewable energy output
- Economic benefit to SSEG/ES/controllable load owners
- Cost and complexity

## 6.3 Development Approach

The cost and complexity criteria are used as a basis for an incremental approach to the development of a centralised control system. Therefore, the first systems are simple in terms of measurement requirements and the sophistication of the control algorithm. Subsequent systems are more complex and are thus likely to be more expensive when implemented in an LV distribution network to enable the concept of the SSEZ.

### 6.3.1 Active network management techniques for Experimental SSEZ centralised control systems

Generation curtailment is the only active network management technique used in the development of these centralised control systems. The following active network management techniques, previously described in chapter three, are not used: -

1. Reactive power compensation – The effect of reactive power flow on the phase-neutral voltages of the Experimental SSEZ was found to be very small in common with many LV distribution networks.
2. OLTC control – The voltage at the terminals of the network connection emulator will not be controlled by the centralised control system. In an LV distribution network, this control function would not be directly available to the control system of an SSEZ. This is because secondary distribution transformers do not feature an OLTC.
3. Load management – A centralised control system is likely to initially interact only with the generation in the system. This is because generation is likely to be the justification for any control system implementation.
4. Energy storage control – Simultaneous communications between the PC, hosting the centralised control system, and the energy storage system and SSEGs in the Experimental SSEZ was found to degrade greatly the operation of the entire system. This is a practical consideration of the Experimental SSEZ due to the communications requirements of the inverters for the PV, wind turbine and energy storage systems. This architecture therefore, was not considered for the development of centralised controllers but should be considered for future work.
5. Network reconfiguration – No control over the configuration of the LV network of the Experimental SSEZ is available at present.

### 6.3.2 Experimental SSEZ centralised control system development

The initial system uses a simple case based control system to control the voltage at the remote end of the LV network of the Experimental SSEZ. The initial systems have voltage control capabilities only, as this is seen as the most limiting of the network

constraints described in chapter two [9, 41]. Subsequent control systems feature a feedback control design, utilise more measurements and are also capable of ensuring that thermal and percentage voltage unbalance limits are observed.

The first control system utilises a simple case based [145] control algorithms, a single, local system parameter and control capability over the wind turbine generation only. Case selection is by utilising the remote end voltage estimate, based on a single-phase current measurement. After a voltage excursion event has been detected the generation is curtailed by a user defined amount based on previous experience. When the remote end voltage has been estimated to drop below the defined limits the generation curtailment command is removed.

This system considered one case only and the system only fulfilled the initial voltage constraint voltage requirements under a limited range of generation and load conditions. To ensure satisfactory operation for more generation and load conditions would require the development of a database of previous cases. This was deemed to be excessively complex both for the development of a control system for the Experimental SSEZ and also for an SSEZ. Moreover, as SSEGs are likely to be deployed on the LV distribution network in a “fit and forget” fashion [14, 23-24, 99, 117] it is possible that this complex database may need be revised regularly increasing greatly the lifetime cost of the system.

A feedback control based system is thus proposed which would provide a simpler and more scalable solution. The initial implementations of feedback control used the remote end voltage estimator described earlier to estimate remote end voltage. The subsequent control system utilises the voltage at the network connection node to improve the accuracy of the remote end voltage estimate.

The following set of control systems utilise a distributed voltage measurement located at or near the remote end of the network. The process variable for the feedback control system is now provided from a distributed location.

It has been established previously that the voltages on a three-phase four-line LV network are likely to be unbalanced. Therefore, a control system utilising distributed voltage measurements on all three-phases was developed.

The operation of these voltage control systems may result in a reduction in thermal limit and voltage unbalance violations but do not directly control these quantities. Therefore, direct thermal limit control functionality is added to the system and local three-phase current measurements at the network connection point were now used as process variables for the control system. The network connection point has been previously identified to be the most likely location for a thermal limit violation on a radial network [22, 41].

The final centralised control system has control techniques that mitigate against voltage rise and thermal limits on each phase of the LV network and also operates to ensure that percentage voltage unbalance limits are observed. This is the most complex centralised control system described in this work. As this system is the most complex and it would be the most costly topology to implement on a radial LV distribution network. This final centralised control system is illustrated diagrammatically in Figure 6.1.

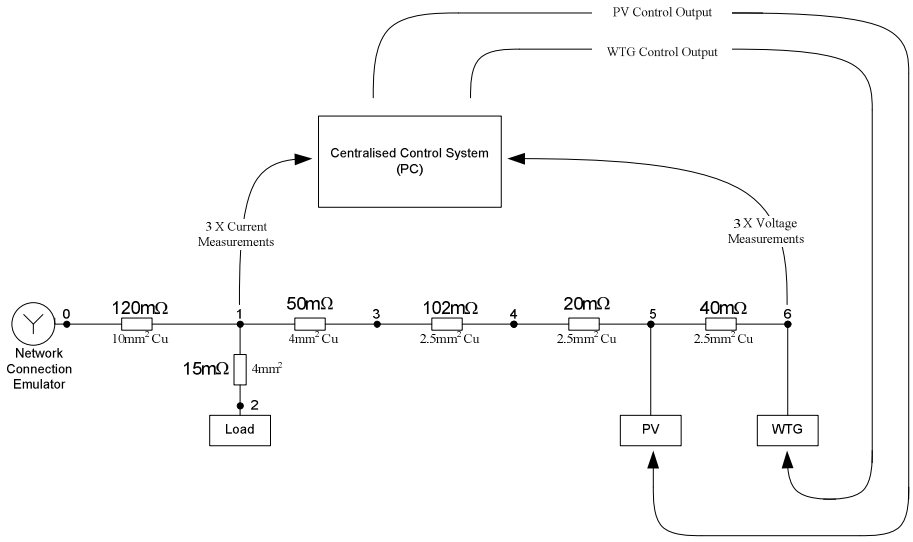


**Figure 6.1: Architecture of final centralised control system design for the Experimental SSEZ**

## 6.4 Centralised Control System Evaluation Program

To assist development and evaluate the operation of the control systems, with regard to the observance of network constraints, an evaluation program has been devised. A successful system will ensure that excursions from the defined operational limits of the system will be minimised. However, due to errors in the estimation of a particular parameter, for example remote end voltage, the system may fail to control generation to observe the system network constraints. In the development of these centralised control systems assumptions and idealisations are made regarding the operation of the LV network of the Experimental SSEZ. These tests are designed to investigate the operation of these control systems with regard to network constraints while considering these idealisations and assumptions.

The tests were therefore categorised, based on the network constraints identified previously, are as follows: -

1. Steady-state voltage rise
2. Thermal limit
3. Percentage voltage unbalance factor ( %VUF)

The initial control systems assumed an unbalanced LV network with generation greatest on phase C. No load is connected to either phase B and C and the generation is located at node 4 and node 5 of the LV network of the Experimental SSEZ. *Test A* results in system operation consistent with the assumptions and idealisations made in the development of the initial control systems. In *Test B*, this is no longer the case and load is connected to phase B and phase C. The generation is moved electrically further from the network connection point, to node 5 and node 6 of the Experimental SSEZ, in *Test C*. The generation and load are moved from phase C to phase A in *Test D*. *Test E* is used to investigate the operation of control systems that have thermal limit control facility. Similarly, *Test F* is used to evaluate the operation of control systems with a percentage voltage unbalance control capability.

### 6.4.1 Steady-State Voltage Rise Tests

Under normal operating conditions, the Experimental SSEZ is operated such that steady-state voltages are maintained within the designated limits. In order to cause a voltage violation, an increase in generation and/or a reduction in load can be initiated. For the purposes of these tests, the nominal voltage was defined as 225.5V, while the allowable voltage rise limit was defined as 232V.

#### *Test A*

This is the first voltage rise scenario with voltage limit violations occurring on phase C of the LV network of the Experimental SSEZ. All the generation is connected to phase C of the LV network. The PV generation emulator is connected at node 4 and the wind turbine generator emulator at node 5. It has been previously shown in [9] that the worst scenario for voltage rise in a radial LV network is if all generation is connected to a single phase.

Initially, the prime mover of the wind turbine generator emulator is instructed to operate at a speed that results in the export of 0.4kW to the system, the PV generator emulator is instructed to export 1.5kW and the load imports approximately 0.9kW on phase C only. It should be noted that the PV generator begins synchronisation before the test begins. However, the time it takes to synchronise and connect with the LV network, so that PV emulator may export power to the Experimental SSEZ, is inconsistent and therefore it does not always synchronise before the test begins. At time t = 230s the prime mover of the wind turbine generator emulator is instructed to accelerate to a speed that results in the export of 1.2kW to the system as illustrated in Figure 6.2(a). The power import of the load emulator and the power export of the PV generator emulator initially remain constant. At time t = 320s and at 90s intervals thereafter the load is reduced by approximately 0.2kW until the demand is reduced to zero as illustrated in Figure 6.2(b).

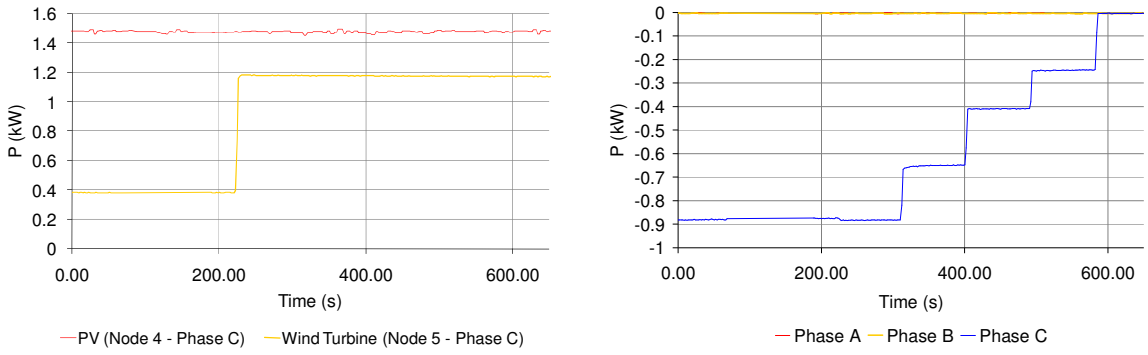


**(a) Generation** **(b) Load**

**Figure 6.2: Generation and load power profiles for *Test A***

The effect of the operation of the generation and the changing load profile on the remote end (node 5) network voltages is illustrated in Figure 6.3. It can be seen that the voltage on phase C in this case exceeds the defined voltage rise limit of 232V following the increase in wind generation and thereafter the decrease in demand.

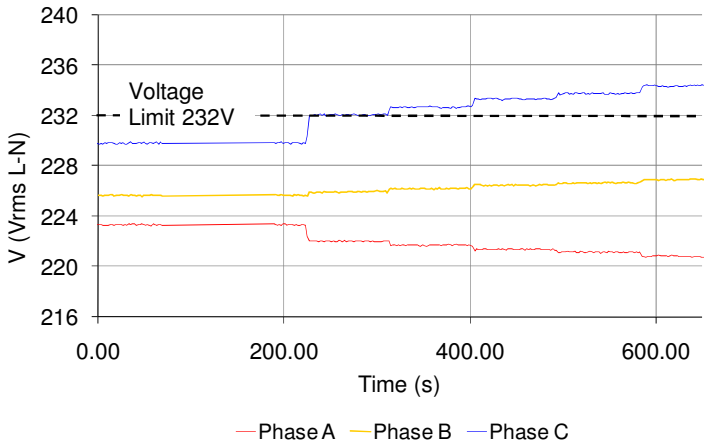


**Figure 6.3: Remote end (node 5) voltages of Experimental SSEZ during *Test A* (No control system deployed)**

### *Test B*

This is similar to *Test A* but in this instance the load emulator is instructed to import a constant load of 0.8kW for the duration of the test on phases A and B. This has the effect of increasing the phase C remote end voltage due to the current flows in all three phases of the synchronous machine as described in chapter four. The resultant load and generation profiles are illustrated in Figure 6.4. This test is designed to illustrate the limitation of assuming that the voltage at the network connection point is constant when estimating the remote end voltage.

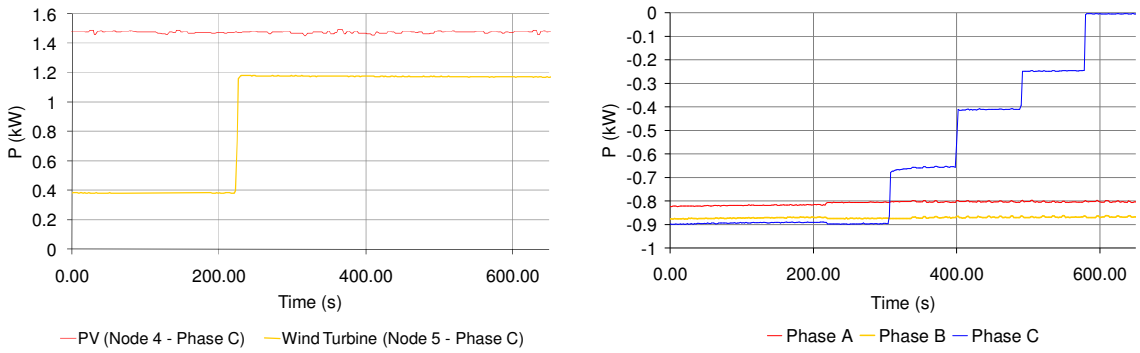


**(a) Generation** **(b) Load**

**Figure 6.4: Generation and load power flows for *Test B***

The effect of the operation of these generation and load profiles on the remote end voltages is illustrated in Figure 6.5. The phase C, remote end voltage again exceeds the defined upper voltage limit of 232V following the increase in wind generation and thereafter the decrease in demand. The voltages during this test on phase C are higher than at the same point during *Test A*.

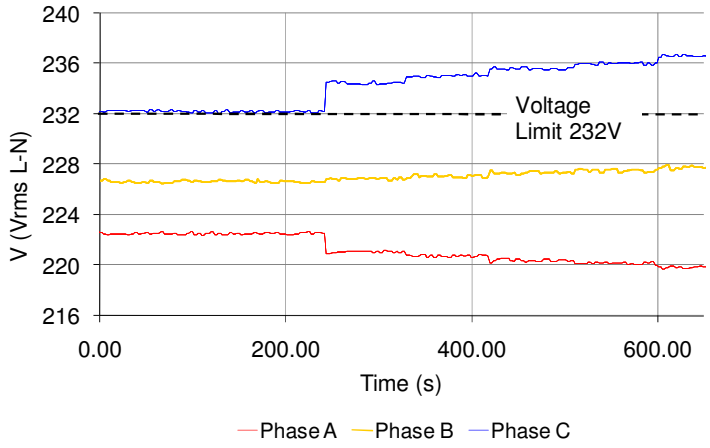


**Figure 6.5: Remote end (node 5) voltages of Experimental SSEZ during *Test B* (No control system deployed)**

### *Test C*

*Test C* is designed to investigate how the centralised control systems performed following a change in the distribution of generation on the LV network of the Experimental SSEZ. In this test, the PV and wind turbine generator emulators are moved to nodes 5 and 6 respectively of the Experimental SSEZ LV network. The load and generation profiles used in *Test A*, as illustrated in Figure 6.2 are implemented during this test. The remote end of the LV network in this test is moved from node 5 to node 6.

The effect of this change in the distribution of load on the LV network remote end voltages is illustrated in Figure 6.6. The remote end, phase C voltages are always greater than the remote end, phase C voltage measured at the same point during *Test A* as illustrated in Figure 6.3. This is due to the location of the generation which is electrically

further from the network connection emulator. This is analogous to a scenario where extra generation is introduced at the remote end of an LV distribution network resulting in higher remote end voltages.

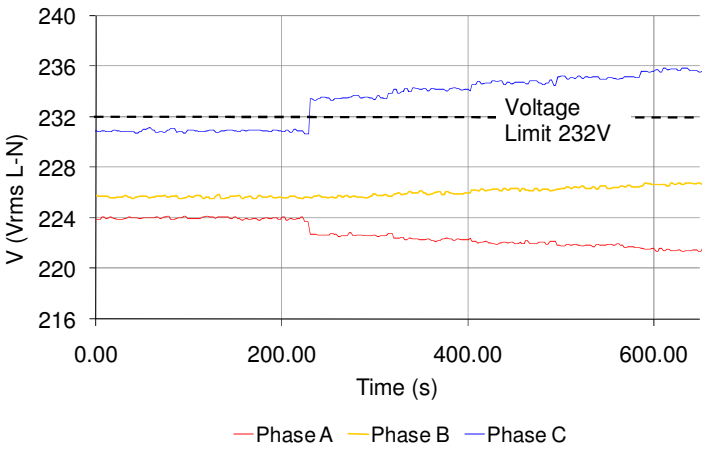


**Figure 6.6: Voltages at remote end (node 6) of Experimental SSEZ during *Test C* (No control system deployed)**

### *Test D*

As in the case of *Test C*, *Test D* seeks to investigate the impact of changes to the distribution of generation on the LV network on the operation of centralised voltage control systems. In this test, the PV and wind turbine generation are connected to phase A of the LV network of the Experimental SSEZ at nodes 5 and 6 respectively. The generation profiles are similar to the previous tests and are illustrated in Figure 6.7 (b). There is no load connected to phase B and phase C of the LV network. A load profile, as per Figure 6.7(b), is implemented on phase A of the LV network.

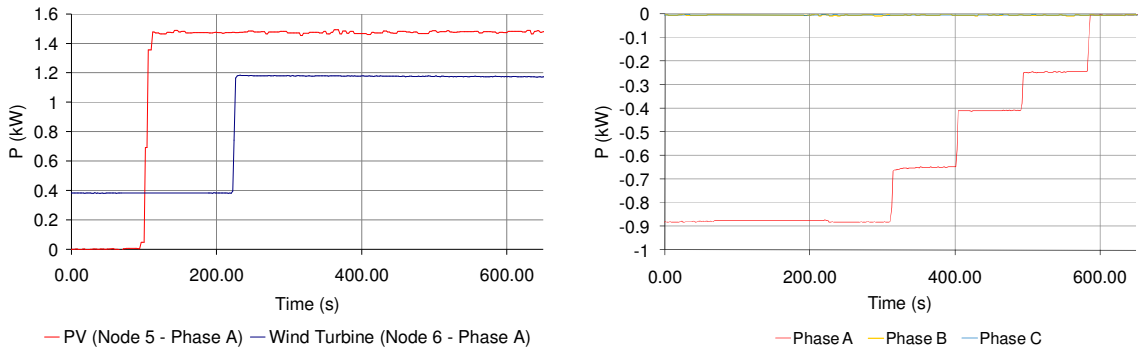


**(a) Generation** **(b) Load**

**Figure 6.7: Generation and load active power flows during *Test D* (No control system deployed)**

The effect of the configuration and the operation of these generation and load profiles on the remote end voltages is illustrated in Figure 6.8. The remote end of the LV network is again node 6. Phase A, remote end voltages now rise above the defined voltage limit of 232V. This test seeks to investigate the limitations of control systems which assume that the LV network is balanced or that voltage rise is likely to occur on a particular phase of the LV network.

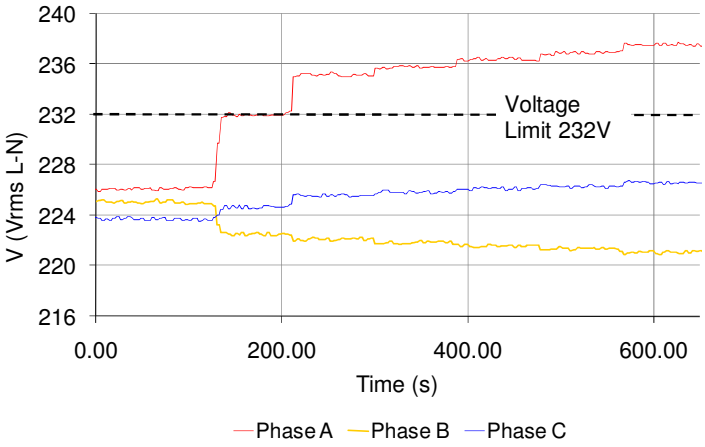


**Figure 6.8: Voltages at remote end (node 6) of Experimental SSEZ during *Test D* (No control system deployed)**

### 6.4.2 Current Limit Test

***Test E***

As the Experimental SSEZ is a radial network, the most thermally stressed cable section is likely to be between node 0 and node 1 [22, 41]. A similar test sequence is devised to that of the steady-voltage rise investigation, *Test D*. The PV and wind turbine generation are connected to phase A of the LV network and load appears on phase A only. Figure 6.9 illustrates the effect of the operation of the PV generator emulator, wind turbine generator emulator and load emulator on the current flow of the cable section under consideration, without the generation curtailment capabilities provided by a control system. The current limit is defined to be 8A and is violated for extended periods of time on phase A during this test as illustrated in Figure 6.9.

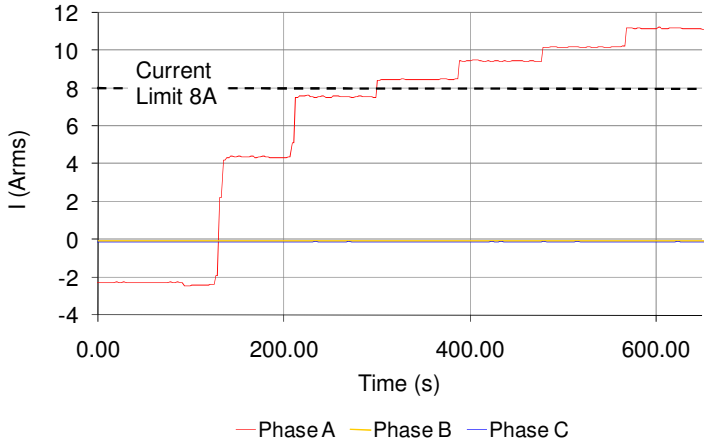


**Figure 6.9: Current at node 1 of Experimental SSEZ during *Test E* (No control system deployed)**

### 6.4.3 %VUF Test

#### *Test F*

It was established in chapter seven that the percentage voltage unbalance (%VUF) is greatest at the remote end of the Experimental SSEZ LV network. This test sequence is similar to the steady-voltage rise investigation *Test D* and the current limit test, *Test E*. Load and generation are connected to phase A of the Experimental SSEZ LV network. Figure 6.9 illustrates the effect of these load and generation profiles on the %VUF at the remote end without any control system deployed. The %VUF limit for this test is defined

to be 1.5%. The %VUF exceeds the defined limit of 1.5%, at nodes 2, 5 and 6 for extended periods following the increase in generation. The largest values of %VUF are measured at the remote end (node 6) of the LV network. Similarly, in radial LV networks the %VUF is also found to be greatest at the remote end [8-9].

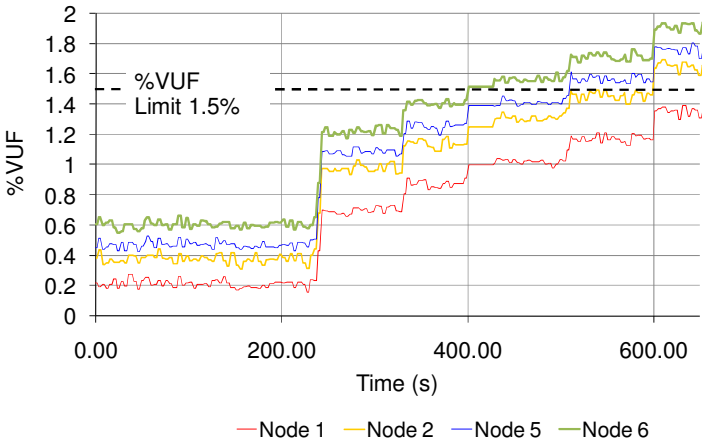


**Figure 6.10: %VUF at node 6 of Experimental SSEZ during *Test F* (No control system deployed)**

## 6.5 Centralised Voltage Control System – Centralised Single-Phase Current Estimator (Wind Turbine Generator Curtailment)

The first control system developed on the Experimental SSEZ utilises a single-phase current measurement (phase C) at node 1 to estimate the remote end voltage. This is similar to the operation of an LDC on the tap-changers of primary distribution transformers as described in chapter three [26, 95].

### 6.5.1 Remote end voltage estimation

To estimate the remote end voltage of the LV network of the Experimental SSEZ, a number of assumptions are needed. The simple remote end voltage estimator in this instance is based on the voltage rise equation (2.2) which assumes that the system is balanced and symmetrical.

$$\left|\overline{E}-\overline{V}\right|=\left|\Delta\overline{V}\right|=\left|\overline{I}\right|\left[R\cos\theta+X\sin\theta\right] \tag{2.2}$$

Many of the active network management control strategies for voltage control, described in chapter three, are proposed for MV distribution networks [92-102, 104-108]. These systems are often assumed to be balanced and symmetrical. This idealisation is also made in the development of this remote end voltage estimator and so only a single phase C measurement is required ($\left|\overline{I_c}\right|$). Using these assumptions and assuming that the LV network under consideration is resistive and power is assumed to be generated and consumed at unity power factor then it is possible to write: -

$$\left|\overline{E_c}\right|=\left|\overline{I_c}\right|\left[R_c\right]+\left|\overline{V_c}\right| \tag{6.1}$$

A first stage control system is developed which assumes that the system is operating at zero load and the generation is operating at unity power factor at the end of the network through a resistive network with an effective impedance of $R_{1-5}$. There is no voltage measurement at node 1 in this algorithm therefore it is necessary to assume that the voltage at node 1 is defined to be the nominal voltage of the system ($V_{nom}$). The remote end voltage estimation $V_5^{Est}$ is then defined: -

$$V_5^{Est}=I_{1c}R_{1-5}+V_{nom} \tag{6.2}$$

While this equation can be used to estimate the voltage at the remote end of a radial distribution network in LV distribution networks the settings are usually set based on a compromise based on the remote end voltage and the load on the network [35].

### 6.5.2 Simple case based control system

This first stage, centralised voltage control system uses a simple case based control system which utilises the estimated remote end voltage to decide on a predetermined curtailment in generation. This is similar to the operation of the system described in [13]

where generation is reduced in steps of 33% depending on the estimated network conditions. The remote end voltage estimation is derived from (6.2). When the remote end voltage estimation drops below a lower threshold level the control action is released and the generation curtailment constraint on generation is removed.

In this initial implementation only the wind generation in the Experimental SSEZ is curtailed. A simplified block diagram of the LabVIEW™ visual code for this active voltage control system is shown in Figure 6.11.

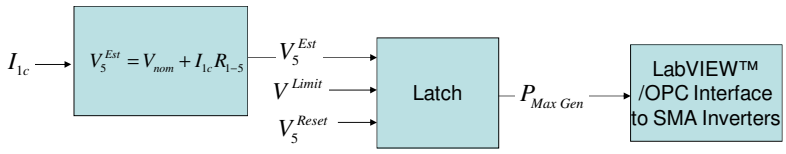


**Figure 6.11: Simplified block diagram of initial single-phase current based centralised voltage control system**

*Test A* is used to investigate two cases of this control system as illustrated in Figure 6.12. In the trace titled *Case A,* a generator curtailment operation is triggered if the remote end voltage estimation is greater than 232V. The remote end voltage estimation assumed zero load. This corresponds to a flow of current of greater than 11A at node 1 under no load conditions. The control system ensured that generation is curtailed until the remote end voltage estimation dropped below 230V. During curtailed generation operation the output of the wind turbine generation is reduced by 75%.

The remote end voltage estimation can be inaccurate as the load, which is situated electrically closer to the network connection emulator has very little effect on the voltage rise at the remote end of the network. The assumptions made therefore to estimate the remote end voltage are only valid when demand is very low. *Case A* does not curtail generation until the end of the test when the load is zero as illustrated in Figure 6.12.

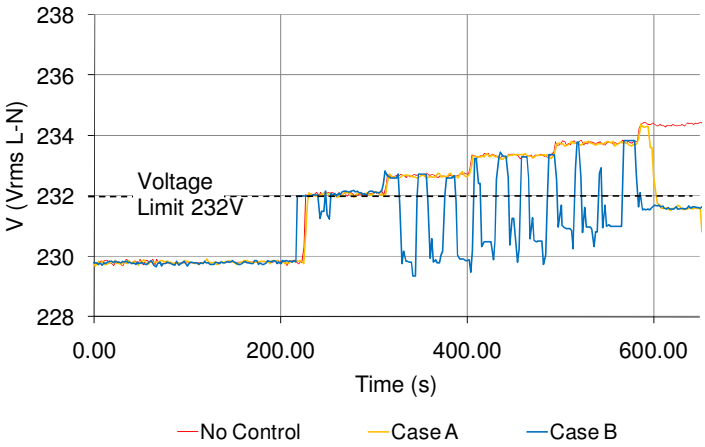


**Figure 6.12: Remote end voltage (node 5 - phase C) with simple case based control system – *Test A***

In *Case B*, the remote end voltage estimate assumes that maximum load is connected to the LV network. The operation of this system is illustrated in Figure 6.12. Again the wind turbine generation is reduced by 75% when the system detected an over voltage condition. This generation curtailment resulted in the estimated and actual voltage of the system to drop below the value of the reset limit of the latch. Once the latch is reset the active control system increased the power export limit to 100% installed capacity. This resulted in a reoccurrence of the steady-state voltage limit. The system with the *Case B* controller finally became stable when minimum load conditions were approached at t = 600s.

This simple system ensures that voltage rise is controlled only under a limited number of scenarios. It has been shown that this initial control system does not provide satisfactory operation but this could be improved by adding further cases to the control system and improving the operation of the system between cases. In addition, the generation curtailment would have to be determined for each case. This would result in a complex, customised system which is likely be too complex and expensive for implementation in an SSEZ.

### 6.5.3 Proportional Control system

In order to improve the performance of the control system detailed in the previous section a proportional feedback control is implemented. A simplified block diagram of the LabVIEW™ visual code for this control system is shown in Figure 6.13. As in the simple caes based system, this system curtails the generation of the wind turbine generator only.

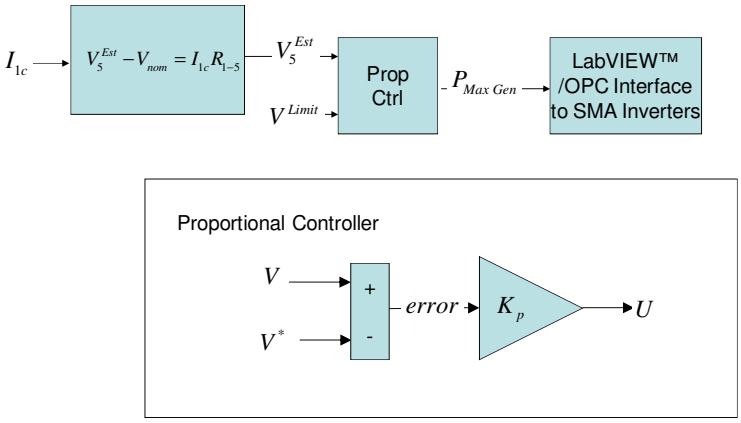


**Figure 6.13: Simplified block diagram of proportional voltage control system**

*Test A* is again used to investigate the effect of the proportional gain of this controller on the voltage excursions of the system as illustrated in Figure 6.14. Low proportional gains were used initially and were unable to control the system to below the required voltage level. When the gains are increased the response of the system became oscillatory.

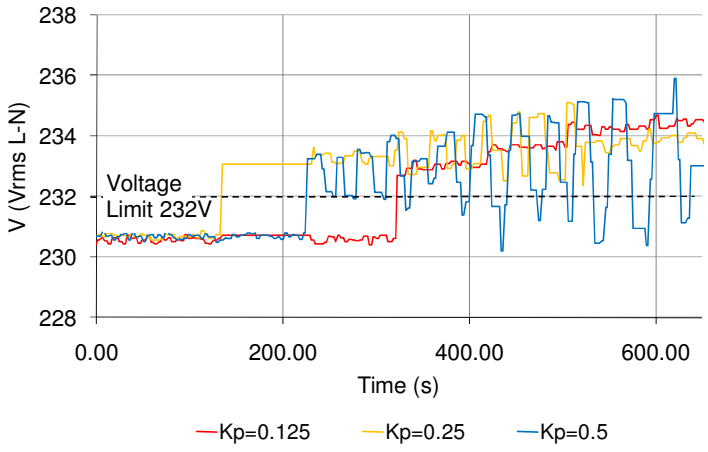


**Figure 6.14: Remote end voltage (phase C – node 5) with simple current based proportional voltage control system – *Test A***

### 6.5.4 Proportional and Integral Control system

In order to achieve acceptable performance from the feedback based control system a proportional and integral (PI) controller was developed. A PI controller, as illustrated in Figure 6.15, is a feedback controller which uses the difference between the set point ($V^*$) and the measured process variable ($V$) to generate an error ($e$). The integral and proportional gain system thus changes the output ($U$) of the controller, which is the input to the process, in order to reduce the error between the set point and the measured process variable to zero.

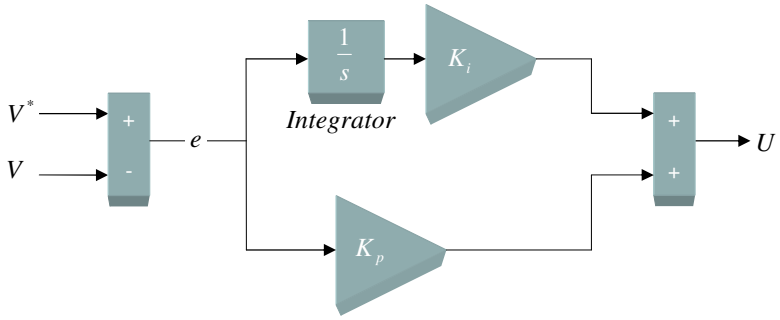


**Figure 6.15: PI Controller**

As in the previous centralised control system implementations, only the wind turbine generator active power export is curtailed. A simplified block diagram of the LabVIEW™ visual code for this control system is shown in Figure 6.16.

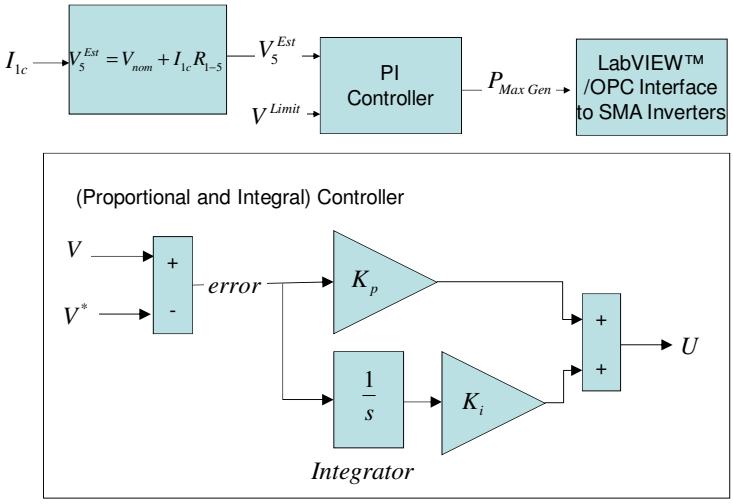


**Figure 6.16: Simplified block diagram of single-phase proportional and integral based centralised voltage control system**

*Test A* was again used to investigate the effect of the PI based system control system on the voltage violations measured on the LV network as illustrated in Figure 6.18.

The initial PI based central control system did not operate to reduce system voltage as shown in the trace titled *PI* in Figure 6.18. During normal operation when the remote end voltage estimate is less than voltage limit, the value of the integrator increases but the maximum value of generation is limited by the installed capacity of the SSEG. This results in the accumulation of large positive values of the integrator. If a voltage rise situation is then detected the output of the controller remains positive until the negative error reduces the value of the integrator. This could take a long time especially if the voltages had remained within the defined limits for extended periods of time. Eventually the output of the PI controller would curtail the maximum exportable active power of the SSEG, thus reducing the voltages at the remote end of the LV network.

This effect, which is common when PI controllers are used to control non-linear systems, is known as integral wind-up [146-147]. Integral windup occurs in a PI or Proportional Integral and Derivative controller when the integrator continues to integrate the error indefinitely which occurs when the controller's output no longer affect the controlled

variable. This is typically caused by process saturation, that is the output of the process is limited at the top or bottom of its scale, resulting in a constant error. Two control algorithms were used to evaluate the use of anti-integral wind-up algorithms to control voltage in the Experimental SSEZ and are illustrated diagrammatically in Figure 6.17 [146-147].

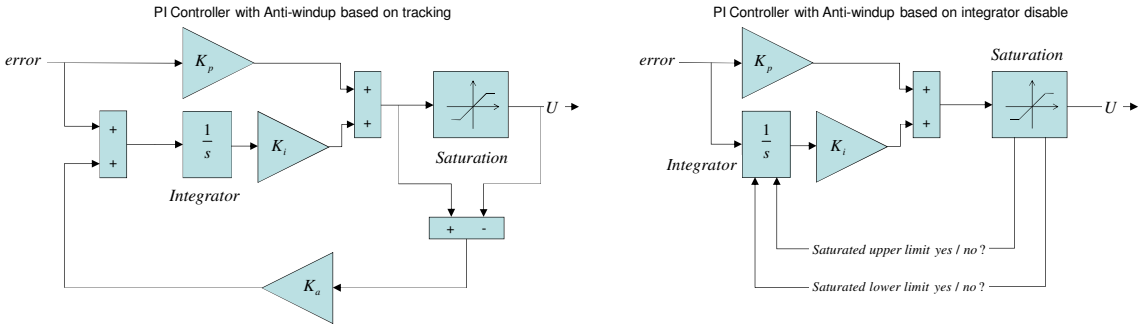


**Figure 6.17: Anti-integral windup PI controllers**

All three PI based control systems, whose results are illustrated in Figure 6.18, use the same proportional and integral gains. It can be seen from the trace titled *PI & Integrator Disable Anti-Integral* in Figure 6.18 that the PI controller with the integrator disable, anti-integral wind-up algorithm offers the most satisfactory operation.

This anti-integral wind-up algorithm disables the addition of negative error to the integrator when the output of the integrator is below the minimum limit and disables the addition of positive error when the output of the control system is above the maximum limit. This limits the accumulation of large positive or negative values on the integrator. The tracking algorithm, as illustrated by the trace titled *PI & Tracking Anti-Integral*, did not bring the integrator out of saturated operation until the end of the test. All the PI controllers were tuned using a modified version of the Ziegler-Nichols method.

It should be noted that the use of a single current measurement to estimate the remote end voltage is likely to be more accurate in an LV distribution network than in the Experimental SSEZ. This is because load and generation are likely to be distributed more

evenly about the LV network. In addition, future work could include the development of a control system that utilises historical load data to estimate the load, thus enabling more precise estimation of remote end voltage.

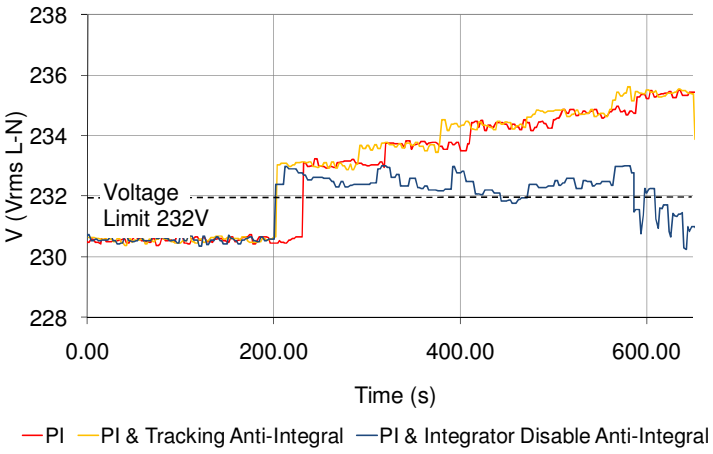


**Figure 6.18: Remote end voltage (phase C – node 5) with PI based voltage control system – *Test A***

As the all the system measurements are located at the same location these centralised control systems are relatively resilient to communications malfunction. However, a failure in the measurement sensor or in the control system could result in the complete failure of the control system.

These systems provide a certain degree of scalability as a limited amount of extra SSEGs can be added, which are not integrated into the control system, can be added to the system without the requirement for reprogramming of the system. However, large changes in the penetration level and distribution of SSEG may result in inaccurate remote end voltage estimations and therefore unacceptable system operation. In addition, if extra SSEGs are to be integrated into the control system some modifications to the control system will be required.

The communications system in this architecture would be required to control the wind turbine generation but none are required for data acquisition as this is done locally. The renewable energy output of the system is high in comparison to schemes where

generation curtailment duty is equitably shared between all the generators in the network, as generation curtailment at the remote end of the LV network has been shown have the greatest impact on voltage rise. As the wind turbine generation is curtailed whenever the estimated remote end voltage rises above the defined limit, the renewable energy export of the wind turbine generator is less than if it was not integrated into the control system. The renewable energy export of the PV generation, by contrast is not curtailed.

## 6.6 Centralised Voltage Control System – Centralised Single-Phase Current and Voltage Estimator (Wind Turbine Generator Curtailment)

The control strategies described in the previous section assumed that the voltage at the network connection emulator remains at the nominal voltage ($V_{nom}$) under all generation and load conditions. In chapter five however, it was demonstrated that the voltages at the terminals of the network connection emulator were dependent on the flow of current in the three-phases of the synchronous machine. Consequently, the remote end voltage (phase C) in *Test B* is greater than in *Test A* even though the current flow (phase C) is the same at node 1 of the network connection emulator. *Test B* is therefore used to evaluate the effect of changing the voltage at the network connection point would have on centralised remote end voltage control systems. In an LV distribution network this could occur if the tap position of the tap-changer of the primary distribution transformer is changed or if unbalanced currents were flowing thought the secondary distribution transformer. A control system was designed which used the network connection emulator measurements to increase the accuracy of the remote end voltage estimation as illustrated in Figure 6.19.

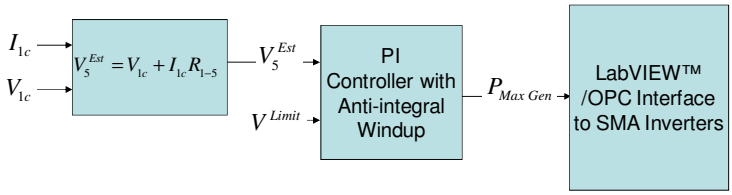


**Figure 6.19: Simplified block diagram of single-phase current and voltage based centralised voltage control system**

This control system uses the same PI controller and the more successful anti-integral wind-up algorithm described in the previous section. *Test B* was used to evaluate this revised centralised control system in comparison with the control system using a single-phase current measurement to estimate remote end voltage presented in the previous section. It can be seen that the control system without the additional voltage measurement attempts to control the remote end voltage to a slightly higher value. This is due to inaccuracies in the simpler remote end voltage estimator. As in the case of the previous control systems only the maximum power export of the wind turbine generation is curtailed.

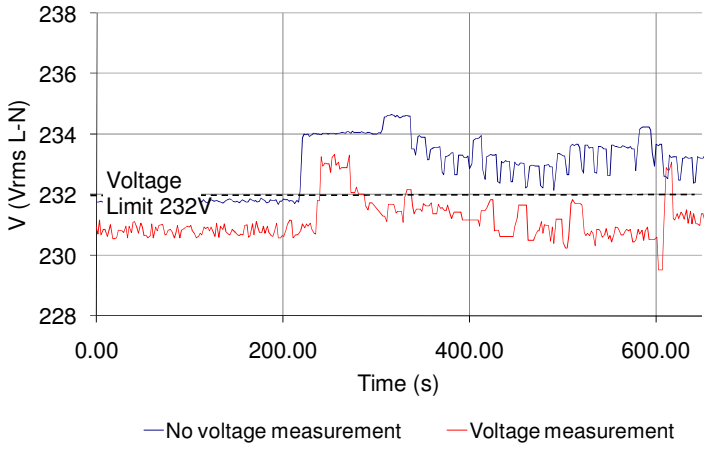


**Figure 6.20: Remote end voltage (phase C – node 5) with current based and revised current and voltage based localised remote end voltage estimators– *Test B***

As the system measurements are again located at the same location these centralised control systems are relatively resilient to communications malfunction. Communications

failures may result in the loss in control of some of the SSEGs integrated into the control system.

As in the case of the control system described in the previous section, this system provides a certain degree of scalability as a limited number of extra SSEGs, which are not integrated into the control system, can be added to the system without the requirement for reprogramming of the system.

Similarly to the previous control system, the communications system in this architecture would be required to control remote end SSEGs but communications are not required for data acquisition as this is done locally. As the generation curtailment scheme is similar to the previous control system, renewable energy output of the system is likely to be high in comparison to schemes where the duty of generation curtailment is equitably shared. As in the previous example, the wind turbine generator energy export is reduced if it is integrated into the control system in contrast to the PV generation.

To control the voltage below the upper voltage limit of 232V requires the wind turbine generator output to be constrained to very low power levels as illustrated in Figure 6.21. The power export by the wind turbine generator is reduced by 1.1kW to 0.1kW by the end of the test. As PV generation remains at 1.5kW for the duration of this test the overall renewable energy output is reduced by 41%. It can be seen that the wind turbine generation cannot be reduced much further if more extreme voltage rise conditions were present.

In the next section both the wind turbine generation and PV generation are curtailed which enables mitigation against more extreme voltage rise conditions. In addition, the duty of mitigating against these conditions is borne by both generators results in greater energy yields for the wind turbine generator but a reduction in the energy yield for the PV generator.

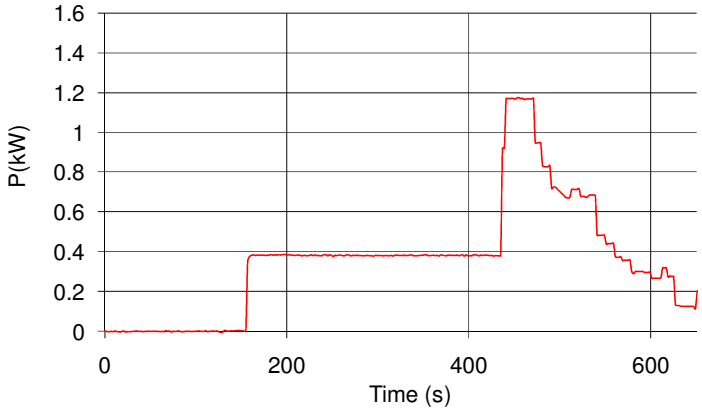


**Figure 6.21: Active power export of wind turbine generation with current and voltage based PI voltage control system – *Test B***

## 6.7 Centralised Voltage Control System – Centralised Single-Phase Current and Voltage Estimator (Wind Turbine and PV Generator Curtailment)

The control algorithm used in the previous section was used as the basis for a control algorithm that curtails the active power export of both the wind turbine generator and PV generator to regulate the voltage at the remote end. A simplified block diagram of the LabVIEW™ code used to implement the first two active control systems is illustrated in Figure 6.24.

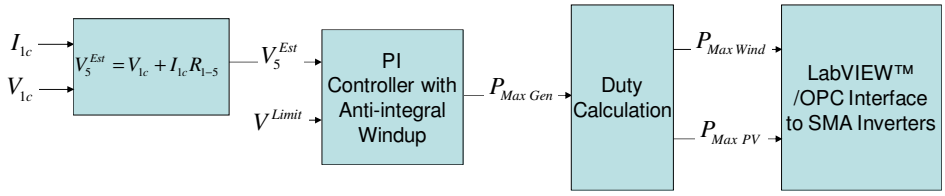


**Figure 6.22: Simplified block diagram of single-phase current and voltage based centralised voltage control system with wind turbine and PV generation curtailment**

The block titled *Duty Calculation* block apportions the duty of generation curtailment between the two generators. In addition, in order to reduce the frequency of control signal

commands to the SMA inverters a deadband block is implemented on the output of the third control system as illustrated in Figure 6.23.

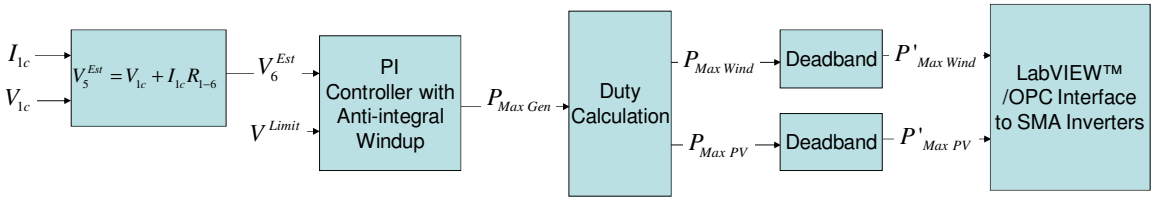


**Figure 6.23: Simplified block diagram of single-phase current and voltage based centralised voltage control system including deadband with wind turbine and PV generation curtailment**

The *Duty Calculation* in these centralised control system implementations apportions the duty of generation curtailment relative to their installed capacity. This is a simple strategy but more complicated strategies could also be used as described in chapter three [101]. For example, if the total installed capacity of a wind generator is 2kW and a PV generator is 1kW, the total installed generation is 3kW. The maximum allowable generation ( $P_{Max\ Gen}$ ) can vary between 3kW (installed capacity) and zero generation. Therefore if $P_{Max\ Gen}$ is 1.5kW, the maximum allowable wind turbine generation ( $P_{Max\ Wind}$ ) is 1kW and the maximum allowable PV generation ( $P_{Max\ PV}$ ) is 0.5kW.

The first control system, whose operation is illustrated by the trace titled *Kp, Ki original* uses the topology illustrated in Figure 6.22 and uses the same proportional and integral gains as the active control system developed in section 6.6 where curtailment of wind turbine generation is used to control the remote end voltage in the system. The operation of this control system resulted in large oscillatory changes to the generation curtailment set points which as a consequence resulted in oscillatory changes to the remote end voltage as illustrated in Figure 6.24.

The second control system, whose operation is illustrated by the trace titled *Kp, Ki reduced,* in Figure 6.24, uses reduced gains and appears to control the system but the

operation of the system is slow and when the system does react, the voltage is reduced far below the defined voltage limit.

Following further investigation into the operation of this active control system it was determined that the large numbers of control actions, that take place during the operation of this control system, places a large burden on the communications system. As the data acquisition system and control system run on the same computer large numbers of control commands result in poor operation of both of these systems.

To reduce the burden on the communications infrastructure, deadband blocks are implemented, as illustrated in Figure 6.23, whose output only changes if the output from the control system changes by more than 200W. As there are less control commands the performance of the both system is greatly improved. Deadband techniques are also used in existing distribution network control, an example of which is their implementation in the control systems for transformer tap-changers [4, 35].

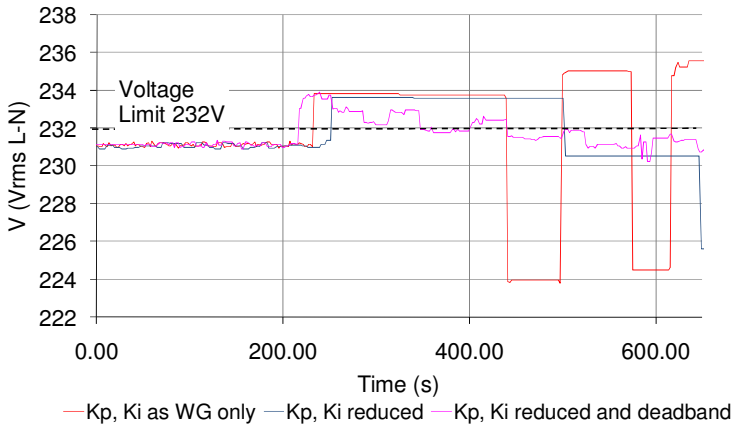


**Figure 6.24: Remote end voltages (phase C – node 5) with centralised voltage control system with control of wind turbine and PV generation – *Test C***

It can be seen from Figure 6.24 that the control system with reduced gains and a deadband function enables the best control of the voltage at remote end of the system to below the defined limit.

This control system uses the same remote end voltage estimator described previously and is subject to the same sources of failure as the earlier control systems. As more curtailable generation units are available a greater degree of redundancy is available. If a communications link fails to one of the generating units, another generating unit can take over the duty to mitigate against the network constraint.

As in the previous control systems a limited amount of extra SSEG, which are not integrated into the control system, could be added. However, the development of this control algorithm demonstrates that changes are required in a control system when extra controllable generation is added which indicates limited scalability when dispatchable generation is available to the system.

During the development of this control system a deadband block was found to greatly improve the operation of the control system. As a larger number of controllable entities (PV and wind turbine generation) were integrated into the control communications traffic was increased. The deadband block reduced the number of control actions and thus reduced the communications traffic on the system.

The sharing of the duty of the generation curtailment of PV and wind turbine generation during the operation of the control system featuring the deadband filter is illustrated in Figure 6.25. It can be seen that the duty of generation curtailment duty is borne by all the SSEGs rather than the wind turbine generation. In this case, the wind turbine generation output drops by 0.6kW and the PV generation drops by 0.7kW. Therefore, the overall the reduction in renewable energy output by the end of the test is 1.3kW in comparison to the previous system where wind turbine generation only was curtailed and renewable generation power output was reduced by 1.1kW. Overall renewable generation output power is reduced by 48% in comparison to the previous system where renewable generation output is reduced by 41%. As both generators are curtailed in this control

system, the overall energy yield from both generators is reduced. Moreover, the overall energy renewable energy export is lower than in the previous control systems as the duty of reducing the voltage at the remote end of the system is not confined to the generator at the remote of the radial LV network.

This is because curtailment has been assigned to be a simple function of capacity as described earlier in this section. The centralised control system however would enable any other strategies for curtailment and may be designed so that renewable energy output is maximised and could instruct the most remote generators to curtail initially to maximise renewable generation output. In such a system, the wind turbine generation would respond similarly to the system where only wind generation was curtailed in *Test C.*

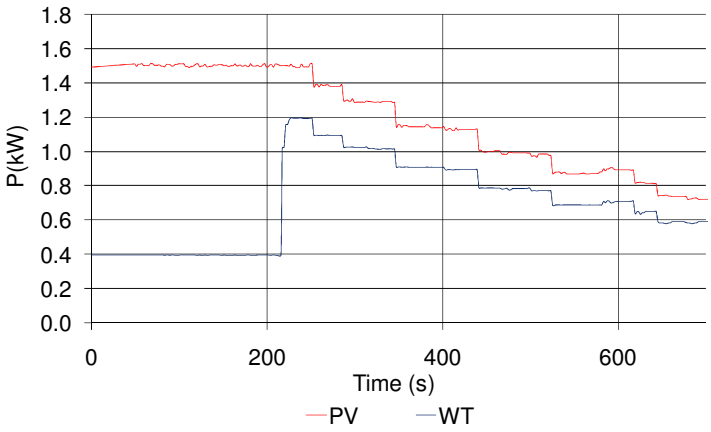


**Figure 6.25: Curtailed PV and wind turbine active power generation controlled by centralised voltage control system with deadband – *Test C***

## 6.8 Centralised Voltage Control System – Distributed Single-Phase Voltage Measurement (Wind turbine and PV generator Curtailment)

To get a more accurate estimation of the voltages in an LV network, a distributed voltage measurement at the remote end of the LV network can be used. The GenAVC™ system

uses distributed voltage measurement(s) to increase the accuracy of a state estimation of the distribution network under consideration [92, 97-98, 148]. This centralised control system will again curtail the maximum active power export of the PV and wind turbine generation to reduce the voltage at the remote end of the Experimental SSEZ LV network. A simplified block diagram of the LabVIEW™ control system is illustrated in Figure 6.26.

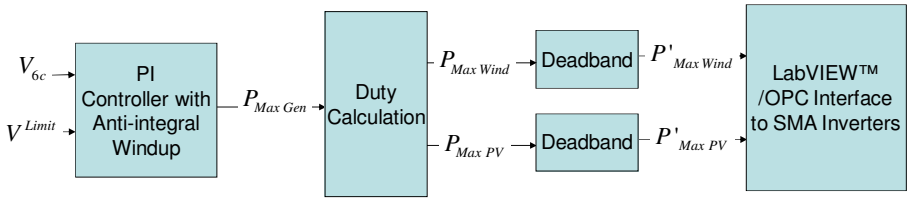


**Figure 6.26: Simplified block diagram of remote end voltage sensing centralised voltage control system with PV and wind turbine generation curtailment**

To determine the gains for this system the PI controller the integral gain $K_i$ was set to zero so the controller was operated as a proportional controller. A number of proportional gains were investigated and some of the test results are illustrated in Figure 6.27. This was done to establish the proportional control gains required for the PI controller using a modified version of the Ziegler-Nichols method.

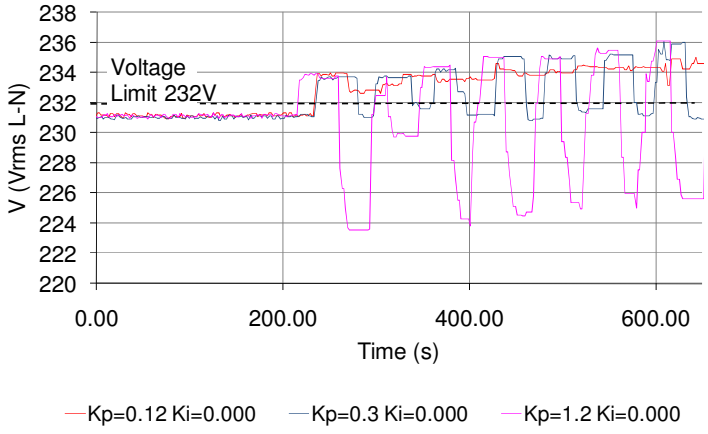


**Figure 6.27: Remote end voltages (phase C – node 6) with centralised voltage control system with control of PV and wind turbine generation (Proportional control) – *Test C***

A proportional gain of 0.12 was selected. A number of integral gains $K_i$ were then tested using the same scenario. A selection of the results is shown in Figure 6.28. The active control systems operated successfully in regulating the voltage at the remote end of the LV network with differences in their speed of operation and oscillations around the operating points once the system is in voltage regulation mode.

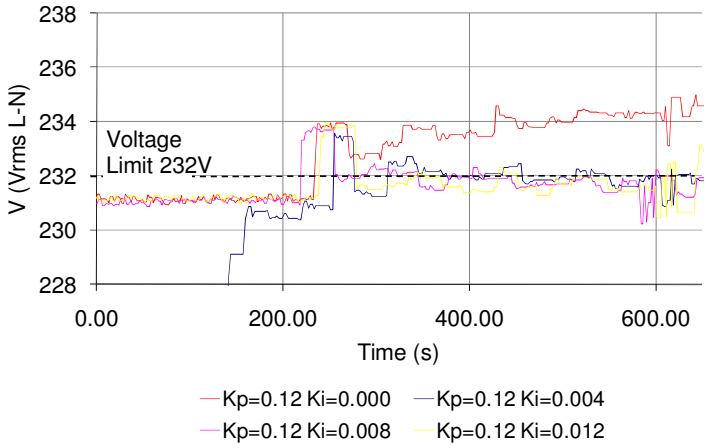


**Figure 6.28: Remote end voltages (phase C – node 6) with centralised voltage control system with distributed voltage measurement – *Test C***

It can be seen Figure 6.28 that the control system, after appropriate tuning of the control system, ensures that the defined voltage rise limit is observed. This operation as in the previous cases is contingent on the correct selection of gains for the system.

In this control system, in contrast to the previous systems, some measurement nodes are located at distributed locations. Malfunctions in the remote measurement sensors or their associated communication systems could result in errors or even failure in the operation of the system.

The same observations apply to this control system as the previous control systems with regard to scalability as small changes in penetration levels and distribution of SSEG can be accommodated but large changes in penetrations levels or the addition of extra controllable SSEG may entail modifications to the control system.

The importance of communications traffic in this system is increased as a distributed voltage measurement is essential for the operation of the system. In addition, the communications system must be fast enough to ensure that the reaction of the control system to a change in the LV network is not slowed.

As in the system described in the previous section both generators are curtailed and therefore the energy export of both PV and wind turbine generation is reduced when the remote end voltage violates the defined upper limit.

As established earlier, the largest magnitude of voltage rise is likely to occur at the remote end of a radial distribution network. Therefore, the remote end of a radial distribution network is a good location to make a voltage measurement available to an active centralised control system. However, in LV distribution networks, change in the configuration or distribution of SSEG may result in the measurement sensor not remaining at the remote end of the LV network. The effect of the location of the voltage measurement on the operation of the control system developed is illustrated in Figure 6.29. The same control system is deployed in both cases. In the traces titled *Node 5 Meas* and *Node 6 Meas* the voltage is measured at node 5 and node 6 respectively. The voltage is not regulated below 232V when the voltage measurement is at node 5 using this control system. However, this could be compensated for by estimating the voltage at node 6 based on measurements at node 5 or other available nodal measurements.

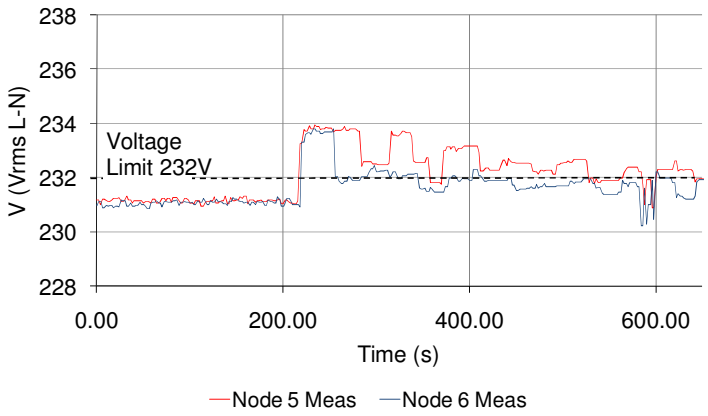


**Figure 6.29: Remote end voltages (phase C) with centralised voltage control system with distributed voltage measurements at node 5 and node 6– *Test C***

## 6.9 Centralised Voltage Control System – Distributed Three-Phase Voltage Measurement (Wind Turbine and PV Generator Curtailment)

In chapter two, the single-phase nature of domestic load and future SSEG was demonstrated. This can lead to unbalanced voltages on an LV distribution network. It may be necessary, therefore, to measure or estimate the voltages on all three phases of an LV distribution network in order to determine how to coordinate load and generation so that voltage limits are not violated. *Test D* is used to investigate the operation of a voltage control system where voltage rises above the defined limits on phase A. The three-phase control systems are based on the single-phase control system developed earlier. A simplified block diagram of the system is illustrated in Figure 6.30.

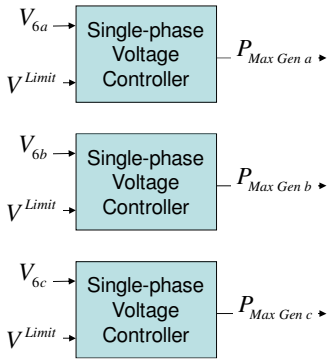


**Figure 6.30: Simplified block diagram of three-phase voltage control system**

The effect of the operation of the single-phase voltage control system developed previously, on the phase A remote end voltage is illustrated by the trace titled *Single-phase control system* in Figure 6.31. The trace titled *Three-phase control system I* illustrates the operation of the three-phase voltage control system and utilises the same controller gains that are used in the single-phase control system developed in the previous section. This control system exhibits oscillatory behaviour that was not observed when the identical controller was deployed on phase C with identical generation. This is due to the differences in impedances between the two phases, the effect of the AVR on this phase of the LV network and the asymmetries in the synchronous machine. The operation of the control system when the gains have been reduced to achieve more stable operation is illustrated by the trace titled *Three-phase control system II*.

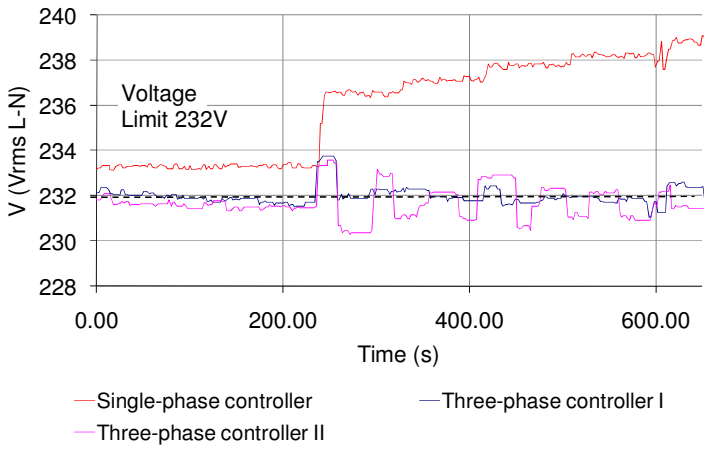


**Figure 6.31: Remote end voltages (phase A – node 6) with three—phase centralised voltage control – *Test D***

It can be seen in Figure 6.31 that the three-phase voltage measurement based control ensures that the defined voltage rise limit is on phase A of the LV network. In addition, this control system has been found to mitigate against voltage rise on phase B of the network also. It was found, however that identical controller implementations did not result in identical operation on each phase of the LV network due to asymmetries in the system.

In this control system there are more sources of failure in the system. Malfunctions in any of the remote measurement sensors and their associated communication system could result in errors or even failure in the operation of the system. However, as three voltage measurements are available to the control system a degree of redundancy could be included in a development of this control system.

The same observations apply to this control system as the previous control system, which integrates wind turbine and PV generation into the control system, with regard to scalability.

Communications traffic is again increased in this system is increased as three distributed voltage measurements are required. As in the system described in the previous section

both generators are curtailed and therefore the energy export of both PV and wind turbine generation is reduced when the remote end voltage violates the defined upper limit.

## 6.10 Centralised Power Flow and Voltage Control System

The design and development of voltage control systems of varying degrees of functionality and complexity are described in the previous sections. However, as established in chapter two, thermal limits are also a constraint that may be encountered when large concentrations of SSEG are installed on distribution networks. The design of a centralised power flow or current limit control system is described in this section that operates in parallel with one of the voltage control systems described in the previous sections. The centralised voltage control system with remote end measurement is modified so that thermal limiting is part of the functionality of the control algorithm. The same modifications could also be applied to the other earlier voltage control systems to extend their functionality.

Two PI controllers are deployed in parallel to control both voltage and current. As in the case of the three-phase voltage control algorithm, each phase has its own active voltage and current control system. A simplified block diagram of the phase A section of the control system is illustrated in Figure 6.33. The phase B and phase C sections of the control algorithm are identical.

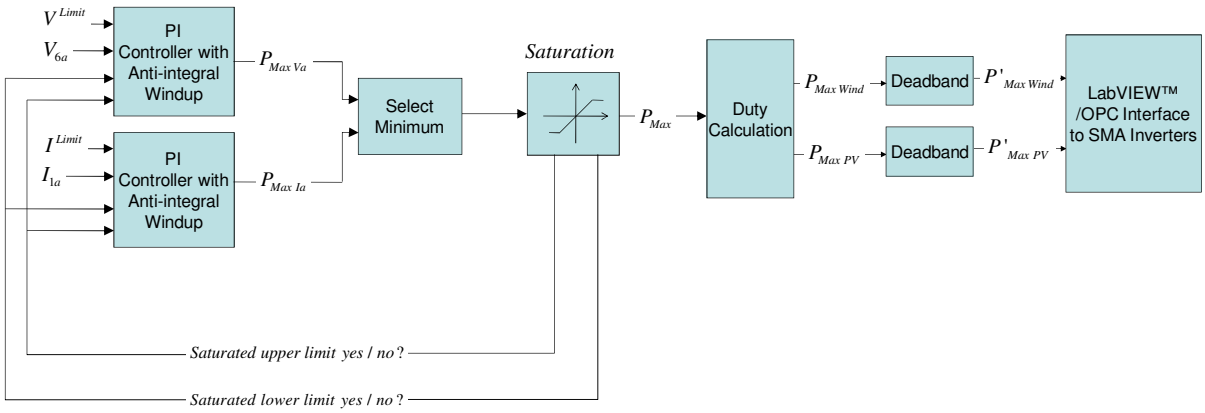


**Figure 6.32: Block diagram of phase A control scheme for current and voltage controlling centralised control system**

In order to evaluate the operation of the current limit scheme it was necessary to change the defined voltage limit programmed into the control system to 240V. This is because a voltage rise condition occurs in the Experimental SSEZ before there is a violation of the current limits using the limits defined previously for this testing program. Results illustrating the operation of the current limit scheme are shown in Figure 6.33. The controllers were tuned using the same Ziegler-Nichols method used earlier to tune the voltage controllers. Both sets of controller gains are successful in mitigating against the thermal limit violation. The control loop with the higher gains exhibits a more unstable response to the changing network conditions.

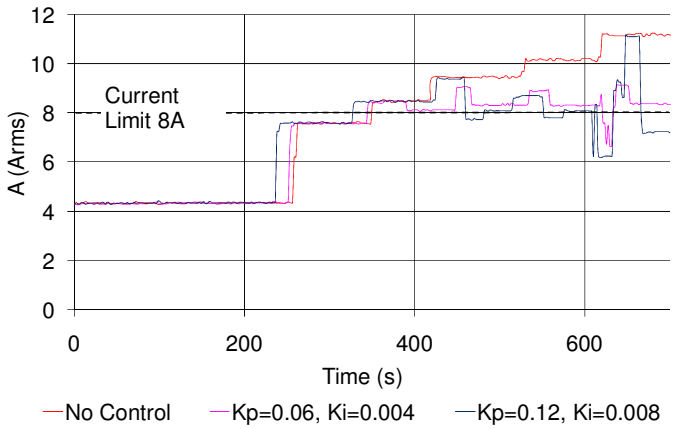


**Figure 6.33: Current limiting operation of combined voltage and thermal centralised control system (Phase A) – *Test E***

It can be seen in Figure 6.33, after appropriate tuning of the PI controllers, the control system control generation so that the defined current limits are observed on phase A. In addition, the control system has been found to control the generation on the system so that the thermal limits are observed on phase B and phase C of the LV network.

In this control system there more sources of failure in the system. Malfunctions in any of the remote measurement sensors and their associated communication system could again result in errors or even failure in the operation of the system.

As in the case with the voltage rise only system, this control system is capable of accommodating extra SSEG. Large numbers of extra SSEG or the addition of extra controllable SSEG may entail modifications to the control system.

Communications traffic is similar to the last voltage rise only control system. This is because the additional current measurement sensors are located locally (network connection emulator). As in the system described in the previous section both generators are curtailed and therefore the energy export of both PV and wind turbine generation is reduced when the current violated the defined upper limit.

## 6.11 Centralised Voltage Unbalance, Power Flow and Voltage Control System

In the previous section, the design and development of a centralised thermal and voltage control systems is described. This system monitors and controls each phase independently on a central control platform. Voltage unbalance is an inherently three-phase phenomenon and may require the co-ordination of the controllable resources of the three-phases to maintain system operation within statutory limits.

A scheme is proposed that utilises the thermal and voltage control systems developed in earlier sections. It has been shown previously that, in common with voltage rise, the remote end of a radial LV network is likely to experience the largest %VUF [8, 41]. Therefore it is proposed to control the voltages at the remote end of the network to reduce the %VUF measured on the LV network.

As %VUF increases the feedback control system will reduce the voltage limits on the network. The control systems developed previously will then act to curtail the generation on the network. The phase with largest magnitude of remote end voltage will be required to curtail the largest amount of generation. This will have the effect of reducing the %VUF as the differences in the magnitude of the phase-neutral voltages, of each of the phases, is reduced. The bandwidth of the voltage control loops is higher than the %VUF control loop which controls the voltage limit on the voltage loop. These loops form a PI set of PI cascade control loops [149]. A simplified block diagram of the system is illustrated in Figure 6.34.

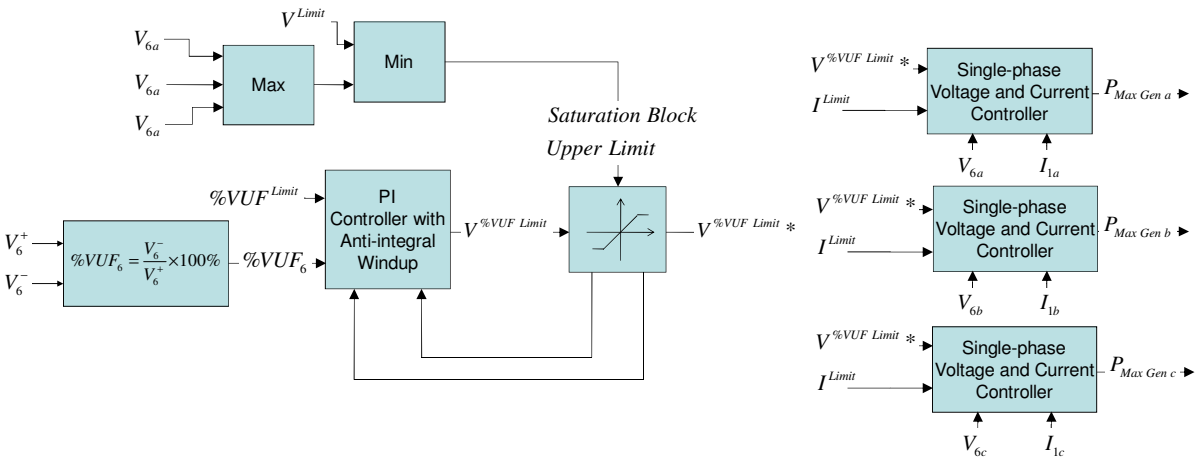


**Figure 6.34: Centralised %VUF, thermal and voltage control system for the Experimental SSEZ**

To investigate the operation of control systems based on this topology *Test F* detailed earlier in this chapter is used. As in the thermal control system investigation, the limits on voltage were relaxed as these are the first constraint encountered during this test. The results of an implementation of this control topology are illustrated in Figure 6.35.

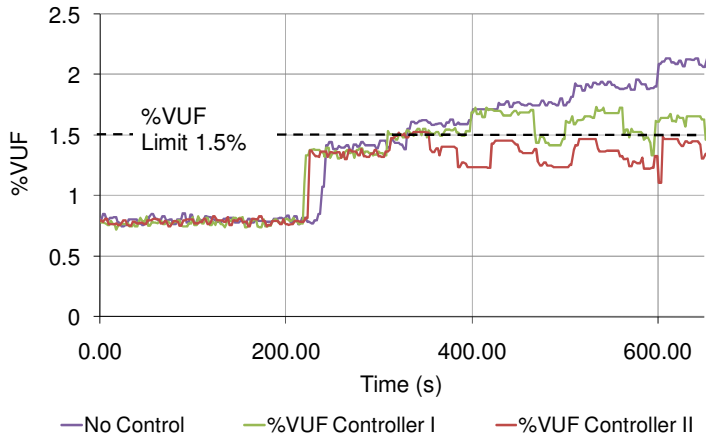


**Figure 6.35: %VUF control operation of %VUF, thermal and voltage centralised control system – *Test F***

The trace titled *%VUF Control system I* illustrates the operation of a first stage control system with the integrator disable logic feedback from the %VUF saturation block only. An improved response is observed however if feedback is also provided from the saturation blocks of each of the three voltage and current controller loops. The operation of this more advanced system is illustrated by the trace titled *%VUF Control system II.*

More advanced measurement sensors are required to realise this system. Phase and magnitude measurements are required to calculate the %VUF at the remote end of the LV network. This would also result in an increase in the communications requirements.

The reliability of this system is likely to be comparable to the systems described earlier with distributed measurement requirements.

As in the case of the earlier systems, this control system is capable of accommodating extra SSEG. Large numbers of extra SSEG or the integration of extra controllable SSEG into the control system may entail modifications to the control system.

As in the case of the system described in the previous section, both generators are curtailed and therefore the energy export of both PV and wind turbine generation is reduced when the %VUF violated the defined upper limit.

## 6.12 Conclusions

A series of centralised control systems are developed in this chapter which were developed incrementally from a single-phase current based, case based voltage control system until a three-phase control system, utilising a PI feedback based control system is developed. This system is capable of controlling the SSEG so that voltage, thermal and %VUF limits were observed.

Due to the nature of centralised control systems failures in hardware, communications or software may result in the malfunction or complete failure of the centralised control system. If reliability is a major consideration in the development of a control system, redundant systems may be used. Communications systems are particularly prone to failure as they may have to share infrastructure with other systems in an SSEZ to reduce costs. Control system which utilise localised measurement data to estimate system parameters also may be useful to mitigate against this danger.

It was determined that a certain amount of extra generation may be accommodated in an LV distribution network controlled by a centralised control system. However, large changes in the penetration level or distribution of SSEG could affect the performance of centralised control systems if no modifications are made to the control algorithm. Furthermore, if extra SSEGs are to be integrated into the control system then a change in the control system would be required. This would be very impractical if large numbers of SSEGs were connected incrememental ly in an LV distribution network. However, modularised designs may limit the requirement for extensive redevelopment of the control algorithms as SSEGs are connected to the LV distribution network under consideration.

The communications traffic in the centralised control architectures, examined in this chapter, is a function of the data acquisition system and the number of SSEGs integrated into the control system. In addition, the speed of the communications infrastructure, when implementing a distributed data acquisition system, has a large impact on the bandwidth of the feedback controllers within the control systems.

The renewable energy export of each control system architecture is dependent on how the duty of mitigating against the network constraint under consideration is divided. If this duty is taken by the generators at the remote end of the radial LV network, when controlling, voltage rise and percentage voltage unbalance, the renewable energy export is maximised. In an actual LV distribution network, however, owners of SSEG towards the remote end of the network would have a disproportionately reduced ability to generate renewable energy and could be penalised economically.

Due to time constraints operational goal functionality was not implemented in any of the centralised control systems. However, modifications to the power flow algorithm could be used to easily to achieve this functionality.

The control systems which used fewer, localised measurements could result in cheaper and more reliable systems when realised in an LV distribution network. However, to maintain acceptable operation in these systems while minimising sensor requirements the LV distribution network should be operated so that voltage unbalance is kept low. In addition, extra load and generation should be evenly distributed throughout the LV network so that the assumptions and idealisation used in the development of the controllers can be maintained. Otherwise it would be necessary to update these idealisations in the control system algorithm or alternatively more measurement sensors can be distributed throughout the network. Either option increases the overall cost of the control system. In addition, if SSEGs can be integrated into the control system in a modular way it would also increase the scalability of the system and reduce the cost of extending the centralised control system.

The next chapter will introduce a distributed control system developed to mitigate the same constraints as the centralised control systems developed in this chapter.

# 7 DESIGN AND LABORATORY IMPLEMENTATION OF A DISTRIBUTED CONTROL SYSTEM

## 7.1 Introduction

The previous chapter detailed the design and development of a centralised control system which ensures that voltages, power flows and voltage unbalance stay within the defined limits. In this chapter, the design and development of distributed control systems for the Experimental SSEZ is described. A distributed control system for the purposes of this research, as defined in chapter three, consists of a number of independent devices or control systems that appear to its users as a single system [85-86].

The criteria for evaluation of a distributed control system for the Experimental SSEZ, based on the literature reviewed in chapter three, are initially presented. The development approach, based on a distributed control framework for the SSEZ concept developed at Durham University, is then presented. This is followed by a description of the design and development of the distributed control systems. This description includes results illustrating the effect of their operation on the LV network of the Experimental SSEZ. Finally, conclusions are drawn from the implementation and operation of these distributed control systems on the Experimental SSEZ LV network and the implications of their possible deployment on LV distribution networks are identified.

## 7.2 Evaluation Criteria for Distributed Control Systems

To be consistent with the criteria proposed in the previous chapter, the following are again used in evaluating the operation of the distributed control system: -

- Ensure system operation within network constraints
- Resilience and reliability

- Scalability
- Communications requirements
- Renewable energy output
- Economic benefit to SSEG/ES/controllable load owners
- Cost and complexity

## 7.3 Development approach

The development approach utilises a framework for the development of an agent-based distributed control system developed by a colleague of the author at Durham University [14, 23-24, 103]. This approach was chosen as it provides a framework for mitigating the constraints identified previously in chapter two.

The initial distributed control system consists of first-stage agents which operate as simple local voltage controllers. These agents are then developed so that they are capable of interacting with other. The final distributed control system consists of a number of independently operating agents which are capable of interacting with each other to ensure that the defined network constraints are observed within the LV network.

### 7.3.1 Active network management techniques for Experimental SSEZ distributed control systems

Generation curtailment, load management and energy storage control are used as active network management techniques in the development of the distributed control systems detailed later in this chapter. Load management is used in the distributed control system as it is likely that the "plug and play" nature of an agent-based distributed control system would make it relatively easy to modify the operation of existing load with the addition of an agent enabling integration into the distributed control system. In addition, it is proposed to also use energy storage, as load management and energy storage control can

be realised simultaneously on the Experimental SSEZ. The following active network management techniques, previously described in chapter three, are not used in the development of distributed control systems for the Experimental SSEZ: -

1. Reactive power compensation – The effect of reactive power flow on the phase-neutral voltages of the Experimental SSEZ was found to be very small in common with many LV distribution networks.
2. OLTC control – The voltage at the terminals of the network connection emulator will not be controlled by an agent of a distributed control system. In an LV distribution network, this control function would not be directly available to the control system of an SSEZ. This is because secondary distribution transformers do not feature an OLTC.
3. Network reconfiguration – No control over the configuration of the LV network of the Experimental SSEZ is available at present.

### 7.3.2 Experimental SSEZ distributed control system development

An agent-based distributed control framework for the SSEZ concept, developed at Durham University by a colleague of the author, is used to ensure that defined voltage, thermal and voltage unbalance limits are observed during the dynamic operation of the Experimental SSEZ and enable operational goals [14, 23-24, 103].

Three types of agents have been identified previously, in order to satisfy the specific control requirements of an SSEZ and adhere to the specifications developed by the Foundation of Intelligent Physical Agents (FIPA) [150]: -

- Direct control agents - (Generator Agent, Consumer Demand Agent and Energy Storage Agent) use local measurements to directly control a power system entity (SSEG, ESU or controllable load) within the SSEZ [14, 23-24, 103].

- Indirect control agents - (Operational Goals Agent, Unbalance Agent and Thermal Limits Agent) use global measurements to indirectly control one or more power system entities within the SSEZ [14, 23-24, 103].
- Utility agents - (Agent Management System and Directory Facilitator) perform administrative duties in order to facilitate the efficient operation of the direct and indirect control agents and they are in alignment with FIPA specifications [14, 23-24, 103].

Initially, the agent systems are used to overcome steady-state voltage rise issues which are seen as the most likely limiting network constraint to the operation of SSEGs on radial LV networks [7, 9, 41]. The first-stage distributed control system for the Experimental SSEZ implements the following agents on the Experimental SSEZ using the LabVIEW™ visual programming environment, as illustrated in Figure 7.1: -

- Generator Agents (GAs) - one GA controlling the wind turbine generator emulator and one GA controlling the PV generator emulator [14, 23-24, 103].
- Consumer Demand Agent (CDA) - one CDA controlling the load emulator [14, 23-24, 103].
- Energy Storage Agent (ESA) - one ESA controlling the ESU emulator [14, 23-24, 103].

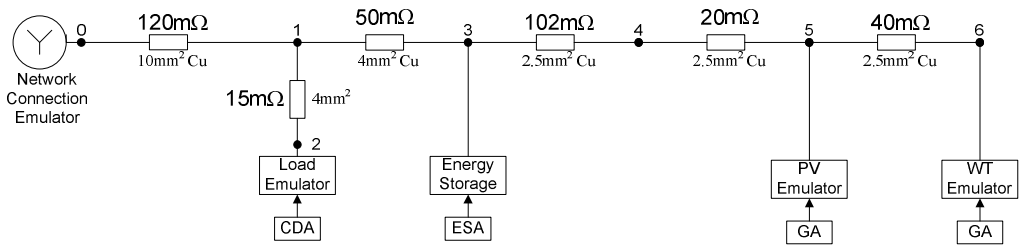


**Figure 7.1: First-stage agent-based distributed control system on the Experimental SSEZ**

Steady state voltage rise is mitigated by: (i) generation curtailment of wind turbine or PV generation through their respective GA; (ii) controlling the power import of the ESU through the ESA; and/or (iii) managing the controllable load through the CDA. The operation of each of the first-stage agents deployed individually on the system was investigated initially. Subsequent developments of this initial control system deploy multiple agents on the LV network to mitigate voltage rise conditions.

A simple communications and control structure that enables inter-agent communication was developed. The system was integrated into the control systems of each of the agents to enable collaborative operation. These are second-stage agents. Due to practical issues associated with the Experimental SSEZ only the following direct agent combinations were investigated: -

- GA (PV) and GA (WTG)
- GA (PV), GA (WTG) and CDA
- ESA and CDA

A combination of all four direct agents was not implemented due to the slow operation of the RS485 communications system when the ESU, PV generator emulator and wind turbine generator are controlled by the Experimental SSEZ communications system. The initial distributed control systems are voltage control systems and are therefore unable to ensure that the system observes the defined thermal and voltage unbalance limits. To enable this functionality indirect agents are added to the system [14, 23-24, 103]. The indirect agents utilised in the distributed control system of the Experimental SSEZ are: -

- Thermal Limits Agent (TLA – Indirect Agent) - the TLA controls the power flow at the network connection emulator to reduce the current flow so that thermal limits on the system are observed [14, 23-24, 103].

- Unbalance Agent (UA – Indirect Agent) – the UA indirectly balances the power flow across each of the three phases to reduce the percentage voltage unbalance factor below the defined limits [14, 23-24, 103].
- Voltage Agent[1] (VA – Indirect Agent) – the VA indirectly ensures that the voltages at the remote end of the network are within the defined limits.

These indirect agents interact with the direct agents using the same inter-agent communications system. The deployment of the agents in the final distributed control system is illustrated in Figure 7.2.

[1] A VA is not always required as GAs and ESAs may exist at the remote end of the network which enables voltage control. This agent could be required if generation or energy storage is connected to the LV network which are not integrated into the distributed control system.

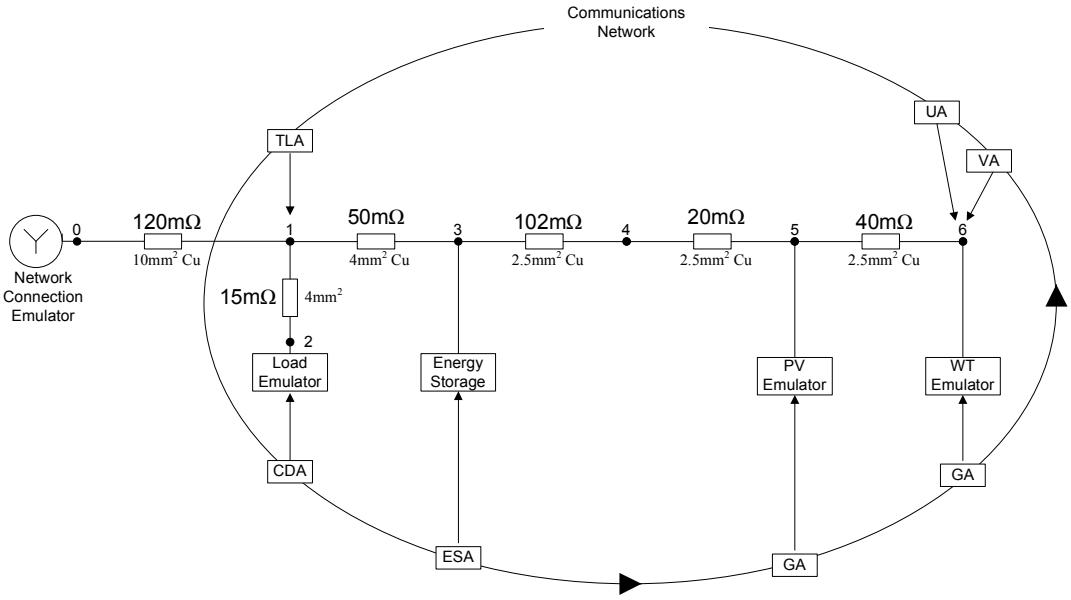


**Figure 7.2: Second-stage agent-based control approach for the Experimental SSEZ including inter-agent communication**

The thermal limit agent is located at node 1 as the most thermally stressed cable section is likely to be between node 0 and node 1 as observed previously [22, 41]. The voltage unbalance agent is located at 6 as the remote end of a radial LV network is likely to experience the largest voltage unbalance [8, 41].

These indirect agents have PI feedback controllers integrated into their control algorithm and are therefore susceptible to anti-integral windup effects that were discussed in chapter six. Therefore, anti-integral windup algorithms were devised for each indirect agent implementation.

## 7.4 Distributed Control System Evaluation Program

To assist development and evaluate the operation of the distributed control systems for the Experimental SSEZ, with regard to the observance of network constraints, an evaluation program was devised. As in the case of the centralised control system development, a successful system will ensure that excursions from the defined operational limits of the system will be minimised.

Three tests were developed that seek to investigate the performance of the distributed control systems with regard to voltage rise, thermal limits and voltage unbalance. The *Steady-state voltage rise test* seeks to investigate the operation of a distributed control system when generating and load conditions result in the voltages on the system exceeding their defined limits. No load is connected to phase B or phase C and generation is located at node 5 and node 6 of the LV network of the Experimental SSEZ.

The operation of distributed control systems that have a power flow control capability is investigated in the *Thermal limit test*. As in the *Steady-state voltage rise test* generation is connected to phase A only but similar load profiles are implemented all three-phases on the load emulator. This is to ensure that there is current flow in all three-phases during the test. In addition, this test has a longer duration than the *Steady-state voltage rise test* as it is used to evaluate the operation of the anti-integral windup algorithms proposed for the thermal limit agent. This is achieved by using generating and load profiles that return the LV network to a state where thermal limits are not violated even though there is now no control system intervention reducing generation or increasing load.

In the *Voltage unbalance test,* unbalanced conditions are recreated in the LV network of the Experimental SSEZ to investigate the operation of distributed control systems that have a voltage unbalance control capability. Generation and load in this case are now connected to phase C of the LV network as this has been shown in chapter five to result in the greatest values of percentage voltage unbalance factor. As in the case of the *Thermal limit test*, the generating and load profiles return the LV network to a state where percentage voltage unbalance limits are not violated even though there is now no control system intervention.

### 7.4.1 Steady-State Voltage Rise Test

As in the case of the steady-state voltage rise tests developed for the centralised control system the nominal phase-neutral voltage for this system is defined to be 225.5V and the defined voltage phase-neutral limit for this system is 232V.

Voltage limit violations occur on phase A of the LV network of the Experimental SSEZ during the operation of this test. All the generation is connected on phase A of the LV network. The PV generation emulator is connected at node 5 and the wind turbine generator emulator at node 6. Initially, the prime mover of the wind turbine generator emulator was instructed to operate at a speed that results in a power output of 0.4kW to the system, the PV generator emulator was instructed to export 1.5kW and the load imports approximately 0.8kW on phase A only. At time t = 230s, the prime mover of the wind turbine generator emulator was instructed to accelerate to a speed that resulted in the export of 1.2kW to the system as illustrated in Figure 6.7 (a). Load is connected to phase A only during this test. The power import of the load emulator and the power export of the PV generator emulator initially remain constant. At time t = 320s and at 90s intervals thereafter the load is reduced by approximately 0.2kW until the demand is reduced to zero as illustrated in Figure 6.7(b).

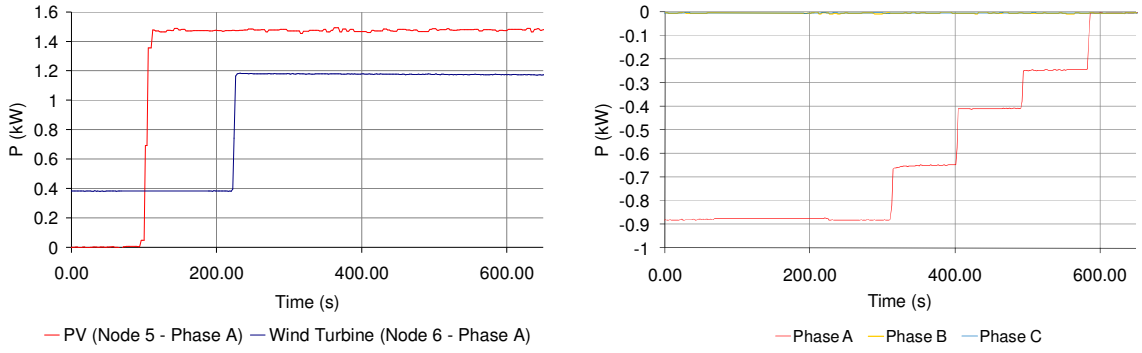


**(a) Generation** **(b) Load**

**Figure 7.3: Generation and load power flows for *Steady-state voltage rise test* (No control system deployed)**

The effect of the operation of these generation and load profiles on the remote end network voltages is illustrated in Figure 6.8. It can be seen that the voltage on phase A at node 6 now rises above the defined voltage limit of 232V.

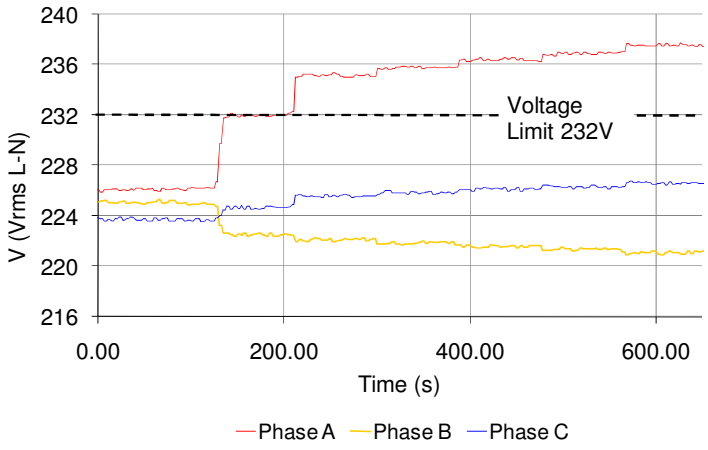


**Figure 7.4: Voltages at node 6 of Experimental SSEZ during *Steady-state voltage rise test* (No control system deployed)**

### 7.4.2 Thermal limit test

As in the case of the thermal limit test developed for the centralised control system the defined current limit for this system is 8A.

The centralised control system, developed in the previous chapter, utilises a thermal limiting algorithm that had direct access to the information on the saturation of the output

of the generators which enabled detection of integral wind-up. However, the indirect thermal limit agent (TLA) implemented has limited information about the status of each agent. This test therefore will also seek to investigate integral wind-up effects by emulating thermally onerous conditions and then reducing current flow so that these conditions are relaxed on the LV network of the Experimental SSEZ.

In the *Thermal limit test*, the PV and wind turbine generation are again connected on phase A of the LV network as in the *Steady-state voltage rise test*. The PV generation is again connected at node 5 and the wind turbine generation at node 6. Initially, the prime mover of the wind turbine generator emulator was instructed to operate at a speed that results in a power output of 0.4kW to the system, the PV generator emulator was instructed to export 1.5kW and the load imports approximately 0.9kW on all three phases. At time t = 230s the prime mover of the wind turbine generator emulator was instructed to accelerate to a speed that resulted in the export of 1.2kW and at time t = 600s it is decelerated to a speed that results in a power export to the system of 0.4kW as illustrated in Figure 7.5(a). At time t = 320s and at 90s intervals thereafter the load is reduced by approximately 0.2kW until the demand is reduced to zero as illustrated in Figure 7.5(b). At time t = 680s the load is increased again, at 90s intervals, in steps of approximately 0.2kW until the load on all three-phases increases to 0.9kW. This extension to the test sequence is included to ensure that the TLA removes generation curtailment, load management and energy storage import when they are no longer required. This is to maximise renewable energy output, minimise customer load management and remove the requirement of energy storage import which is finite.

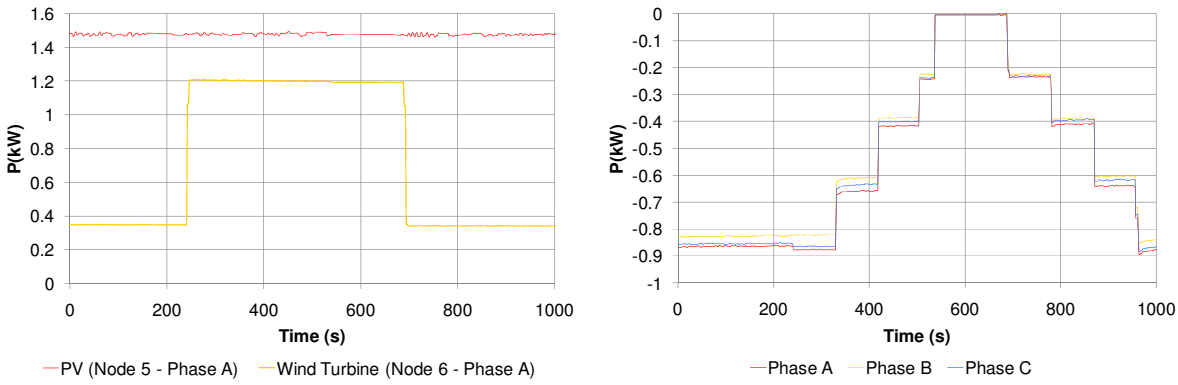


**(a) Generation** **(b) Load**

**Figure 7.5: Generation and load power flows for *Thermal limit test* (No control system deployed)**

Figure 7.6 illustrates the effect of the operation of the PV generator emulator, wind turbine generator emulator and load emulator on the current of the cable section under consideration, without active network management in the system. It can be seen that the current in this case exceeds the defined current limit of 8A on phase A following the increase in generation and then decreases following the decrease in generation and increase in load.

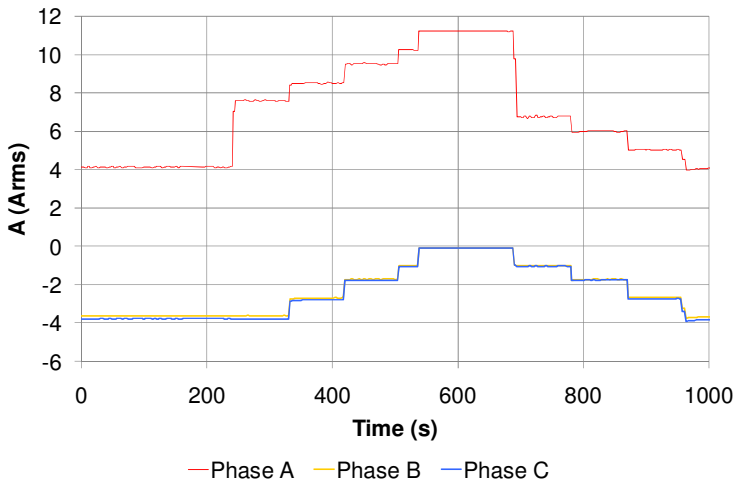


**Figure 7.6: Current at node 1 of Experimental SSEZ during *Thermal limit test* (No control system deployed)**

### 7.4.3 Voltage unbalance test

As in the case of the voltage unbalance test developed for the centralised control system the defined percentage voltage unbalance factor (%VUF) for this system is 1.5%.

A similar test sequence to that of the *Thermal limit test* was devised for the *Voltage unbalance test*. In this test however, the load and generation are all connected to phase C of the Experimental SSEZ LV network as this has been shown in chapter five to result in the highest values of percentage voltage unbalance.

As in the case of distributed thermal limit strategies described earlier, the indirect voltage unbalance agent may have limited information about the status of each individual local agent. This test therefore will also seek to investigate integral wind-up effects by emulating scenarios with high values of percentage voltage unbalance conditions and then changing the system conditions so that the percentage voltage unbalance values in the LV network are reduced.

The PV generation is again connected at node 5 and the wind turbine generation at node 6. Both generators in this case export active power to phase C of the Experimental SSEZ LV network. Initially, the prime mover of the wind turbine generator emulator was instructed to operate at a speed that results in a power output of 0.4kW to the system, the PV generator emulator was instructed to export 1.5kW and the load imports approximately 0.9kW on phase C. At time t = 230s the prime mover of the wind turbine generator emulator was instructed to accelerate to a speed that resulted in the export of 1.2kW and at time t = 650s it is decelerated to a speed that results in a power export to the system of 0.4kW as illustrated in Figure 7.7(a). At time t = 320s and at 90s intervals thereafter the load is reduced on phase C by approximately 0.2kW until the demand is reduced to zero as illustrated in Figure 7.7(b). At time t = 650s the load is increased again, at 90s intervals, in steps of approximately 0.2kW until the load level returns to 0.9kW.

This extension to the test sequence is again included to ensure that the voltage unbalance agent removes generation curtailment, load management and energy storage import when they are no longer required to ensure satisfactory system operation. This is to maximise renewable energy output, minimise customer load management and remove the requirement of energy storage import which is finite.

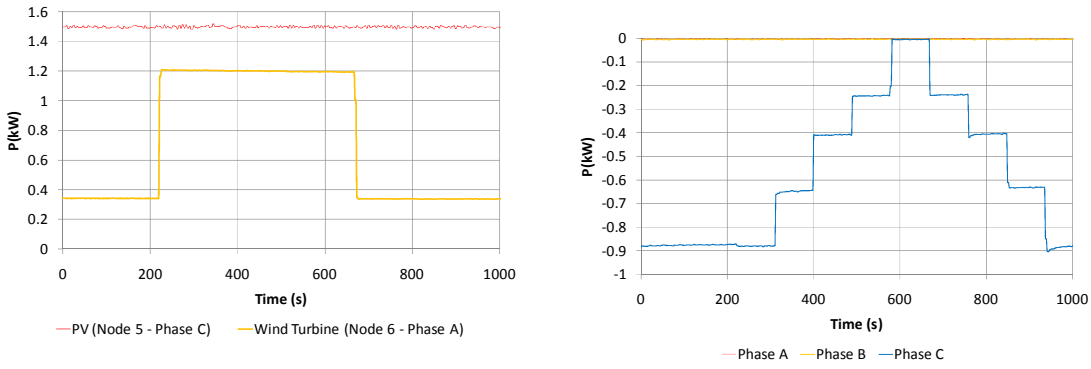


**(a) Generation** **(b) Load**

**Figure 7.7: Generation and load power flows for *Voltage unbalance test* (No control system deployed)**

Figure 7.8 illustrates the effect of the operation of the PV generator emulator, wind turbine generator emulator and load emulator on the %VUF observed on the LV network of the Experimental SSEZ without active network management in the system. It can be seen that the %VUF in this case exceeds the defined current limit of 1.5% following the increase in generation and then reduces as the generation is decreased. The highest values of %VUF are at the remote end of the LV network as expected. As the load is increased the %VUF is also decreased as the load on the system is equalising the generation.

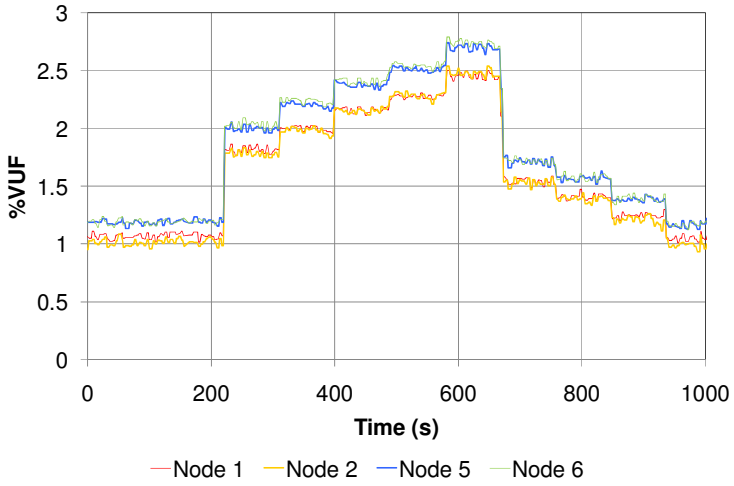


**Figure 7.8: %VUF at node 6 of Experimental SSEZ during *Voltage unbalance test* (No control system deployed)**

## 7.5 Initial Direct Agent Development and Laboratory Implementation

In chapter three, distribution network control system architectures have been classified as either centralised or distributed. However, many distributed control system architectures have characteristics of both classes. An example of this is the Multi-Agent System (MAS) system developed at NTUA which consists of local controllers and also a Microgrid centralised control system (MGCC) which operates as an interface between the DNO and/or the operator of the electricity system [15-18].

In this section, a series of first-stage direct agents which react to local voltage conditions are developed. This is a highly distributed system with no inter-agent communication. They operate autonomously to mitigate violations of the defined upper voltage limit in the LV network. As the agents are controlling single-phase SSEG, ESUs or controllable load without any inter-agent communication they are unable to co-operate to ensure that thermal and voltage unbalance limits are adhered to.

### 7.5.1 First-Stage Generator Agent

The initial, first-stage generator agents (PVGA I and WGA I) monitor the local voltage and then instruct the grid interface inverters of the wind turbine emulator or PV generator emulator to curtail active power export to achieve satisfactory system operation. In this implementation, the wind turbine and PV generation are located at node 5 and node 6 respectively. Load is connected at node 2 as per the centralised control system investigation.

This first-stage agent implementation is realised using a PI controller and a deadband block which are deployed in a control loop in LabVIEW™ on the hosting PC. The deadband block is used to reduce the number of control actions executed by the communications system and improve the overall operation of the Experimental SSEZ. A simplified block diagram of a first-stage generator agent is illustrated in Figure 7.1.

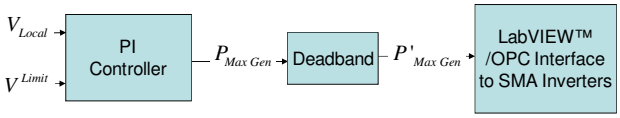


**Figure 7.9: Simplified block diagram of first-stage generator agent (GA I)**

A PI controller utilising the integrator disable strategy, described in chapter six, for anti-integral wind up is integrated into the GA I algorithm. During normal operation the measured voltage is below the defined limit and the error is negative. As the gains of the controller are negative the output of the controller eventually saturates to installed capacity. The agent will therefore instruct the grid interface inverter to export maximum generation. In this mode of operation the anti-integral windup system disables addition to the integrator but allows subtraction.

During a voltage limit violation the error becomes positive. As the gains of the controller are negative the proportional part of the controller will become negative and the integral section reduces in value. As addition to the integrator is disabled when the voltage is

below the defined voltage limit the value of the integrator is not so large that it does not keep the output of the controller saturated and can therefore quickly assist in the control of the output. The agent will therefore instruct the inverter interface to curtail the generation. Once the controller output leaves the saturated area of operation the anti-integral windup system allows addition and subtraction to the integrator of the PI controller.

The gains for the PI controller for the agents were established by using the Ziegler-Nichols method. Figure 6.27 compares the opeation of the first-stage wind turbine generator agent (WGA I) and PV generator agent (PVGA I) operating individually on the Experimental SSEZ to mitigate the steady-state voltage rise.

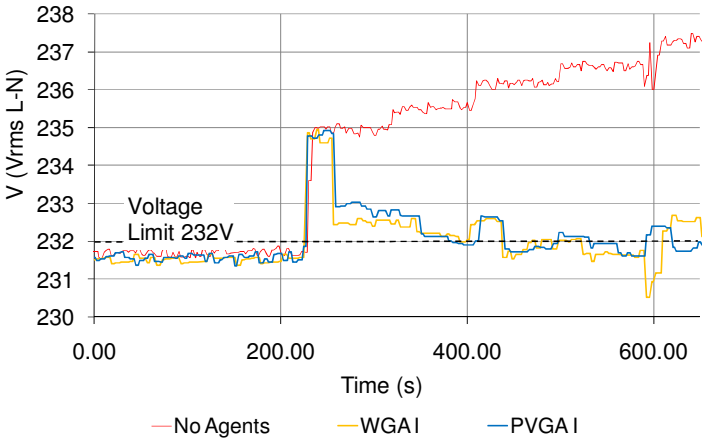


**Figure 7.10: Remote end voltage (phase A) of Experimental SSEZ LV network with first-stage generator agents (PVGA I and WGA I) – *Steady-state voltage rise test***

To control the voltage below the upper limit of 232V requires the wind turbine and PV generation to be constrained to very low power levels as illustrated in Figure 7.11. The power export of the wind turbine generator is reduced by 1.1kW to 0.1kW by the end of the test which is a 91% reduction in generation. Moreover, as the PV generation is not located at the remote end its active power export is reduced by a larger amount, 1.4kW

from 1.5kW to 0.1kW which is a 93% reduction in generation. It can be seen that neither generator cannot be reduced much further if higher voltages were present.

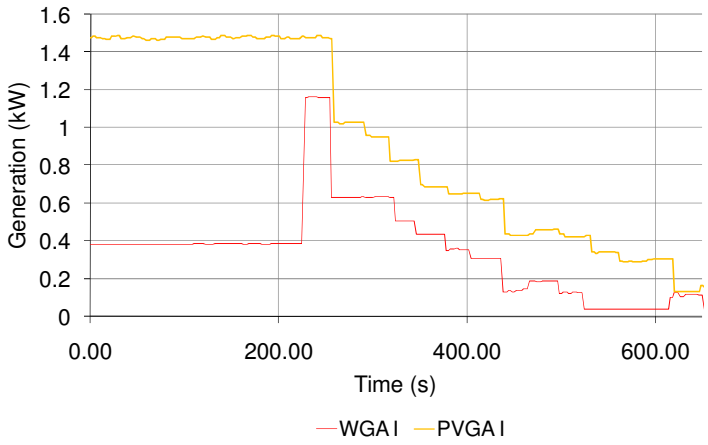


**Figure 7.11: Active power export of wind turbine generation when controlled by WGA I and PV generation when controlled by PVGA I– *Steady-state voltage rise test***

### 7.5.2 First-Stage Energy Storage Agent (ESA I)

The initial, first-stage energy storage (ESA I) is similar to the generating agent described previously but in this case power is imported to charge the energy storage device. ESA I monitors the local voltage and then instructs the grid interface inverter of the energy storage unit to increase the power import until satisfactory system operation is achieved. This has the effect of charging the energy storage device. In this implementation the energy storage unit is connected at node 3 of the LV network. In contrast to generation curtailment, the energy storage unit cannot be charged indefinitely and therefore ESA I will instruct the inverter of the grid interface inverter to stop charging the energy storage once the energy stored by the device reaches a threshold level. In this implementation the State-of-Charge (SOC) is monitored by the agent and once this goes above a threshold value charging stops.

This first-stage agent implementation of an energy storage agent is again realised using a PI controller and deadband block algorithm which is similar to the first-stage generator

agent described previously. The PI controller is modified to include the SOC monitor, stopping the charging of the battery when the threshold upper SOC level is reached. In addition, the control algorithm also interacts with the PI loop so that integral windup effects are minimised. A simplified block diagram of ESA I is illustrated in Figure 7.12.

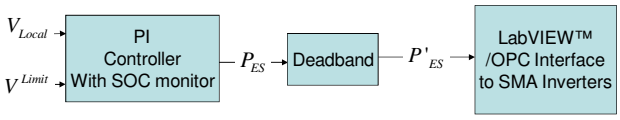


**Figure 7.12: Simplified block diagram of first-stage energy storage agent (ESA I)**

The voltage at node 3 does not exceed the defined upper limit during the *Steady-state voltage rise test,* as the energy storage system is located at node 3. ESA I therefore does not instruct the grid interface inverter to import active power even though the remote end voltage exceeds the defined upper limit as illustrated in Figure 7.13.

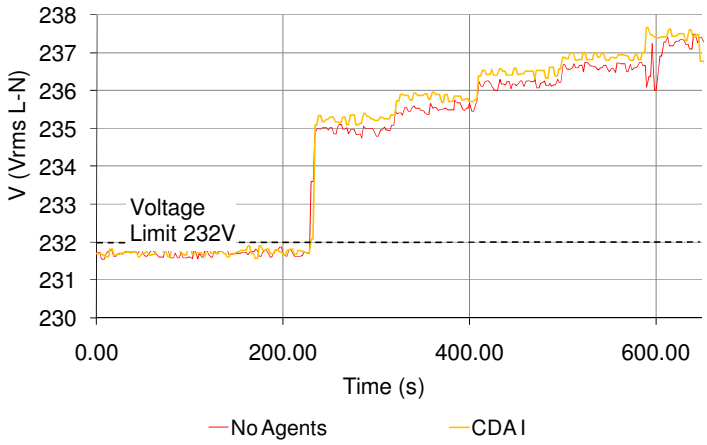


**Figure 7.13: Remote end voltage (phase A) of Experimental SSEZ LV network with first-stage energy storage agent (ESA I) – *Steady-state voltage rise test***

### 7.5.3 First-Stage Consumer Demand Agent (CDA I)

The initial, first-stage consumer demand agent (CDA I) is very similar to the operation of ESA I described previously. CDA I monitors the local voltage and then aims to manage controllable load to restore satisfactory system operation. In this implementation all load is located at node 2 of the LV network. This load is three-phase with controllable load, under the management of CDA I, is available on phase A.

In LV distribution networks short-term controllable load are likely to be thermostatically controlled loads which consumers could leave to be managed by an autonomous controller. These thermostatically controlled loads however are limited in the time that they can be switched or else this could result in temperatures of air, water or refrigeration leaving the temperature limits defined by the consumer.

This first-stage agent implementation of a CDA is again realised using a similar PI controller and deadband block algorithm which was used in the first-stage agents described previously. This PI controller is modified to a timer which mimics the effect of a thermostatically controlled load for demand side management. A simplified block diagram of CDA I is illustrated in Figure 7.14.


**Figure 7.14: Simplified block diagram of first-stage consumer demand agent (CDA I)**

The voltage at node 2 does not exceed the defined upper voltage rise limit during the *Steady-state voltage rise test.* As the load managed by CDA I is located at node 2, CDA I therefore does not switch in controllable load even though the remote end voltage exceeds the defined upper limit. Figure 7.15 illustrates the operation of CDA I and the operation of the system without any agents on the system.

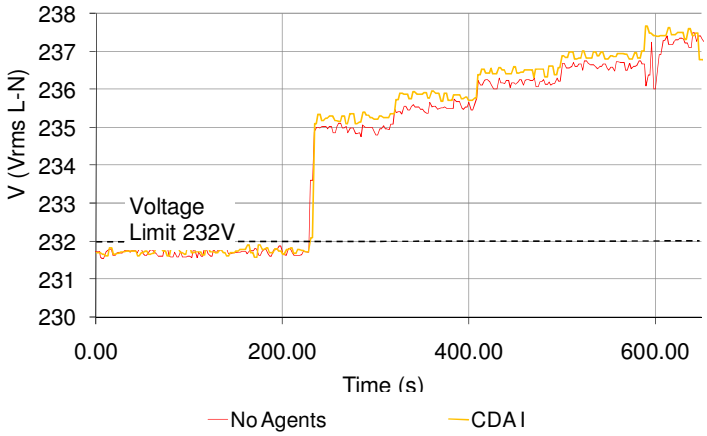


**Figure 7.15: Remote end voltage (phase A) of Experimental SSEZ LV network with first-stage consumer demand agent (CDA I) – *Steady-state voltage rise test***

### 7.5.4 Multi-agent deployment on LV network (First-stage agents)

The initial, first-stage generator agents developed earlier are deployed on the Experimental SSEZ at the same time to investigate their combined operation. In the previous section it was shown that using this control system architecture, only the agent systems at the remote end of the network (PVGA I and WGA I) were able to ensure that the voltage was reduced below the defined limits.

The agents were initially not modified from their previous implementation on their own in the LV network and therefore the agent controller gains were the same as in the

previous implementation. The trace titled *PVGA I & WGA I* in Figure 7.16 illustrates the combined operation of the generator agents to mitigate steady-state voltage rise. An oscillatory response is now observed on the system which was not apparent when each of these agents were deployed individually on the Experimental SSEZ. The gains on both controllers were revised to dampen the response of the overall voltage control system. This response is illustrated in the trace titled *PVGA I and WGA I (Revised Gains).* As previously, the gains of the controllers were determined using the Ziegler-Nichols method.

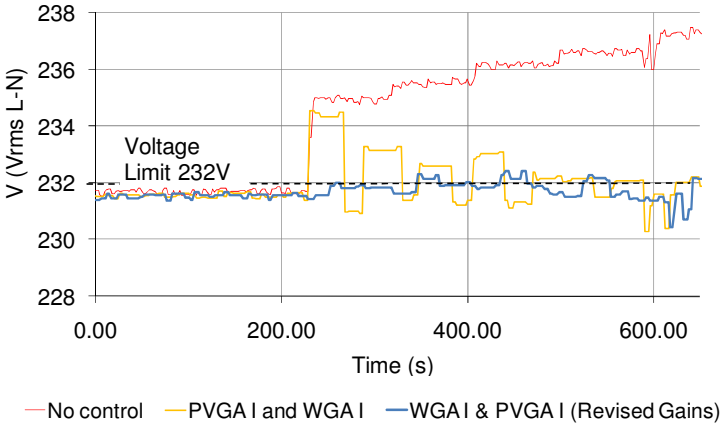


**Figure 7.16: Remote end voltage (phase A) of Experimental SSEZ LV network with both first-stage generator agents implemented (PVGA I and WGA I) – *Steady-state voltage rise test***

To control the voltage below the upper limit of 232V requires the wind turbine and PV generation to be constrained as illustrated in Figure 7.17. The duty of active power generation curtailment between the two SSEGs is shared. This is not equitable however as the agent at the remote end of the network (WGA I) measures a higher voltage than the agent that is closer to the network connection emulator (PVGA I). Wind turbine active power export is reduced from 1.2kW to about 0.2kW which is a reduction of 83% in generation when the original gains are used. PV active power export is reduced from 1.5kW to 1.2kW which is a reduction of 20%. The duty of mitigating the voltage rise is

even more inequitably shared when the gains are reduced to dampen the response. Wind turbine active power export is reduced from almost zero and PV generation remains at 1.5kW. This response is due to the operation of the dead-band resulting in no initial response from the PVGA I resulting in WGA I taking the duty of mitigating the voltage rise.

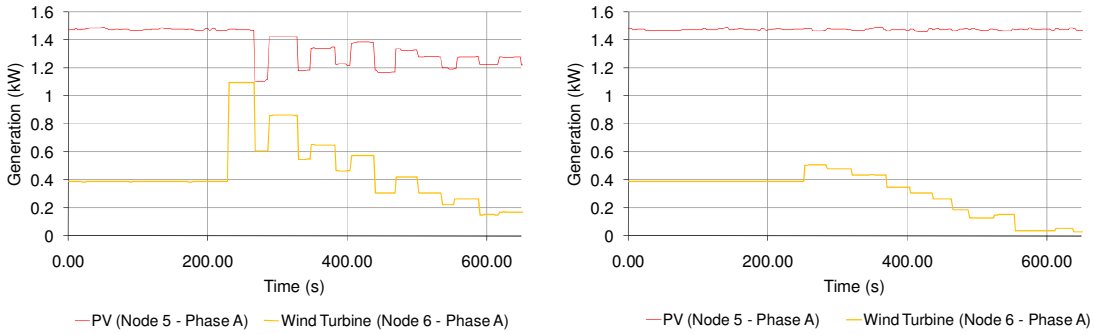


**(a) (Standard)** **(b) (Revised Gains)**

**Figure 7.17: Active power export of wind turbine and PV generation when controlled by WGA I and PVGA I (Combined operation) – *Steady-state voltage rise test***

### 7.5.5 Discussion

Both the generator agents were able to restore system operation that gave satisfactory voltage excursions. By contrast, the energy storage and consumer demand agents were unable to achieve this but this was not attributable to the agent operation but was in fact a function of their location on the LV network. If either of these agents were located near the remote end of the network they may have been able to control remote end voltage. A limitation of energy storage systems and demand side management systems is that they can only act to control voltage for a finite period of time. In the case of the energy storage agent this is governed by the SOC of the battery and in the case of the consumer demand agent the limitations of the thermostatic loads. In addition, the combined operation of agents operating autonomously is different from when they are operating on their own in the Experimental SSEZ.

The response of the distributed control system became more oscillatory after an extra agent is introduced although in this instance the system did not become remain oscillatory for the duration of the test. Reducing the gains on both agents damped the response of the system. It can be seen therefore that a limited number of extra SSEGs may be added but modifications to the gains of the PI controllers of the agents may be required if many agent controlled SSEGs are added.

There is no communication system in these architectures as the voltage measurement and control of the SSEZ entity is local. These distributed control systems are likely therefore to be rugged and reliable if they were deployed on an LV distribution network.

When multiple agents were deployed on the system the SSEG at the remote end bore the largest duty in generation curtailment. This is better than sharing the duty equally among all the generators from an export of renewable energy point of view. This is because the SSEG at the remote end has the greatest impact on voltage rise as stated previously. As before, however, the owner of an SSEG at the remote end would be disproportionately affected economically as their ability to export renewable energy would be less than a consumer nearer the network connection point.

In the next section, an inter-agent communication system is proposed to enable second-stage agents interact so they can act collaboratively to reduce the voltages on the system below the defined limits. This will enable a more equitable sharing of the duty of mitigating voltage rise. In addition, the system will enable the ESA and CDA to participate in restoring satisfactory system operation even though the voltage measured by these agents does not violate the defined limit. The impact that this collaborative operation of the developed agents on the operation of the LV network is then examined.

## 7.6 Design of Agent Communication System for Experimental SSEZ

The droop operation proposed in [17-18, 135, 151] is used to ensure power balance within an islanded area of LV network. As described in chapter six this operation is analogous to the operation of primary control on large scale power systems. This is not useful however when considering the grid connected LV network of an SSEZ where the frequency is fixed to that of the grid. In [15-18, 152], communications protocols between agents based on FIPA [150] compliance is proposed. In addition, in the agent ontology proposed by a colleague of the author at Durham University, a FIPA compliant inter-agent communications structure is proposed [14, 23-24, 103].

In this work, however a simpler solution is proposed that is inspired by the droop operation proposed for the grid interfaced inverters in [17-18, 135, 151] and the secondary control structure of a large-scale power system [153]. In this system, each agent creates a pseudo-frequency ($f_n$) which is available to all agents in the system. If this pseudo-frequency is greater than 50Hz system frequency ($f_0$) the agents operate to reduce generation.

However, many pseudo-frequencies within the distributed control system may exist. To arbitrate, the pseudo-frequency with the largest deviation from $f_0$ is used by all agents as an input to their PI based inter-agent control system. Secondary control systems in large-scale power systems also utilise PI based controllers to bring frequency back to 50Hz after the operation of primary frequency control [153]. The difference in this implementation is that the PI control is distributed and is part of the functionality of each direct agent. A block diagram of the control stage of a second-stage generator agent is illustrated in Figure 7.18.

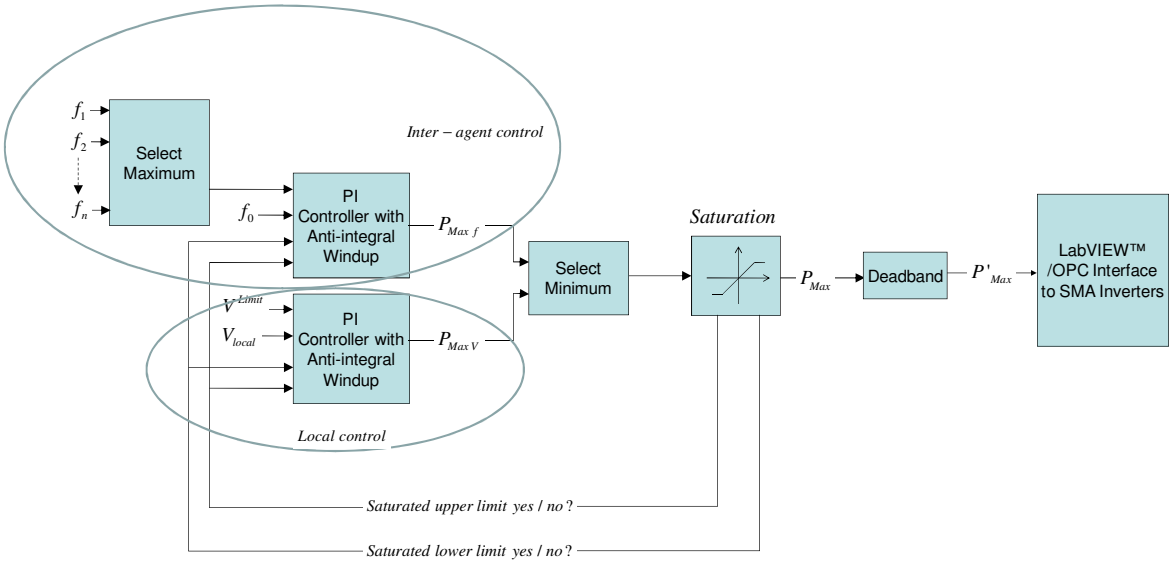


**Figure 7.18: Simplified block diagram of second-stage generator agent control system**

The initial objective of this second-stage distributed control system is to more equitably distribute the duty of mitigating the violation of the network constraints in the LV network. To achieve this it is proposed that the gains of the secondary controller of the agent are multiples of base proportional and integral gains. The multiplying factors are based on the rated active power output of the generation, the rated active power import of the energy storage or the rating of the controllable load under the control of each direct agent.

The pseudo-frequency generated by each agent is dependent on what type of agent is under consideration. The direct agents relate the pseudo-frequency to the local voltage. If for example the local voltage goes above the defined limit then the pseudo-frequency will rise above $f_0$ as illustrated by the block diagram in Figure 7.19.

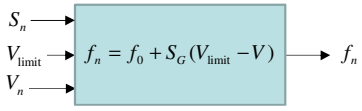


**Figure 7.19: Block diagram of pseudo frequency calculator for direct agents**

## 7.7 Second-Stage Direct Agent Development (Collaborative operation)

In this section three different agent deployments are considered to investigate the operation of the communications system and collaborative operation of the agents in the distributed control system for the Experimental SSEZ. These are second-stage agents employing the inter-agent communication and control algorithms described in the previous section. The direct agents investigated in this section are: -

1. PVGA II – Second-stage PV generation agent
2. WGA II – Second-stage wind turbine generation agent
3. CDA II – Second-stage consumer demand agent
4. ESA II – Second-stage energy storage agent

The PVGA II and WGA II are not used in conjunction with the ESA II agent as it has been found that simultaneous control of all three grid tied inverters in the Experimental SSEZ result in greatly degraded performance of the control and data acquisition systems of the Experimental SSEZ.

### 7.7.1 PV and wind turbine generation agent deployment (Collaborative operation)

The second-stage generator agents are both deployed on the Experimental SSEZ to investigate their combined operation. Figure 7.20 illustrates the collaborative operation of the second-stage PV Generator Agent (PVGA II) and Wind turbine Generator Agent (WGA II) to mitigate the steady-state voltage rise. The gains for the inter-agent PI controllers for each agent were again determined by using the Ziegler-Nichols method.

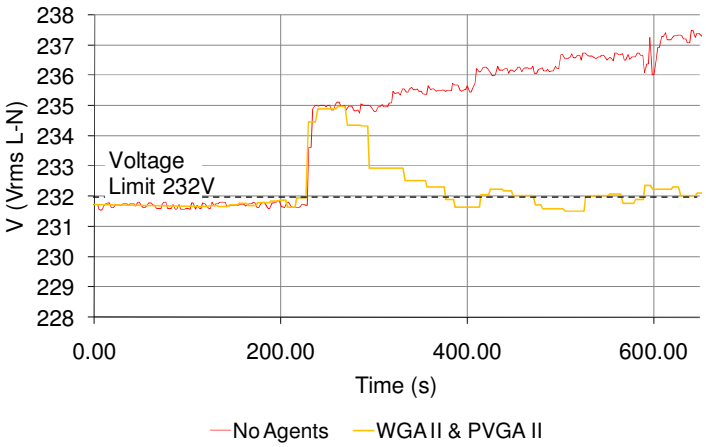


**Figure 7.20: Remote end voltage (phase A) of Experimental SSEZ LV network with both first-stage generator agents implemented (PVGA II and WGA II) – *Steady-state voltage rise test***

To control the voltage below the upper voltage limit of 232V the wind turbine and PV generation is constrained as illustrated in Figure 7.21. The duty of active power generation curtailment between the two SSEGs is more equitably shared than when the first-stage agents were deployed together in section 7.5.4. This collaborative operation of the direct agents results in PV generation reducing from 1.5kW to 0.8kW and the wind turbine generation from 1.2 kW to 0.6kW, which is a reduction of 50% in both cases, by the end of the *Steady-state voltage rise test*.

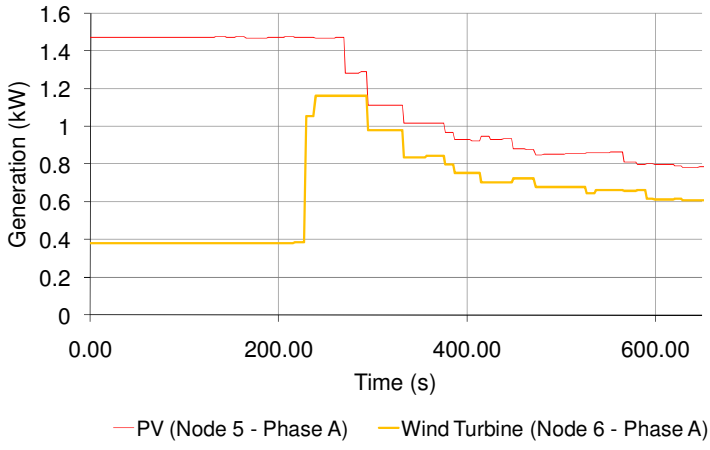


**Figure 7.21: Active power export of wind turbine and PV generation when controlled by WGA II and PVGA II (Collaborative operation) – *Steady-state voltage rise test***

### 7.7.2 PV and wind turbine generation and consumer demand agent deployment (Collaborative operation)

The second-stage generator agents and the consumer demand agent are all deployed on the Experimental SSEZ to investigate their combined operation. As the second-stage consumer demand agent (CDA II) is also capable of interacting with the other agents it is able to participate in sharing the duty of mitigating voltage rise. Figure 7.22 illustrates the collaborative operation of PVGA II, WGA II and CDA II to mitigate the steady-state voltage rise. The gain sets for the inter-agent PI controllers for the agents were kept from the previous system.

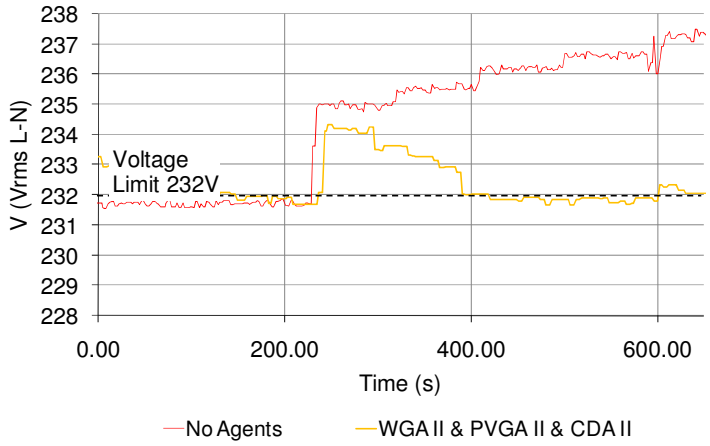


**Figure 7.22: Remote end voltage (phase A) of Experimental SSEZ LV network with both second-stage generator agents and consumer demand agent implemented (PVGA II, WGA II and CDA II) – *Steady-state voltage rise test***

To control the voltage below the upper voltage limit of 232V requires the wind turbine and PV generation to be constrained and an increase in the controllable load as illustrated Figure 7.23 and Figure 7.24. The duty of active power generation curtailment between the two SSEGs is equitably shared as in the previous example. This collaborative operation of the direct generator agents results in PV generation reducing from 1.5kW to just over 0.8kW and the wind turbine generation from 1.2 kW to 0.65kW, which is again a reduction of just less than 50%, by the end of the *Steady-state voltage rise test*. The

generation is not curtailed as much as in the previous example as CDA II also manages the controlled load to reduce the remote end voltage.

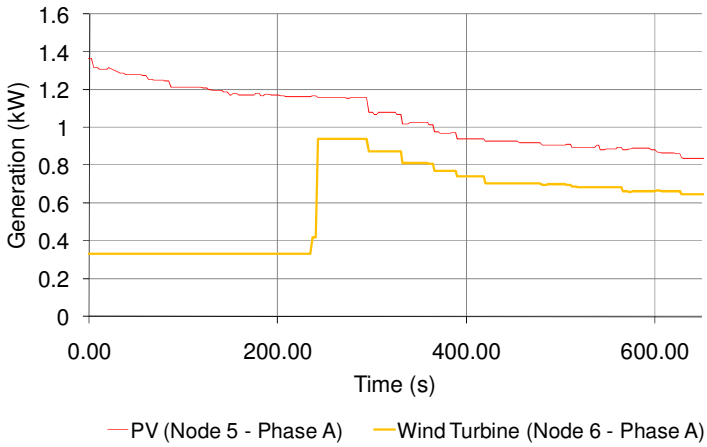


**Figure 7.23: Active power export of wind turbine and PV generation when controlled by WGA II, PVGA II and CDA II distributed control system (Collaborative operation) – *Steady-state voltage rise test***

In Figure 7.24 the effect of DSM controlled by CDA II is illustrated by the trace titled *Base Load and DSM*. The load without the intervention of a distributed control system is illustrated by the trace titled *Base Load.* Initially, no load is required to control the voltage. At time t = 70s, 0.25kW of controllable load is switched in to control the voltage at the remote end of the network. At t = 400s this load is increased to 0.5kW as more generation curtailment and load are required to control the remote end voltage below the defined limit. At t = 600s the DSM drops to 0.25kW as the control system estimates that the remote end voltage violation has disappeared and DSM is reduced.

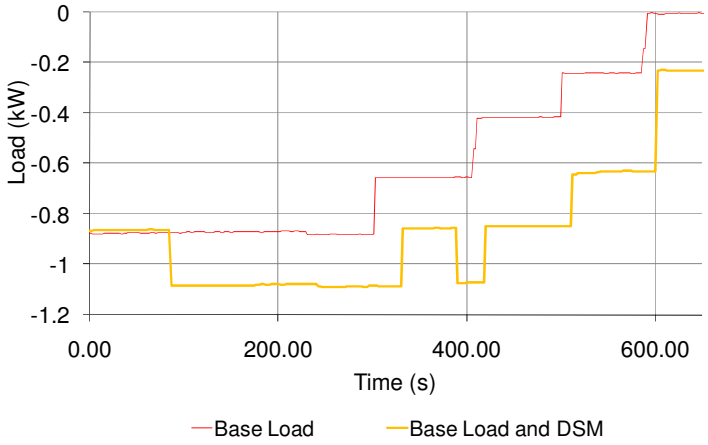


**Figure 7.24: Active power import of base load and base load and DSM when controlled by WGA II, PVGA II and CDA II distributed system (Collaborative operation) – *Steady-state voltage rise test***

### 7.7.3 Consumer demand and energy storage agent deployment (Collaborative operation)

The second-stage energy storage agent and the consumer demand agent are deployed on the Experimental SSEZ to investigate their combined operation. This implementation does not successfully control the remote end voltage below the defined limit. This is because the voltages at node 2 or node 3 do not exceed the defined upper voltage rise limit during the *Steady-state voltage rise test.* As the load managed by CDA II is located at node 2, CDA II therefore does not switch in controllable load even though the remote end voltage exceeds the defined upper limit. Similarly, as the energy storage unit managed by ESA II is located at node 3, ESA II does not instruct the grid tied inverter to import energy from the LV network and charge the battery even though the remote end voltage exceeds the defined upper limit. This behaviour is illustrated by the trace titled *ESA II & CDA II* in Figure 7.25. In order to illustrate the collaborative operation of these two agents another simple agent is introduced which monitors remote end voltage and interacts with other agents and is designated a Voltage Agent (VA). The collaborative operation of these three agents is illustrated by the trace titled *ESA II & CDA II & VA* in Figure 7.25.

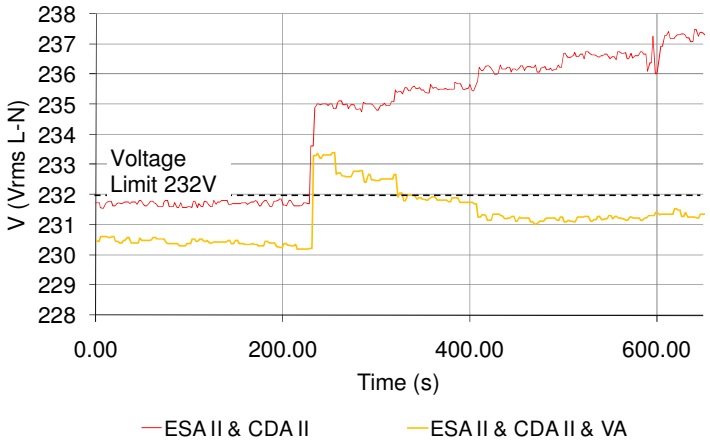


**Figure 7.25: Remote end voltage (phase A) of Experimental SSEZ LV network with first-stage consumer demand agent (CDA I) – *Steady-state voltage rise test***

As both ESA II, CDA II and VA operate collaboratively to control the voltage at the remote end by increasing the power imported into the energy storage system and increasing controllable load, no renewable energy is curtailed during this test as illustrated in Figure 7.26.

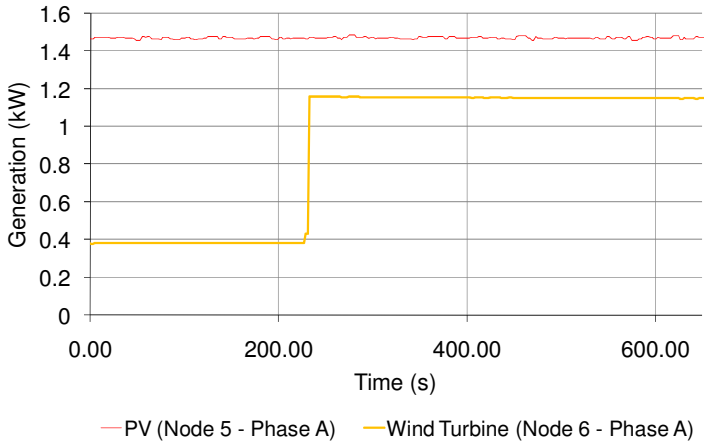


**Figure 7.26: Active power export of wind turbine and PV generation with distributed control system with ESA II and CDA II (Combined operation) – *Steady-state voltage rise test***

In Figure 7.27 the effect of DSM controlled by CDA II is illustrated by the trace titled *Base Load and DSM*. The load without the intervention of a distributed control system is illustrated by the trace titled *Base Load.* The energy imported by the energy storage system which is controlled by ESA II is illustrated by the trace titled *Energy Storage.*

Initially, 0.25kW of load is required to control the voltage and about 0.1kW is imported by the energy storage system. As the test progresses both ESA II and CDA II control energy storage and controllable load so that the voltage limits are observed. Eventually both controllers saturate as the rated value of controllable load is approximately 0.8kW and ESA II limits the energy storage power import to approximately 0.5kW.

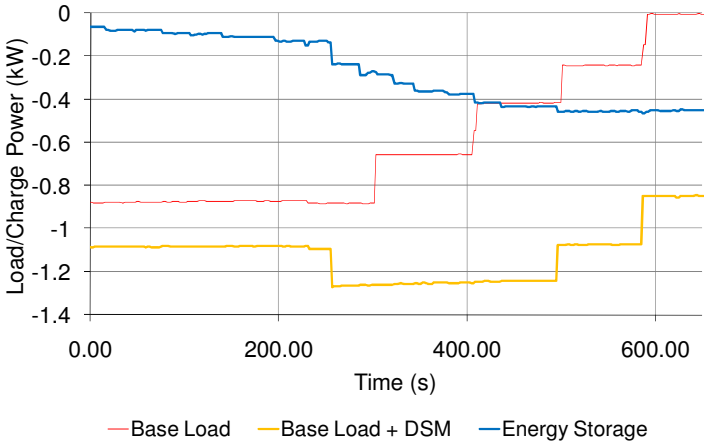


**Figure 7.27: Active power import of load and energy storage unit with distributed control system with ESA II and CDA II (Combined operation) – *Steady-state voltage rise test***

### 7.7.4 Discussion

Only one of the collaborative agent systems was unable to restore satisfactory system operation. The energy storage and consumer demand agents on their own were unable to mitigate voltage rise but the voltage agent at the remote end of the network enabled voltage control. As stated previously a limitation of energy storage and demand side management systems is that they can only act to control voltage for a finite period of time.

As there is a communication system in these architectures they may not be considered to be as rugged and reliable as the systems described previously. However, as each agent features a local control system as well as a system control system, even if there is a failure

in the inter-agent communication system, the direct agents, depending on their location, can ensure that the defined voltage limits are observed.

When generator agents were used collaboratively to mitigate voltage rise the duty was shared between both generators equally. This has been shown previously not to be the most effective way of mitigating voltage rise as remote end generation curtailment has been found to be the most effective. However, as stated previously the most effective way of mitigating voltage rise is if the generation is curtailed at the remote end. When a consumer demand agent is added the generation curtailment required to mitigate voltage rise is reduced but this reduction is small. This is due to the location of the controllable load in the Experimental SSEZ. No generation is curtailed in the distributed control system where the consumer demand agent, controllable load agent and voltage agent are deployed and this system exports the greatest amount of renewable energy.

## 7.8 Thermal Limit Agent (TLA)

In this section, the development of a thermal limit indirect agent which extends the functionality of the agent based distributed control system is described and results are presented illustrating its operation in collaboration with the different combinations of the second-stage direct agents. This indirect agent interacts with the direct agents utilising the inter-agent communication system described previously.

### 7.8.1 Thermal limit agent development

The TLA monitors the current flow at the network connection emulator and then determines a pseudo-frequency that is available to all agents via the inter-agent communication system. A simplified block diagram of the control algorithm is illustrated in Figure 7.28.

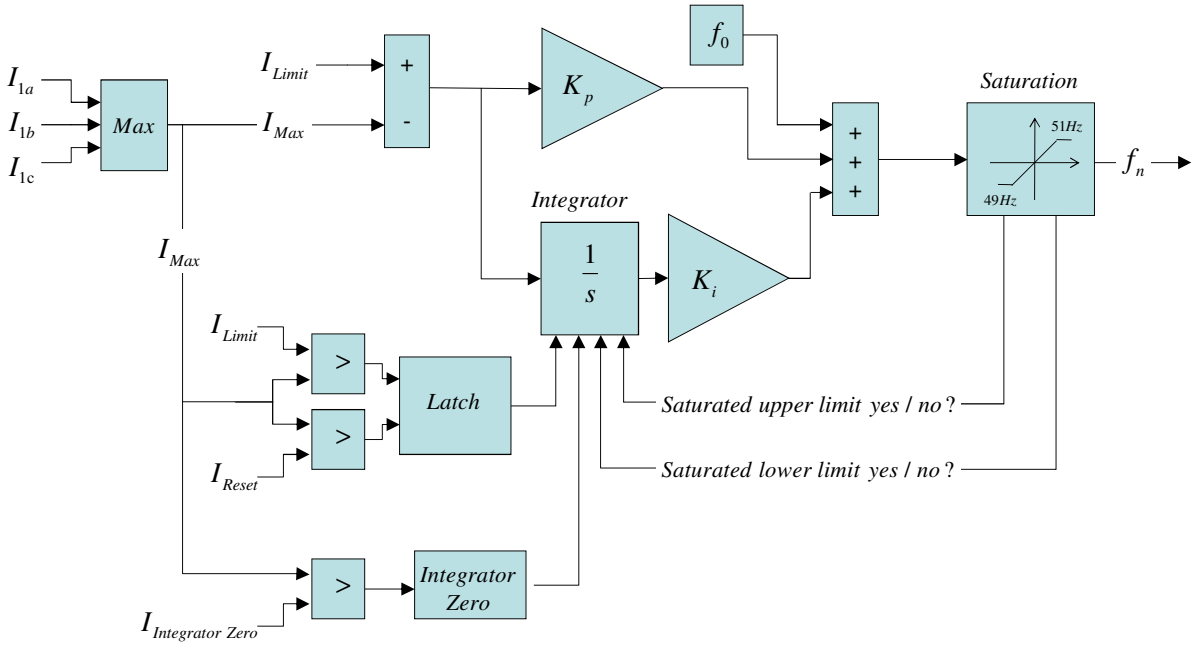


**Figure 7.28: Simplified block diagram of Thermal Limit Agent (TLA)**

This first-stage TLA measures the current flow on each of the phases. If the maximum current flow on any of these phases is greater than the defined limit then a PI controller is made operational within the agent.

The integral operation of the controller is triggered once the current rises above the defined limits. This is achieved using the latch illustrated in Figure 7.28. As in the case of the direct agents the output of this controller is limited to a band of between 49Hz and 50Hz. The pseudo-frequency output of this PI controller is limited in case it becomes too high or low resulting in large dynamic changes in the power flows in the network. In addition, when the maximum current falls below $I_{Integrator\ Zero}$ the integrator is reset to zero so that after the system exits thermal limiting operation so that the integrator does not retain high or low integrator values from a previous thermal limiting control routine. This improves the performance thermal limiting routine when a thermal overload condition is again detected by the TLA.

When enabled, the output of the PI controller system rises above $f_0$ and begins to curtail the generation in the same way that voltage was controlled in the previous section. As this PI control system is outside the inner PI control loops for local and system voltage control described earlier this loop must be slower.

### 7.8.2 Thermal limit agent implementation (PV and wind turbine generation agents)

The thermal limit agent (TLA) is deployed along with the second-stage generator agents (PVGA II and WGA II) on the Experimental SSEZ. Figure 7.29 illustrates the collaborative operation of the second-stage PV generator agent (PVGA II) and Wind turbine generator Agent (WGA II) to ensure that thermal limits are observed. The direct agent gains remained the same as in the previous implementations.

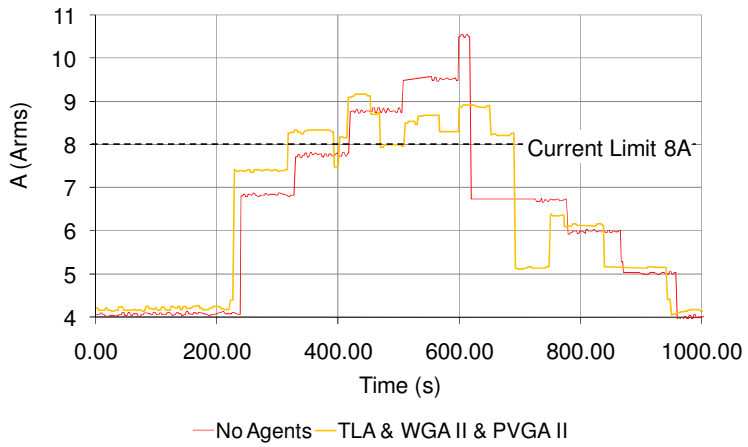


**Figure 7.29 Current flow at network connection emulator (phase A) of Experimental SSEZ LV network with TLA, PVGA II and WGA II – *Thermal limit test***

To control the current below 8A, the wind turbine and PV generation are constrained as illustrated in Figure 7.30. The duty of active power generation curtailment between the two SSEGs is again equally shared. PVGA II instructs the PV generator to curtail generation from 1.5kW to a minimum of 1.0kW and the wind turbine generation from 1.2 kW to 0.8kW during the *Thermal limit test*. The maximum curtailment of each generator

during the test is approximately 33%. It can also be seen in Figure 7.30 that after the reduction in wind generation, the curtailment on PV generation is released demonstrating the operation of the anti-integral windup algorithm of the TLA.

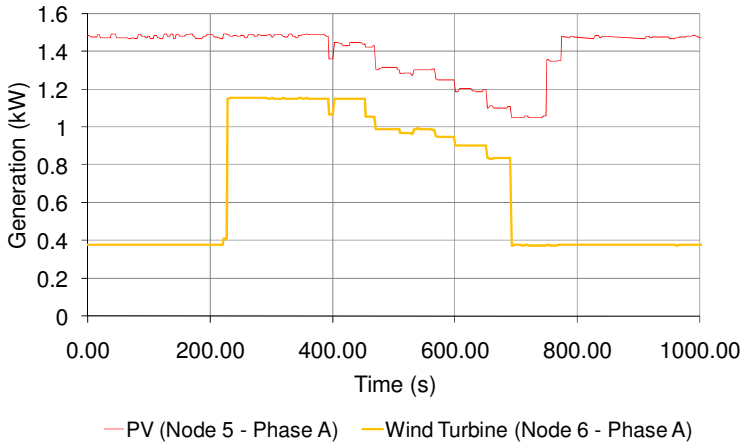


**Figure 7.30: Active power export of wind turbine and PV generation during operation of TLA – *Thermal limit test***

### 7.8.3 Thermal limit agent implementation (PV and wind turbine generation agents and consumer demand agent)

In this implementation, the TLA is deployed in conjunctions with the PVGA II and WGA II and CDA II in the Experimental SSEZ. Figure 7.31 illustrates the collaborative operation of the PVGA II, WGA II and CDA II to to ensure that thermal limits are observed. The gains of the direct and indirect agent gains remained the same as in the previous example.

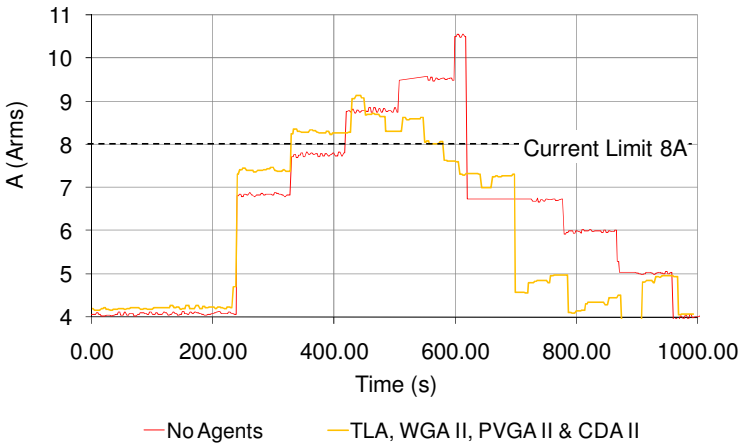


**Figure 7.31 Current flow at network connection emulator (phase A) of Experimental SSEZ LV network with thermal limit agent, generator agents and consumer demand agent – *Thermal limit test***

To control the current flow below the defined current limit requires the wind turbine and PV generation to be constrained and an increase in the controllable load as illustrated in Figure 7.32 and Figure 7.33. The duty of active power generation curtailment is evenly shared between both SSEGs. PVGA II instructs the PV generator to curtail generation from 1.5kW to a minimum of 1.1kW and the wind turbine generation from 1.2 kW to just over 0.8kW during the *Thermal limit test*. The maximum curtailment of each generator during the test is approximately 27%. It can also be seen again in Figure 7.32 that after the reduction in wind generation, the curtailment on PV generation is released demonstrating the operation of the anti-integral windup algorithm of the TLA.

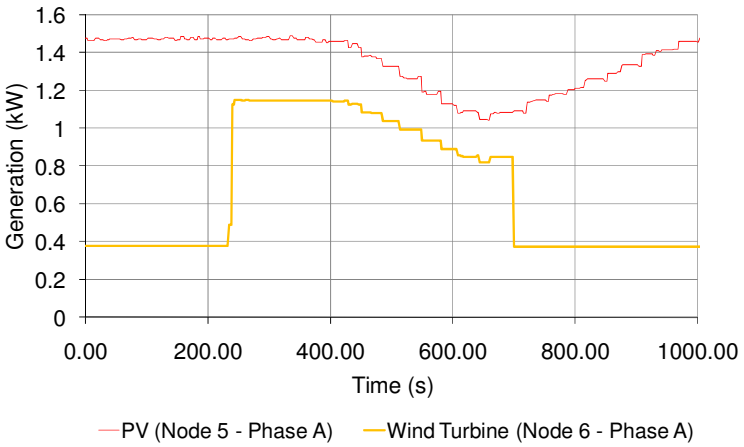


**Figure 7.32: Active power export of wind turbine and PV generation when controlled by TLA, WGA II, PVGA II and CDA II distributed control system – *Thermal limit test***

In Figure 7.33 the effect of DSM controlled by CDA II is illustrated by the trace titled *Base Load and DSM*. The load without the intervention of a distributed control system is illustrated by the trace titled *Base Load.* It can be seen that CDA II does not switch in any controllable load until t = 600s through the test. This is because the load is connected in 0.25kW steps and the calculated controllable load requirement was less than this. After t = 600s the 0.25kW of controllable load remains connected due to integral-windup effects but this is finally disconnected after t = 900s.

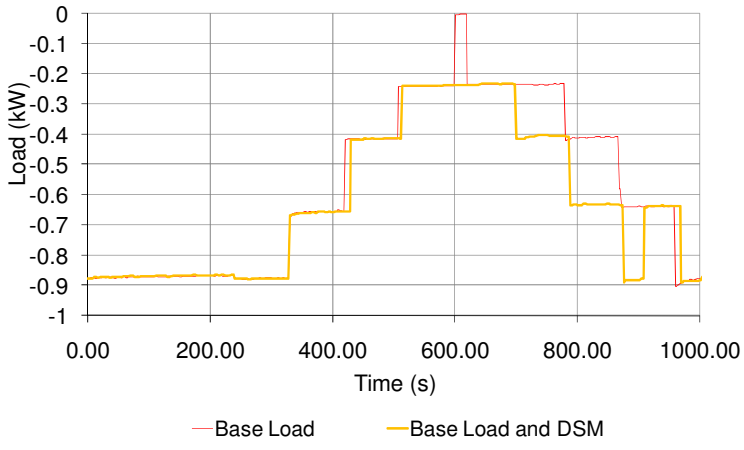


**Figure 7.33: Active power import of base load and base load and DSM when controlled by TLA, WGA II, PVGA II and CDA II distributed system –*Thermal limit test***

### 7.8.4 Thermal limit agent implementation (Consumer demand agent and Energy Storage Agent)

In this implementation, the TLA is deployed in conjunctions with CDA II and ESA II on the Experimental SSEZ. Figure 7.34 illustrates the collaborative operation of these agent to ensure that thermal limits are observed. The gains of the direct and indirect agent gains remained the same as in previous examples.

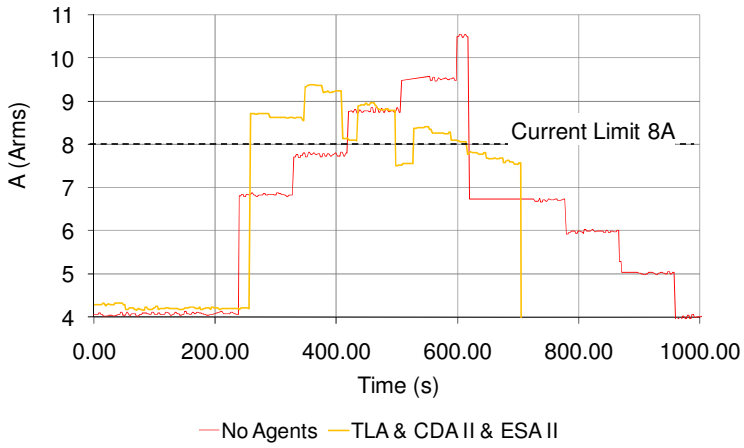


**Figure 7.34: Current flow at network connection emulator (phase A) of Experimental SSEZ LV network with TLA, CDA II and ESA II – *Thermal limit test***

As both ESA II, CDA II and TLA operate collaboratively to ensure that the thermal limits are observed by increasing the power imported into the energy storage system and increasing controllable load. Thus no renewable energy is curtailed during this test as illustrated in Figure 7.35. It can be seen however that the current limits are exceeded in the system with TLA implemented before it is exceeded in the system with no control. This is due to the poor reactive power control achieved with the energy storage unit.

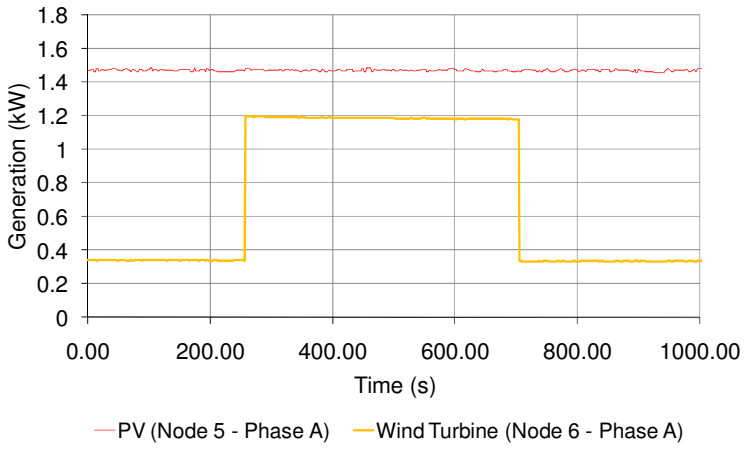


**Figure 7.35: Active power export of wind turbine and PV generation with distributed control system with TLA, ESA II and CDA II – *Thermal limit test***

In Figure 7.36 the effect of DSM controlled by CDA II is illustrated by the trace titled *Base Load and DSM*. The load without the intervention of a distributed control system is illustrated by the trace titled *Base Load.* The energy imported by the energy storage system which is controlled by ESA II is illustrated by the trace titled *Energy Storage.* As the test progresses both ESA II and CDA II control energy storage and controllable load to ensure that the thermal limits are observed. However, some integral windup behaviour is observed as the energy storage and DSM both continue to import power after the thermal limit conditions disappear at the network connection emulator.

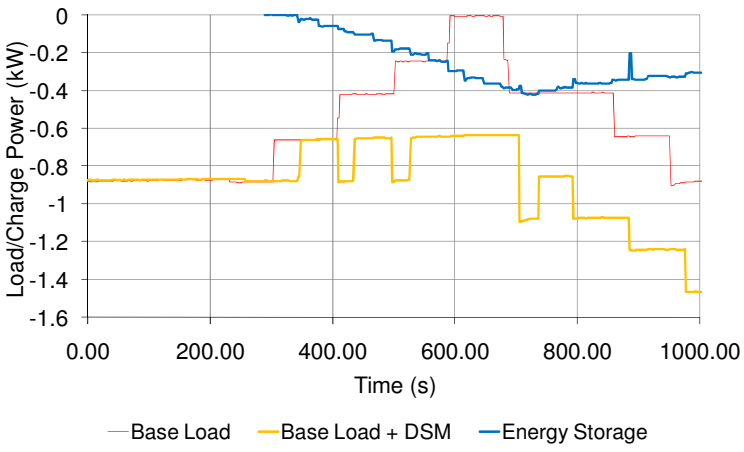


**Figure 7.36: Active power import of load and energy storage unit with distributed control system with TLA, ESA II and CDA II – *Thermal limit test***

### 7.8.5 Discussion

All of the collaborative agent systems were able to restore satisfactory system operation following an increase in the flow of current at the network connection emulator. As power flow is directly related to current flow at the network connection emulator the location of the SSEZ entity does not impact on the operation of power flow control in the distributed control system.

If inter-agent communications fail between thermal limit agent and any of the direct agents the system can still control the current at the network connection emulator by interacting with the remaining direct agents below the defined limits. However, if there is a failure in the thermal limit agent the current at the network connection emulator is not controlled.

## 7.9 Voltage Unbalance Agent (UA)

In this section, the development of a voltage unbalance indirect agent which extends the functionality of the agent based distributed control system is described and results are presented illustrating its operation in collaboration with the different combinations of the second-stage direct agents. This indirect agent interacts with the direct agents utilising the inter-agent communication system described previously.

### 7.9.1 Voltage unbalance agent development

The UA monitors the voltage unbalance at the remote end ($\%VUF_6$) of the LV network and then determines a pseudo-frequency that is available to all agents via the inter-agent communication system. A simplified block diagram of the control algorithm is illustrated in Figure 7.37.

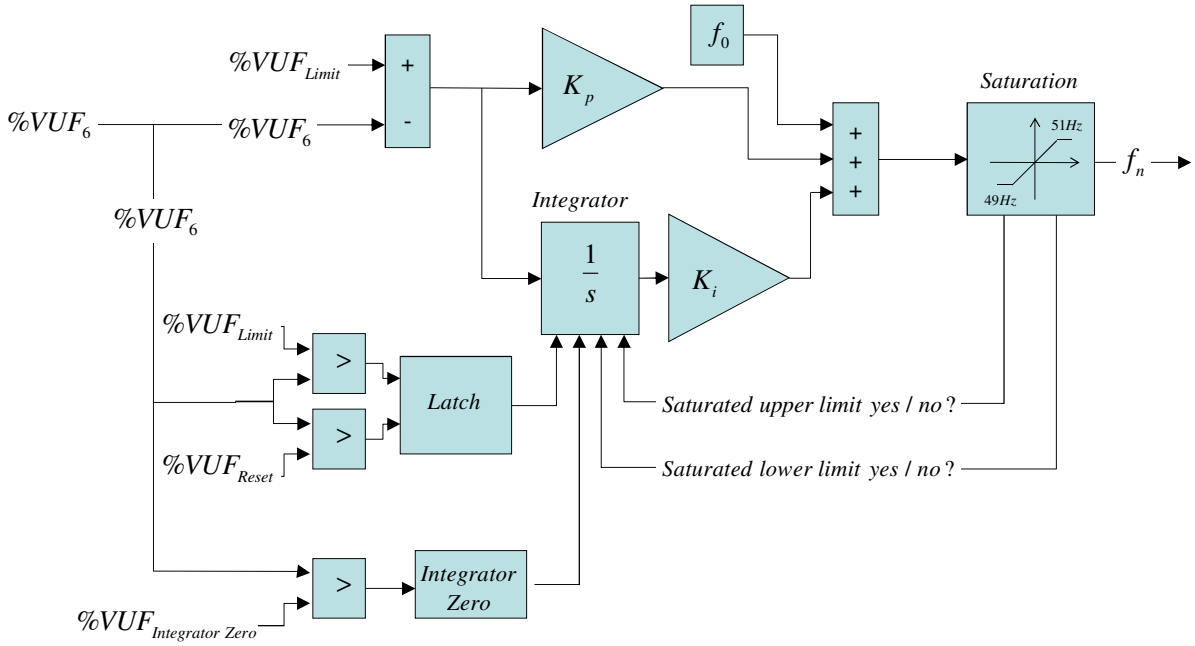


**Figure 7.37: Simplified block diagram of voltage unbalance agent (UA)**

This UA measures the phase and magnitude of the remote end voltages. These quantities are used to calculate the sequence voltage components at the remote end of the network and these are then used to calculate the percentage voltage unbalance factor. If the percentage voltage unbalance factor is greater than the defined limit then a PI controller is made operational within the agent. This system is similar in design to the TLA described in the previous section and operates in a similar manner.

When enabled, the output of the PI controller system rises above $f_0$ and begins to curtail the generation in the same way that current was controlled in the previous section. As this PI control system is also outside the inner PI control loops for local and system voltage control this loop must be slower.

### 7.9.2 Voltage unbalance agent implementation (PV and wind turbine generation agents)

A voltage unbalance agent (UA) is initially deployed along with the second-stage generator agents (PVGA II and WGA II) on the Experimental SSEZ. Figure 7.38

illustrates the collaborative operation of the second-stage PV generator agent (PVGA II) and wind turbine generator agent (WGA II) to ensure that the percentage voltage limits are observed. The direct agent gains remained the same as in the previous thermal limit agent implementations.

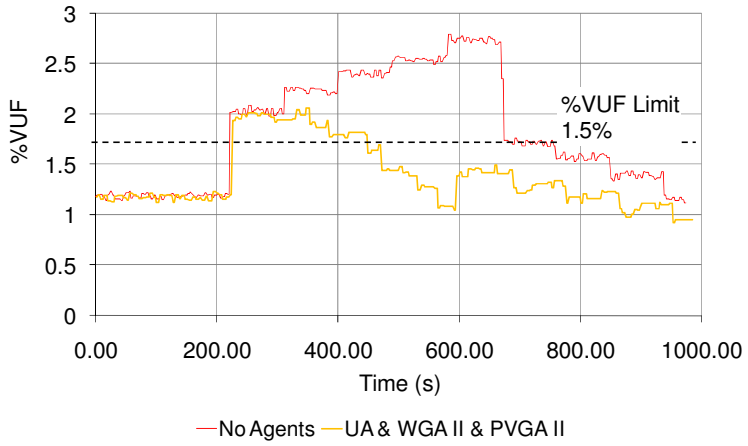


**Figure 7.38 %VUF at remote end (node 6) of Experimental SSEZ LV network with voltage unbalance agent and generator agents – *Voltage unbalance test***

To ensure that the defined percentage voltage balance limit is not reached. the wind turbine and PV generation are constrained as illustrated in Figure 7.39. The duty of active power generation curtailment between the two SSEGs is again equally shared. PVGA II instructs the PV generator to curtail generation from 1.5kW to a minimum of 0.5kW and the wind turbine generation from 1.2 kW to 0.5kW during the *Voltage unbalance test*. The maximum curtailment of each generator during the test is approximately 66%. It can also be seen in Figure 7.39 that after the reduction in wind generation, the curtailment on PV generation is released demonstrating the operation of the anti-integral windup algorithm of the UA.

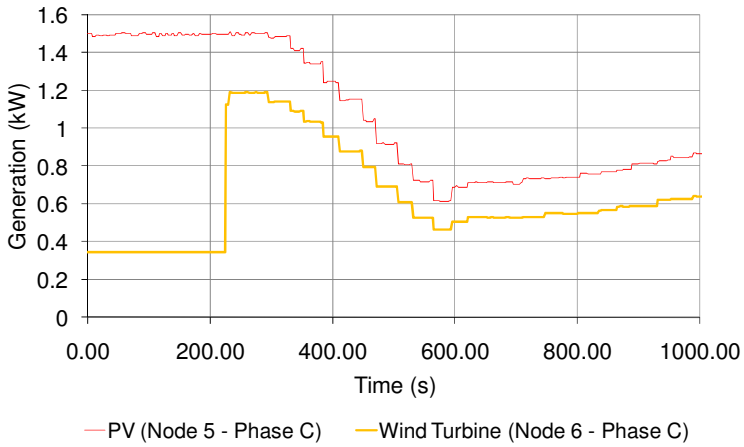


**Figure 7.39: Active power export of wind turbine and PV generation during operation of UA–*Voltage unbalance test***

### 7.9.3 Voltage unbalance agent implementation (PV and wind turbine generation agents and consumer demand agent)

In this implementation, the voltage unbalance agent (UA) is deployed in conjunction with the second-stage generator agents (PVGA II and WGA II) and the second-stage consumer demand agent (CDA II) in the Experimental SSEZ. Figure 7.40 illustrates the collaborative operation of the second-stage PV generator agent (PVGA II), wind turbine generator agent (WGA II) and consumer demand agent (CDA II) to to ensure that voltage unbalance limits are observed. The gains of the direct and indirect agent gains are the same as in the previous section.

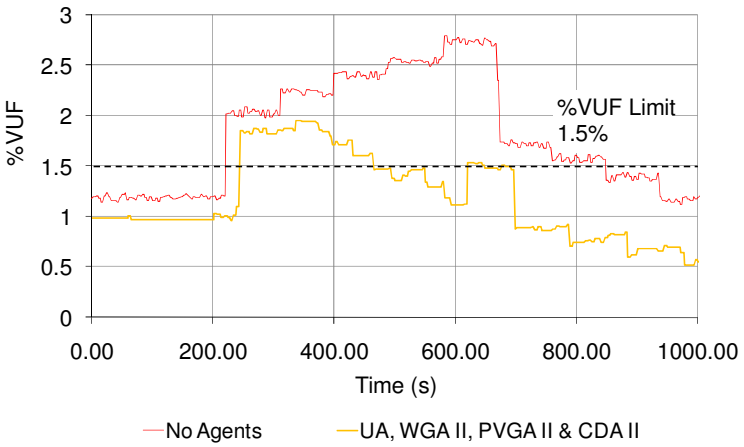


**Figure 7.40 %VUF at remote end of Experimental SSEZ LV network with voltage unbalance agent, generator agents and consumer demand agent – *Voltage unbalance test***

To ensure that the defined percentage voltage balance limit is not reached requires the wind turbine and PV generation to be constrained and an increase in the controllable load as illustrated in Figure 7.41 and Figure 7.42. The duty of active power generation curtailment is again evenly shared between both SSEGs. PVGA II instructs the PV generator to curtail generation from 1.5kW to a minimum of 0.9kW and the wind turbine generation from 1.2 kW to just over 0.7kW during the *Voltage unbalance test*. The maximum curtailment of each generator during the test is approximately 40%. It can also be seen again in Figure 7.41 that after the reduction in wind generation, the curtailment on PV generation is released demonstrating the operation of the anti-integral windup algorithm of the UA.

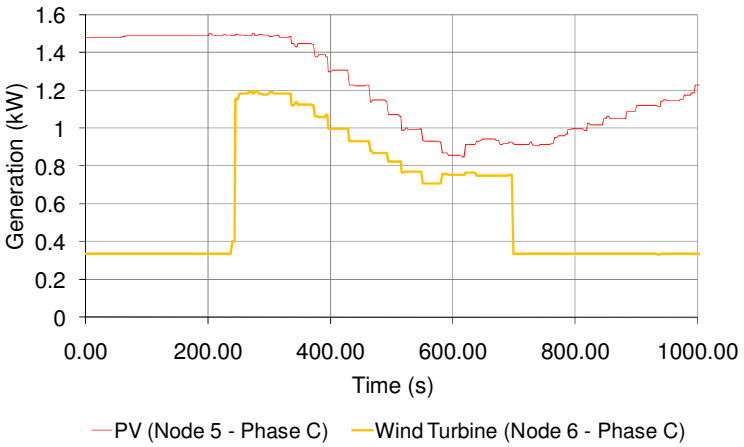


**Figure 7.41: Active power export of wind turbine and PV generation when controlled by UA, WGA II, PVGA II and CDA II distributed control system – *Voltage unbalance test***

In Figure 7.42 the effect of DSM controlled by CDA II is illustrated by the trace titled *Base Load and DSM*. The load without the intervention of a distributed control system is illustrated by the trace titled *Base Load.* It can be seen that CDA II does not switch in any controllable load until t = 420s through the test. This is because the load is connected in 0.25kW steps and the calculated controllable load requirement was less than this.

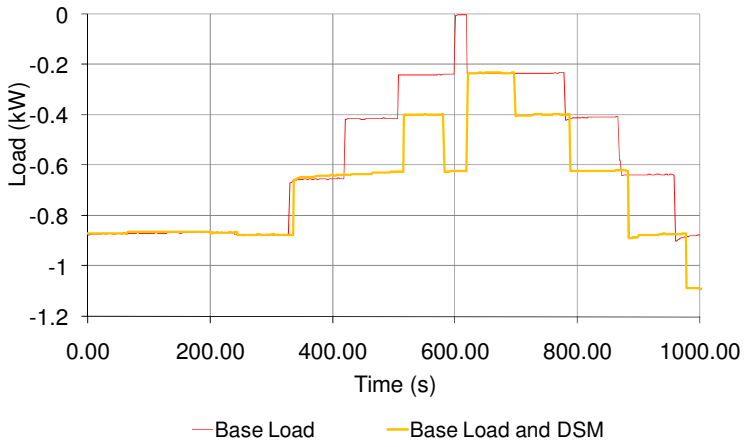


**Figure 7.42: Active power import of base load and base load and DSM when controlled by UA, WGA II, PVGA II and CDA II distributed system –*Voltage unbalance test***

### 7.9.4 Voltage unbalance agent implementation (Consumer demand agent and Energy Storage Agent)

In this implementation, the UA is deployed in conjunctions with CDA II and ESA II on the Experimental SSEZ. Figure 7.43 illustrates the collaborative operation of these agents to ensure that voltage unbalance limits are observed. The gains of the direct and indirect agent gains remained the same as in the previous implementations.

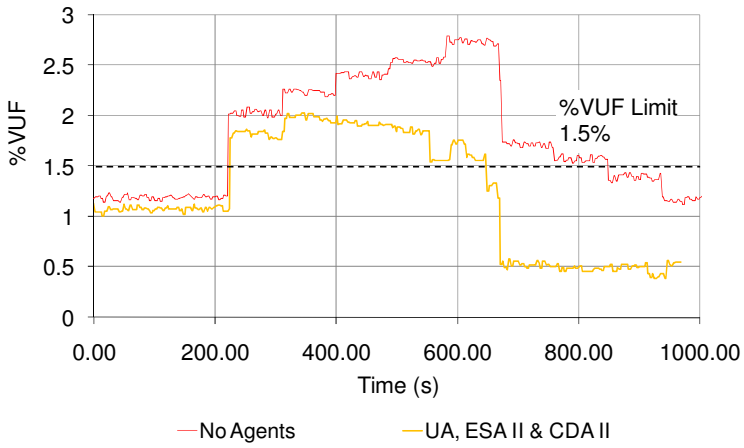


**Figure 7.43: %VUF at remote end of Experimental SSEZ LV network with UA, CDA II and ESA II – *Voltage unbalance test***

As both ESA II, CDA II and UA operate collaboratively to ensure that the voltage unbalances are observed by increasing the power imported into the energy storage system and increasing controllable load. Thus no renewable energy is curtailed during this test as illustrated in Figure 7.44.

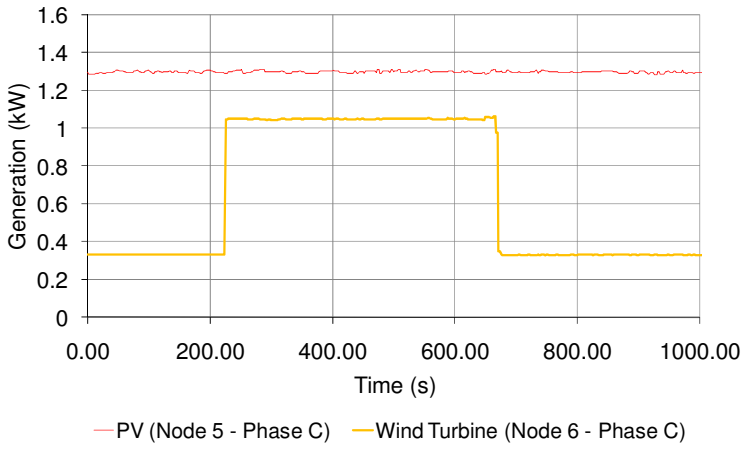


**Figure 7.44: Active power export of wind turbine and PV generation with distributed control system with UA, ESA II and CDA II – *Voltage unbalance test***

In Figure 7.45 the effect of DSM controlled by CDA II is illustrated by the trace titled *Base Load and DSM*. The load without the intervention of a distributed control system is illustrated by the trace titled *Base Load.* The energy imported by the energy storage system which is controlled by ESA II is illustrated by the trace titled *Energy Storage.* As the test progresses both ESA II and CDA II control energy storage and controllable load to ensure that the voltage unbalance limits are observed. However, some integral windup behaviour is observed as the energy storage and DSM both continue to import power after the voltage unbalance conditions disappear at the network connection emulator.

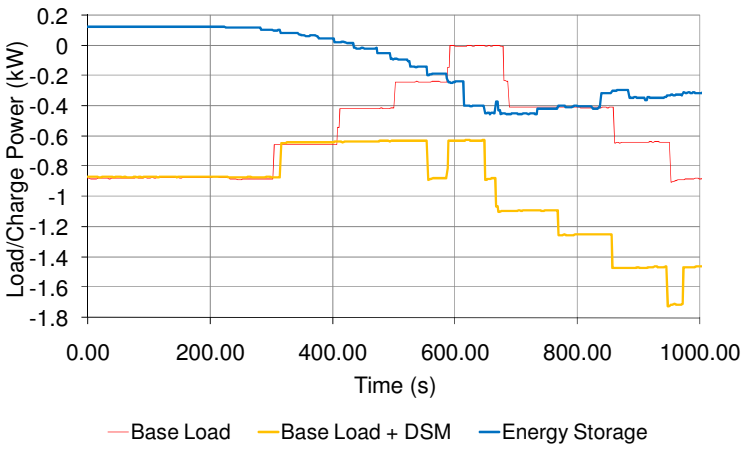


**Figure 7.45: Active power import of load and energy storage unit with distributed control system with UA, ESA II and CDA II – *Voltage unbalance test***

## 7.10 Conclusion

The development of the distributed control system based on the agent framework described in [14, 23-24, 103] is described in this chapter. The initial systems consisted of direct agents for generation, consumer demand and energy storage working on their own and collectively to reduce voltage rise on the system without any inter-agent communication. The agent functionality was then extended to include inter-agent communication to enable collaborative operation between the agents to mitigate voltage rise. To ensure that thermal and voltage unbalance limits were observed, indirect thermal and voltage unbalance agents (TLA and UA) were developed and integrated into the system using the inter-agent communication. These distributed control systems are capable of controlling SSEG, controllable load and energy storage so that the defined voltage, thermal and voltage unbalance limits are observed.

As the distributed control system proposed in this chapter consists of autonomous agents the distributed control system can still continue functioning even if the inter-agent communications system fails. In addition, if any of the direct agents fail the system will continue to operate and ensure that voltage rise, thermal and voltage unbalance limits are observed. However, if either of the indirect agents fails then that functionality of the distributed control system would be lost even though the system would continue to control voltage in a distributed manner and would control the remaining network constraints using the relevant indirect agents. The resilience of the system could also be compromised if multiple agents reside on a single hardware platform. An example of this architecture would be the Microgrid centralised controller (MGCC) in which multiple agents are hosted [15-18]. However, as there are relatively few indirect agents proposed for an SSEZ the possibility of using an extra redundant set of indirect agents on another hardware platform is a possibility to increase reliability with consequent extra costs.

Extra SSEZ entities were easily accommodated into the distributed control system deployed on the Experimental SSEZ. It should be noted however that the gains of the local and system PI controllers in each agent may need to be changed as the penetration level of agent equipped SSEZ entities increased. If the gains chosen are too low initially the performance of the distributed control system could be sluggish. This would improve as more agent equipped SSEZ entities are added to the system. However, if too many entities are added it may result in the system becoming unstable. This is illustrated in Figure 7.16.

The communications traffic in these agent based distributed control architectures, examined in this chapter, is a function of the number of agents that are deployed. The communications traffic is likely to be quite low, however as each agent transmits its own pseudo-frequency described earlier. Each agent however will need to be able to receive all the pseudo-frequencies from the other agents.

The renewable energy export of each distributed control system is dependent on the method used to assign duty of mitigating the network constraint under consideration. It does not depend on the control system architecture. As controllable load and energy storage is integrated into the agent-based distributed control system in some of the agent implementations renewable energy curtailment is reduced to zero and is instead stored as thermal or battery based energy storage using the controllable load and the energy storage system.

Due to time constraints operational goal functionality was not implemented in any of the distributed control systems. However, the introduction of an operational goal agent (OGA) based on the thermal limit agent (TLA) could be used to achieve this functionality.

The overall cost of a distributed control systems is difficult to determine. Each system will require dedicated measurement equipment to measure current flow near the network connection emulator to enable operation of the thermal limit agent and any operational goal agents that are deployed on the LV network. In addition, to control voltage unbalance, measurements are required at the remote end of the network. This could be achieved by using a dedicated three-phase measurement system located at the remote end of the network, as used in the Experimental SSEZ implementation, or by agents at the remote of the network which could be configured to transmit voltage data to the voltage unbalance agent. Communications are also required that will allow all SSEZ entities to transmit a pseudo-frequency and receive all pseudo-frequencies from the other agents. The cost of this communications system could be a major factor in assessing the future cost of these systems. It is possible however that no extra infrastructure may be required if existing communications infrastructure was employed. Another option may be to use Power Line Carrier (PLC) or WLAN modules which would be integrated into each hardware platform hosting the agents at each SSEZ entity. In addition, costs will also increase with the addition of each direct agent to the system as a hosting hardware platform together with interfaces to the communications system and the SSEZ entity. This cost however could be borne by individual customers as this system facilitates a “plug and play” infrastructure.

# 8 DISCUSSION

## 8.1 Introduction

The previous two chapters detailed the design and development of centralised and distributed control systems for the Experimental SSEZ which ensured that the defined voltage rise, thermal and voltage unbalance limits are complied with. A centralised control system has been defined previously to imply a control system located at the secondary distribution substation which acquires data from nodes throughout the LV network. A distributed control system by contrast consists of a number of independent devices or control systems that appear to its users as a single system [85-86]. In this chapter, the relative value of these control system architectures with regard to their deployment on an LV distribution network is investigated.

The criteria for evaluation of the control system architectures are initially restated. The ability of centralised and distributed control system architectures to meet these requirements is then discussed, based on the work presented in the previous two chapters. Finally conclusions on the implementation of centralised and distributed control systems on LV distribution networks are drawn.

## 8.2 Evaluation Criteria for Distributed Control System Architectures

The following criteria are used to evaluate distributed and centralised control system architectures in the following sections: -

- Ensure system operates within network constraints
- Resilience and reliability
- Scalability

- Communications requirements
- Renewable energy output
- Economic benefit to SSEG/ES/controllable load owners
- Cost and complexity

In order to facilitate evaluation of these networks in the context of evaluating the SSEZ concept, the UK generic LV network described previously is used to facilitate comparison between centralised and distributed control systems in an SSEZ [9]. In addition, to illustrate the differences in the implementation of centralised and distributed control systems, from a cost and complexity point of view, a generic European LV network is introduced for comparison [36]. These generic networks are illustrated Figure 8.1. More details on these generic LV distribution network can be found in Appendix B-3.

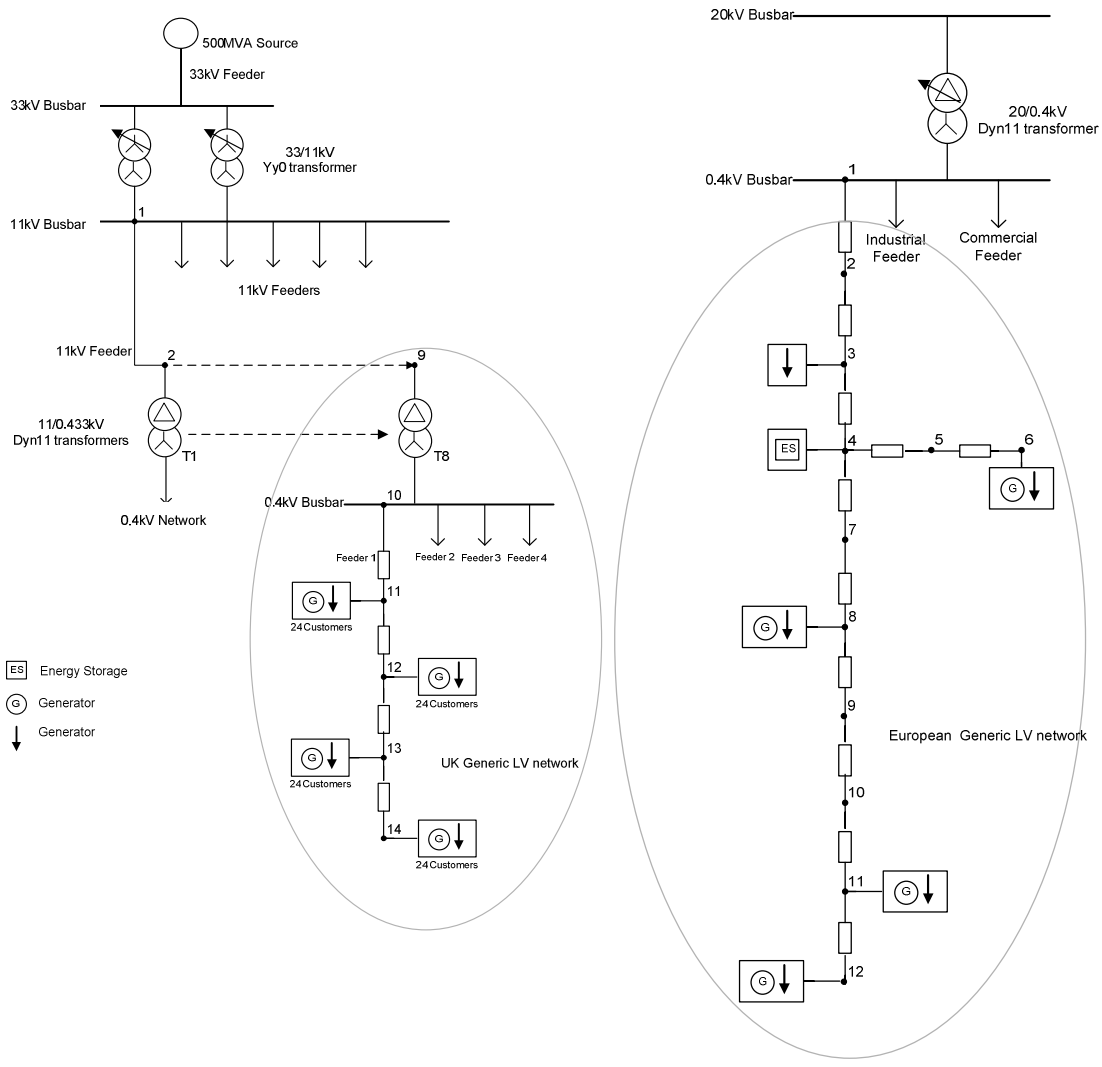


**(UK)** **(European)**

**Figure 8.1: UK Generic and European Generic Network Models**

## 8.3 Ensure System Operates within Network Constraints

Centralised and distributed control systems were developed that were able to mitigate voltage rise, thermal and voltage unbalance limit violations. In the centralised control system, in order to reduce the number of measurements, assumptions were made regarding the operation and distribution of load and generation of the LV network. The centralised evaluation program was used to investigate the limitations of these assumptions. The assumptions include: -

1. LV network is balanced.
2. Voltage at network connection is constant.
3. Load and generation is distributed evenly across the network.
4. Voltage rise is greatest at the remote end.
5. Thermal limit violations occur first at the cable section emanating from the network connection.
6. Voltage unbalance is greatest at the remote end.

The first four assumptions are used to determine voltage rise. It was shown in chapter six, however, that each of the first three of these assumptions may not be valid under certain conditions. This could result in voltages that exceed the defined limits of the system. However, these conditions are worst case scenarios and in an LV distribution network many of these assumptions are likely to be valid under normal operating conditions.

A distributed control system overcomes the lack of measurements from a point of view of voltage rise as each agent has local voltage measurement which is integrated into the control system. However, in common with the centralised control system the thermal limit and voltage unbalance limit agents are effectively centralised unless multiple thermal and voltage unbalance agents are deployed on the system.

## 8.4 Resilience and Reliability

Failures in centralised control systems' hardware, communications or software may result in the malfunction or complete failure of the centralised control system. This risk can be reduced in some instances by using redundant systems. However, the failure in the communications system of SSEG entities such as generation, energy storage or controllable load would not be likely to result in the failure of the system. The addition of these systems can increase the cost of the system. The distributed control system in

contrast described in chapter seven utilises autonomous agents that are able to continue mitigating voltage rise even if the inter-agent communication system fails. Moreover, if some of the direct agents fail the functionality of the system is not affected.

To illustrate the differences in the operation of each of these control systems it is worth considering the UK generic LV distribution network. In order to assess the reliability of both control systems the principal elements of each control system are considered using the architectures described in the previous chapters and the loss of each of these elements to the functionality of the control system is considered. When each of these systems are applied to the UK generic LV network there are 96 SSEGs. The centralised control system has individual control of each SSEG and similarly each SSEG in the distributed system is equipped with a GA.

| Centralised Control | | Distributed Control | |
|---|---|---|---|
| ***Control System Element (No. Of elements)*** | ***Failure operation*** | ***Control System Element (No. Of elements)*** | ***Failure operation*** |
| *Voltage rise sensor and communications (1)* | Failure of voltage control subsystem | *Generator Agents (GAs) and communications (96)* | Loss of collaborative operation of single SSEZ energy element, voltage control functionality retained |
| *Thermal limit sensor and communications (1)* | Thermal limit control subsystem failure | *Thermal Limit Agent (TLA) and communications (1)* | Thermal limit control failure |
| *Voltage unbalance sensor and communications (1)* | Voltage unbalance control subsystem failure | *Voltage Unbalance Agent (UA) and communications (1)* | Voltage unbalance control failure |
| *Communications system* | System failure | *Communications system* | Voltage control still available. |
| *Communications to SSEZ energy element (96)* | No control of SSEZ energy element | | |
| *Central controller (1)* | Complete system failure | | |

**Table 8.1: Resilience and reliability comparison between centralised and distributed control systems using UK generic LV network**

The table above illustrates the similarities and the differences in the failure modes of both control systems. However, it can be seen that the centralised control system is more vulnerable to failure of any of its elements. In particular, a fault in the central controller may result in the failure of the entire control system. In contrast, if the communications

system fails completely in the distributed control system, voltage control which has been shown to be the most onerous of network constraints in LV systems, remains while the centralised control system fails.

## 8.5 Scalability

As both the centralised and distributed control system developed for the Experimental SSEZ are based on proportional and integral feedback control loops their response to the addition of extra generation, energy storage and controllable load systems have similarities.

Large changes in the penetration level or distribution of SSEGs affects the operation of both centralised and distributed control systems if no modifications are made to the control algorithm. It was found that the gains of the controller may need to be modified. An approach to solving this problem is to ensure that the system gains are low so that the addition of substantial amounts of controllable SSEZ entities does not result in oscillatory or unstable operation. This would result in a system that could have sluggish operating characteristics and if too many SSEZ entities are added the control system operation may become unstable.

In an actual SSEZ implementation it would be necessary to update these gains either manually or automatically as extra SSEGs are added. In addition, communications links between the central controller and the new SSEGs, controllable load or energy storage unit would also need to be made.

In the distributed control system a utility agent, as previously described in the agent framework, and an inter-agent communication system that is more complex than is proposed could be easily designed to provide this functionality.

## 8.6 Communications Requirements

Communications traffic for centralised and distributed control architectures in an SSEZ are very different. In the centralised control system all communications need to be routed through the central controller. By contrast a distributed controller is likely to use a bus communications system such as IEC 61850 [154] over an Ethernet communications network [155].

The primary requirements for communications in the centralised control system are data acquisition from a limited number of locations and a centralised generation curtailment, energy storage import or export and load control signal. Extra communications could also be useful in determining control system actions which include available generation capacity, energy storage capacity and availability of controllable load. These would increase the communications requirements but may improve the operation of the system.

The communications system in the distributed control system described in chapter seven is a function of the number of agents that are deployed but the only information that is uploaded onto the communications bus is the pseudo-frequency but all agents need to be able to access all the pseudo-frequencies. This requirement could be eliminated either by introducing an arbitration system within the communications protocol or introducing another agent that reads all the pseudo-frequencies and then uploads the highest pseudo-frequency onto the communications bus.

To illustrate the differences in the operation of each of the communications systems in distributed and centralised control systems it is again worth considering the UK generic LV distribution network shown in Figure 8.1. Each of the control system functionalities are reviewed with respect to their communications requirements. As in the investigation into resilience and reliability of the control systems 96 SSEGs are connected to each

network. The centralised control system has individual control of each SSEG and similarly each SSEG in the distributed system is equipped with a GA.

| Control Function | Centralised | | Distributed | |
|---|---|---|---|---|
| | **Send** | **Receive** | **Send** | **Receive** |
| *Voltage rise* | 96 | 1 | 0 (96[1]) | 0 (1[1]) |
| *Thermal limit* | 96 | 1 | 1 | 1[2] |
| *Voltage unbalance* | 96 | 1 | 1 | 1[2] |

**Table 8.2: Communications requirements comparison between centralised and distributed control systems using UK generic LV network**

The table above illustrates how the distributed system can reduce the communications requirements as the decisions regarding voltage can be made locally. In addition, as voltage rise has been shown previously to be the most onerous of the technical constraints and which requires the most immediate action as defined in [29] the ability of the distributed control system to control voltage without communications would result in a reduction in the bandwidth required in the communications systems.

## 8.7 Renewable Energy Output

The distributed control system, which utilised energy storage and controllable load to mitigate voltage rise, thermal limits and voltage unbalance, resulted in the largest renewable energy output during the testing program, as no generation was curtailed.

[1] If the system is operating in an entirely distributed manner no communication is necessary to control voltage. However, to enable collaborative operation communications are necessary to enable interaction between the agent controllers and therefore all voltage controlling agents may send signals.

[2] All generator agents only need to receive a single communications signal, which is the highest pseudo-frequency on the system described in chapter seven.

However, these systems could also be used in conjunction with the centralised control system.

A distributed control system, similar to that described in chapter seven, may have limited flexibility with regard to apportioning the duty of mitigating the network constraints. This was shown to be particularly important when voltage and voltage unbalance limits violate their limits, as reducing generation at the remote end of a radial feeder has a greater effect than reducing generation that is located nearer the network connection. This was illustrated in chapter seven when curtailing wind generation output to control voltage below the defined limits required a 40% reduction in overall renewable generation. When the duty of controlling the voltage was divided equally between the PV and wind turbine generation a reduction of 48% in overall renewable generation was required to control the voltage within the defined limits. The contribution of each agent controlled system is therefore fixed unless, as in the case of energy storage or controllable load, the SSEZ entity is unavailable to take part in the control action.

In the centralised system each SSEZ entity can be controlled independently by the central controller. As a centralised control system could have access to information on the status of the SSEZ entities, it is likely that the decisions regarding coordinating generation, energy storage and controllable load could provide a better overall solution than a distributed control system.

In summary, while the renewable energy export can be the same from both architectures, a distributed control system, with a limited communications system, may not provide as much flexibility when determining the contribution from each SSEZ entity to the operation of the system.

## 8.8 Economic Benefit to SSEG/ES/Controllable Load Owners

Renewable energy export and off-setting local load are the primary advantages of SSEG for individual consumers. In addition, as proposed in chapter three, each participating SSEZ entity owner is compensated in proportion to their generation/storage/consumption capacity. This implies that the economic benefit to the owner of a controllable load of 1kW which is activated for ten minutes receives the same financial compensation that the owner of an SSEG who reduces his generation by 1kW for ten minutes.

Both architectures are capable of interacting with generation, energy storage and controllable load to mitigate network constraints and achieving operational goals. A purely distributed approach to voltage control where no communications or collaboration between agents was enabled was discussed in chapter seven. In this case the possible owner of the wind turbine generator would be exporting between 83-95% less renewable generation at the end of the *Steady-State Voltage Rise Test* depending on the gains used in the first stage agents. In contrast, the owner of the PV generator had power curtailed by between 0-15% depending on the gains used during the same test.

However, a more distributed approach may offer some advantages for maximising the economic benefit for owners of SSEZ entities as each direct agent would be hosted on an intelligent hardware platform located at the SSEZ entity. This offers the possibility of the consumer interacting with a more advanced version of the direct agents proposed in chapter seven in a way that could maximise their economic benefits. In contrast, this functionality may prove to prohibitively difficult and expensive in a centralised system where all the individual user data would need to be processed by the centralised controller.

## 8.9 Cost and Complexity

As it is speculative to estimate at present what the cost of each of the control elements of both systems may cost if they reach production, it is proposed to compare them simply in terms of complexity. This is assessed by determining the number of elements that are likely to be in each control system considering both systems proposed in chapters six and seven are deployed on the UK Generic LV network and the European Generic LV network.

| | **UK Generic LV Network** | | **European Generic LV Network** | |
|---|---|---|---|---|
| | ***Centralised*** | ***Distributed*** | ***Centralised*** | ***Distributed*** |
| Voltage rise, voltage unbalance and thermal sensors and communications | 3 | 2 | 3 | 2 |
| Communications system | 96 dedicated links | 1 bus | 6 dedicated links | 1 bus |
| Controllers | 1 central controller | 96 direct agents + 2 indirect agents | 1 central controller | 8 direct agents + 2 indirect agents |

**Table 8.3: Complexity comparison between centralised and distributed control systems in the UK and European Generic LV Networks**

It can be seen from Table 8.3 that while the distributed control system has many more controller/agents many of these agents are very similar. In addition, a single bus communications structure is feasible to implement control. The centralised controller has dedicated communications and control links to each SSEZ entity. This seems like a reasonable option when only 6 larger SSEZ entities are controlled as in the case of the European generic LV network. However when larger numbers of SSEZ entities are deployed as in the case of the UK generic LV network this option may become prohibitively complex.

In addition to the complexity, the cost of implementation would also depend on the existing infrastructure, the LV network, and the size and distribution of the SSEZ entities. Moreover, one must also consider the future cost of adding extra SSEZ entities. Centralised control systems can consist of simple current sensing system which estimate parameters around the network based on these measurements and a small number of large generators, energy storage units and controlled load integrated into the system. Extra measurements could be incorporated into the system along with extra SSEZ entities but this could require changes to the control algorithm to accommodate these changes which is likely to be costly. However, if these upgrades of the system can be carried out in a modular way it would control these costs. In addition, as extra SSEZ entities and measurements are added this may also require extra dedicated communications links. A distributed control system would not require this and an extra SSEZ entity could be added to the communications bus. An extra cost associated with the deployment of a distributed control system is the requirement for a hosting hardware platform for each direct agent together with interfaces to the communications system and the SSEZ entity. This cost, however, as stated previously could be borne by individual customers as this system facilitates a “plug and play” infrastructure.

# 9 CONCLUSIONS

This chapter describes the conclusions that have been drawn as a result of this research. Finally, future work is proposed that could augment the value of this research.

## 9.1 Conclusions

It has been shown that many of the initial requirements for the development of an LV distribution network laboratory were met during the development by this author of the Experimental SSEZ at Durham University. The Experimental SSEZ had power balance and frequency regulation functionality provided by the network connection emulator. The LV network is radial and tapered with industry standard inverters to connect the SSEG emulators. The data acquisition systems is capable of measuring the phase and magnitude of voltages and currents on all three-phases. The system is therefore able to measure voltage unbalance also. In addition, the LabVIEW™ based control system infrastructure enables the investigation of both centralised and distributed control algorithms. Some limitations of the system were identified during the course of the research. An example of this is the behaviour of the synchronous machine of the network connection emulator which is different in a number of ways to that of an MV/LV distribution network transformer. The LV network of the Experimental SSEZ is much smaller in comparison to an LV distribution network and much fewer SSEGs are deployed than in the projected future scenarios. In addition, the load emulator of the Experimental SSEZ operates in 250W steps and is incapable of emulating phase or harmonic distortion effects. However, the main objective for the development of the Experimental SSEZ, which was to enable the development of control system architectures for the SSEZ concept, was enabled.

In the centralised control system development a number of strategies for controlling voltage rise were investigated. PI using anti-integral wind-up algorithms were chosen to

provide feedback control in the final implementations of these systems as these provided the best performance. Voltage rise, thermal limit and voltage unbalance control capabilities were integrated into this centralised control system. Anti-integral wind-up algorithms were also chosen and successfully implemented in the algorithms for the agents used in the distributed control system. The distributed control system also integrated voltage rise, thermal limit and voltage unbalance control.

It was shown that the centralised control system is more vulnerable to failure of any of its elements. In particular, a fault in the central controller may result in the failure of the entire control system. In contrast, if the communications system fails completely in the distributed control system, voltage control capability which has been shown to be the most onerous of network constraints in LV systems, remains while the centralised control system fails.

Both of the control systems investigated in this work exhibited a capability to integrate extra SSEZ entities into the control systems. However, it was shown that the projected incremental growth in SSEG penetrations in future LV distribution networks is more suited to a distributed control architecture rather than a centralised one.

In chapter seven it was demonstrated how the distributed system can reduce the communications requirements as the decisions regarding voltage can be made locally. In addition, as voltage rise has been shown previously to be the most onerous of the technical constraints and which requires the most immediate action as defined in [29] the ability of the distributed control system to control voltage without communications would result in a reduction in the bandwidth required in the communications systems.

The renewable energy export can be the same from both architectures, a distributed control system, with a limited communications system infrastructure, may not provide as

much flexibility when determining the contribution from each SSEZ entity to the operation of the system.

The distributed approach may offer some advantages for maximising the economic benefit for owners of SSEZ entities as each direct agent would be hosted on an intelligent hardware platform located at the SSEZ entity. This offers the possibility of the consumer interacting with a more advanced version of the direct agents proposed in chapter seven in a way that could maximise their economic benefits. In contrast, this functionality may prove to prohibitively difficult and expensive in a centralised system where all the individual user data would need to be processed by the centralised controller.

Cost and complexity is the most difficult of the control system architecture criteria to assess because this encompasses almost all the other criteria. As well as the reasons described in the legislative framework that could exist to incentivise the deployment of SSEG, energy storage and controllable load in an SSEZ or controllable energy zone are difficult to predict. However, it is possible that a simple centralised control system presiding over an LV network with fewer, larger SSEG with larger consumers and where the addition of further generation is likely to be slow may prove to be a more economical. In contrast, a dynamic, rapidly evolving LV network with large numbers of existing and possibly future SSEGs might be better served by an agent-based distributed control system architectures.

Therefore, in each case load, generation and the configuration of the LV distribution network must be considered on its merits when deciding which control architecture to adopt. This research, therefore, should be useful in informing design decisions when developing and implementing an active distribution network management system on an LV network. A summary of the assessment of the centralised and distributed control system architectures is given in tabular form in Table 9.1.

| Evaluation Criteria | Centralised | Distributed |
|---|---|---|
| *Ensure system operates within network constraints* | Can ensure satisfactory operation | Can ensure satisfactory operation |
| *Resilience and reliability* | Many sources of system failure. Central controller or communications can result in non-operation of the system. | Robust system, voltage control can be maintained without any communications or if some Generator Agents fail. |
| *Scalability* | Does not easily facilitate expansion, modular approach can help. | Facilitates easy expansion and "plug and play" operation. Agents need communications to ensure stable operation. |
| *Communications requirements* | Large communications requirements if many SSEZ energy elements are present on the system. | System can still maintain critical voltage control functionality even if communications fail. |
| *Renewable energy output* | Localised decision making and/or limited communications may reduce renewable energy output. | System flexible enough to maximise renewable energy output whilst ensuring network constraints are adhered to. |
| *Economic benefit to SSEG/ES/controllable load owners* | Intelligent distributed controllers could maximise the economic benefit for each owner. | Developing a customised controller that processes the requirements of each owner could be prohibitively complex and expensive |
| *Cost and complexity* | Less complex and probably costly system when fewer SSEZ entities are in system. | Less complex and probably costly system when a greater number of SSEZ entities are in system. |

**Table 9.1: Summary of assessment of centralised and distributed control system architectures**

## 9.2 Future Work

A number of limitations to the operation of the Experimental SSEZ LV network in comparison with actual LV distribution network have been identified. The addition of a transformer coupled to the synchronous machine of the network connection emulator would be a more accurate representation of a distribution network transformer.

The load system at present is resistive which is in contrast to the load on LV distribution networks which import reactive power as a result of phase and harmonic distortion of the load. In addition, while generation is distributed over a number of locations on the Experimental SSEZ LV network, controllable load is installed at one node only. Therefore, the addition of a number of three-phase load systems capable of importing or exporting reactive as well as real power would improve the evaluation of the control system architectures and enable the transformation described in Appendix H to be used in a larger number of real world scenarios. Another option, to augment the capabilities of the Experimental SSEZ is to introduce a Real Time Digital System Simulator (RTDS®) or a VPS (Virtual Power System) [156-157]. The LV distribution network topology, distribution of load and generation could also be changed in order to increase the coincidence between the Experimental SSEZ and the UK and European generic LV networks.

Finally, in order to fully realise the centralised and distributed control systems on the Experimental SSEZ more computing power is required. Improvements to the available bandwidth of data acquisition systems would also facilitate analysis of the harmonics introduced into the system. As mentioned earlier in the work the deployment of control systems, data acquisition and emulation was straining the capacity of the host PC platform. This could be realised by the addition of extra PCs to handle the control system rather than multi-tasking on one host PC. Another advantage of this approach would be

that each SSEZ energy entity could have a dedicated controller which would facilitate the investigation of distributed control systems.

# References


[1] "Engineering Recommendation G83/1, Recommendations for the connection of small-scale embedded generators (up to 16 A per phase) in parallel with public low-voltage distribution networks", Energy Association, 2003, Available: www.energynetworks.org.uk.

[2] "Energy Act," in Section 82, c. 20, 2004, p. 65, Available: http://www.opsi.gov.uk/acts/acts2004/20040020.htm.

[3] "Meeting the Energy Challenge, A White Paper on Energy", Department of Trade and Industry Report No. CM7124, 2007.

[4] "System Integration of Additional Micro-Generation Costs and Benefits – Final Draft Report", Mott MacDonald, London, UK, June, 2004.

[5] "Potential for Microgeneration - Study and analysis", Energy Saving Trust, London, UK, 2005.

[6] L. M. Cipcigan and P. C. Taylor, "Investigation of the reverse power flow requirements of high penetrations of small-scale embedded generation", *IET Renewable Power Generation*, vol. 1, No. 3, pp. 160 - 166, October 2007.

[7] P. F. Lyons, P. C. Taylor, L. M. Cipcigan, P. Trichakis, and A. Wilson, "Small scale energy zones and the impacts of high concentrations of small scale embedded generators" presented at *International Universities Power Engineering Conference; UPEC 2006*, Newcastle upon Tyne, 6 - 8 Sept., 2006.

[8] P. Trichakis, P. C. Taylor, L. M. Cipcigan, P. F. Lyons, R. Hair, and T. Ma, "An investigation of voltage unbalance in low voltage distribution networks with high levels of SSEG" presented at *International Universities Power Engineering Conference; UPEC 2006*, Newcastle upon Tyne, 6 -8 Sept., 2006.

[9] P. Trichakis, P. C. Taylor, P. F. Lyons, and R. Hair, "Predicting the technical impacts of high levels of small scale embedded generators on low voltage networks", *Proceedings of the Institution of Engineering and Technology, Renewable Power Generation*, vol. 2, No. 4 . pp. 249-262 2008.

[10] "International Electrotechnical Vocabulary - Part 601: Generation, transmission and distribution of electricity - General - Low Voltage," 601-01-26, 2009, Available: http://www.electropedia.org/iev/iev.nsf/display?openform&ievref=601-01-26.

[11] "International Electrotechnical Vocabulary - Part 601: Generation, transmission and distribution of electricity - General - Medium Voltage," 601-01-28, 2009, Available: http://www.electropedia.org/iev/iev.nsf/display?openform&ievref=601-01-28.

[12] "International Electrotechnical Vocabulary - Part 601: Generation, transmission and distribution of electricity - General - High Voltage," 601-01-27, 2009, Available: http://www.electropedia.org/iev/iev.nsf/display?openform&ievref=601-01-27.

[13] D. A. Roberts, "Network Management Systems for Active Distribution Networks - A Feasibility Study", DTI, 2004.

[14] P. Trichakis, P. C. Taylor, G. Coates, and L. M. Cipcigan, "Distributed control approach for small-scale energy zones", *Proceedings of the I MECH E Part A Journal of Power and Energy*, vol. 222, pp. 137 2008, Available: http://www.ingentaconnect.com/content/pep/jpe/2008/00000222/00000002/art00001.

[15] A. Dimeas and N. Hatziargyriou, "A multi-agent system for microgrids" presented at *IEEE PES General Meeting*, Denver, Colorado, USA, June 6-10, 2004.

[16] A. Dimeas and N. Hatziargyriou, "A multi-agent system for microgrids", *Methods and Applications of Artificial Intelligence, Proceedings*, vol. 3025, pp. 447-455 2004, Available: <Go to ISI>://000221610800047.

[17] A. Dimeas and N. Hatziargyriou, "A MAS Architecture for Microgrids Control", *Proc. IEEE Intelligent Systems Application to Power Systems*, pp. 402 – 406, November 2005.

[18] A. L. Dimeas and N. D. Hatziargyriou, "Operation of a multiagent system for Microgrid control", *IEEE Transactions on Power Systems*, vol. 20, No. 3, pp. 1447-1455, Aug 2005, Available: <Go to ISI>://000231001900030.

[19] N. Hatziargyriou, H. Asano, R. Iravani, and C. Marnay, "Microgrids", *IEEE Power & Energy Magazine*, vol. 5, No. 4, pp. 78-94, Jul-Aug 2007, Available: <Go to ISI>://000250081400009.

[20] R. H. Lasseter, "Microgrids and distributed generation", *Journal of Energy Engineering-ASCE*, vol. 133, No. 3, pp. 144-149, Sep 2007, Available: <Go to ISI>://000248971000005.

[21] L. M. Cipcigan and P. C. Taylor, "A generic model of a virtual power station consisting of small scale energy zones" presented at *CIRED 2007*, Vienna, Austria, 21-24 May, 2007.

[22] L. M. Cipcigan, P. C. Taylor, and P. F. Lyons, "Evaluation and Mitigation of Low Voltage Network Thermal Constraints" presented at *IASTED - Power and Energy Systems - 2008*, Baltimore, Maryland, USA, 16th - 18th April, 2008.

[23] P. F. Lyons, P. Trichakis, P. C. Taylor, and G. Coates, "A practical implementation of a distributed control approach for microgrids", *Intelligent Automation and Soft Computing, An International Journal*, , Accepted, Expected publication quarter 3 2009.

[24] P. Trichakis, P. C. Taylor, P. Lyons, R. Hair, and G. Coates, "An agent based control approach for Microgrids" presented at *PowerGrid 08*, Milan, Italy, 2008.

[25] C. Marnay and G. Venkataramanan, "Microgrids in the Evolving Electricity Generation and Delivery Infrastructure" presented at *2006 IEEE Power Engineering Society General Meeting*, 2006.

[26] T. Gonen, *Electric Power Distribution System Engineering*. USA: McGraw-Hill, 1986.

[27] C. L. Sulzberger, "Triumph of AC - from Pearl Street to Niagara", *Power and Energy Magazine, IEEE*, vol. 1, No. 3, pp. 64 2003.

[28] "Seven Year Statement": National Grid plc., 2002, Available: http://www.nationalgrid.com/.

[29] "The Electricity Safety, Quality and Continuity Regulations," 2002.

[30] "Costs and Benefits of Underground Powerlines": Edison Electrical Institute, 2006, Available: http://www.eei.org/industry_issues/energy_infrastructure/distribution/UnderVSOver.pdf.

[31] A. E. Kiprakis and A. R. Wallace, "Maximising energy capture from distributed generators in weak networks", *Generation, Transmission and Distribution, IEE Proceedings*- vol. 151, No. 5, pp. 611 - 618, 13 Sept 2004.

[32] E. Lakervi and E. J. Holmes, *Electricity distribution network design*. London, UK, 2003.

[33] T. H. Chen and W. C. Yang, "Analysis of Multi-Grounded Four-Wire Distribution Systems Considering the Neutral Grounding", *IEEE Trans. Power Delivery*, vol. 16, No. 4, pp. 710-717, October 2001.

[34] "BS 7430: Code of Practice for Earthing" in *BS 7430*: British Standards Institution, London, UK, 1998.

[35] W. H. Kersting, *Distribution System Modelling and Analysis*: CRC Press, 2002.

[36] S. Papathanassiou, N. Hatziargyiou, and K. Strunz, "A benchmark low voltage microgrid network" presented at *Proc. CIGRE Symposium "Power Systems with Dispersed Generation"*, April, 2005, Available: http://www.sense.tu-berlin.de/publication/conference/2005/papathanassiou_hatziargyriou_strunz_lv_benchmark_cigre05.pdf.

[37] M. tenDonkelaar and M. J. J. Scheepers, "A socio-economic analysis of technical solutions and practices for the integration of distributed generation", Dispower, ECN, Report No. ECN-C--04-011, July, 2004, Available: http://www.ecn.nl/docs/library/report/2004/c04011.pdf.

[38] "Seven Year Statement": National Grid plc., 2009, Available: http://www.nationalgrid.com/.

[39] Wikipedia, "Northeast Blackout of 2003", 2008, Available: http://en.wikipedia.org/wiki/2003_North_America_blackout.

[40] K. H. LaCommare and J. H. Eto, "Cost of power interruptions to electricity consumers in the United States (US)", *Energy*, vol. 31, No. 12, pp. 1845 2006, Available: http://www.sciencedirect.com/science/article/B6V2S-4JN2NPP-1/2/179c3944b84953282b784acc0930cecd

[41] S. Ingram, S. Probert, and K. Jackson, "The impact of small scale embedded generation on the operating parameters of distribution networks", Department of Trade and Industry, London, UK, Report No. K/EL/00303/04/01, June, 2003, Available: http://www.ensg.gov.uk/assets/22_01_2004_phase1b_report_v10b_web_site_final.pdf.

[42] "EN 50160: Voltage characteristics of electricity supplied by public distribution systems," Brussels, Belgium: CENELEC, 1999.

[43] M. E. Galey, "Benefits of Performing Unbalanced Voltage Calculations", *IEEE Transactions on Industry Applications*, vol. 24, No. 1, pp. 15-24, Jan-Feb 1988, Available: <Go to ISI>://A1988M601600003.

[44] "Engineering Recommendation P29: Planning limits for voltage unbalance in the United Kingdom", The Electricity Association, London, UK, 1990.

[45] V. Levi, M. Kay, and I. Povey, "Reverse power flow capability of tap-changers", *IEE Conference Publications*, vol. 2005, No. CP504, pp. v4-43 2005, Available: http://link.aip.org/link/abstract/IEECPS/v2005/iCP504/pv4-43/s1

[46] "Accommodating Distributed Generation", Econnect Consulting, Department of Trade and Industry, London, UK, 2006.

[47] Whispergen, "Whispergen", 2008, Available: http://www.whispergen.com/.

[48] Microgen, "Microgen", 2008, Available: http://www.microgen.com/microgen/.

[49] Infinia, "Infinia Corporation", 2008, Available: http://www.infiniacorp.com/applications/combined_heat_power.php.

[50] Disenco, "Disenco", 2008, Available: http://www.disenco.com/html/mchp.htm.

[51] J. Cockroft and N. Kelly, "A comparative assessment of future heat and power sources for the UK domestic sector", *Energy Conversion and Management* vol. 47, No. 15-16, pp. 2349-2360 2006.

[52] "Honda Motor Co. Ltd Press Release", 2004, Available: http://world.honda.com/news/2004/c041020.html.

[53] G. Hoogers, *Fuel cell technology handbook*. Boca Raton: CRC Press, 2004.

[54] M.-F. Cell, "Microchap - Fuel Cell", 2008, Available: http://www.microchap.info/fuel_cell.htm.

[55] I. Staffell, R. Green, and K. Kendall, "Cost targets for domestic fuel cell CHP", *Journal of Power Sources*, vol. 181, No. 2, pp. 339 2008, Available:

http://www.sciencedirect.com/science/article/B6TH1-4R7J85K-2/2/c5901a2f29af278fa09bd3fe128e83b7

[56] J. Aabakken, "Chapter 2" in *Power Technologies Energy Data Book*. Golden, Colorado, USA: National Renewable Energy Laboratory, August 2006.

[57] "Bradford West City Tower Blocks Wind Energy Feasibility Study", Energy for Sustainable Development Ltd., Bradford, UK, December, 2003.

[58] S. Eriksson, H. Bernhoff, and M. Leijon, "Evaluation of different turbine concepts for wind power", *Renewable and Sustainable Energy Reviews*, vol. 12, No. 5, pp. 1419 2008, Available: http://www.sciencedirect.com/science/article/B6VMY-4N68049-1/2/cd2b3f0dc193eb9c6f9260b18e460eb4

[59] "HAWT versus VAWT: Small VAWTs find a clear niche", *Refocus*, vol. 4, No. 4, pp. 44 2003, Available: http://www.sciencedirect.com/science/article/B73D8-49BY4XR-15/2/329fac3e642ab9e2e350055437f7882a

[60] Renewable_Energy_UK, "Renewable Energy UK", 2008, Available: http://www.reuk.co.uk/Savonius-Wind-Turbines.htm.

[61] C. Concepts, "Carbon Concepts", 2008, Available: www.carbonconcepts.co.uk.

[62] *Windy Boy 2500 - Windy Boy 3000 - Operating Instructions*: SMA Regelsysteme GmbH, 2005.

[63] M. J. Currie, J. K. Mapel, T. D. Heidel, S. Goffri, and M. A. Baldo, "High-Efficiency Organic Solar Concentrators for Photovoltaics", *Science*, vol. 321, No. 5886, pp. 226-228, July 11, 2008 2008, Available: http://www.sciencemag.org/cgi/content/abstract/321/5886/226

[64] *Sunny Boy and Sunny Mini Central String Inverters for Photovoltaic Plants - Operating Instructions*: SMA Regelsysteme GmbH, 2005.

[65] J. Machowski, J. W. Bialek, and J. R. Bumby, *Power System Dynamics and Stability*: Wiley, 1997.

[66] C. Concordia and S. Ihara, "Load Representation in Power System Stability Studies", *IEEE Transactions on Power Apparatus and Systems*, vol. 101, No. 4, pp. 969-977 1982, Available: <Go to ISI>://A1982NG31500025.

[67] "Market Transformation Programme Policy Brief - UK Energy Consumption of Industrial Electric Motor Systems", 2006, Available: http://www.bpma-energy.org.uk/USERIMAGES/MTP%20Motor-Pump%20Policy%20Brief%20update%2020%20june%202006(1).pdf.

[68] A. von Jouanne and B. Banerjee, "Assessment of voltage unbalance", *Power Delivery, IEEE Transactions on*, vol. 16, No. 4, pp. 782 2001.

[69] "Load representation for dynamic performance analysis [of power systems]", *IEEE Task Force on Load Representation for Dynamic Performance, Power Systems, IEEE Transactions on*, vol. 8, No. 2, pp. 472-482, May 1993.

[70] B. Design, "Building Design - Osram", 2008, Available: http://www.buildingdesign.co.uk/elec/osram/osram-7.htm.

[71] "Energy consumption in the United Kingdom", BERR, London, Report No. URN 02/1049, 2002, Available: http://www.berr.gov.uk/files/file11250.pdf.

[72] BERR, "Energy consumption in the United Kingdom: domestic data tables. 2008 update", 2007, Available: http://www.berr.gov.uk/files/file47214.xls.

[73] "Worldwide Trends in Energy Use and Efficiency - Key Insights from IEA Indicator Analysis ", International Energy Agency, 2008, Available: http://www.iea.org/Textbase/Papers/2008/Indicators_2008.pdf.

[74] C. W. Gellings and W. M. Smith, "Integrating demand-side management into utility planning", *Proceedings of the IEEE*, vol. 77, No. 6, pp. 908 1989.

[75] D. R. Limaye, "Implementation of demand-side management programs", *Proceedings of the IEEE*, vol. 73, No. 10, pp. 1503 1985.

[76] F. Kreith and D. Y. Goswami, *Handbook of Energy Efficiency and Renewable Energy*: CRC Press, 2007.

[77] T. H. Bradley and A. A. Frank, "Design, demonstrations and sustainability impact assessments for plug-in hybrid electric vehicles", *Renewable and Sustainable Energy Reviews*, vol. 13, No. 1, pp. 115 2009, Available: http://www.sciencedirect.com/science/article/B6VMY-4P9T8GG-2/2/b9a7f473b53f091947abbd832457818b

[78] A. Price, G. Thijssen, and P. Symons, "Electricity Storage, A solution in network operation?" presented at *Distributech Europe*, Miami Beach FL, USA, 12 October, 2000.

[79] W. Kempton and J. Tomic, "Vehicle-to-grid power fundamentals: Calculating capacity and net revenue", *Journal of Power Sources*, vol. 144, No. 1, pp. 268 2005, Available: http://www.sciencedirect.com/science/article/B6TH1-4FXHJ9P-2/2/48041eee0ade5e17263795a6ddcd2b53

[80] R. Baxter, *Energy Storage: A Nontechnical Guide*: PennWell Books, 2006.

[81] C.-H. Dustmann, "The Swiss ZEBRA battery system" presented at *17th Electric Vehicle Symposium EVS-17*, Montreal, October 21-24, 2000.

[82] T. Sels, C. Dragu, T. Van Craenenbrock, and R. Belmans, "New energy storage devices for an improved load managing on distribution level" presented at *Power Tech Proceedings, 2001 IEEE Porto*, vol. 4, 2001.

[83] K. Thomas, "Ford unveils plug-in hybrid vehicle" in *Washington Post*, 2007.

[84] S. Freeman, "GM pledges to make plug-in hybrid vehicle" in *Washington Post*, 2006.

[85] O. Gehrke, S. Ropenus, and P. Venne, "Distributed Energy Resources and Control: A power system point of view", *R-1608*, pp. 248-257 2005, Available: www.risoe.dk/rispubl/reports/ris-r-1608_248-257.pdf

[86] F. F. Wu, K. Moslehi, and A. Bose, "Power System Control Centers: Past, Present and Future", *Proceedings of the IEEE*, vol. 93, No. 11, pp. 1890 - 1908, November 2005.

[87] I. Roytelman and V. Ganesan, "Coordinated local and centralized control in distribution management systems", *Power Delivery, IEEE Transactions on*, vol. 15, No. 2, pp. 718 2000.

[88] D. Botting, "Technical Architecture - A First Report: The Way Ahead", IEE Power Systems and Equipment Professional Network, 4th June, 2005, Available: http://www.ofgem.gov.uk/Pages/MoreInformation.aspx?docid=159&refer=NETWORKS/ELECDIST/POLICY/DISTGEN.

[89] R. H. Lasseter, "Certs Microgrid" presented at *System of Systems Engineering, 2007. SoSE '07. IEEE International Conference on*, 2007.

[90] J. Oyarzabal, J. Jimeno, A. Engler, C. Hardt, and J. Ruela, "Agent based Micro Grid Management System " presented at *International Conference on Future Power Systems*, November, 2005.

[91] M. M. Nordman and M. Lehtonen, "Distributed agent-based state estimation for electrical distribution networks", *IEEE Transactions on Power Systems*, vol. 20, No. 2, pp. 652-658, April 2005, Available: <Go to ISI>://000228778800016.

[92] M. Hird, N. Jenkins, and P. Taylor, "An Active 11kV Voltage Controller: Practical Considerations" presented at *13th International Conference and Exhibition on Electricity Distribution, CIRED 2003 - Part 1: Contributions*, vol. 1, 2003.

[93] A. Shafiu, T. Bopp, I. Chilvers, and G. A. Strbac, "Active management and protection of distribution networks with distributed generation" presented at *Power Engineering Society General Meeting, 2004. IEEE*, vol. 1, 10 June, 2004.

[94] T. Xu and P. Taylor, "Voltage control techniques for electrical distribution networks including distributed generation" presented at *IFAC 2008*, Seoul, South Korea, 2008.

[95] J. D. Crabtree, Y. Dickson, L. Kerford, and A. Wright, "Methods to accomodate embedded generation without degrading network voltage regulation", DTI, London, Report No. DTI/Pub URN 01/1005, 2001.

[96] J. Hill, V. Thornley, C. Barbier, A. Maloyd, and A. Oliver, "Innovative voltage control techniques for optimum connection of renewable and intermittent generation to distribution networks" presented at *40th International Universities Power Engineering Conference*, Cork, Ireland, 2005.

[97] S. White, "Active local distribution network management for embedded generation", DTI, Report No. 05/1588, 2005.

[98] S. K. Salman and Z. G. Wan, "Voltage control of distribution network with high penetration of renewable energy-based embedded generation" presented at *39th International Universities Power Engineering Conference, UPEC 2004*, vol. 2, 2004.

[99] P. N. Vovos, A. E. Kiprakis, A. R. Wallace, and G. P. Harrison, "Centralized and Distributed Voltage Control: Impact on Distributed Generation Penetration", *Power Systems, IEEE Transactions on*, vol. 22, No. 1, pp. 476 2007.

[100] S. Bose, Y. Liu, K. Bahei-Eldin, J. de Bedout, and M. Adamiak, "Tieline controls in microgrid applications" presented at *Bulk Power System Dynamics and Control - VII. Revitalizing Operational Reliability, 2007 iREP Symposium*, 2007.

[101] Q. Zhou and J. W. Bialek, "Generation curtailment to manage voltage constraints in distribution networks", *Generation, Transmission & Distribution, IET*, vol. 1, No. 3, pp. 492 2007.

[102] P. Taylor, T. Xu, S. McArthur, G. Ault, E. Davidson, M. Dolan, C. Yuen, M. Larsson, D. D. Botting, D. Roberts, and P. Lang, "Integrating voltage control and power flow management in AURA-NMS" presented at *CIRED Smart Grids*, Frankfurt, Germany, 2008.

[103] P. Trichakis, P. Taylor, P. Lyons, and R. Hair, "Transforming Low Voltage Distribution Networks Into Small Scale Energy Zones", *Proceedings of ICE: Energy* publication due 2009.

[104] T. Tran-Quoc, E. Monnot, G. Rami, A. Almeida, C. Kieny, and N. Hadjsaid, "Intelligent Voltage Control in Distribution Network with Distributed Generation" presented at *19th International Conference on Electricity Distribution - CIRED 2007*, Vienna, Austria, 21 - 24 May, 2007.

[105] L. Y. Seng and P. Taylor, "Innovative Application of Demand Side Management to Power Systems" presented at *Industrial and Information Systems, First International Conference on*, Peradeniya, Sri Lanka, 8 - 11 August, 2006.

[106] E. F. Mogos and X. Guillaud, "A voltage regulation system for distributed generation" presented at *Power Systems Conference and Exposition, 2004. IEEE PES*, 2004.

[107] P. D. Lund and J. V. Paatero, "Energy storage options for improving wind power quality" presented at *Nordic Wind Power Conference*, Espoo, Finland, 22 - 23 May, 2006.

[108] M. A. Kashem and G. Ledwich, "Energy requirement for distributed energy resources with battery energy storage for voltage support in three-phase distribution lines", *Electric Power Systems Research*, vol. 77, No. 1, pp. 10 2007, Available:

http://www.sciencedirect.com/science/article/B6V30-4JCSK4V-1/2/55be4b72fc8d417e9e5578f2be436d4a

[109] M. Braun, "Technological Control Capabilities of DER to Provide Future Ancillary Services" in *Use of Electronic-Based Power Conversion for Distributed and Renewable Energy Sources: 20 Years of Research on Power Conversion Systems.*, P. Zacharias, Ed. Magdeberg, Germany: ISET, 2008, pp. 321 - 331.

[110] J. McDonald, "Adaptive intelligent power systems: active distribution networks", State of Science Reviews - Infrastructure, Foresight, 5th July, 2006, Available: www.foresight.gov.uk.

[111] L. Kuang, L. Jinjun, W. Zhaoan, and W. Biao, "Strategies and Operating Point Optimization of STATCOM Control for Voltage Unbalance Mitigation in Three-Phase Three-Wire Systems", *Power Delivery, IEEE Transactions on*, vol. 22, No. 1, pp. 413 2007.

[112] B. Singh, K. Al-Haddad, and A. Chandra, "Harmonic elimination, reactive power compensation and load balancing in three-phase, four-wire electric distribution systems supplying non-linear loads", *Electric Power Systems Research*, vol. 44, No. 2, pp. 93 1998, Available: http://www.sciencedirect.com/science/article/B6V30-3TW320D-D/2/f7365d122e463c844347fa6d26813202

[113] P. Salmeron, J. C. Montano, J. R. Vazquez, J. Prieto, and A. Perez, "Compensation in nonsinusoidal, unbalanced three-phase four-wire systems with active power-line conditioner", *Power Delivery, IEEE Transactions on*, vol. 19, No. 4, pp. 1968 2004.

[114] H. Ding, S. Shuangyan, D. Xianzhong, and G. Jun, "A novel dynamic voltage restorer and its unbalanced control strategy based on space vector PWM", *International Journal of Electrical Power & Energy Systems*, vol. 24, No. 9, pp. 693 2002,

Available: http://www.sciencedirect.com/science/article/B6V2T-451DMBB-1/2/37189e56752dd6a8f9a0a79d94da774a

[115] R. A. F. Currie, G. W. Ault, C. E. T. Foote, and J. R. McDonald, "Active power-flow management utilising operating margins for the increased connection of distributed generation", *Generation, Transmission & Distribution, IET*, vol. 1, No. 1, pp. 197 2007.

[116] S. Jupe, P. Taylor, and C. Berry, "Assessing the value of active constrained connection managers for distribution networks" presented at *SmartGrids for Distribution, 2008. IET-CIRED. CIRED Seminar*, 2008.

[117] A. Collinson, F. Dai, A. Beddoes, and J. Crabtree, "Solutions for the connection and operation of distributed generation", Distributed generation co-ordinating group technical steering group, DTI, Report No. URN 03/ K/EL/00303/00/01/REP

July, 2004, Available: http://www.ensg.gov.uk/assets/solutions.pdf.

[118] "VRB Power Announces Progress with Sorne Hill Project and Hires Kieran O'Brien to Assist in Developing Energy Storage Adoption in Irish Market". Reuters, 2008, Available: http://www.reuters.com/article/pressRelease/idUS208517+08-Jul-2008+PRN20080708.

[119] J. P. Barton and D. G. Infield, "Energy storage and its use with intermittent renewable energy", *Energy Conversion, IEEE Transaction on*, vol. 19, No. 2, pp. 441 2004.

[120] O. Osika, T. Degner, C. Hardt, H. Lange, M. Vandenbergh, A. Dimeas, D. Georgakis, A. Kamarinopoulos, S. Papathanassiou, A. J. Goodwin, K. Elmasides, G. Iliadis, M. Barnes, C. Fitzer, and G. Kariniotakis, "Description of the laboratory micro-grids", Microgrids project report DH1, Report No. DH1, 2005.

[121] M. Barnes, A. Dimeas, A. Engler, C. Fitzer, N. Hatziargryriou, C. Jones, M. Papathanassiou, and M. Vandenbergh, "MicroGrid Laboratory Test Facilities"

presented at *International Conference on Future Power Systems*, vol. 2, 18 November, 2005.

[122] Y. Zong, A. Andersson, O. Gehrke, F. Sottini, H. Bindner, and P. Norgord . In: , "Implementation of a load management research facility in a distributed power system" presented at *Proceedings of the Nordic wind power conference (NWPC 2007)*, Risoe, Denmark, 1 - 2 Nov., 2007, Available: http://www.risoe.dtu.dk/rispubl/reports/ris-r-1624.pdf.

[123] *More MicroGrids*, NTUA, 2006 - 2009, Last accessed: November 2008, Available: http://www.microgrids.eu/index.php?page=index.

[124] R. Lasseter, A. Akhil, C. Marnay, J. Stephens, J. Dagle, R. Guttromson, A. S. Meliopoulous, R. Yinger, and J. Eto, "Integration of Distributed Energy Resources: The CERTS MicroGrid Concept", Report No. LBNL-50829, April, 2004, Available: http://certs.lbl.gov/CERTS_P_DER.html.

[125] J. A. Momoh, *Electric power distribution, automation, protections, and control*. London: CRC Press, 2008.

[126] Mathworks, "Simulink", 2008, Available: http://www.mathworks.com/products/simulink/.

[127] "Distributed Power Generation", Available: http://www.dispowergen.com/.

[128] ABB, "ABB industrial drives - ACS800, single drives, 0.55 to 5600 kW - Technical catalogue": ABB, Available: http://library.abb.com/global/scot/scot201.nsf/veritydisplay/198ccd2d35e3cdb7c125743d002766c4/$File/13725_ACS800_Single_drive_catalogue_68375126_Rev_I_lowres.pdf.

[129] "IEC 60364-1 Low-voltage electrical installations – Part 1: Fundamental principles, assessment of general characteristics, definitions", International Electrotechnical Commission, 1 November, 2005.

[130] B. Lacroix and R. Calvas, "Earthing systems worldwide and evolutions", Cahier Technique, Schneider Electric, 1995.

[131] B. Lacroix and R. Calvas, "Earthing Systems in LV", Cahier Technique, Schneider Electric, 2000.

[132] *Sunny Island - Installation and Operating Instructions. Bidirectional Battery Inverter SI4500 for stand-alone applications, V.3.1* SMA Regelsysteme GmbH, Year to be found.

[133] University_of_Kassel, "University of Kassel‘s Institute for Electrical Energy Technology", 2008, Available: http://www.evs.e-technik.uni-kassel.de/EVSFrameset.html.

[134] ISET, "ISET", 2008, Available: http://www.iset.uni-kassel.de/pls/w3isetdad/www_iset_new.main_page.

[135] A. Arulampalam, M. Barnes, A. Engler, A. Goodwin, and N. Jenkins, "Control of power electronic interfaces in distributed generation Microgrids", *International Journal of Electronics*, vol. 91, No. 9, pp. 503-523, Sep 2004, Available: <Go to ISI>://000225571700001.

[136] Elecsol, "Elecsol Batteries", 2008, Available: http://www.elecsolbatteries.com/.

[137] National_Instruments, "National Instruments LabVIEW", 2008, Available: http://www.ni.com/labview/.

[138] National_Instruments, "National Instruments Website", 2008, Available: www.ni.com

[139] "LEM website Technical Reports ", Available: www.lem.com

[140] C. Crabtree, *Investigation into the Impacts of Small Scale Embedded Generation on Low Voltage Distribution Networks*, MEng Thesis, 2006, School of Engineering, Durham University.

[141] W. D. Kellogg, M. H. Nehrir, G. Venkataramanan, and V. Gerez, "Generation unit sizing and cost analysis for stand-alone wind, photovoltaic, and hybrid wind/PV systems", *IEEE Transactions on Energy Conversion*, vol. 13, No. 1, pp. 70-75, Mar 1998.

[142] NaREC, "Energy LINK Laboratory": NaREC, 2008, Available: http://www.narec.co.uk/main/st1703/distributed_generation.htm.

[143] A. R. Bergen and V. Vittal, "Generator Voltage Control" in *Power System Analysis*, Second ed. New Jersey: Prentice Hall, 2000, pp. 273 - 293.

[144] C. V. Jones, *Unified Theory of Electrical Machines*: Butterworth, 1967.

[145] A. Aamodt and E. Plaza, "Case-based reasoning: Foundational issues, methodological variations, and system approaches", *Artificial Intelligence Communications*, vol. 7, No. 1, pp. 39 - 52 1994.

[146] L. Rundqwist, *Anti-reset windup for PID controllers*, PhD Thesis, 1991, Department of Automatic Control, Lund Institute of Technology.

[147] C. Bohn and D. P. Atherton, "An analysis package comparing pid antiwindup strategies", *IEEE Systems Magazine*, vol. 15, No. 2, pp. 34 - 40, April 1995.

[148] V. Thornley, N. Jenkins, P. Reay, J. Hill, and C. Barbier, "Field Experience with Active Network Managment of Distribution Networks with Distributed Generation" presented at *19th International Conference on Electricity Distribution, CIRED 2007*, Vienna, Austria, 21 - 24 May, 2007.

[149] R. Lestage, A. Pomerleau, and A. Desbiens, "Improved constrained cascade control for parallel processes", *Control Engineering Practice*, vol. 7, pp. 969 1999, Available:

http://www.ingentaconnect.com/content/els/09670661/1999/00000007/00000008/art00049.

[150] *The Foundation for Intelligent Physical Agents - FIPA Agent Management Specification*, Last accessed: August 2008, Available: http://www.fipa.org/specs/fipa00023/SC00023K.pdf.

[151] SMA, *Sunny Island - Installation and Operating Instructions. Bidirectional Battery Inverter SI4500 for stand-alone applications, V.3.1* SMA Regelsysteme GmbH, 2003.

[152] S. D. J. McArthur, E. M. Davidson, V. M. Catterson, A. Dimeas, N. Hatziargyriou, F. Ponci, and T. Funabashi, "Multi-Agent Systems for Power Engineering Applications: Concepts, Approaches and Technical Challenges", *IEEE MAS Technical White Paper* 2006.

[153] UCTE, "UCTE Operation Handbook", 20th July, 2004, Available: www.ucte.org/resources/publications/ophandbook/.

[154] "Overview of IEC 61850", 2008, Available: http://www.61850.com/.

[155] G. Kariniotakis, J. Oyarzabal, A. Amorim, J. F. G. Cobben, F. v. Overbeeke, B. Buchholz, O. Perego, J. E. Nielsen, and V. Keivanidis, "WPF Periodic Activity Report 2006", January, 2007.

[156] M. Armstrong, D. J. Atkinson, A. G. Jack, and S. Turner, "Power system emulation using a real time, 145 kW, virtual power system" presented at *Power Electronics and Applications, 2005 European Conference on*, 2005.

[157] S. Turner, D. J. Atkinson, A. G. Jack, and M. Armstrong, "Development of a high bandwidth multi-phase multilevel power supply for electricity supply network emulation" presented at *Power Electronics and Applications, 2005 European Conference on*, 2005.

[158] H. J. Slater, D. J. Atkinson, and A. G. Jack, "Real-time emulation for power equipment development. II. The virtual machine", *Electric Power Applications, IEE Proceedings* -, vol. 145, No. 3, pp. 153 1998.

[159] Highly_Distributed_Power_Systems, "Highly Distributed Power Systems": UK Research Council Supergen project grant GR/T28836/01, 2005-2009, Available: http://www.supergen-hdps.org/.

[160] D. Pudjianto, C. Ramsay, and G. Strbac, "Virtual power plant and system integration of distributed energy resources", *Proceedings of the IET - Generation, Transmission and Distribution*, vol. 1, No. 1, pp. 10 - 16, March 2007.

[161] UK-Microgrids, "UK-Microgrids": UK Research Council EPSRC grant EP/C00177X/1, 2005-8, Available: http://gow.epsrc.ac.uk/ViewGrant.aspx?GrantRef=EP/C00177X/1.

[162] US_Department_of_Energy, "Advanced Distribution Technologies and Operating Concepts -Microgrids": US Department of Energy Electricity Distribution Programme, 2008, Available: http://www.electricdistribution.ctc.com/microgrids.htm.

[163] *International Journal of Distributed Energy Resources, Microgrids Special Issue*, 2006/7.

[164] M. Barnes, J. Kondoh, H. Asano, J. Oyarzabal, G. Ventakaramanan, R. Lasseter, N. Hatziargyriou, and T. Green, "Real-World MicroGrids An Overview" presented at *IEEE International Conference on System of Systems Engineering, 2007. SoSE '07*, 2007.

[165] More_MicroGrids, "More MicroGrids": European Research Project, 2006-2009, Available: http://www.microgrids.eu/index.php?page=index.

[166] T. Degner and P. Strauss, "Laboratory for Distributed Generation", Project Highlight document no. 3, EC Project DISPOWER, Available: http://www.iset.uni-kassel.de/.

[167] E. Sanchez, F. J. Santiago, and J. Oyarzabal, "MoreMicroGrids - WPF: Alternative µGrids Designs - DF2 - Part I – Labein's MicroGrid description", Labein, Labein, 6th November, 2006.

[168] H. Bindner, P. Anm, and O. Ibsen, "Vanadium redox-flow batteries - Installation at Riso for characterisation measurements" presented at *Energy solutions for sustainable development - Proceedings of the Riso international energy conference 2007*, Roskilde, Denmark, 22 - 24 May 2007, Available: http://www.risoe.dtu.dk/rispubl/reports/ris-r-1608.pdf.

[169] *SYSLAB*, Risoe, 2008, Last accessed: November 2008, Available: http://www.risoe.dk/research/sustainable_energy/wind_energy/projects/syslab.aspx/.

[170] Siemens, "WinCC", 2008, Available: http://www.automation.siemens.com/hmi/html_76/products/software/wincc/index.htm .

[171] D. Nestle, C. Bendel, and J. Ringelstein, "Bi-directional energy management interface (BEMI) - integration of the low voltage level into grid communication and control" presented at *Proceedings of Ninth International Conference on Electricity Distribution (CIRED) 2007*, Vienna, Austria, 21-24 May 2007, 2007, Available: http://www.cired.be/CIRED07/pdfs/CIRED2007_0520_paper.pdf.

[172] Dranetz_BMI, "Signature System", 2008, Available: http://www.dranetz-bmi.com/products/prod2.cfm?prodcat=5.

[173] J. A. Baroudi, V. Dinavahi, and A. M. Knight, "A review of power converter topologies for wind generators", *Renewable Energy*, vol. 32, No. 14, pp. 2369 2007, Available: http://www.sciencedirect.com/science/article/B6V4S-4MVN01F-2/2/c9dc0dafbbea3b1778d55acb650baeee

[174] LabJack, "LabJack", 2008, Available: http://www.labjack.com/.

[175] "EU Research Project MicroGrids [Online]", Available: http://micro-grids.power.ece.ntua.gr.

[176] dSPACE_GmBH, "dSPACE": dSPACE_GmBH, 2008, Available: http://www.dspaceinc.com/ww/en/inc/home.cfm.

[177] A. Engler and C. Hardt, "Operation of a prototype Microgrid system based on micro-sources equipped with fast-acting power electronics interfaces" presented at *31st Power Electronics Specialists Conference 2004*, Aachen, 20-25 June, 2004.

[178] J. C. Das, *Power system analysis : short-circuit load flow and harmonics*. New York: Marcel Dekker, 2002.

[179] *PSCAD™ Users Guide Version Ver. 4.2.0*: Manitoba HVDC Research Centre Inc., 2005.

[180] *EMTDC™ Users Guide Ver. 4.2.0*: Manitoba HVDC Research Centre Inc., 2005.

[181] M. E. Baran and F. F. Wu, "Network reconfiguration in distribution systems for loss reduction and load balancing", *Power Delivery, IEEE Transactions on*, vol. 4, No. 2, pp. 1401 1989.

[182] G. B. Jasmon and L. H. C. C. Lee, "Distribution network reduction for voltage stability analysis and loadflow calculations", *International Journal of Electrical Power & Energy Systems*, vol. 13, No. 1, pp. 9 1991, Available: http://www.sciencedirect.com/science/article/B6V2T-47X77CN-34/2/8e30de6a81a2247356a8bada80e9e171

[183] P. Subburaj, K. Ramar, L. Ganesan, and P. Venkatesh, "Distribution System Reconfiguration for Loss Reduction using Genetic Algorithm", *Journal of Electrical Systems*, vol. 2, No. 4, pp. 198-207, December 2006.

[184] C. S. Cheng and D. Shirmohammadi, "A 3-Phase Power-Flow Method for Real-Time Distribution-System Analysis", *IEEE Transactions on Power Systems*, vol. 10, No. 2, pp. 671-678, May 1995, Available: <Go to ISI>://A1995RB28900020.

[185] R. M. Ciric, A. P. Feltrin, and L. F. Ochoa, "Power flow in four-wire distribution networks - General approach", *IEEE Transactions on Power Systems*, vol. 18, No. 4, pp. 1283-1290, Nov 2003, Available: <Go to ISI>://000186590300008.

[186] R. M. Ciric, L. F. Ochoa, A. Padilla-Feltrin, and H. Nouri, "Fault analysis in four-wire distribution networks", *IEE Proceedings-Generation Transmission and Distribution*, vol. 152, No. 6, pp. 977-982, Nov 2005, Available: <Go to ISI>://000233379800030.

[187] "Specification for planning & design of greenfield low voltage housing estates", Scottish Power, April, 2003.

[188] "Framework for underground networks (and associated HV/LV distribution substations) in EDF Energy's three distribution networks (EPN, LPN and SPN)", EDF Energy, December, 2004.

[189] "Framework for design and planning for low voltage housing developments underground network installations and associated new HV/LV distribution substations", Western Power Distribution, January, 2005.

# Appendix A PUBLICATIONS

## *Journal Articles*

L. Cipcigan, P. Taylor, and **P. Lyons**, "A Dynamic Virtual Power Station Model Comprising Small Scale Energy Zones", *International Journal of Renewable Energy Technology*, Vol. 1, Issue 2, pp 172 -191, 2009.

**P. Lyons**, P. Trichakis, P. Taylor and G. Coates, "A Practical Implementation of a Distributed Control Approach for MicroGrids", *Autosoft - Intelligent Automation and Soft Computing Journal, MicroGrids Special Edition* Vol. 16, Issue 2, pp 315 -330, 2009.

P. Trichakis, P. Taylor, **P. Lyons**, and R. Hair, "Transforming Low Voltage Networks Into Small Scale Energy Zones", *Proceedings of the Institution of Civil Engineers, Journal of Energy* Vol. 162, Issue 1, pp. 37 – 46, February 2009.

P. Trichakis, P. Taylor, R. Hair and **P. Lyons**, "Predicting the technical impacts of high levels of small scale embedded generators on low voltage networks" *IET Renewable Power Generation,* Vol. 2, Issue 4, pp.249 – 262, December 2008.

## *Conference Proceedings*

P. Taylor, S. Jupe, P. Trichakis, A. Michiorri, and **P. Lyons**, "Active MV and LV Distribution networks", CIGRE NGN, Paris, France, 2008.

P. Trichakis, P. Taylor, **P. Lyons**, R. Hair, and G. Coates, "An agent based control approach for Microgrids". *PowerGrid 08*, Milan, Italy, 3-5 June 2008.

L. Cipcigan, P. Taylor, P and **P. Lyons**, "Evaluation and mitigation of low voltage network thermal constraints", *IASTED 2008*, Baltimore, USA, 16-18 April 2008.

P. Trichakis, P. Taylor, L. Cipcigan, **P. Lyons**, R. Hair and T. Ma, "An Investigation of Voltage Unbalance in Low Voltage Distribution Networks with High Levels of SSEG",

*41st Universities Power Engineering Conference, UPEC 2006*, Newcastle, UK, 6-8 September 2006.

**P. Lyons**, P. Taylor, P., L. Cipcigan, P. Trichakis and A. Wilson, "Small Scale Energy Zones and the Impacts of High Concentrations of Small Scale Embedded Generators", *41st Universities Power Engineering Conference, UPEC 2006*, Newcastle, UK, 6-8 September 2006.

# Appendix B EXPERIMENTAL REQUIREMENTS FOR INVESTIGATION OF SSEZ CONCEPT

## Appendix B-1 Introduction

Intelligent active distribution network control architectures and techniques, as outlined in the chapter three, have different definitions depending on the network topology, the rating and mixture of distributed generation, operational aims and their specific controller implementations.

However, before centralised or distributed control algorithms can be implemented in actual networks it is useful to implement them in laboratory emulation facilities. The role of these facilities in all cases is to: -

1. Assess the impact of SSEGs on distribution networks.
2. Validate models.
3. Implement, test and refine the control algorithms developed during research programs.

The first of these roles can also be investigated through simulation. However, simulations are limited by the mathematical approximations of the models used in each study which require validation. LV distribution networks and LV network emulation laboratories use physical LV networks, with power converters and small scale generation in contrast to simulations of LV distribution networks.

However, the validation and implementation of control algorithms on an actual distribution network could cause considerable disruption to both network operation and service to customers, therefore electricity operators are very slow to implement a testing program that might jeopardise supply to customers. Moreover, as real SSEG and load customers are connected to distribution networks, repeatable tests will be impossible to

implement. This is in contrast to SSEG emulation based LV network emulation laboratories.

This section will initially describe and illustrate the advantages of emulation in the development of LV distribution network laboratories. This is followed by an investigation into the requirements for each element of an LV distribution network laboratory considering proposed future generic LV networks with large concentrations of SSEG, energy storage and controllable load, data acquisition systems and the development of active network control infrastructure compatible with the SSEZ concept. In order to fully exploit the advantages accruing from laboratory test facilities they need to be designed to reflect, as much as possible, the nature of the envisaged future active distribution network.

## Appendix B-2 Emulation

LV distribution network laboratories, in this work, are defined as scaled versions of LV networks with less generation, energy storage and load and with a much smaller electrical network. In addition, if accurate data is available the other constituent network components may also be emulated. An example of this would be to use a virtual machine [158] to mimic the operation of a specific small scale wind turbine and synchronous generator in a particular wind scenario. The output of the virtual machine could then be rectified and inverted using commercial products preserving the accuracy of the system.

In addition, to the power system modelling, control systems and signals also need to be modelled accurately if a realistic representation of the system is to be achieved. In contrast to simulation, emulation laboratories use actual signals and a real control system.

LV distribution network emulation laboratories therefore are powerful tools to enable investigation of large penetrations of SSEG and the control systems that will mitigate the undesirable effects of high penetrations of SSEG and augment their value.

## Appendix B-3 LV Network Topology

In this research two generic LV distribution network models that have been used as benchmark future distribution networks are considered. The first one is based on a typical UK urban distribution network model illustrated in Figure B-1, as approved by UK DNOs [41] and is referred to in this research as the UK generic LV network [9]. The second LV distribution network model based on the benchmark LV MicroGrid network, is a radial suburban LV distribution network [36]. The benchmark LV MicroGrid network has been adopted as a benchmark LV system by CIGRE TF C6.04.02: "Computational Tools and Techniques for Analysis, Design and Validation of Distributed Generation Systems" and is also illustrated in Figure B-1. These are not actual networks and are instead networks designed to capture the salient characteristics of the LV distribution networks of the UK and Europe.

The UK generic LV network proposed in [9] refers to the connection of SSEGs on just one 0.4kV substation of the distribution network in [41]. The entire LV network in this system consists of four radial 300m long feeders of underground cable distribution system serving 384 evenly-distributed customers [41].

This benchmark LV MicroGrid network comprises of a single 20/0.4kV 400kVA ground-mounted distribution transformer and three 0.4kV outgoing feeders: one residential, one industrial and one commercial. The residential feeder is in total 350m long and supplies 14 single-phase and 12 three-phase connected customers. The industrial feeder is 200m long and supplies a three-phase connected workshop, while the commercial feeder is

330m long and supplies 15 single-phase and 2 three-phase connected customers. Customers are not spread uniformly throughout this network and are connected with different service cables, which are typically 30m long. The residential feeder is defined in this work as the European generic LV network [9].

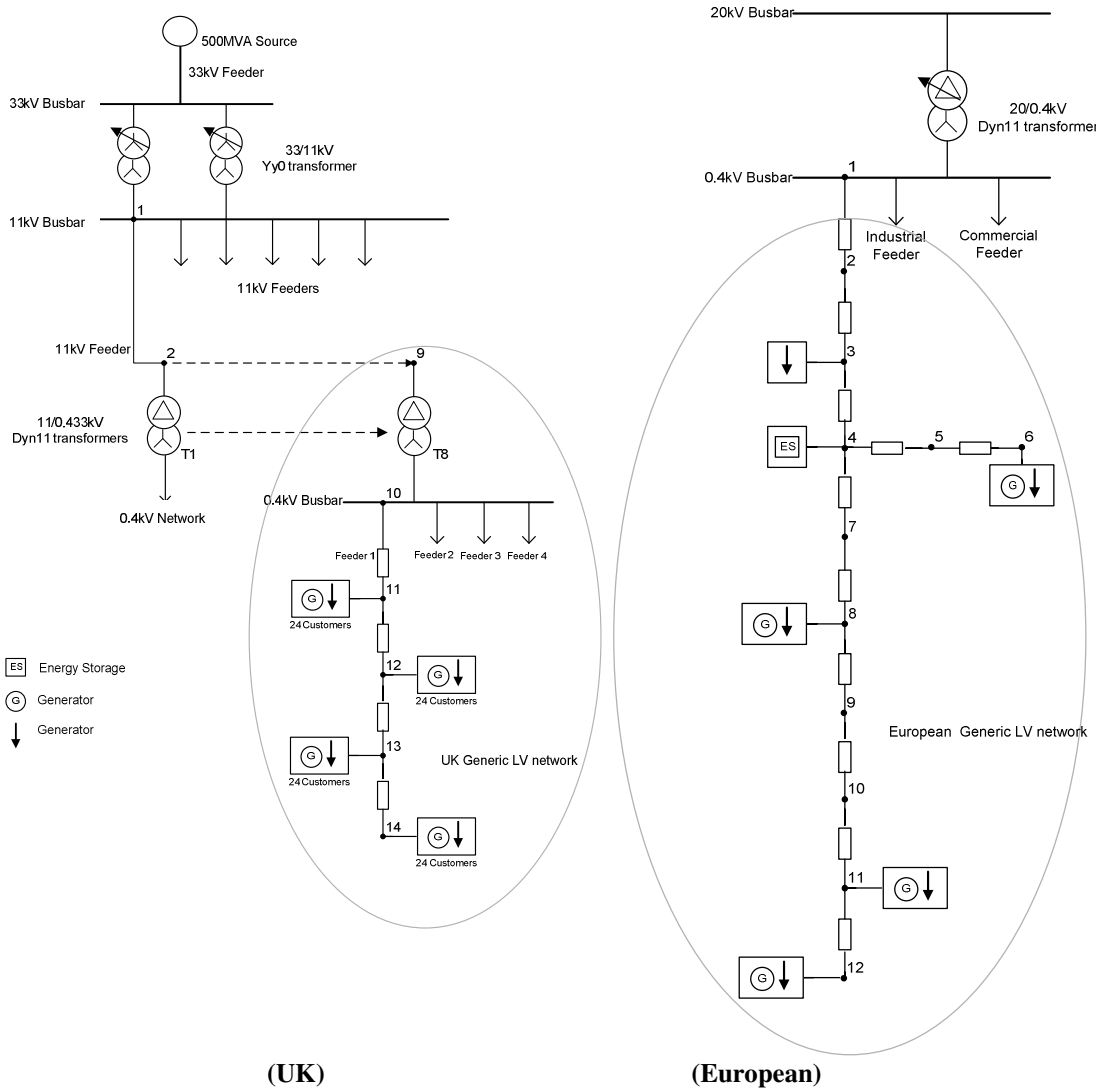


**Figure B-1: UK Generic and European Generic Network Models**

Ideally, an LV distribution network emulator should consist of three-phase networks which are tapered and are of radial construction as in the generic LV networks. The network connection emulator should be able to emulate the action of a transformer and

provide power balance to the LV system. The UK generic LV network has a uniform distribution of generation and load whereas the European generic LV network does not. As actual LV networks are non-uniform the LV network of the emulator should facilitate different distribution of load and generation. In addition, the system network impedances should be chosen judiciously to ensure that measured voltage and voltage unbalance deviations are large enough to facilitate measurement during changes in load or generation on the system.

## Appendix B-4 Generation Technologies

A single-phase generator believed to be typical of the size of domestic generator in development has been previously modelled at each house in the UK generic LV network resulting in a uniform distribution of SSEG. This generator has an output of 1.1kW operating at power factor of 0.95 lagging or unity [41] which is comparable to some commercially available dCHP units [47].

The largest generator in the benchmark European generic LV network is a 30kW three-phase microturbine connected approximately 105m along the LV feeder via a 105m lateral. Four 2.5kW single-phase photovoltaic generators are the smallest generators on the system and are distributed unequally among the three phases. These are located approximately 175m along the LV feeder. In addition, there is wind turbine generation and a fuel cell at other nodes within the system. Generation is therefore not uniformly distributed both in terms of phase and geographical distribution on this LV network. No data is available on the power factor of the generators in the system and therefore unity power factor is assumed.

In the UK, regulations exist that ensure that power is connected to the LV network at power factor of between 0.95 leading and 0.95 lagging [1]. Many SSEGs require inverter

interfaces or, in the case of some dCHP units, single-phase induction motors with a capacitor supplying the reactive power requirements, to connect to the LV distribution network.

The generation in an LV distribution network emulator should ideally include inverter coupled single-phase and three-phase generation emulation. All currently important or emerging SSEG sources should be available; wind, photovoltaic and fuel cells [36]. In addition, single-phase, induction machine coupled dCHP could also be included in the system. Accurate emulation enables repeatable testing under a wide variety of conditions independent of weather conditions. Ideally, actual SSEG systems should also be included for validation of the generation emulation systems.

## Appendix B-5 Load

In the UK generic LV network maximum and minimum domestic load figures were taken from Electricity Association sources, which state that the minimum and maximum demand figures of each domestic single-phase load are 0.16kVA and 1.3kVA After Diversity Maximum Demand (ADMD) respectively at a power factor of 0.95 [26]. The load is evenly distributed throughout this LV distribution network. An actual LV distribution network however would not have load evenly distributed and therefore this is not realistic.

The distribution of load in the European generic LV network is non-uniform. Load figures based on standardized coincidence factors for residential, industrial and commercial customers were used, as described in [36]. The power factor of the loads is assumed to be 0.85 lagging. The total maximum demand is 272.1kW, or 68% of transformer capacity, while the total minimum demand is 85.2kW, equal to 21.3% of

transformer capacity. The load is unevenly distributed though the network both in terms of position on the radial network and phase [36].

The reactive power due to load in both models is assumed to be due to phase distortion. In practice this is not true, as low power factor may also be due to harmonic distortion caused by load characteristics outlined in chapter two. The expected continued increase in home appliance load and loads supplied using switched mode power supplies (SMPS) are likely to result in their continuous increase in their share of future load. While in the commercial sector load attributable to air conditioning units is likely to increase its share of the load mix.

The load in an LV distribution network emulation laboratory should therefore consist of a number of sophisticated load emulators which would seek to emulate, on a smaller scale, the operation of the aggregated effects of the different categories of load at different points on the network. The load emulator therefore would need to be able to emulate the phase and the harmonic distortion associated with each load category. In addition, a set of actual household loads which could be easily connected to the system could be utilised to investigate the interaction between these systems and actual SSEGs.

## Appendix B-6 Energy Storage Technologies

Energy storage is not included in the UK generic LV network. In the European generic LV network a centralised central storage unit is considered [36]. This is to facilitate islanded operation by providing balance of power and frequency regulation within the LV network. It should be noted however, that these facilities may also be provided by a number of local energy storage units with a decentralised balance of power and frequency regulation control system [120]. In addition, the probability of large distributions of domestic fuel cells, EVs or PHEVs on LV networks also providing energy storage in

future distribution networks would indicate that distributed energy storage would be useful for an LV distribution network emulator. ESUs can operate as generators as well as loads and therefore inverter coupling devices must observe the same connection requirements as SSEGs [1].

## Appendix B-7 Data Acquisition Systems

The data acquisition system for an LV distribution network emulation laboratory must be able to accurately determine the parameters associated with the network constraints identified in chapter two. The data acquisition system therefore should be able to measure root mean squared (RMS) voltage and current on each phase of the LV network and at a number locations within the network as identified in Figure B-1 but in particular at the remote end and at the network connection point. In addition, the system should also be able to accurately detect phase difference between all voltage and current waveforms relative to a reference waveform.

## Appendix B-8 Active Network Control Infrastructure

The LV distribution network emulation laboratory should provide a platform to develop centralised and distributed control algorithms in grid connected operation. The centralised and distributed control algorithms, when adequately designed, should be able to interact with SSEGs, ESUs and controllable load to return the network to satisfactory operation within the defined limits following a disturbance to the system.

# Appendix C REVIEW OF EXISTING LOW VOLTAGE DISTRIBUTION NETWORK EMULATION LABORATORIES

## Appendix C-1 Introduction

In order to satisfy the experimental requirements for the design of an active, LV distribution network laboratory, a review of existing network emulation laboratories is required to determine the state-of-the-art in this area. A number of laboratory test facilities, whose objective being proof of concept of active distribution network control systems, have been reviewed previously [15, 120, 123-124, 159-163]. Many of these facilities are primarily concerned with three-phase distributed generating units rather than single-phase SSEGs that are central to the SSEZ concept. However, European laboratories at NTUA [120-121, 164-165] in Athens, Greece, DeMoTec [120-121, 164-166] at Kassel, Germany, Labein's Experimental Centre in Bilbao, Spain [164-165, 167], and the SYSLAB at Risø, Denmark [168-169] are useful for comparison. In addition, UK laboratories, NaREC's EnergyLINK Laboratory [7, 142] in Blyth, Northumbria and the University of Manchester Microgrid/Flywheel energy storage prototype [120-121, 164-165], are also considered in this investigation. These laboratory facilities are evaluated with reference to the following criteria: -

- LV Network Topology
- Generation technologies
- Load
- Energy Storage Technologies
- Data Acquisition Systems
- Active Network Control Infrastructure

This approach is taken to be consistent with the requirements for the LV distribution network emulation laboratory proposed in Appendix B.

## Appendix C-2 MicroGrid Test Facility at NTUA (Athens)

At NTUA a single-phase grid connection provides power balance during normal operation [120-121, 123, 164-165]. The LV network topology is single-phase with a relay to switch between islanded and grid connected operation [121].

Small-scale wind and PV generation are coupled to the single-phase LV network via G83 compliant inverters but no SSEG emulation facilities exist [120-121, 123, 164-165]. The laboratory scale microgrid system uses a selection of household loads, which are controlled by a programmable logic controller (PLC) system. This PLC system is interfaced with the MAS system deployed in this laboratory [120-121, 164-165].

Lead acid batteries in conjunction with another inverter, is used to provide energy storage capability at this facility [120-121, 164-165].

Each inverter has an RS232 serial communications link to a PC running WinCC [170] and LabVIEW™ [137] programming environments [120-121]. This is possible as a proprietary OPC (OLE for process control where OLE represents Object Linking and Embedding) server is available to interface with the SMA inverters. These inverter systems provide measurements of the parameters of the battery, PV and wind turbine systems (voltage, current and frequency, state of the batteries etc.).

In addition to this data acquisition functionality, the RS232 serial communications enables online modification of the parameters of the battery inverter droop controller [120-121]. The active and reactive power import/export can therefore be regulated. Due to the communications limitations of this system it has been observed that new set points can be sent no quicker than every 5 seconds. Finally, a controllable load is coupled to the

LV network, which is implemented using various load types and a relay panel controlled manually, by a Programmable Logic Controller (PLC) or a PC-Card [120-121, 164-165].

## Appendix C-3 DeMoTec (Kassel)

DeMoTec features a three-phase multiple bus system where load, generation or energy storage can be easily configured into various power system topologies. In addition, an MV network emulator is provided, known as the *Distribution System Simulator,* where impedance values can be varied to investigate different lengths and types of conductors. In addition, a three-phase synchronous machine coupled to a DC machine and drive rated to 80kVA can be used to emulate the network connection. This system is capable of supplying the LV network at 50Hz or 60Hz. Two MV/LV transformers, rated at 400kVA and 175kVA, connected on the MV side to the utility grid, are also available which provide power balance to the system [120-121, 123, 164-166].

Actual PV and dCHP systems can be used to export power to the LV network. Furthermore, the system also features a 5kW wind turbine emulator [120-121, 123, 164-166] to enable repeatable testing.

A workshop with typical loads like refrigerators, lighting, a pump drive, drilling equipment and a welding machine is also available for connection to the LV network. In addition, load emulation of non-unity power factor loads is possible using combinations of resistive, inductive and capacitive elements. However, load harmonic distortion effects are not emulated by this system [120-121, 164-166].

Fuel cells, lead acid battery banks and a flywheel are also available for connection to the LV network [120-121, 164-166].

Data acquisition is managed by specialist software for visualisation and industrial process control [120-121, 164]. The communication protocol for this system is an lnterbus-S

control line. To enable system monitoring a proprietary SCADA [125] system has been developed.

The SCADA system also controls the generators. XML-RPC was selected as communication protocol between the generators themselves which is carried on a separate Ethernet system [120-121, 164]. In addition, a distributed controller designated Bi-directional Energy Management Interface (BEMI) [171] is used to interface with domestic load, energy storage and generation utilising IEC 61850 [154] which is a standard for the design of substation automation systems, using a variety of communication systems such WLAN and Ethernet [171].

## Appendix C-4 Labein Experimental Centre (Bilbao)

At Labein, the *μGrid Switchboard* is used to connect any generator, load or energy storage unit to one of the three, three-phase LV busbars. An LV network emulator, known as the *Line Simulator,* is also available enabling the investigation into the effect of X/R conductor ratios on LV networks with high concentrations of SSEG. Power balancing is provided by 2 X 1250kVA transformers MV/LV transformers. In addition, a 110kVA network connection emulator is also available which enables the emulation of a variety of network conditions [164, 167].

Actual PV and wind SSEG systems are available for connection to the LV network. The dCHP unit however is above the defined SSEG power levels [164, 167]. None of these systems are emulated.

A system of computer controlled resistive loads are used to emulate the effect of load [164, 167]. A limitation of using resistive loads is that unity power factor load can be emulated only.

Ultra capacitors, lead acid battery banks and a flywheel are available for energy storage purposes [164, 167].

An integrated web-based platform known as the DRANETZ-BMI Signature System [172] that allows users to remotely monitor power systems in real time has been installed. The system enables measurement of hundreds power quality, energy and process parameters including half-cycle RMS triggering on voltage and current, current harmonic and inter-harmonic measurement [167].

The control system is built around IEC 61850 [154] over an Ethernet communications network [155].

## Appendix C-5 SYSLAB (Risø)

The SYSLAB at Risø utilises a 45kVA back-to-back converter [173], acting as a network connection emulator, to provide power balance to the system and also provides flexibility in voltage and frequency settings [168-169]. Three sites are interconnected using an LV network with the distances from the middle site to the other two equal to 300m and 700m respectively.

An 11kW small-scale wind turbine generator system and a 7kW PV system are also installed [168-169].

A lumped resistive load is used in conjunction with 10kW of time deferrable space heating load. Furthermore, this system is equipped with a small, freestanding office building, titled *FlexHouse* [107, 122]. This facility has been specifically designed to investigate active load management. The individual loads in the building are controlled by a central computer [122]. The combined peak load of the *FlexHouse* system is almost 20kW.

A 120kWh, Vanadium Redox Battery (VRB) [82] with a maximum power output of 15kW provides the primary source of energy storage at this site [168]. In addition, a hybrid electrical vehicle has been retrofitted with 9kWh of lithium iron phosphate ($LiFePO_4$) battery cells and a charger to operate as a PHEV [122, 168].

Each component on the LV network is equipped with its own dedicated computer which includes a monitoring module. A high-speed communications network links all the computers in the system [168] to enable an integrated data acquisition system.

All components in the grid are remotely controllable and locally supervised by a "node" computer associated with each unit or entity. A high-speed communications network connects all these nodes and together they form a distributed control platform infrastructure [122, 168] using the IEC 61850 protocol [154].

## Appendix C-6 EnergyLINK Laboratory (NaREC, Blyth)

A three-phase, configurable, multiple-bus system for connecting generation, energy storage and load is available at the EnergyLINK Laboratory at NaREC, Blyth, Northumbria. The laboratory also features a LV network emulator with variable impedances. A bespoke 145kW virtual machine [156], a 7.5kW virtual power supply [157] or the grid can be connected to any of the LV buses to provide power balance to the system and emulate the network connection. The virtual power supply and virtual machine can be used to approximate of the effect of power flows on the voltages of the terminals of a secondary distribution transformers. In addition, these systems are capable of operating at a variety of frequencies and voltages.

Wind, PV and dCHP small-scale generation systems can be coupled to the LV network [142]. In addition, a 15kW linear generator for wave generation emulation is also

available for connection. Furthermore, the virtual power supply, described above could also be used to emulate three-phase small-scale generation [157].

Load facilities consist of domestic load simulator and also a resistive load bank [142] and a flywheel provides energy storage capabilities [142].

Voltage and current transducers providing galvanic isolation [139] are used in conjunction with a distributed high speed National Instruments™ [138] data acquisition system and LabVIEW™ [137]. This system is supplemented with an Ethernet based LabJack [174] system which integrates into the overall LabVIEW™ data acquisition system. No active network control infrastructure is installed at present.

## Appendix C-7 University of Manchester Microgrid

Power balancing functionality at the University of Manchester Microgrid is provided by the flywheel and the three-phase laboratory supply, connected via a three-phase circuit breaker [121].

A computer controlled DC machine coupled to a three-phase synchronous machine is used to emulate SSEG. A limitation of this system is that the coupling to the LV network is with a grid synchronised three-phase, synchronous machine which is not seen as a likely interface for SSEGs [120-121, 123].

The laboratory utilises a selection of household loads to emulate the load of an LV distribution network [120-121] and the flywheel provides energy storage capability [120-121].

A set of interface boards using current and voltage transducers [175] providing galvanic isolation have been developed in order to interface with a dSPACE® [176] system.

Simulink® [126] and dSPACE® [176] are used to provide a human hardware interface, control tasks within the active network and provide a platform to develop intelligent controllers within the system [120-121].

# Appendix D SUNNY ISLAND 4500 – REAL AND REACTIVE POWER CONTROL SYSTEMS

The Sunny Island 4500™ has three basic operating modes. These are: -

- Grid forming – in this mode the Sunny Island 4500™ keeps the voltage and frequency of the grid at a constant level.
- Grid-tied – in this mode the Sunny Island 4500™ complies with the voltage and frequency that is defined by an additional component. This is typically the utility LV connection or a generator connection.
- Droop mode – This is typically for islanded grid forming operation with other droop mode enabled generation units. In this mode the Sunny Island 4500™ varies the grid's frequency with real power and the grid's voltage depending on the reactive power requirements. In addition, it also controls the grid frequency depending on the condition of the associated battery system.

The operation of the droop mode is illustrated diagrammatically in Figure D-1 [132, 135, 177].

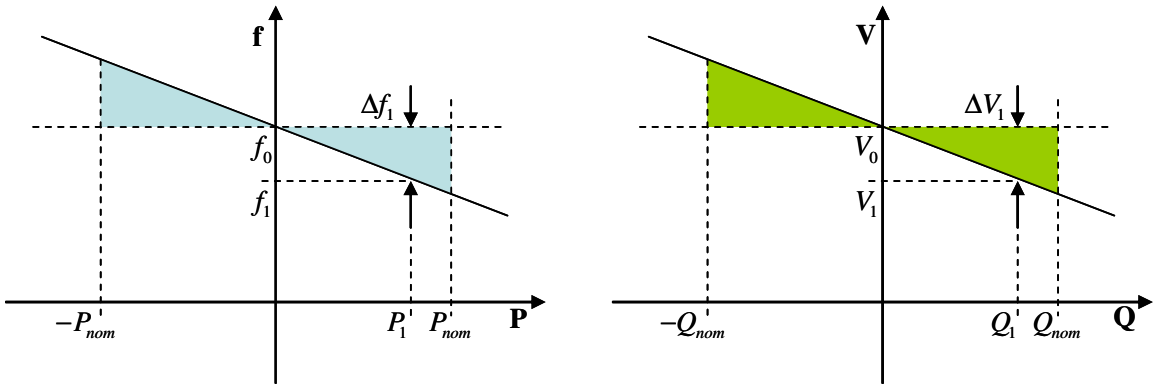


**Figure D-1: Sunny Island 4500™ Frequency/Power and Voltage/Reactive Power Droop Characteristics**

These droop characteristics are analogous in operation to the droop characteristic of generating units in large-scale power systems where multiple generators participate in ensuring that the instantaneous active and reactive power balance within the system is

met. To illustrate this operation, consider a full-scale power system where there is a surfeit of generation. The generating machines will tend to speed up slightly resulting in an increase in system frequency. The governors on all the machines will react to this change and begin to reduce their output power in accordance with their droop characteristic reducing the surplus generation. Eventually, the frequency becomes stable and the power balance is restored within the system.

The use of these droop characteristics in conjunction with the Sunny Island 4500™ at NTUA and at DeMoTec to facilitate islanded operation has been well documented [15, 17-18, 136]. In this system a Sunny Island 4500™ or multiple units are used to balance active and reactive power in the system and also provide frequency regulation. The regulation of power import/export is described by (D.1).

$$P_{ac} = \left( \frac{f - f_0}{f_{droop}} \right) P_{nom} \qquad \text{(D.1)}$$

Where: -

$f$ is the frequency of the LV network (Hz)

$f_0$ is the nominal frequency (Hz)

$P_{nom}$ is the nominal power rating of the Sunny Island 4500™ (kW)

$P_{ac}$ is the required output power of the Sunny Island 4500™ (kW)

$f_{droop}$ droop frequency. If the system frequency deviates by this much from nominal frequency the Sunny Island 4500™ will supply/feed $P_{nom}$ into the LV network (Hz)

The parameter $f_0$ can be set in the LabVIEW™ programming environment thus controlling the power flow in or out of the batteries. Similarly, control of reactive power flow exported or imported by the Sunny Island 4500™ can be implemented by changing the nominal voltage parameter.

The Sunny Island 4500™ is often used in three-phase applications where three sets of batteries are connected to three Sunny Island 4500™ inverters, one on each phase. To ensure charge equalisation between three battery banks in this system an extra offset is included into the droop characteristic. This offset is defined as a function of the State of Charge (SOC) and the state of the battery: -

$$\Delta f = (SOC - 80\%) \times 0.005 + (BatState - 7) \times 0.067 \qquad \text{(D.2)}$$

This offset is included in the compensated power control algorithm by adding $\Delta f$ to $f_0$ which is the nominal frequency to be used in calculations.

# Appendix E EXPERIMENTAL SSEZ DATA ACQUISITION AND CONTROL SYSTEM

| **Transducer Base** | **SSEG Component** | **Description** | | |
|---|---|---|---|---|
| | | *No. of Signals* | *Signal Description* | *Rating* |
| A | Network Emulator | 6 | 3 X Line Voltages<br>3 X Line Currents | 400V (Peak)<br>70A (Peak) |
| B | Load Bank | 6 | 3 X Line Voltages<br>3 X Line Currents | 400V (Peak)<br>70A (Peak) |
| C | Battery Bank and Inverter | 4 | 1 X Line-Neutral Voltage<br>1 X Line Current<br>1 X 48V dc Voltage<br>1 X 48V dc Current | 400V (Peak)<br>70A (Peak)<br>70V (DC)<br>100A (DC) |
| D | PV Emulator | 6 | 3 X Line Voltages<br>3 X Line Currents | 400V (Peak)<br>70A (Peak) |
| E | Wind Turbine Emulator | 6 | 3 X Line Voltages<br>3 X Line Currents | 400V (Peak)<br>70A (Peak) |
| F | dCHP Emulator | 6 | 3 X Line Voltages<br>3 X Line Currents | 400V (Peak)<br>70A (Peak) |

**Table E-1: Data acquisition signal summary**

| SSEZ Component | Signal Description | | | |
|---|---|---|---|---|
| | *No. of Signals* | *Signal Type* | *Signal Control* | *Voltage* |
| Load Bank | 12 | Digital | Power Demand | 0/5V |
| PV Emulator | 1 | Analogue | Power Output | 0->10V |
| Wind Turbine Emulator | 1 | Analogue | Velocity | 0->10V |
| dCHP Emulator | 1 | Analogue | Velocity | +/-10V |

**Table E-2: Control/Emulation system signal summary**

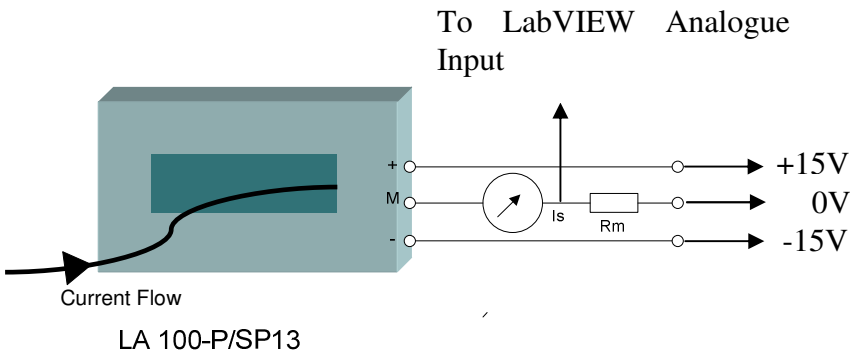


**Figure E-1: Current Transducer System**

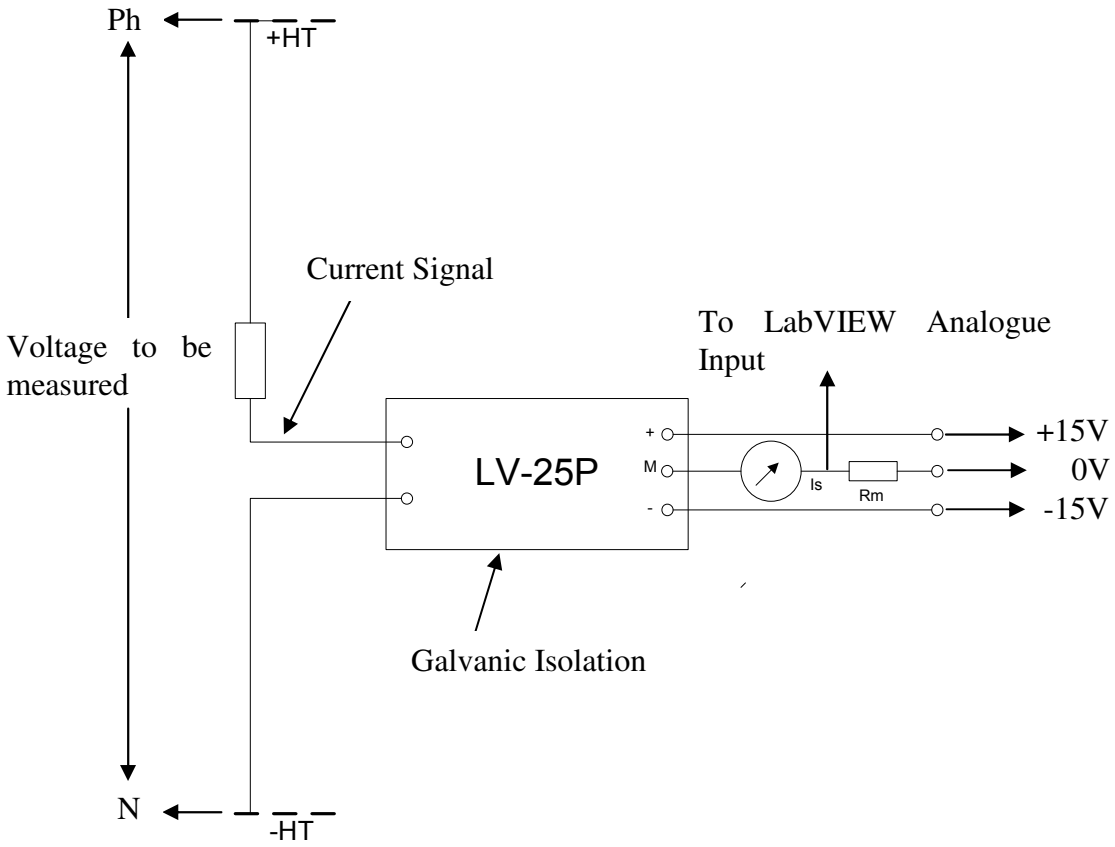


**Figure E-2: Voltage Transducer System**

# Appendix F EXPERIMENTAL SSEZ LV NETWORK IMPEDANCES

| | *Node 1* | *Node 3* | *Node 4* | *Node 5* | *Node 6* |
|---|---|---|---|---|---|
| Distance from Sync Machine (m) | 7 | 15 | 32 | 34.5 | 39.5 |
| Resistance (mΩ) (Estimated) | 9.55 | 44 | 142.7 | 158.6 | 198.5 |
| Phase 1 (Sync machine to node) (mΩ) | 88 | 146 | 240 | 270 | 304 |
| Phase 2 (Sync machine to node) (mΩ) | 139 | 188 | 313 | 337 | 370 |
| Phase 3 (Sync machine to node) (mΩ) | 132 | 194 | 281 | 297 | 325 |
| Neutral (Sync machine to node) (mΩ) | 66 | 67 | 180 | 204 | 245 |
| Reactance (mΩ) (Estimated) | 12.6 | 27 | 57.6 | 62.1 | 71.1 |

# Appendix G INVESTIGATION INTO THE PASSIVE OPERATION OF THE EXPERIMENTAL SSEZ – COMPLETE RESULTS

## Appendix G-1 Voltage Variation and Regulation

### Appendix G-1-1 Scenario I - Balanced Load

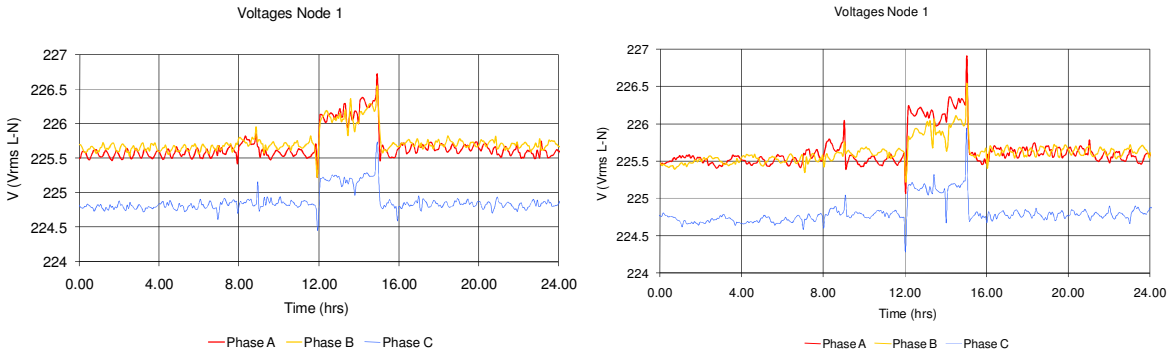


**Configuration I** **Configuration II**

**Figure G-1: Voltages at node 1 during zero generation and balanced load tests**

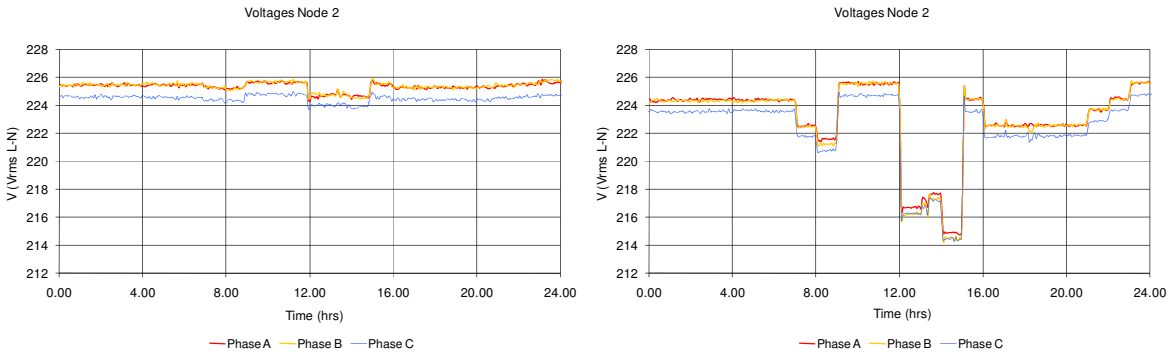


**Configuration I** **Configuration II**

**Figure G-2: Voltages at node 2 during zero generation and balanced load tests**

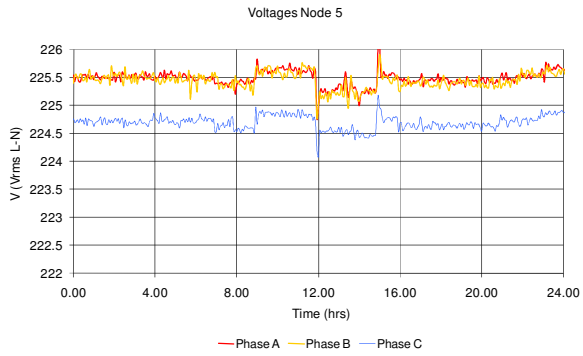


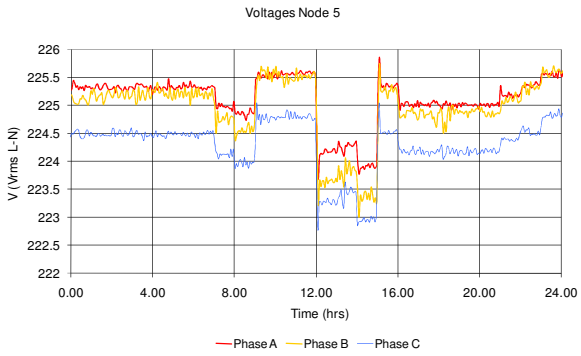


**Configuration I** **Configuration II**

**Figure G-3: Voltages at node 5 during zero generation and balanced load test**

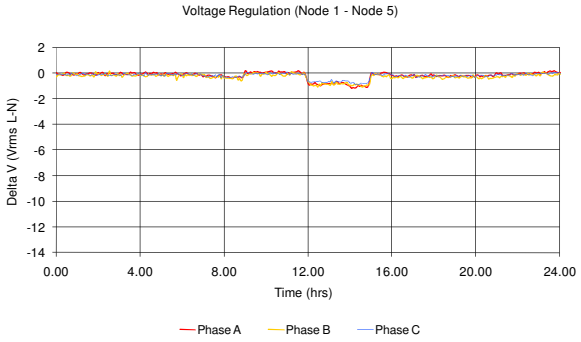


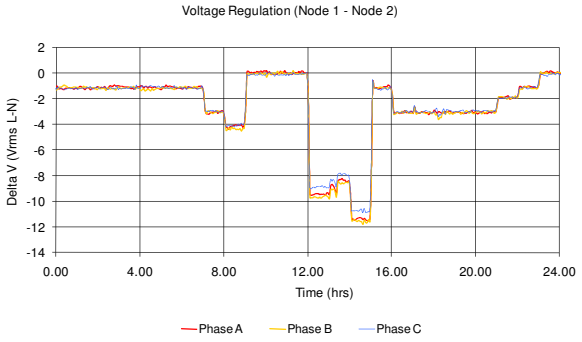


**Configuration I** **Configuration II**

**Figure G-4: Voltage regulation during zero generation and balanced load test**

## Appendix G-1-2 Scenario II - Unbalanced Load (Phase A)

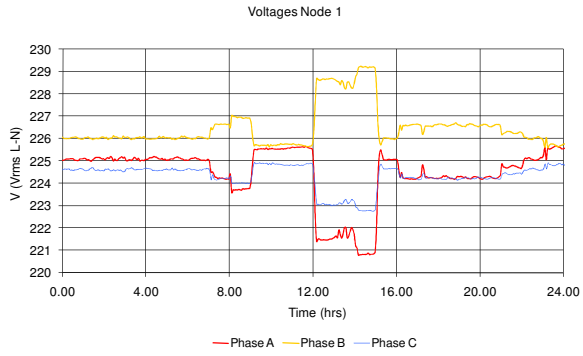


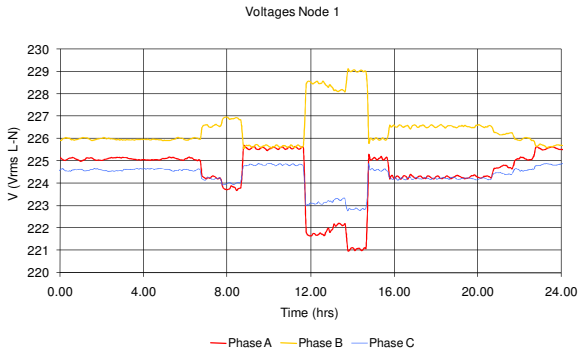


**Configuration I** **Configuration II**

**Figure G-5: Voltages at node 1 during zero generation and unbalanced load (Phase A) tests**

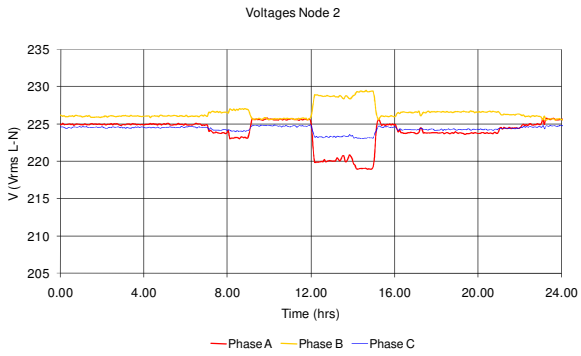


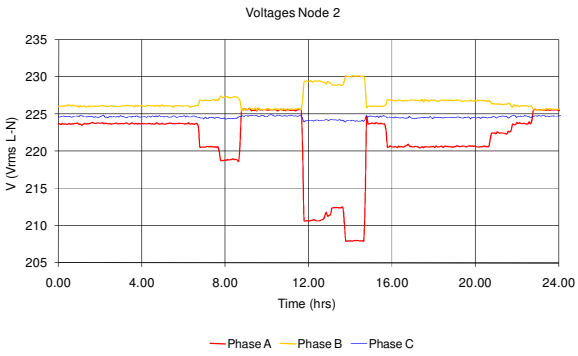


**Configuration I** **Configuration II**

**Figure G-6: Voltages at node 2 during zero generation and unbalanced load (Phase A) tests**

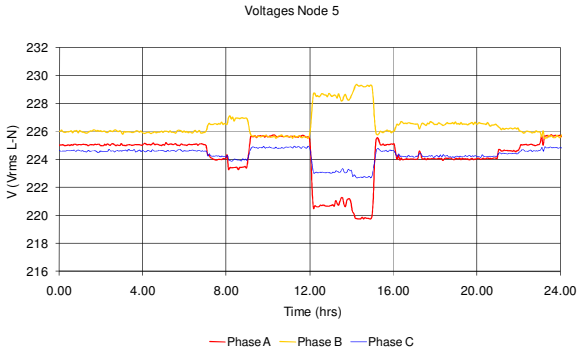


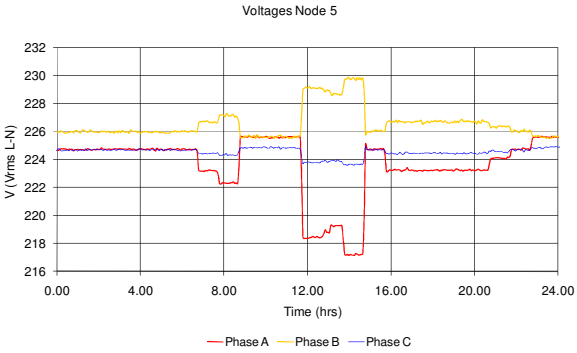


**Configuration I** **Configuration II**

**Figure G-7: Voltages at node 5 during zero generation and unbalanced load (Phase A) tests**

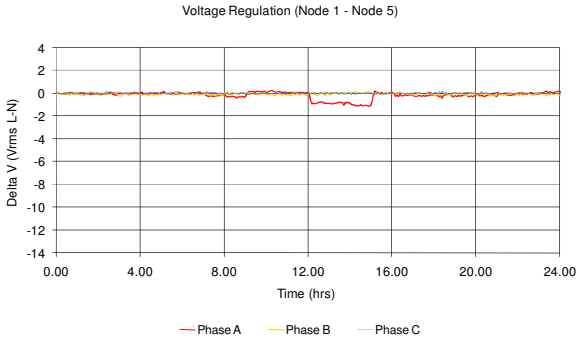


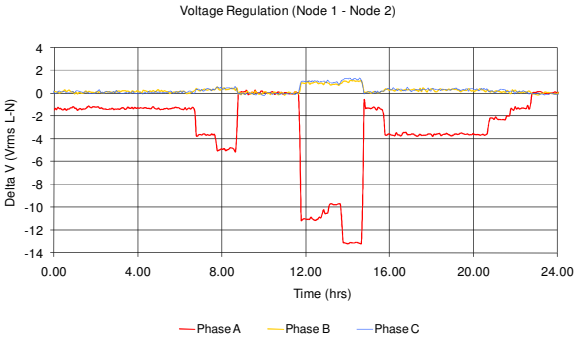


**Configuration I** **Configuration II**

**Figure G-8: Voltage regulation during zero generation and unbalanced load (Phase A) tests**

## Appendix G-1-3 Scenario III - Balanced Loading and Unbalanced Generation (Phase A)

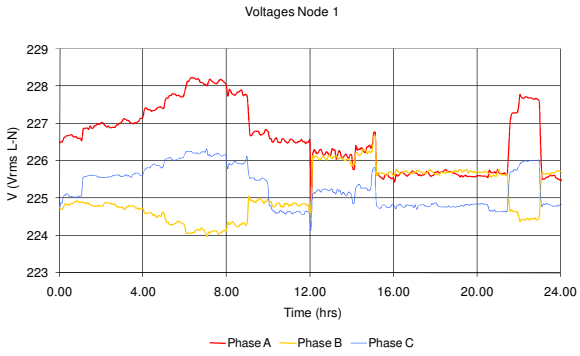


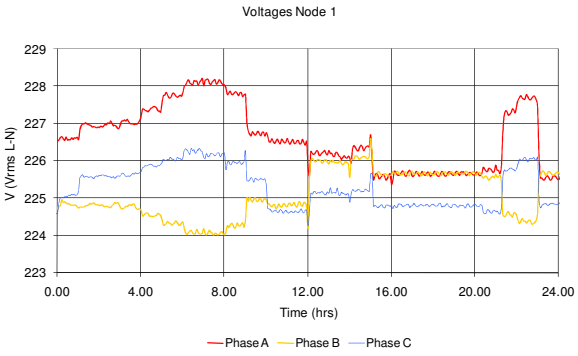


**Configuration I** **Configuration II**

**Figure G-9: Voltages at node 1 during generation and balanced load test**

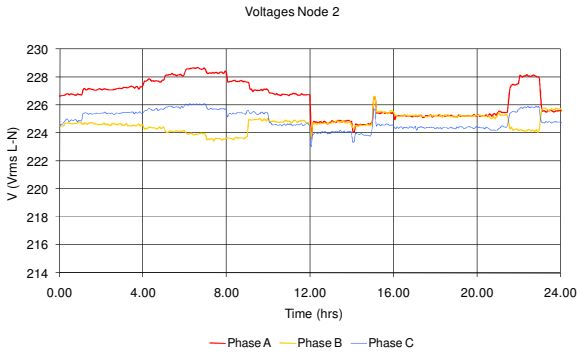


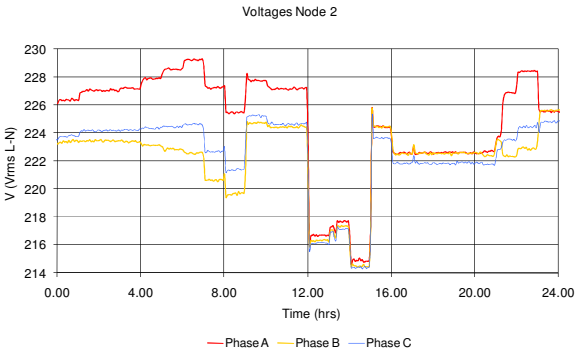


**Configuration I** **Configuration II**

**Figure G-10: Voltages at node 2 during generation and balanced load tests**

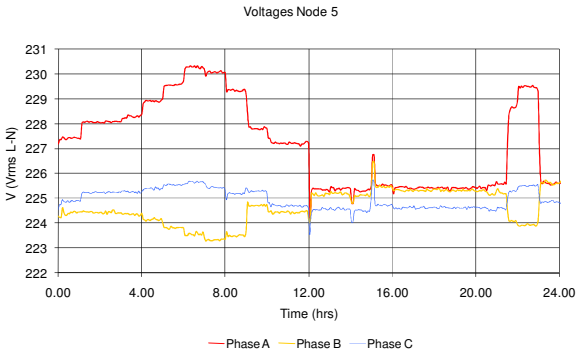


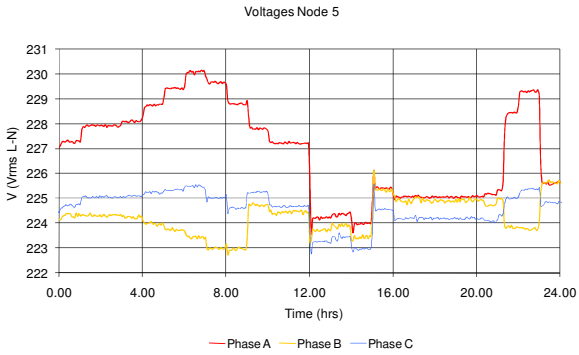


**Configuration I** **Configuration II**

**Figure G-11: Voltages at node 5 during generation and balanced load tests**

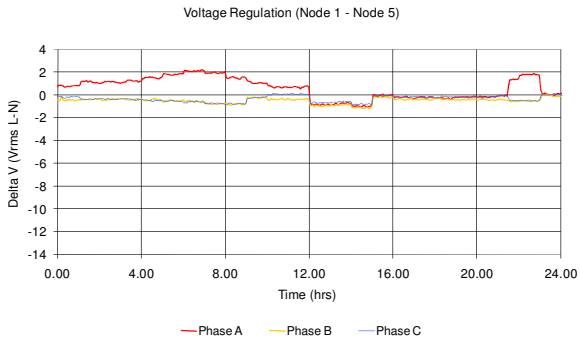


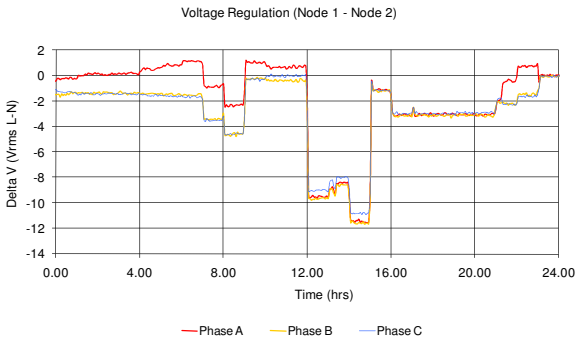


**Configuration I** **Configuration II**

**Figure G-12: Voltage regulation during generation and balanced load tests**

## Appendix G-1-4 Scenario IV- Unbalanced Loading (Phase A) and Unbalanced Generation (Phase A)

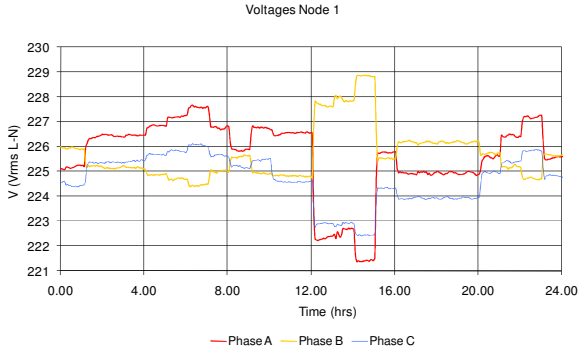


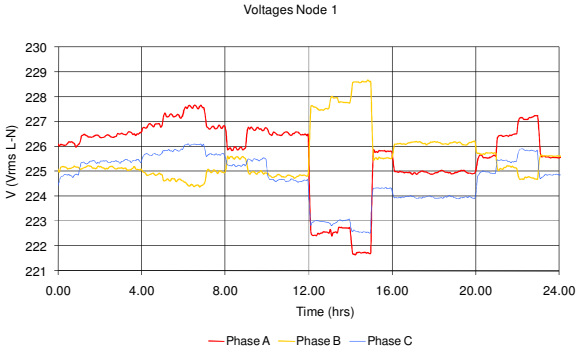


**Configuration I** **Configuration II**

**Figure G-13: Voltages at node 1 during generation and unbalanced load (Phase A) tests**

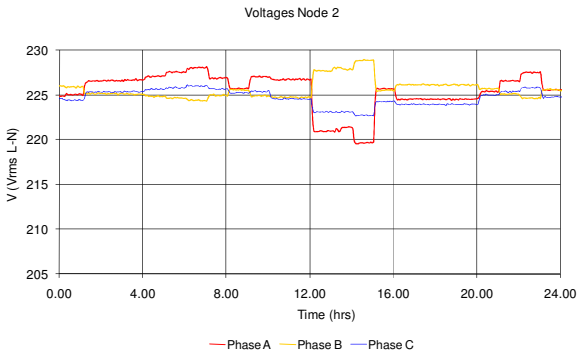


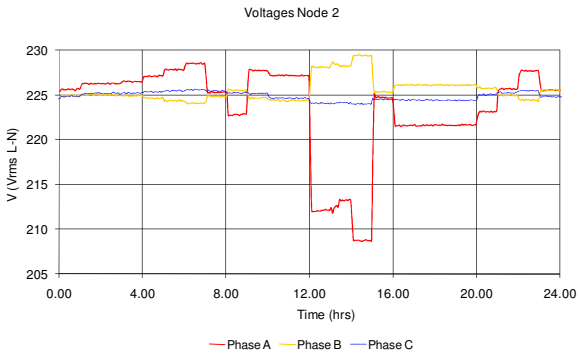


**Configuration I** **Configuration II**

**Figure G-14: Voltages at node 2 during generation and unbalanced load (Phase A) tests**

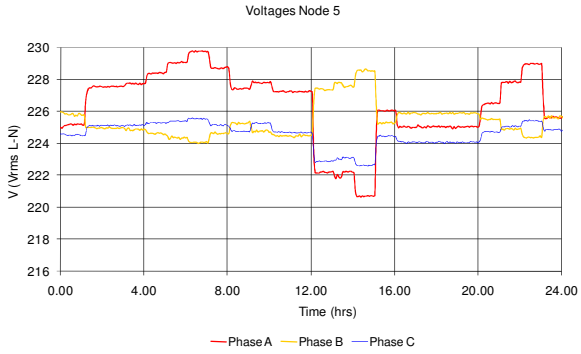


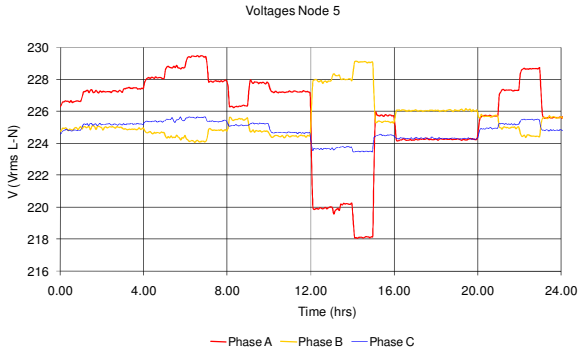


**Configuration I** **Configuration II**

**Figure G-15: Voltages at node 5 during generation and unbalanced load (Phase A) tests**

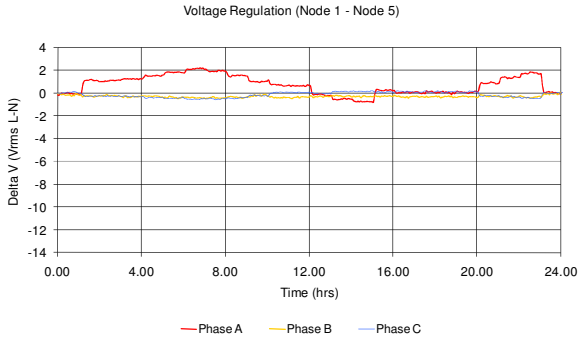


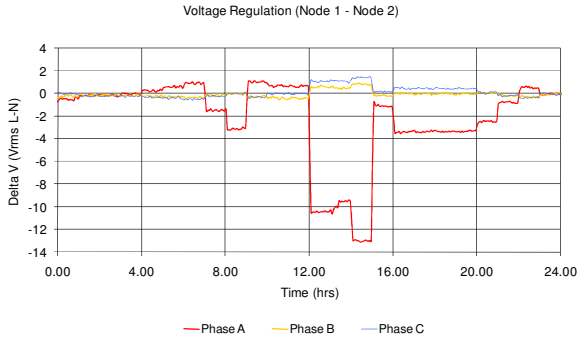


**Configuration I** **Configuration II**

**Figure G-16: Voltages regulation during generation and unbalanced load (Phase A) tests**

## Appendix G-1-5 Scenario V - Non-Unity Power Factor Load

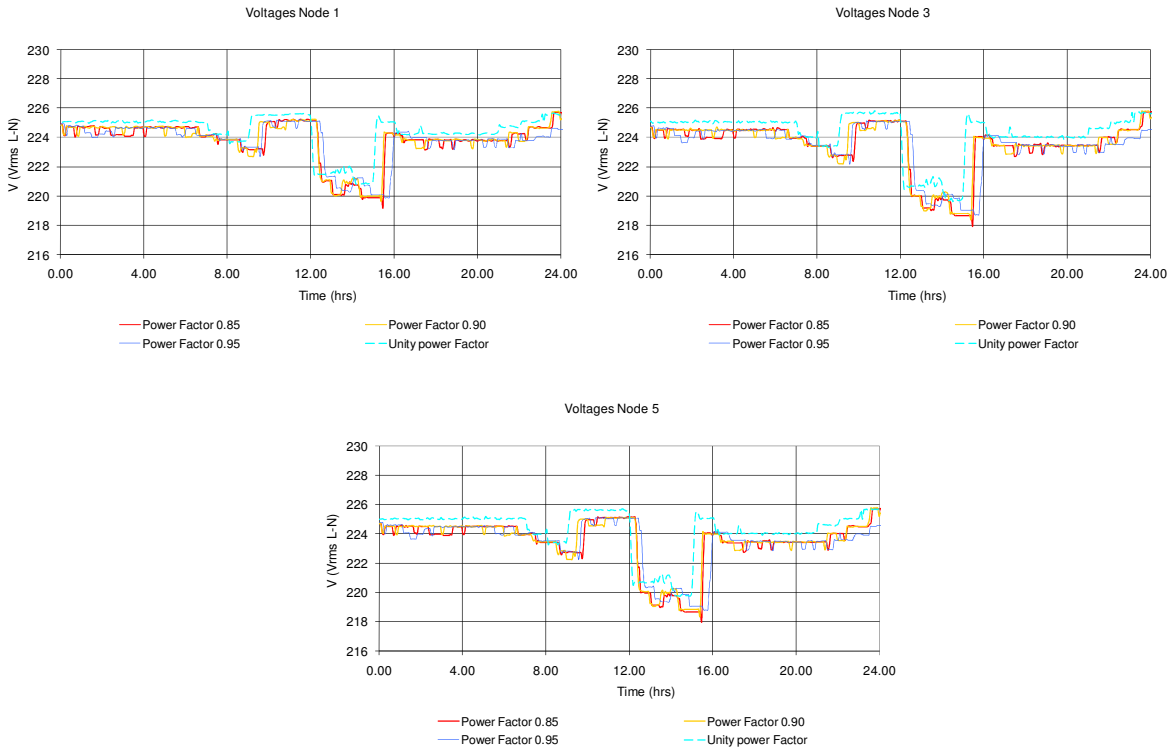


**Figure G-17: Voltages at node 1, node 2 and node 5 during zero generation and non-unity unbalanced load (Phase A)**

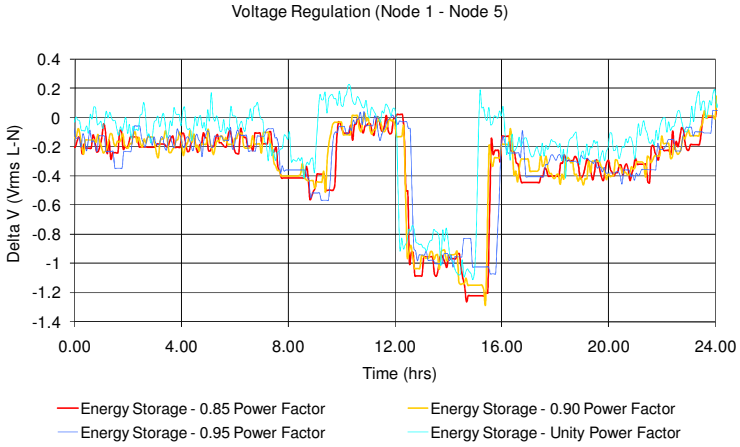


**Figure G-18: Voltages regulation during zero generation and non-unity unbalanced load (Phase A)**

## Appendix G-1-6 Scenario VI - Non-Unity Power Factor Loads and Unity Power Factor Generation

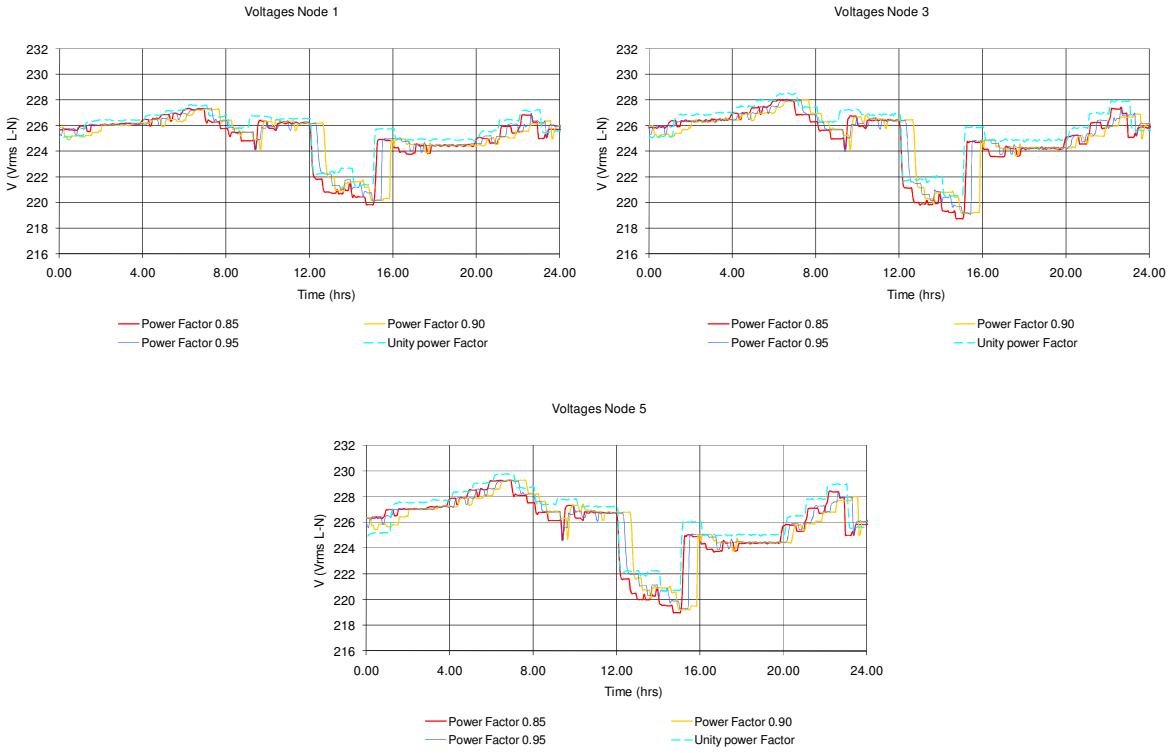


**Figure G-19: Voltages at node 1, node 2 and node 5 during small-scale wind turbine generation and non-unity unbalanced load (Phase A)**

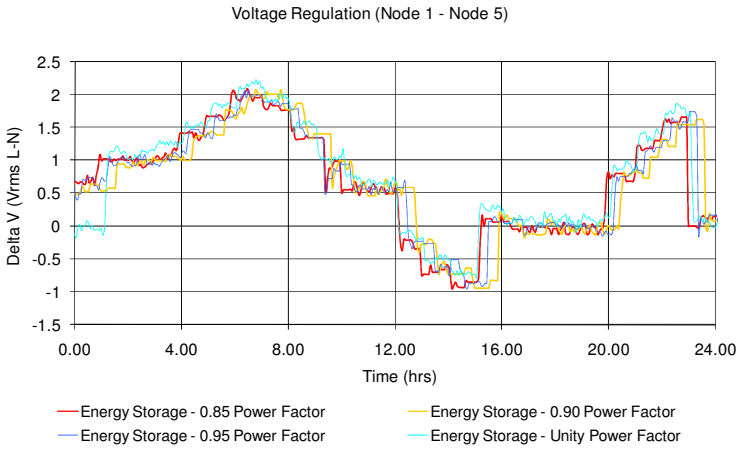


**Figure G-20: Voltage regulation during small-scale wind turbine generation and non-unity unbalanced load (Phase A)**

# Appendix G-2 Voltage Unbalance

## Appendix G-2-1 Scenario I - Balanced Load

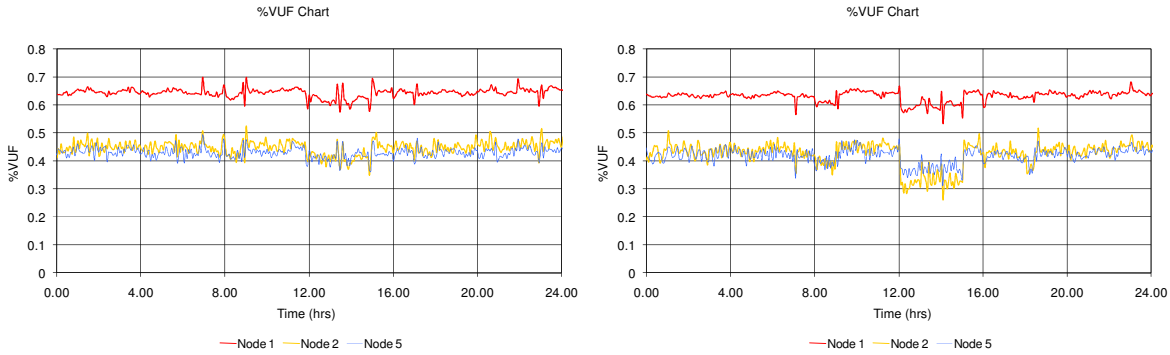


**Configuration I** **Configuration II**

**Figure G-21: Percentage Voltage Unbalance Factors (%VUFs) under balanced load and zero generation.**

## Appendix G-2-2 Scenario II - Unbalanced Loading

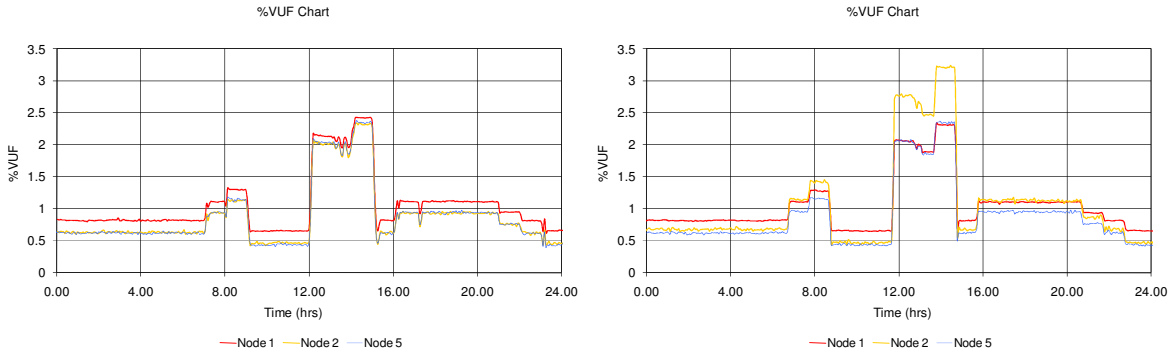


**Configuration I** **Configuration II**

**Figure G-22: Percentage Voltage Unbalance Factors (%VUF) under unbalanced loading conditions**

## Appendix G-2-3 Scenario III - Balanced Load and Unbalanced Generation (Phase A)

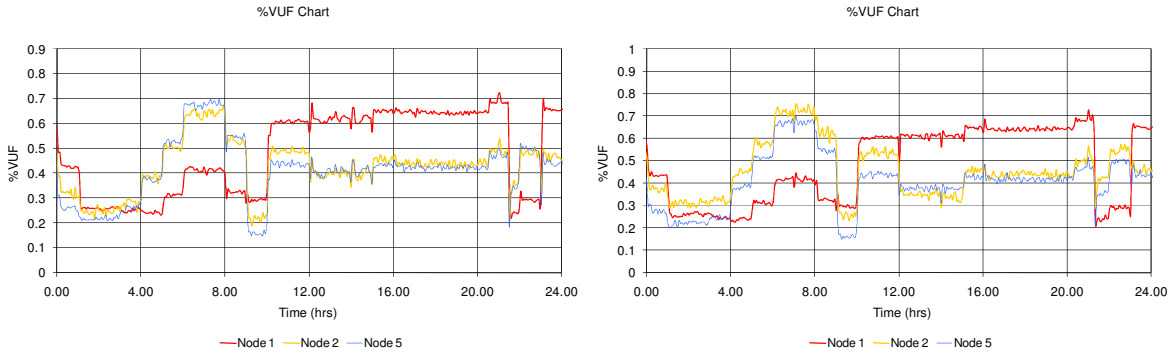


**Configuration I** **Configuration II**

**Figure G-23: Percentage Voltage Unbalance Factors (%VUF) under balanced loading and unbalanced generation conditions (Phase A)**

## Appendix G-2-4 Scenario IV - Unbalanced Load (Phase A) and Unbalanced Generation (Phase A)

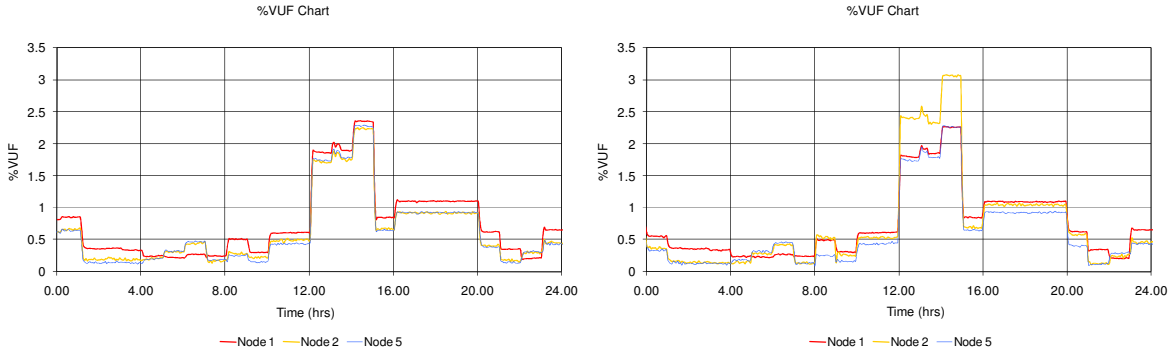


**Configuration I** **Configuration II**

**Figure G-24: Percentage Voltage Unbalance Factors (%VUFs) under unbalanced loading (Phase A) and single-phase generation (Phase A)**

## Appendix G-2-5 Scenario V - Unbalanced Load (Phase B) and Unbalanced Generation (Phase A)

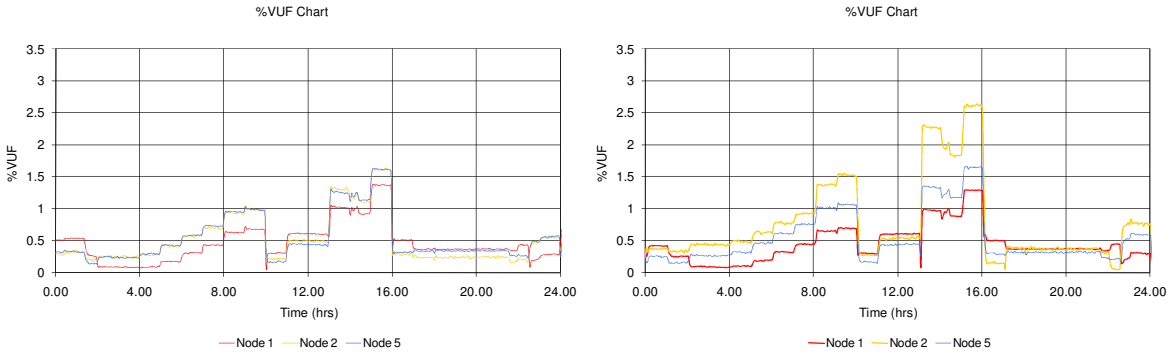


**Configuration I** **Configuration II**

**Figure G-25: Percentage Voltage Unbalance Factors (%VUFs) under unbalanced loading (Phase B) and single-phase generation (Phase A)**

## Appendix G-2-6 Scenario VI - Non-Unity Power Factor Unbalanced Load

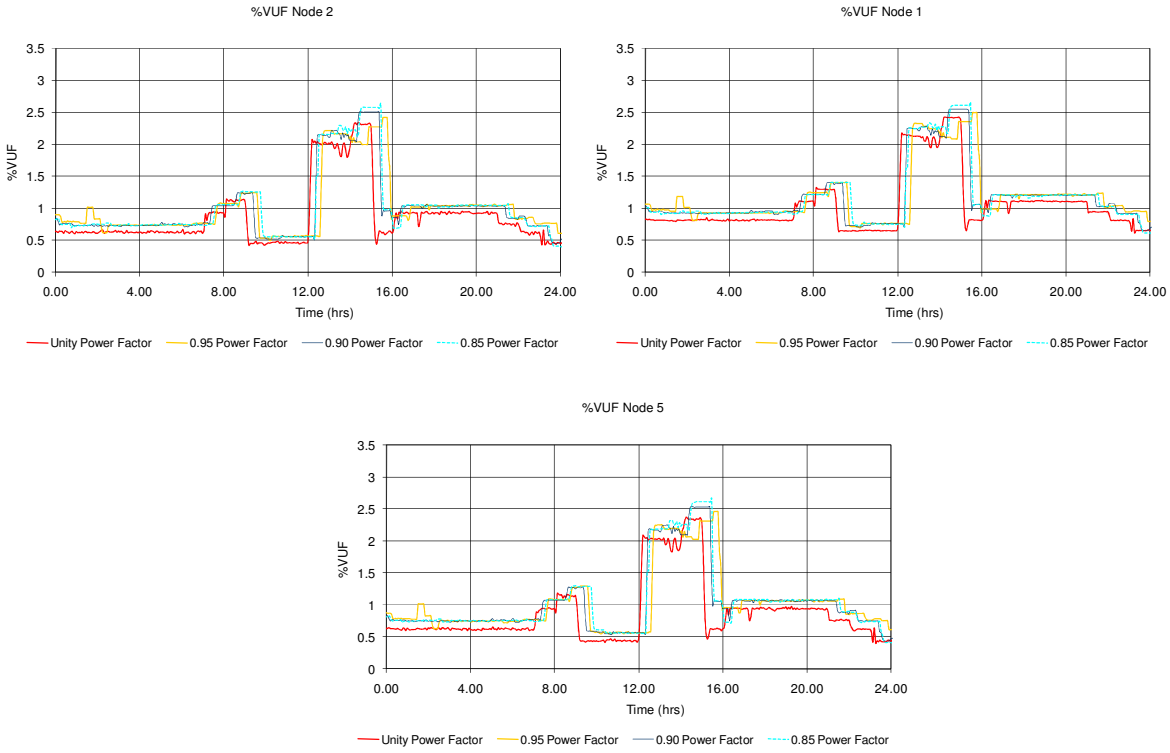


**Figure G-26: Percentage Voltage Unbalance Factors % (%VUF) at during zero generation and unbalanced load (Phase A) and varying power factor**

## Appendix G-2-7 Scenario VII - Non-Unity Power Factor Unbalanced Load (Phase A) and Unity Power Factor Generation (Phase A)

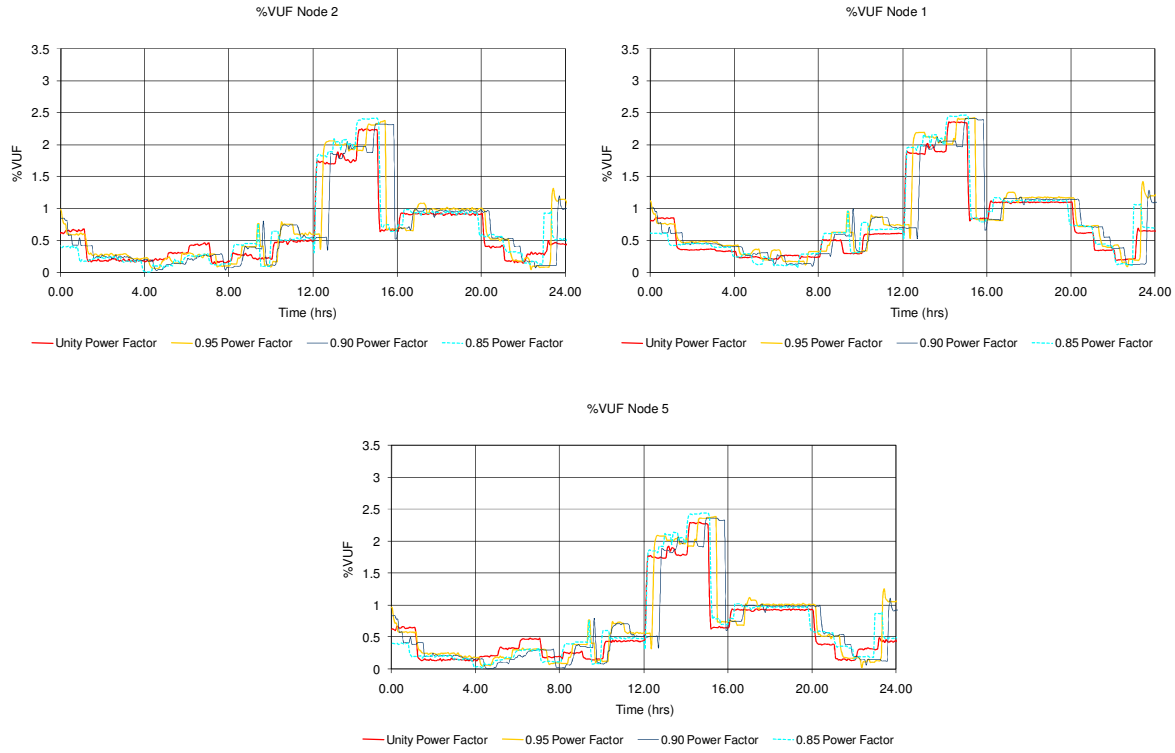


**Figure G-27: Percentage Voltage Unbalance Factors (%VUFs) under unbalanced loading (Phase A) with varying power factor and single-phase generation (Phase A)**

## Appendix G-2-8 Scenario VIII - Non-Unity Power Factor Unbalanced Load (Phase B) and Unity Power Factor Generation (Phase A)

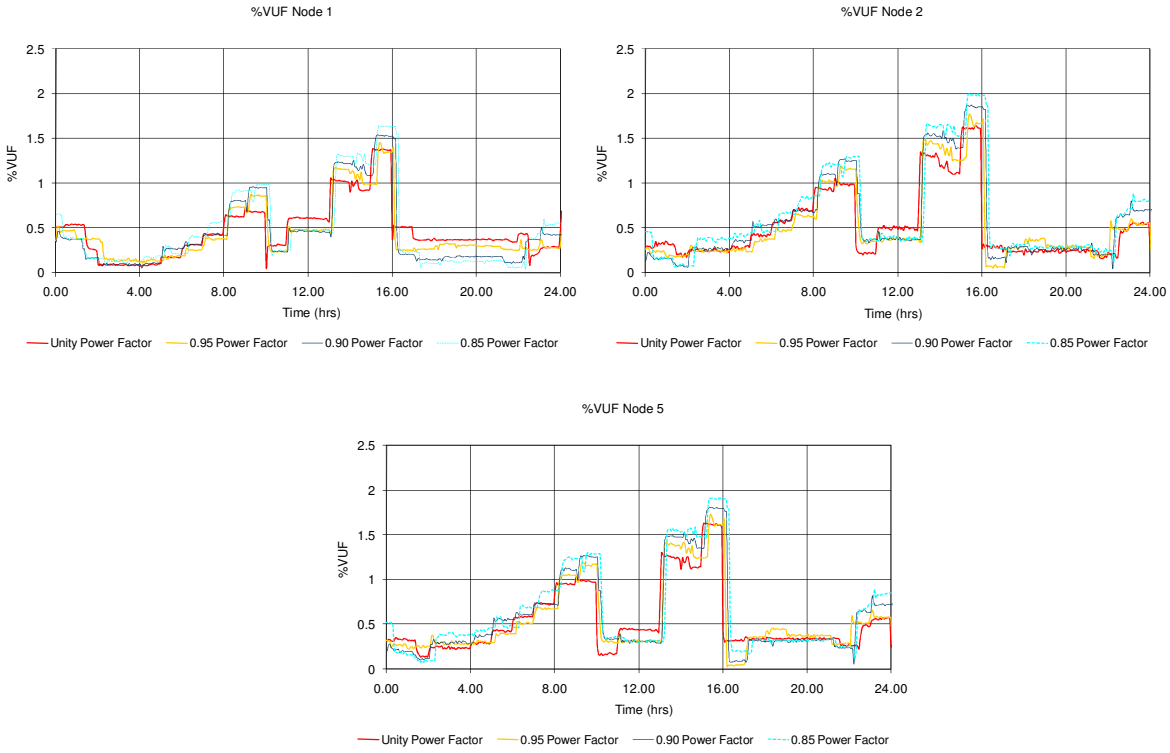


**Figure G-28: Percentage Voltage Unbalance Factors (%VUFs) under unbalanced loading (Phase B) with varying power factor and single-phase generation (Phase A)**

# Appendix G-3 Power Flow

## Appendix G-3-1 Scenario I - Unbalanced Load (Phase A) and Unbalanced Generation (Phase A)

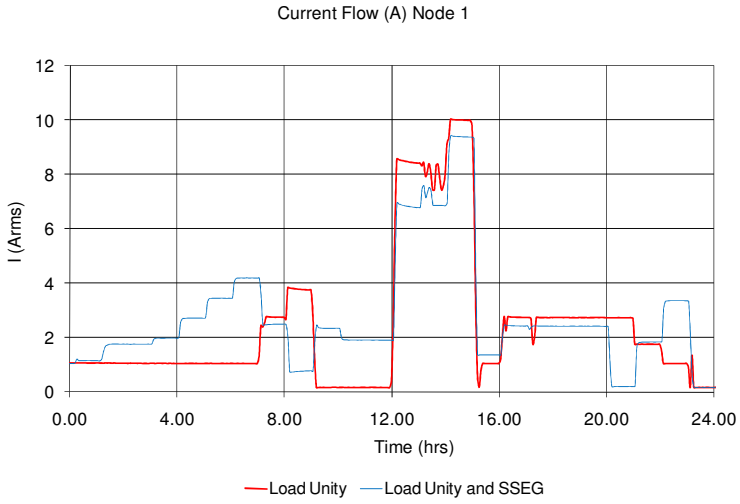


**Figure G-29: Magnitude of current flows through node 1 with and without SSEG**

## Appendix G-3-2 Scenario II – Unbalanced Non-Unity Power Factor Load (Phase A)

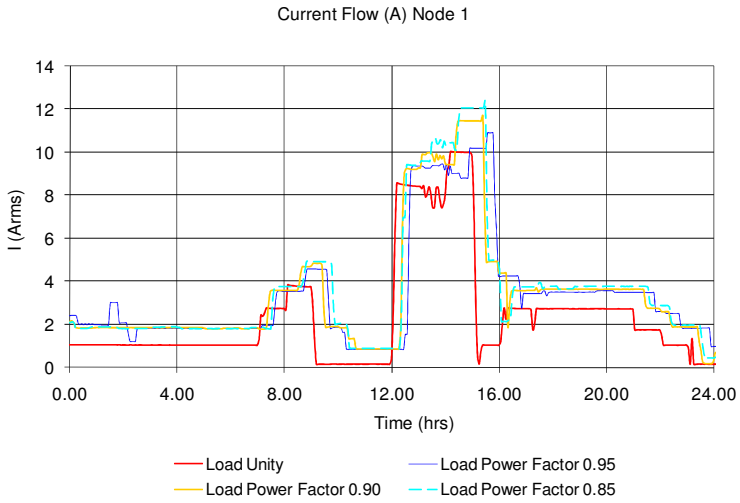


**Figure G-30: Current flows through node 1 with varying load power factors**

## Appendix G-3-3 Scenario III - Unbalanced Non-Unity Power Factor Load (Phase A) and Unbalanced Non-Unity Power Factor Generation (Phase A)

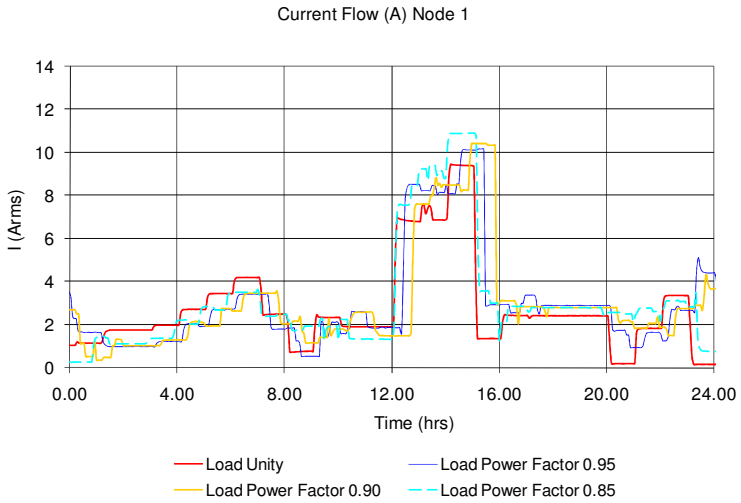


**Figure G-31: Current flows through node 1 with varying load power factors and SSEG**

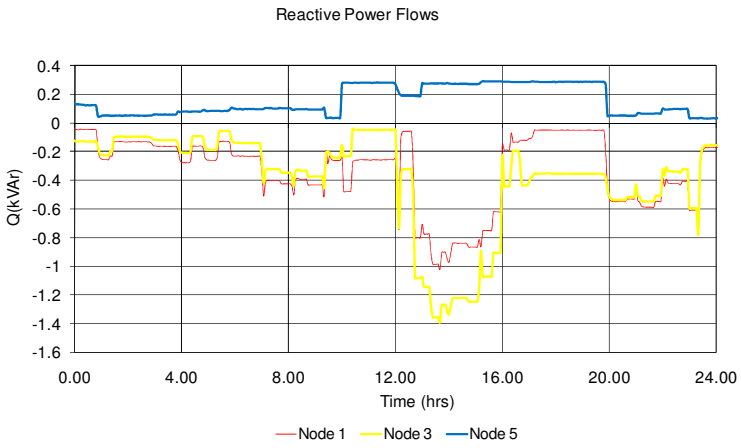


**Figure G-32: Reactive power flows at node 1, 3 and 5 - load (0.85 power factor) and SSEG**

# Appendix H TRANSFORMATION SYSTEM FOR EXPERIMENTAL SSEZ

## Appendix H-1 Introduction

The impacts of load and SSEG on network constraints in the Experimental SSEZ were established in chapter five. In order to relate these impacts to the effects of large concentrations of SSEG on the network constraints of actual or generic LV networks a transformation system is proposed. This transformation system will be derived by a quantitative process of comparison between the Experimental SSEZ and radial LV networks.

The differences between radial LV networks and the Experimental SSEZ have been described in chapter four and five. The impedances from the network connection emulator to remote end of the Experimental SSEZ are less than those of an LV network. In addition, the numbers of individual loads and SSEGs are much greater in any LV network than in the Experimental SSEZ LV network. The transformation system proposed utilises steady-state analysis and some simplifying assumptions to account for these differences that exist between the two systems.

Major differences exist between the network connection emulator and the secondary distribution transformer as illustrated diagrammatically in Figure H-1. Relating the operation of the network connection emulator and the secondary distribution transformer in an LV network has been found to be non-trivial [26, 144, 178]. It is proposed therefore, to use transformed results from the Experimental SSEZ, in conjunction with PSCAD®/EMTDC™ [179-180] MV/LV network models to complete the Experimental SSEZ to LV network transformation.

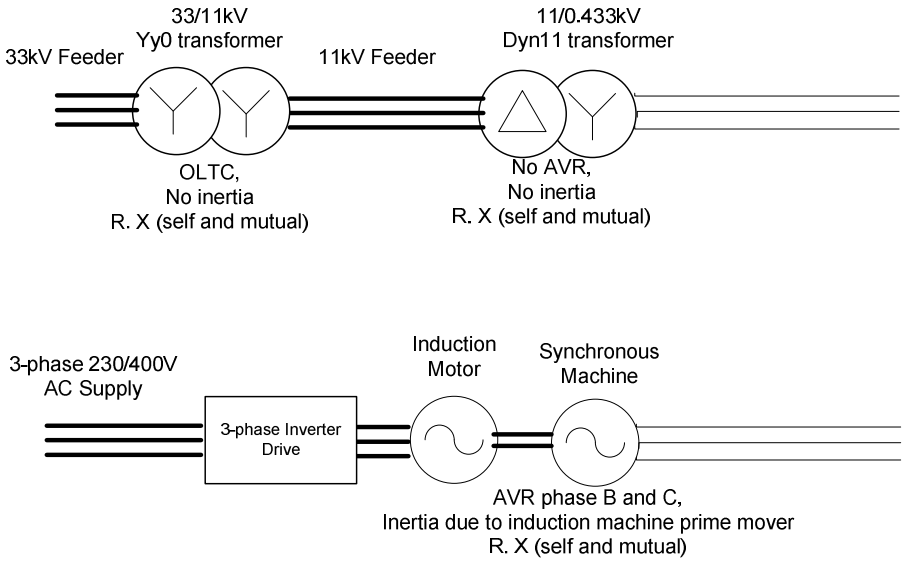


**Figure H-1: Simplified MV/LV distribution system and Experimental SSEZ network emulator**

The proposed methodology for transformation, from the operational parameters of the Experimental SSEZ to those of the LV network can be summarised as follows: -

1. Identify the LV network system parameters that impact on the flow of power and voltages within the LV network.
2. Measure real and reactive power flows at the network connection emulator of Experimental SSEZ and transform to LV network real and reactive power flows.
3. Inject transformed real and reactive power flows into the PSCAD®/EMTDC™ transformer and MV network model. Transformer terminal voltages can then be determined.
4. Experimental SSEZ voltage deviations ($\Delta V^{Ex}$) between the network connection emulator and system remote end node are transformed to LV network voltage deviations ($\Delta V^{LV}$).
5. Transformed LV network voltage deviations ($\Delta V^{LV}$) on each phase are superimposed on the terminal voltages of the LV transformer model to determine LV network remote end voltages.

6. Transformed parameters are now available to evaluate the LV distribution network phenomenon under investigation.

## Appendix H-2 LV Network Parameter Identification

To enable an accurate comparison between the Experimental SSEZ and an LV network a set of identifying parameters are proposed. The parameters to be quantified are expressed in tabular format in Table H-1.

| **Network Component** | **Parameter** | **Unit** |
|---|---|---|
| *LV network conductors* | Conductor impedance | (Ω/km) |
| | Conductor length | (km) |
| *Load* | Total maximum load | (kVA) |
| | Distribution and number of loads | NA |
| | Power factor | NA |
| *SSEG* | Total installed generation | (kW) |
| | Distribution and number of generators | NA |
| | Power factor | NA |
| *MV/LV transformer* | Transformer impedances | % |
| | Nominal voltages | (kV) |
| | Tap changer position (off-load tap changer) | % |
| | MV voltage | (kV) |
| | kVA rating (forward or reverse) | (kVA) |

**Table H-1: MV/LV Network parameters for transformation**

## Appendix H-3 Real and Reactive Power Flow Transformation

In order to relate the real and reactive power flows on the Experimental SSEZ to those in a real network a power transformation factor ($\mu_P$) is defined. The installed real power capabilities of generation and maximum real power demand of the Experimental SSEZ and the LV network are considered when determining $\mu_P$. As the generating and load capabilities of both systems are different, a load scaling factor $\mu_{P_L}$ and a generation scaling factor $\mu_{P_G}$ are initially defined. The larger of these two coefficients is used to define the power scaling factor $\mu_P$ and is used in order to preserve the load and generation profile shapes so that they are not distorted during implementation on the Experimental SSEZ.

$$\mu_{pL} = \frac{P_L^{LV}}{P_L^{Ex}} \qquad \text{(H.1)}$$

$$\mu_{pG} = \frac{P_G^{LV}}{P_G^{Ex}} \qquad \text{(H.2)}$$

where: -

$P_L^{LV}$ is the maximum per-phase load of the LV network under consideration (kW)

$P_L^{Ex}$ is the maximum per-phase load of the Experimental SSEZ (kW)

$P_G^{LV}$ is the installed per-phase generation on the LV network under consideration (kW)

$P_G^{Ex}$ is the maximum per-phase generation available on the Experimental SSEZ (kW)

$\mu_P$ is therefore be defined as: -

$$\mu_p = \max(\mu_{pL}, \mu_{pG}) \tag{H.3}$$

The real-time power flow data from the Experimental SSEZ is now transformed to be indicative of the power flows into the LV windings of the MV/LV transformer at the secondary distribution substation.

$$p_a^{LV}(t) = \mu_p p_a^{Ex}(t) \tag{H.4}$$

$$q_a^{LV}(t) = \mu_p q_a^{Ex}(t) \tag{H.5}$$

where: -

$p_a^{Ex}(t)$ real power import/export on phase A from/to the network connection emulator of the Experimental SSEZ (kW)

$p_a^{LV}(t)$ real power import/export on phase A from/to the MV/LV transformer of the LV network under consideration (kVAr)

$q_a^{Ex}(t)$ reactive power import/export on phase A from/to the network connection emulator of the Experimental SSEZ (kW)

$q_a^{LV}(t)$ reactive power import/export on phase A from/to the MV/LV transformer of the LV network under consideration (kVAr)

The same transformation is used to relate the real and reactive power flow data for phase B and for phase C of the Experimental SSEZ to those of the LV network. The power flow data sets generated by the Experimental SSEZ are used as input data into the PSCAD®/EMTDC™ model system where the power transformation is implemented.

## Appendix H-4 MV/LV Network Modelling System

A PSCAD®/EMTDC™ model system of the MV network and MV/LV transformer was developed to account for some of the differences between the operation of a secondary distribution transformer and the synchronous machine of the network connection

emulator in the Experimental SSEZ. To assist the development of the PSCAD®/EMTDC™ model system a validated model of the UK generic LV network [8] developed by a colleague of the author at Durham University was used. This was modified so that the transformed real and reactive power flow data sets from the Experimental SSEZ representing the import or export of power from one of the MV/LV transformers, can be injected into the model system.

PSCAD®/EMTDC™ does not include a model that enables injection of single-phase real and reactive power/current data sets into the electrical system, based on the output of a data file. A set of three, single-phase inverter models were required to inject the real and reactive power into the MV/LV distribution transformer. The current flows of the inverter models are sinusoidal and do not consider semi-conductor switching effects. The inverters uses a pair of Proportional Integral (PI) controllers to regulate the real and reactive power flow of the current source.

The PI controllers are used to generate a current vector command and this is used to generate a sinusoidal current reference relative to the instantaneous phase-neutral voltage on each phase. The absolute phase of the phase-neutral voltage is measured by a phase detector which utilises a combination of a set of PSCAD™/EMTDC™ *zero detectors* and *sample and hold* models. This is used in preference to the inbuilt PSCAD®/EMTDC™ phase detector as it demonstrated better performance. The overall control system for the single-phase current source inverter is illustrated in Figure H-2.

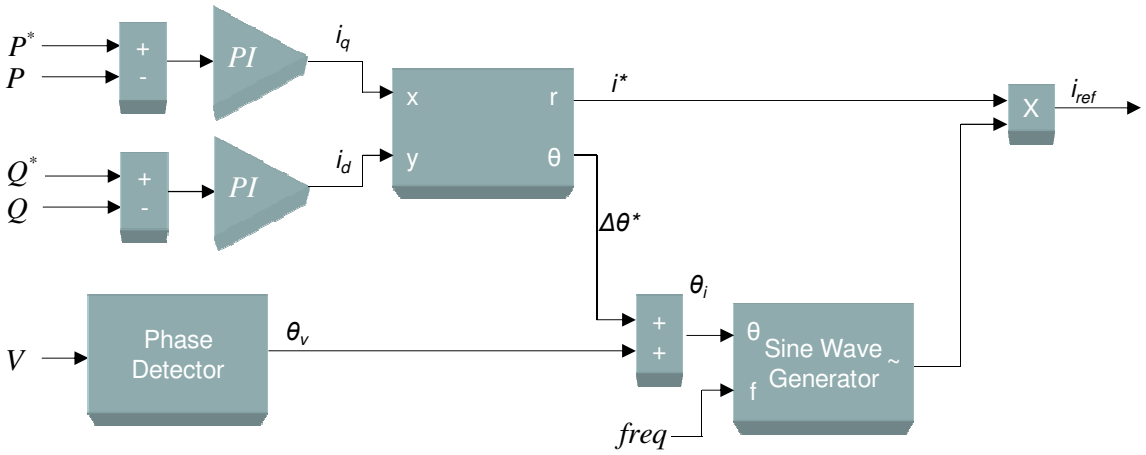


**Figure H-2: Single-phase current source inverter control circuit for power flow injection into secondary distribution transformer model**

Three separate single-phase inverter models were required as individual control of the real and reactive power injections were needed to simulate unbalanced current flow which is typical of LV networks. The single-phase inverter models are then used to inject the real and reactive power into the MV/LV transformer model as illustrated in Figure H-3.

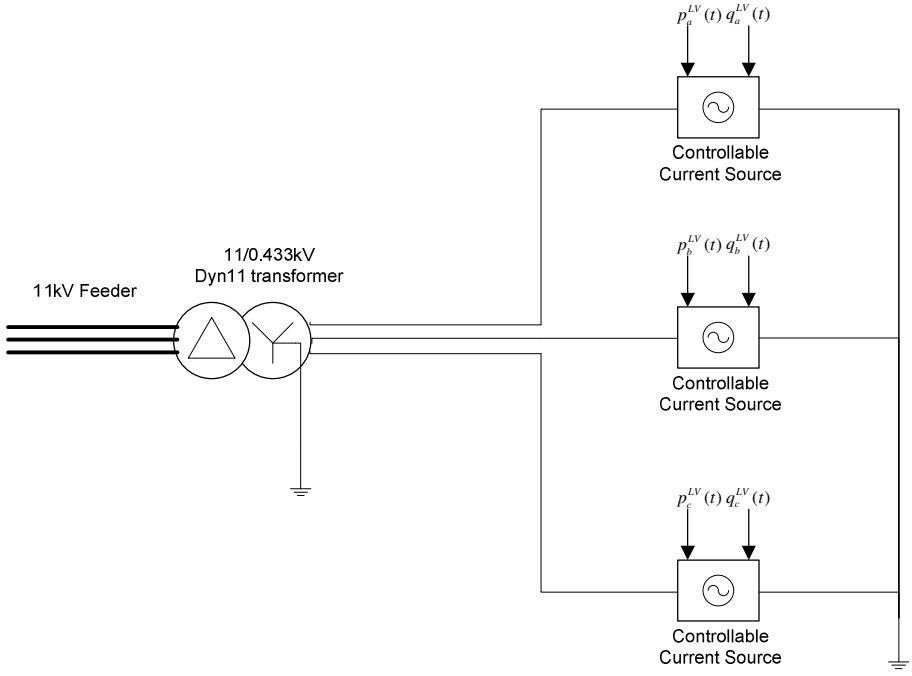


**Figure H-3: PSCAD®/EMTDC™ model of 11kV distribution network connected MV/LV transformer model and controllable current source systems for power transformation**

# Appendix H-5 Voltage Variation Transformation

## Appendix H-5-1 Impedance Transformation

A number of methods exist for reducing the complexity of radial distribution systems in order to decrease the run-time of load flow algorithms and to enable estimation of operating parameters of systems. A number of these methods assume balanced, three-phase conditions [35, 181-184] in reducing radial networks. These reduction systems therefore can be inaccurate when analysing unbalanced systems. In addition, many of these methods can be computationally intensive if one considers many loads, generators and energy storage units.

A method for calculating an "apparent impedance" for an LV distribution network is described in [9] and is used to compare public LV networks with a generic network for the purposes of quickly ascertaining the impact of large penetrations of SSEG on an LV network. This method is modified and extended here so that the apparent impedance enables the estimation of the remote end voltages of four-wire LV feeders.

The apparent impedance of a network location is defined in this work as the sum of the phase and neutral impedances between the secondary substation and any customer connection point multiplied by the number of customers per phase at that location.

$$Z^{i}_{location}{}^{(ap)} = \sum_{k=1}^{m} Z^{k}_{customer}{}^{(ap)} \cong m \cdot Z_{customer}{}^{(ap)} \qquad \text{(H.6)}$$

where: -

$Z^{i}_{location}{}^{(ap)}$ apparent impedance [Ω] of network location $i$ with $m$ customer connections

$m$ number of customers connected per phase to the location

$Z_{customer}^{k\ (ap)}$ sum of the phase and neutral impedances between the substation and customer connection point $k$ [Ω] neglecting the service connection impedances

The sum of apparent impedances of all locations where customers are connected will give the apparent impedance of the feeder.

$$Z_{feeder}^{(ap)} = R_{feeder}^{(ap)} + jX_{feeder}^{(ap)} = \sum_{i=1}^{n} Z_{location}^{i\ (ap)} + Z_{service\ cable}^{max} \qquad \text{(H.7)}$$

where: -

$Z_{feeder}^{(ap)}$ apparent impedance of the LV feeder [Ω]

$R_{feeder}^{(ap)}$, $jX_{feeder}^{(ap)}$ apparent resistance [Ω] and reactance [Ω] of the LV feeder

$n$ number of feeder locations with customer connections

$Z_{service\ cable}^{max}$ the largest of the impedances of service cable connections to each customer [Ω] from the $n^{th}$ network location

The network is assumed to consist of a number of radial feeders as per the UK generic LV network [7-9, 41] and the European generic LV network [9, 36] described in chapter four. In this analysis, the distribution of SSEG on each feeder of the LV network results in the largest values for voltage rise, regulation and unbalance appearing at the remote en of the feeder with the largest apparent impedance. This is a valid assumption as it has been shown in [7-8, 41] that the voltage rise, voltage regulation and voltage unbalance is greatest at the remote end, if the distribution of generation and load is uniform. Moreover, it can be seen from (2.1) and (2.2) that if the concentration of generation is greater near the remote end then this is also the case. If generation is distributed near the network connection that this may not be the case and the results of this translation may therefore be conservative. It is possible to write therefore: -

$$Z_{net}^{(ap)} = R_{net}^{(ap)} + jX_{net}^{(ap)} = \max\left(\mathrm{Re}\left(Z_{feeder1}^{(ap)}\right), .....\mathrm{Re}\left(Z_{feeder\,p}^{(ap)}\right)\right) \quad \text{(H.8)}$$

where: -

| | |
|---|---|
| $Z_{net}^{(ap)}$ | apparent impedance of the LV feeder [Ω] |
| $R_{net}^{(ap)}$, $jX_{net}^{(ap)}$ | apparent resistance [Ω] and reactance [Ω] of the LV network |
| $p$ | number of radial feeders on the LV network |

The complex quantity $\mu_z$ is then defined: -

$$\mu_z = \frac{Z^{LV}}{Z^{Ex}} = \frac{R^{LV} + jX^{LV}}{R^{Ex} + jX^{Ex}} \quad \text{(H.9)}$$

where: -

| | |
|---|---|
| $R^{LV}$ | apparent resistance ( $R_{net}^{(ap)}$ ) of the LV network [Ω] |
| $X^{LV}$ | apparent resistance ( $X_{net}^{(ap)}$ ) of the LV network [Ω] |
| $R^{Ex}$ | sum of the phase and neutral resistances from the network connection emulator to the remote end node of the LV network of the Experimental SSEZ [Ω] |
| $X^{Ex}$ | sum of the phase and neutral reactances from the network connection emulator to the remote end node of the LV network of the Experimental SSEZ [Ω] |

*N.B. In this transformation system the impedances of all three phases of the Experimental SSEZ LV network are assumed to be identical.*

$\mu_z$ can now be used to relate impedances of the LV network to the impedances of the conductors of the Experimental SSEZ. This system assumes that the ratio of impedances between neutral and phase conductors is the same in the Experimental SSEZ and the LV network. However, in common with Experimental SSEZ, the impedance of the neutrals of

many LV networks is approximately equal to or slightly lower than the impedance of the phase conductors.

## Appendix H-6 Three-phase four-wire unbalanced LV network operation

The voltages at intermediate points of existing radial LV networks are determined by the network impedances and the distribution of load. The active power produced by SSEG units, however, will tend to increase steady-state voltage. In addition, the reactive power produced or absorbed by SSEGs will also affect LV network voltages.

Power flow algorithms are the chief tool for analysis of distribution networks with large penetrations of distributed generation. In order to analyse LV networks with neutral wires many power flow algorithms use Kron's reduction [35] to simplify the network by merging the neutral conductor into the phase conductors without sacrificing the accuracy of the result. The 3 X 3 admittance networks used in these algorithms can therefore be preserved and therefore no major adaptation of the power flow engine is required [35].

The limitation of this process is that the currents and voltages in the neutral conductors remain unknown. These parameters are essential however, when determining the impacts of SSEG on LV networks, as these networks are generally unbalanced, due to the single-phase nature of domestic load and SSEG, and LV network construction topologies which result in the flow of current in the neutral conductor and ground. Violation of the thermal limits of the neutral conductor may result even though the current ratings of the phase conductors have not been exceeded. Moreover, the current flow in the neutral conductor and ground can result in a voltage displacement from reference ground of both the remote neutral and ground points.

A 5 x 5 matrix can be used in general to represent the self and mutual impedances of any line impedance $Z_l$ of the line section *l* with 5 conductors (three-phase conductors, neutral and effective earth conductor) as shown in Figure H-4 [185-186].

$$[Z_l] = \begin{bmatrix} Z_{aa} & Z_{ab} & Z_{ac} & Z_{an} & Z_{ag} \\ Z_{ba} & Z_{bb} & Z_{bc} & Z_{bn} & Z_{bg} \\ Z_{ca} & Z_{cb} & Z_{cc} & Z_{cn} & Z_{cg} \\ Z_{na} & Z_{nb} & Z_{nc} & Z_{nn} & Z_{ng} \\ Z_{ga} & Z_{gb} & Z_{gc} & Z_{gn} & Z_{g} \end{bmatrix} \quad \text{(H.10)}$$

where

*a, b, c* phase conductors;

*n* neutral conductor

*g* ground

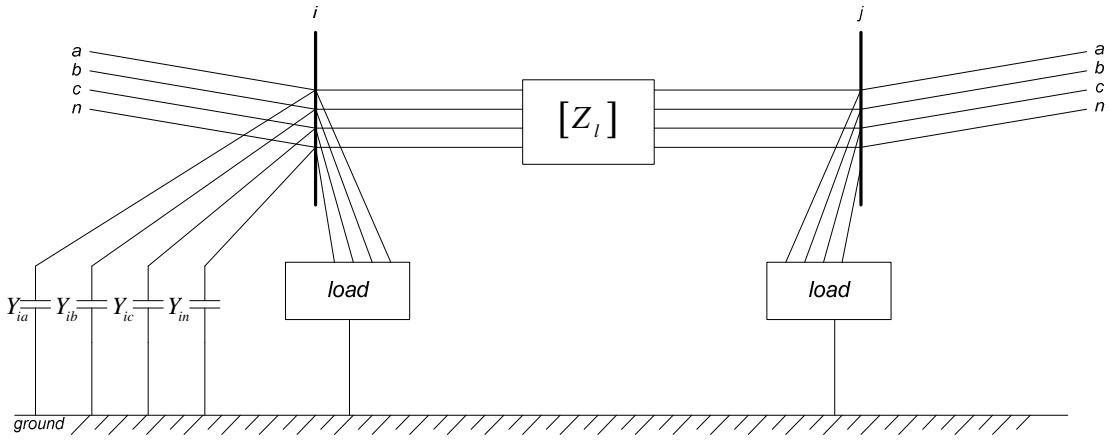


**Figure H-4: Three-phase four-wire line segment including ground of a distribution network [185-186]**

If any of these phase, neutral or earth conducting paths of the line section are of very high impedance or do not exist, the corresponding impedance parameters in (H.10) are infinite. The shunt impedances as illustrated in Figure H-4 can be neglected as this is an LV network. The general model used in this work a for three-phase four-wire distribution line segment is illustrated in Figure H-5 [185-186].

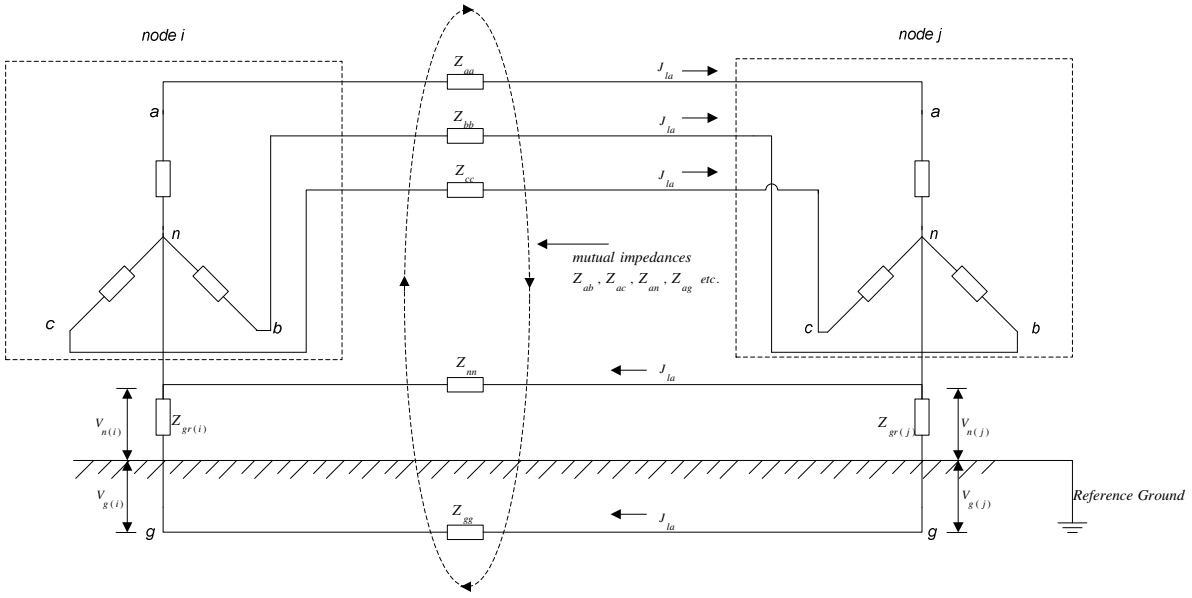


**Figure H-5: Model of the three-phase four-wire distribution line section (*l*) [185-186]**

As described in chapter two unbalanced loading or generating conditions result in return current flowing in the neutral conductor and earth path. In this analysis the LV network under consideration is assumed to have a TT type earthing system, to assist comparison with the Experimental SSEZ as this also has a TT type earthing system. As stated previously this is also a common earthing configuration in rural UK networks. Therefore, in this analysis it is assumed that no current returns through the earthing path.

For the general situation, the voltage drops along a three-phase four-wire line segment which includes the self and mutual coupling between the phase and the neutral conductors can be written [43]: -

$$\begin{bmatrix} \Delta\overline{V}_{AG} \\ \Delta\overline{V}_{BG} \\ \Delta\overline{V}_{CG} \\ \Delta\overline{V}_{NG} \end{bmatrix} = \begin{bmatrix} \overline{Z}_{AA} & \overline{Z}_{AB} & \overline{Z}_{AC} & \overline{Z}_{AN} \\ \overline{Z}_{BA} & \overline{Z}_{BB} & \overline{Z}_{BC} & \overline{Z}_{BN} \\ \overline{Z}_{CA} & \overline{Z}_{CB} & \overline{Z}_{CC} & \overline{Z}_{CN} \\ \overline{Z}_{NA} & \overline{Z}_{NB} & \overline{Z}_{NC} & \overline{Z}_{NN} \end{bmatrix} \begin{bmatrix} \overline{I}_{A} \\ \overline{I}_{B} \\ \overline{I}_{C} \\ \overline{I}_{N} \end{bmatrix} \qquad \text{(H.11)}$$

where: -

$\Delta\overline{V}_{AG}$ voltage drop in phase A with reference to ground (equivalent earth return plane of infinite conductivity) (V)

$\overline{Z}_{AA}$ self impedance of A phase conductor (mΩ)

$\overline{Z}_{AB}$ mutual impedance of A phase and B phase conductor (mΩ)

$\overline{Z}_{AN}$ mutual impedance of A phase and neutral conductor (mΩ)

similarly for phase B,C and for the neutral N.

It is difficult to accurately and consistently measure the mutual impedance between the phases of the Experimental SSEZ. However, the effect of these mutual impedances is often ignored in LV network analysis as they are considerably less than the self impedances of the network. This simplifies (H.11) so that the equation can now be written as: -

$$\begin{bmatrix} \Delta\overline{V}_{AG} \\ \Delta\overline{V}_{BG} \\ \Delta\overline{V}_{CG} \\ \Delta\overline{V}_{NG} \end{bmatrix} = \begin{bmatrix} \overline{Z}_{AA} & 0 & 0 & 0 \\ 0 & \overline{Z}_{BB} & 0 & 0 \\ 0 & 0 & \overline{Z}_{CC} & 0 \\ 0 & 0 & 0 & \overline{Z}_{NN} \end{bmatrix} \begin{bmatrix} \overline{I}_{A} \\ \overline{I}_{B} \\ \overline{I}_{C} \\ \overline{I}_{N} \end{bmatrix} \qquad \text{(H.12)}$$

To relate phase voltages with reference to the neutral point of the load or source, the phase voltage drops with respect to neutral can be expressed as follows [43]: -

$$\Delta\overline{V}_{AN} = \Delta\overline{V}_{AG} - \Delta\overline{V}_{NG} \qquad \text{(H.13)}$$

$$\Delta\overline{V}_{BN} = \Delta\overline{V}_{BG} - \Delta\overline{V}_{NG} \qquad \text{(H.14)}$$

$$\Delta\overline{V}_{CN} = \Delta\overline{V}_{CG} - \Delta\overline{V}_{NG} \qquad \text{(H.15)}$$

where $\Delta\overline{V}_{AN}$, $\Delta\overline{V}_{BN}$ and $\Delta\overline{V}_{CN}$ are the voltage drops with respect to neutral.

Single-phase loads and SSEGs are commonly connected between phase and neutral and therefore any overvoltages that are experienced due to high penetrations of SSEG will be across these connections. It can be assumed that the common neutral of an LV feeder is

effectively grounded at the MV/LV substation. A voltage potential between neutral and earth at the single-phase load/SSEG can therefore contribute to the voltage variation experienced by the customer. The phasor relationship between these quantities is illustrated diagrammatically in Figure H-6 [43].

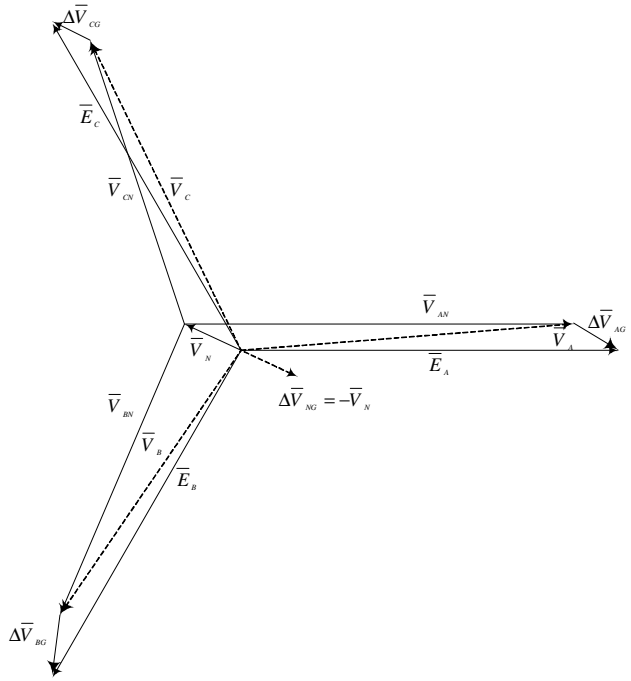


**Figure H-6: Phasor diagram of voltages across line section with an unbalanced load**

where : -

| | |
|---|---|
| $\overline{E}_A$, $\overline{E}_B$ and $\overline{E}_C$ | are sending end voltages |
| $\overline{V}_A$, $\overline{V}_B$ and $\overline{V}_C$ | are receiving end voltage with respect to ground |
| $\overline{V}_{AN}$, $\overline{V}_{BN}$ and $\overline{V}_{CN}$ | are receiving end voltage with respect to neutral |

(H.13), (H.14) and (H.15) can be rewritten using the self impedances described earlier in matrix form as: -

$$\begin{bmatrix} \Delta\overline{V}_{AN} \\ \Delta\overline{V}_{BN} \\ \Delta\overline{V}_{CN} \end{bmatrix} = \begin{bmatrix} \overline{Z}_{AA} & 0 & 0 \\ 0 & \overline{Z}_{BB} & 0 \\ 0 & 0 & \overline{Z}_{CC} \end{bmatrix} \begin{bmatrix} \overline{I}_A \\ \overline{I}_B \\ \overline{I}_C \end{bmatrix} - \overline{Z}_{NN} \begin{bmatrix} \overline{I}_N \\ \overline{I}_N \\ \overline{I}_N \end{bmatrix} \qquad \text{(H.16)}$$

Or alternatively: -

$$\mathbf{\Delta V_{ABC}} = \mathbf{Z_{ABC}} \mathbf{I_{ABC}} - Z_{NN} \mathbf{I_N} \tag{H.17}$$

where: -

$$\mathbf{\Delta V_{ABC}} = \begin{bmatrix} \Delta\overline{V}_{AN} \\ \Delta\overline{V}_{BN} \\ \Delta\overline{V}_{CN} \end{bmatrix}$$

$$\mathbf{Z_{ABC}} = \begin{bmatrix} \overline{Z}_{AA} & 0 & 0 \\ 0 & \overline{Z}_{BB} & 0 \\ 0 & 0 & \overline{Z}_{CC} \end{bmatrix}$$

$$\mathbf{I_{ABC}} = \begin{bmatrix} \overline{I}_{A} \\ \overline{I}_{B} \\ \overline{I}_{C} \end{bmatrix} \quad , \quad \mathbf{I_N} = \begin{bmatrix} \overline{I}_{N} \\ \overline{I}_{N} \\ \overline{I}_{N} \end{bmatrix}$$

## Appendix H-7 Voltage Transformation

The equations developed in the previous section are now used to complete the voltage transformation from the voltages measured on the Experimental SSEZ to values that correspond to those of an LV network. The voltage variation from the secondary substation busbar to the remote end of the LV network can be expressed as: -

$$\mathbf{\Delta V^{LV}_{ABC}} = \mathbf{Z^{LV}_{ABC}} \mathbf{I^{LV}_{ABC}} - Z^{LV}_{NN} \mathbf{I^{LV}_N} \tag{H.18}$$

where: -

$$\mathbf{\Delta V^{LV}_{ABC}} = \begin{bmatrix} \Delta\overline{V}^{LV}_{AN} \\ \Delta\overline{V}^{LV}_{BN} \\ \Delta\overline{V}^{LV}_{CN} \end{bmatrix}$$

$$\mathbf{Z^{LV}_{ABC}} = \begin{bmatrix} \overline{Z}^{LV}_{AA} & 0 & 0 \\ 0 & \overline{Z}^{LV}_{BB} & 0 \\ 0 & 0 & \overline{Z}^{LV}_{CC} \end{bmatrix}$$

$$\mathbf{I}_{\mathbf{ABC}}^{\mathbf{LV}} = \begin{bmatrix} \overline{I}_A^{LV} \\ \overline{I}_B^{LV} \\ \overline{I}_C^{LV} \end{bmatrix} \quad , \quad \mathbf{I}_{\mathbf{N}}^{\mathbf{LV}} = \begin{bmatrix} \overline{I}_N^{LV} \\ \overline{I}_N^{LV} \\ \overline{I}_N^{LV} \end{bmatrix}$$

$\overline{I}_A^{LV}$, $\overline{I}_B^{LV}$, $\overline{I}_C^{LV}$ and $\overline{I}_N^{LV}$ are the average line currents per customer on each phase and neutral. The average line current is defined to be the current flow from the transformer to each phase of the feeder divided by the number of customers on each phase of each feeder.

Similarly, a conservative approximation of the voltage variation measured from the network connection emulator to the remote end of the Experimental SSEZ is defined as: -

$$\mathbf{\Delta V}_{\mathbf{ABC}}^{\mathbf{Ex}} = \mathbf{Z}_{\mathbf{ABC}}^{\mathbf{Ex}} \mathbf{I}_{\mathbf{ABC}}^{\mathbf{Ex}} - Z_{NN}^{Ex} \mathbf{I}_{\mathbf{N}}^{\mathbf{Ex}} \qquad \text{(H.19)}$$

where: -

$$\mathbf{\Delta V}_{\mathbf{ABC}}^{\mathbf{Ex}} = \begin{bmatrix} \Delta\overline{V}_{AN}^{Ex} \\ \Delta\overline{V}_{BN}^{Ex} \\ \Delta\overline{V}_{CN}^{Ex} \end{bmatrix}$$

$$\mathbf{Z}_{\mathbf{ABC}}^{\mathbf{Ex}} = \begin{bmatrix} \overline{Z}_{AA}^{Ex} & 0 & 0 \\ 0 & \overline{Z}_{BB}^{Ex} & 0 \\ 0 & 0 & \overline{Z}_{CC}^{Ex} \end{bmatrix}$$

$$\mathbf{I}_{\mathbf{ABC}}^{\mathbf{Ex}} = \begin{bmatrix} \overline{I}_A^{Ex} \\ \overline{I}_B^{Ex} \\ \overline{I}_C^{Ex} \end{bmatrix} \quad , \quad \mathbf{I}_{\mathbf{N}}^{\mathbf{Ex}} = \begin{bmatrix} \overline{I}_N^{Ex} \\ \overline{I}_N^{Ex} \\ \overline{I}_N^{Ex} \end{bmatrix}$$

The voltage variation parameters measured on the Experimental SSEZ are now transformed so that they are indicative of the voltage variations measured on the case study network under consideration.

If both sides of (H.19) are multiplied by the scalar $\mu_z$.

$$\mu_z \Delta \mathbf{V}_{\mathbf{ABC}}^{\mathbf{Ex}} = \mu_z \mathbf{Z}_{\mathbf{ABC}}^{\mathbf{Ex}} \mathbf{I}_{\mathbf{ABC}}^{\mathbf{Ex}} - \mu_z Z_{NN}^{Ex} \mathbf{I}_{\mathbf{N}}^{\mathbf{Ex}} \tag{H.20}$$

And as the impedances of the Experimental SSEZ and the LV network have been defined to be related by $\mu_z$, it is possible to write: -

$$\mu_z \Delta \mathbf{V}_{\mathbf{ABC}}^{\mathbf{Ex}} = \mathbf{Z}_{\mathbf{ABC}}^{\mathbf{LV}} \mathbf{I}_{\mathbf{ABC}}^{\mathbf{Ex}} - Z_{NN}^{LV} \mathbf{I}_{\mathbf{N}}^{\mathbf{Ex}} \tag{H.21}$$

The current flow in the LV network is defined using the power transformation factor ($\mu_p$) and the nominal phase-neutral voltages of the case study LV network and the Experimental SSEZ.

$$V_{nom}^{Ex} \mu_z \Delta \mathbf{V}_{\mathbf{ABC}}^{\mathbf{Ex}} = V_{nom}^{Ex} \mathbf{Z}_{\mathbf{ABC}}^{\mathbf{LV}} \mathbf{I}_{\mathbf{ABC}}^{\mathbf{Ex}} - V_{nom}^{Ex} Z_{NN}^{LV} \mathbf{I}_{\mathbf{N}}^{\mathbf{Ex}} \tag{H.22}$$

$$V_{nom}^{Ex} \mu_z \Delta \mathbf{V}_{\mathbf{ABC}}^{\mathbf{Ex}} = \mathbf{Z}_{\mathbf{ABC}}^{\mathbf{LV}} \mathbf{S}_{\mathbf{ABC}}^{\mathbf{Ex}} - V_{nom}^{Ex} Z_{NN}^{LV} \mathbf{S}_{\mathbf{N}}^{\mathbf{Ex}} \tag{H.23}$$

The power transformation factor ($\mu_p$) and the number of customers per phase ($q$) are used to transform the Experimental SSEZ power matrices to case study LV network power matrices.

$$\frac{\mu_p V_{nom}^{Ex} \mu_z \Delta \mathbf{V}_{\mathbf{ABC}}^{\mathbf{Ex}}}{q} = \frac{\mu_p \mathbf{Z}_{\mathbf{ABC}}^{\mathbf{LV}} \mathbf{S}_{\mathbf{ABC}}^{\mathbf{Ex}} - \mu_p V_{nom}^{Ex} Z_{NN}^{LV} \mathbf{S}_{\mathbf{N}}^{\mathbf{Ex}}}{q} \tag{H.24}$$

$$\frac{\mu_p V_{nom}^{Ex} \mu_z \Delta \mathbf{V}_{\mathbf{ABC}}^{\mathbf{Ex}}}{q} = \mathbf{Z}_{\mathbf{ABC}}^{\mathbf{LV}} \mathbf{S}_{\mathbf{ABC}}^{\mathbf{LV}} - Z_{NN}^{LV} \mathbf{S}_{\mathbf{N}}^{\mathbf{LV}} \tag{H.25}$$

$$\frac{\mu_p V_{nom}^{Ex} \mu_z \Delta \mathbf{V}_{\mathbf{ABC}}^{\mathbf{Ex}}}{q V_{nom}^{LV}} = \frac{\mathbf{Z}_{\mathbf{ABC}}^{\mathbf{LV}} \mathbf{S}_{\mathbf{ABC}}^{\mathbf{LV}}}{V_{nom}^{LV}} - \frac{Z_{NN}^{LV} \mathbf{S}_{\mathbf{N}}^{\mathbf{LV}}}{V_{nom}^{LV}} \tag{H.26}$$

$$\frac{\mu_p V_{nom}^{Ex} \mu_z \Delta \mathbf{V}_{\mathbf{ABC}}^{\mathbf{Ex}}}{q V_{nom}^{LV}} = \mathbf{Z}_{\mathbf{ABC}}^{\mathbf{LV}} I_{\mathbf{ABC}}^{\mathbf{LV}} - Z_{NN}^{LV} \mathbf{I}_{\mathbf{N}}^{\mathbf{LV}} \tag{H.27}$$

If $\mu_{Vnom}$ is defined: -

$$\mu_{Vnom} = \frac{V_{nom}^{LV}}{V_{nom}^{Ex}} \tag{H.28}$$

It is now possible to write from (H.18), (H.27) and (H.28): -

$$\mathbf{\Delta V_{ABC}^{LV}} = \frac{\mu_p \mu_z}{q \mu_{Vnom}} \mathbf{\Delta V_{ABC}^{Ex}} \tag{H.29}$$

In real-time it is possible to write: -

$$\mathbf{\Delta v_{abc}^{LV}(t)} = \frac{\mu_p \mu_z}{q \mu_{Vnom}} \mathbf{\Delta v_{abc}^{Ex}(t)} \tag{H.30}$$

where: -

$$\mathbf{\Delta v_{abc}^{Ex}(t)} = \begin{bmatrix} \Delta v_a^{Ex}(t) \\ \Delta v_b^{Ex}(t) \\ \Delta v_c^{Ex}(t) \end{bmatrix} \quad , \quad \mathbf{\Delta v_{abc}^{LV}(t)} = \begin{bmatrix} \Delta v_a^{LV}(t) \\ \Delta v_b^{LV}(t) \\ \Delta v_c^{LV}(t) \end{bmatrix} \tag{H.31}$$

And $\Delta v_a^{Ex}(t)$, $\Delta v_b^{Ex}(t)$ and $\Delta v_c^{Ex}(t)$ is the data measured from the Experimental SSEZ and $\Delta v_a^{LV}(t)$, $\Delta v_b^{LV}(t)$ and $\Delta v_c^{LV}(t)$ is the data that is superimposed on the PSCAD™/EMTDC™ system model to determine the remote end voltages.

## Appendix H-8 Discussion

A transformation system has been developed that enables evaluation of the impact of SSEG on low voltage networks using a combination of steady state, four-wire distribution network analysis and a transformer, MV network model system and single-phase controllable current source systems in PSCAD®/EMTDC™.

As the Experimental SSEZ is a highly non-uniform network with limited flexibility, case-study networks need to be developed which facilitate comparison with the Experimental SSEZ in terms of load and generation distribution. The transformation also assumes that the current flows in the LV distribution network under investigation are purely sinusoidal and contain no harmonics. Moreover, as the ratio of phase impedance to neutral impedance is fixed in the Experimental SSEZ, if this ratio is significantly different in the case-study network it increases the error in the results. In the Appendix I, the

transformation system is used to investigate the dynamic operation of a case-study network based on the UK generic LV network. In addition, these dynamic results are compared with the steady results from a previously developed PSCAD®/EMTDC™ model to validate the transformation system.

# Appendix I IMPACT INVESTIGATION AND VALIDATION OF TRANSFORMATION SYSTEM

## Appendix I-1 Introduction

The transformation proposed in Appendix H, will be used to investigate the impact of dynamic unbalanced power flows due to SSEG and load at the LV level, on the operating parameters of a case study LV distribution network, connected to a secondary distribution transformer. These results are also used to validate the transformation using a previously validated steady-state PSCAD®/EMTDC™ model developed at Durham University. The transformation area is defined to be from the secondary distribution substation LV busbar to the remote ends of the feeders of the LV network.

The first step of the transformation is to determine the network parameters identified in Appendix H and the topology of the LV network. The second stage is to implement the real and reactive power parameter data sets, from experimental data from the Experimental SSEZ, in the PSCAD®/EMTDC™ model system. The power transformation described earlier is implemented within the model system, enabling the estimation of the power flows within the case-study LV network in simulated real-time.

The power flow estimates of the case study LV network are injected into the LV network model which makes the estimation of the terminal voltages of the secondary distribution transformer possible. Finally, the voltage variations from the Experimental SSEZ are transformed so that the estimated remote end voltage variations can be calculated. This final stage enables determination of the voltage variation, voltage regulation and voltage unbalance issues in the network during dynamic, unbalance loading and generating conditions.

## Appendix I-2 Case Study Network

A validated PSCAD®/EMTDC™ model of the UK generic network as illustrated in Figure I-1 has been completed by a colleague of the author at Durham University [8]. This network topology has been deemed by UK DNOs to be representative of a typical UK urban distribution network and assumed a uniform distribution of load and SSEG [41]. An LV system associated with one of the secondary distribution substations has been defined as the UK generic LV network as shown in Figure I-1 [9].

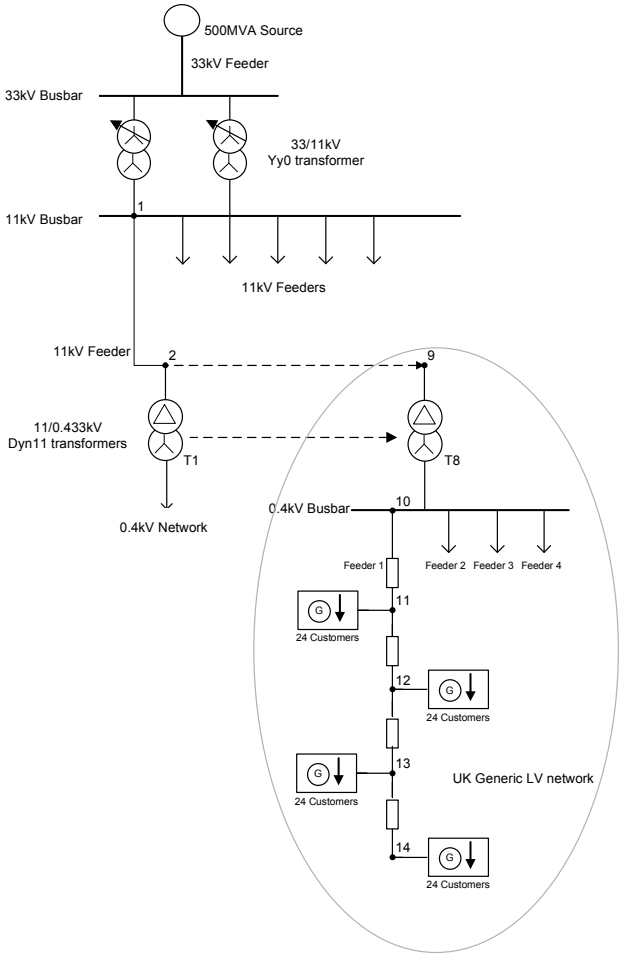


**Figure I-1: UK generic distribution network**

In contrast, to the UK generic LV network, the Experimental SSEZ has a non-uniform distribution of load and generation as would a real system. However, in a real LV distribution network the load and generation are not likely to be evenly distributed. The PSCAD®/EMTDC™ model described previously [8] is modified to reflect the

distribution of load and generation in the Experimental SSEZ. This modification does not significantly detract from the relevance of the case study network as actual LV distribution networks [9] and the generic European LV network [36] do not have uniform distributions of load and generation.

# Appendix I-3 LV Network Parameter Identification

## Appendix I-3-1 LV Network

The UK generic LV network used in this investigation comprises four identical feeders but only one feeder is represented in detail in the model, as illustrated in Figure I-1 from nodes 10 to 14.

The feeder consists four 75m sections of underground aluminium cable emanating from the secondary distribution substation. The feeder is comprised of two sections with a cross sectional area (CSA) of 185mm$^2$ and two sections with a CSA of 95mm$^2$. A network location, as defined earlier in this work, is situated at the end of each of these sections. Finally, at each network location, a total of 24 customers (8 per phase) are connected with a set of 35mm$^2$ service cables. The conductor data for this LV feeder is presented in Table I-1.

| Sending, Receiving Nodes | CSA ($mm^2$) | Length (m) | $R_{ph}$ (mΩ/m) | $X_{ph}$ (mΩ/m) | $R_n$ (mΩ/m) | $X_n$ (mΩ/m) | $I_Z$ (A) (Rating) |
|---|---|---|---|---|---|---|---|
| 10,11 | 185 | 75 | 0.164 | 0.074 | 0.164 | 0.014 | 355 |
| 11,12 | 185 | 75 | 0.164 | 0.074 | 0.164 | 0.014 | 355 |
| 12,13 | 95 | 75 | 0.32 | 0.075 | 0.32 | 0.016 | 235 |
| 13,14 | 95 | 75 | 0.32 | 0.075 | 0.32 | 0.016 | 235 |
| Service cables | 35 | 30 | 0.851 | 0.041 | 0.90 | 0.041 | 140 |

**Table I-1: Conductor data for the cables used in the UK generic LV network [41]**

## Appendix I-3-2 Load Data

In previous work, the After Diversity Maximum Demand (ADMD) is assumed to be 1.3kW per customer [41]. Constant power load models [66, 69] are implemented in this work [41] which is in contrast to the Experimental SSEZ which employs constant impedance loads [66, 69]. In order to investigate a dynamic, thermally onerous condition for the generic LV, the maximum diurnal demand was defined to exceed the MVA limits of the secondary distribution transformer by 50% at nominal voltage. This is not likely to occur in practice as a secondary distribution transformer capacity is greater than the maximum load of the downstream LV network. However, these onerous conditions were used to validate the transformation over a wide variety of network conditions.

The total maximum load on the LV network therefore is 750kW and the power per-phase is 250kW. In each LV feeder, there are 96 customers equally distributed across the three phases and there are four feeders supplied by the secondary distribution transformer making a total of 384 customers. Therefore, the maximum load per customer is 1.95kW (750kW/384 customers).

A power factor of unity is assumed as the load emulator of the Experimental SSEZ utilises resistive loads and the maximum load is assumed to be 2.6kW. The load profiles used in this study are based on data from [141]. This load profile is scaled so that the maximum load per customer is 1.95kW. In order to investigate the most onerous network conditions for voltage regulation, voltage rise and voltage unbalance the load peaks and troughs on each phase are modified. The maximum and minimum loads on phases A (where the generation is connected) and phase B and C occur at times which are likely to result large deviations in voltage regulation, voltage rise and voltage unbalance from zero load and generation conditions. The resultant scaled and modified load data used in this study is illustrated in Figure I-2.

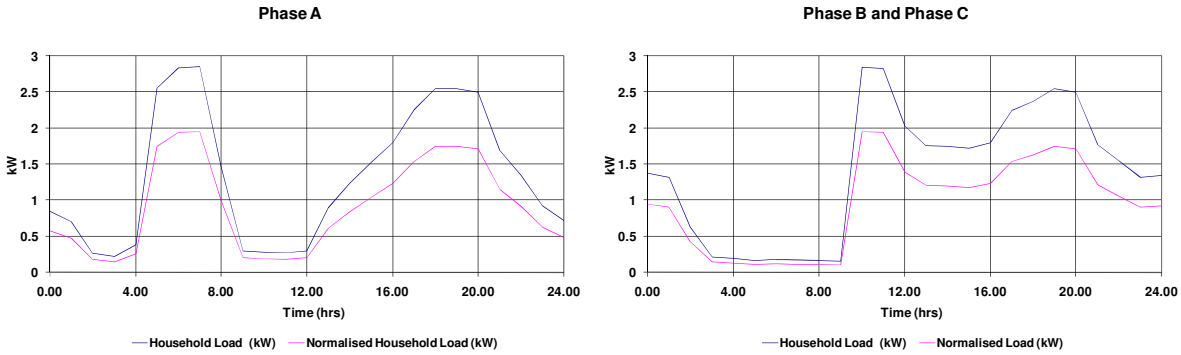


**Figure I-2: Modified household load profiles [141] and scaled profiles for implementation in case study LV network [41]**

## Appendix I-3-3 Small Scale Embedded Generation Data

The installed small scale generation capacity per customer of the UK generic distribution network is 1.1kW at unity power factor which corresponds to 100% penetration of SSEG [41]. An unbalanced generation scenario is investigated in this case study and all generation is assumed to be connected to phase A of the network as in [9] and that the maximum average generation per customer on phase A is 2.2kW. This corresponds to a SSEG penetration of 200%.

This scenario of generation on a single-phase only has been shown to result in the most onerous network conditions for voltage regulation, voltage rise and voltage unbalance [9]. As in the demand scenarios there are 128 customers per phase connected to the LV network. The total installed small scale embedded generation capacity on this LV network therefore is 281.6kW (phase A only). The distribution of the installed generation and maximum load on the case study generic LV network model of Figure I-1 is illustrated in Figure I-3.

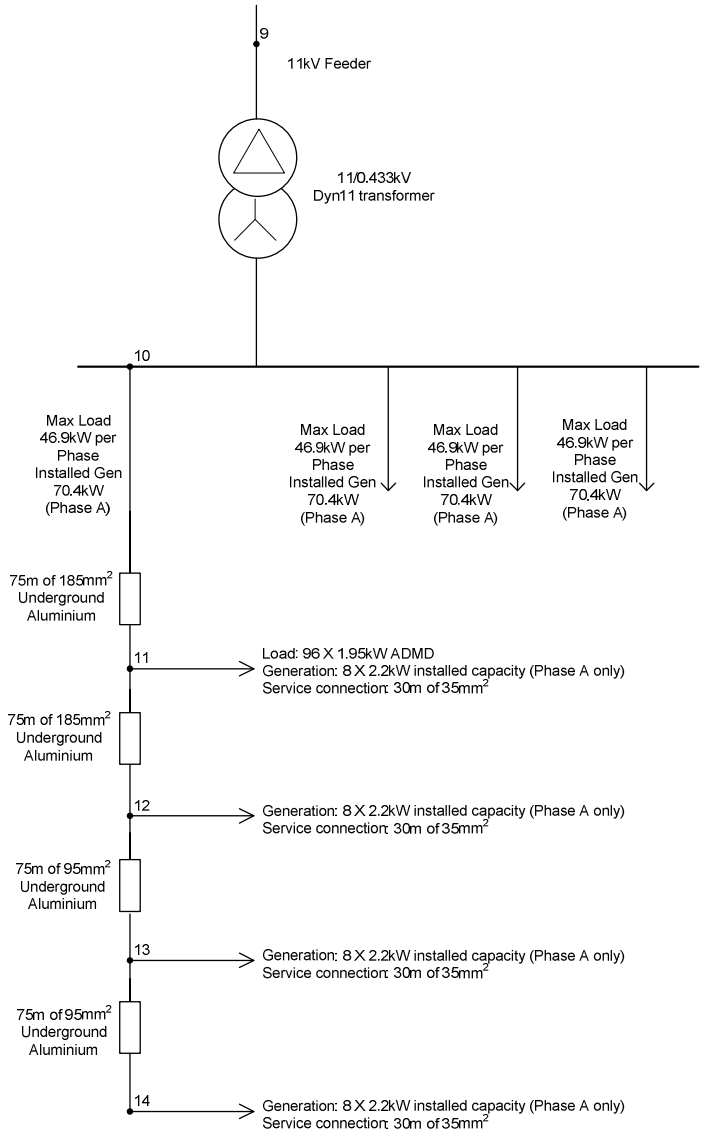


**Figure I-3: Load and generation distribution for case study network for transformation validation**

In this LV distribution network all the load is connected near the network connection unlike the LV distribution network in Figure I-3 where load is uniformly distributed. Wind data for this case study is based on tests at NaREC's, EnergyLINK Laboratory as in chapter five. However, as in the case of the load data in that chapter, the real wind data is manipulated to create more onerous conditions during specific loading conditions for voltage rise, regulation and unbalance and also thermal ratings. At a wind speed of $14.2ms^{-1}$ it is assumed that the SSEGs will be operating at full capacity. This has been defined to correspond to an output power of 1.2kW from the wind turbine generator emulator. The wind profile implemented in this study is shown in Figure I-4.

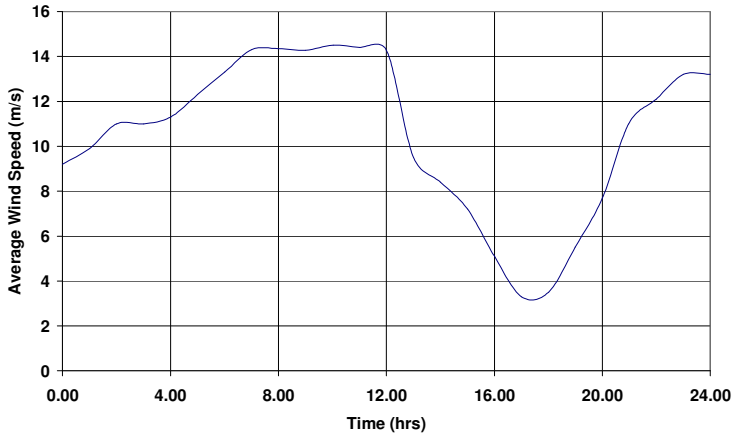


**Figure I-4: Modified wind speed from the EnergyLINK Laboratory, Blyth, Northumbria, UK**

To simplify the analysis and create scenarios that would result in large deviations from those experienced under balanced load and generation and also create thermally onerous conditions a fictitious insolation level which results in a constant output of 1.5kW from the PV generator emulator.

## Appendix I-3-4 MV/LV Secondary Distribution Transformer

The secondary distribution network transformer is located between nodes 9 and 10 of the generic UK distribution network [41] as illustrated in Figure I-3. The transformer has a voltage ratio is 11/0.433kV and its connection group Dyn11. The impedance on the base

MVA is 5%. The tap-changer is a typical UK installation and is an off-load type with a range of +/-5% and in this investigation is set to 0% [41].

## Appendix I-4 Real and Reactive Power Transformation

The maximum load per phase on the LV network is 250kW. The maximum load per phase of the Experimental SSEZ is 2.6kW then from (H.1): -

$$\mu_{pL} = \frac{P_{aL}^{LV}}{P_{aL}^{Ex}} = \frac{250.0}{2.6} = 96.2$$

The maximum generation per phase on the LV network as stated earlier is 281.6kW. The maximum generation per phase of the Experimental SSEZ is 2.7kW at present (1.2kW wind turbine generator emulator and 1.5kW PV generator emulator). Then from (H.2): -

$$\mu_{pG} = \frac{P_{aG}^{LV}}{P_{aG}^{Ex}} = \frac{281.6}{2.7} = 104.3$$

The power transformation factor $\mu_p$, defined according to (H.3) is defined.

$$\mu_p = \max(\mu_{pL}, \mu_{pG}) = 104.3$$

The load data is modified (as $\mu_{p_L}$ is less than $\mu_{p_G}$) so that the load and generation profiles are preserved when they are implemented in the Experimental SSEZ.

## Appendix I-5 Voltage Transformation

The apparent impedance, as defined in this work, of a network location is the sum of the phase and neutral impedances between the substation and any customer connection point, multiplied by the number of customers per phase at that location. The data for this calculation is taken from [41]. First $Z_{customer}^{(ap)}$ is calculated for all the network locations. To illustrate the process the parameter $Z_{customer}^{(ap)}$ at node 14, as shown in Figure I-3, is calculated.

$$
Z_{customer}^{(ap)} = \left.\begin{array}{l}(75\times(0.164+j0.074))\\+(75\times(0.164+j0.074))\\+(75\times(0.320+j0.075))\\+(75\times(0.320+j0.075))\end{array}\right\}\ phase\ impedance
$$

$$
\left.\begin{array}{l}+(75\times(0.164+j0.014))\\+(75\times(0.164+j0.014))\\+(75\times(0.320+j0.016))\\+(75\times(0.320+j0.016))\end{array}\right\}\ neutral\ impedance
$$

$$
= (145.2+j26.85)\,\text{m}\Omega
$$

Using (H.6) it is possible to write: -

$$
\begin{aligned}
Z_{location}^{14\ (ap)} &= \sum_{k=1}^{8} Z_{customer}^{k\ (ap)} \cong m\cdot Z_{customer}^{(ap)} + Z_{service\ cable}\\
&= (8\times(145.2+j26.85))+(30\times(0.851+j0.041))+(30\times(0.41+j0.041))\\
&= (1.344+j0.2441)\Omega
\end{aligned}
$$

Similarly, it is possible to determine the apparent impedance at the other node feeder locations.

$$
\begin{aligned}
Z_{location}^{13\ (ap)} &= (0.7776+j0.2441)\Omega\\
Z_{location}^{12\ (ap)} &= (0.3936+j0.1056)\Omega\\
Z_{location}^{11\ (ap)} &= (0.1968+j0.0528)\Omega
\end{aligned}
$$

The sum of apparent impedances of all locations where customers are connected will give the apparent impedance of the feeder (H.7).

$$
\begin{aligned}
Z_{feeder}^{(ap)} &= R_{feeder}^{(ap)} + jX_{feeder}^{(ap)} = \sum_{i=1}^{n} Z_{location}^{(ap)}\\
&= (0.1968+j0.0528)+(0.3936+j0.1056)+(0.7776+j0.2441)+(1.344+j0.2441)\\
&= (2.712+j0.5627)\Omega
\end{aligned}
$$

As the apparent impedance of all the feeders is the same in this case study network, it is possible to write from (H.8).

$$
\begin{aligned}
Z^{LV} = Z_{net}^{(ap)} &= R_{net}^{(ap)} + jX_{net}^{(ap)} = \max\left(\text{Re}\left(Z_{feeder1}^{(ap)}\right),.....\text{Re}\left(Z_{feeder\,p}^{(ap)}\right)\right)\\
&= (2.712+j0.5627)\Omega
\end{aligned}
$$

Detailed measurements taken from the conductors of the Experimental SSEZ indicate that the sum of the neutral and the phase impedances from the node 1 to node 5, which is the remote end of the Experimental SSEZ in this study, are: -

$$\begin{aligned} Z^{Ex} &= (0.330 + j0.035) + (0.245 + j0.028) \\ &= (0.575 + j0.063)\Omega \end{aligned}$$

The impedance transformation $\mu_z$ is then defined: -

$$\begin{aligned} \mu_z = \frac{Z^{LV}}{Z^{Ex}} &= \frac{R^{LV} + jX^{LV}}{R^{Ex} + jX^{Ex}} \\ &= \frac{(2.712 + j0.5627)}{(0.575 + j0.063)} \\ &= (4.767 + j0.4562) = 4.788\angle 5.466^\circ \end{aligned}$$

$\mu_{Vnom}$ is determined from measurements at the MV/LV secondary distribution transformer of the PSCAD®/EMTDC™ model and the Experimental SSEZ when they are operating under zero import/export conditions (H.29) : -

$$\begin{aligned} \mu_{Vnom} &= \frac{V_{nom}^{LV}}{V_{nom}^{Ex}} \\ &= \frac{250}{225} = 1.111 \end{aligned}$$

The relationship therefore between the complex voltage variations from node 1 (network connection emulator) to node 6 (wind turbine generator emulator) on the Experimental SSEZ and from the secondary distribution network busbar to the remote end of the LV network maybe expressed as (H.31): -

$$\begin{aligned} \Delta\mathbf{v}_{\mathbf{abc}}^{\mathbf{LV}}(\mathbf{t}) &= \frac{\mu_p \mu_z}{q\mu_{Vnom}} \Delta\mathbf{v}_{\mathbf{abc}}^{\mathbf{Ex}}(\mathbf{t}) \\ &= \frac{(104.3)\left(4.788\angle 5.466^\circ\right)}{(128)(1.111)} \Delta\mathbf{v}_{\mathbf{abc}}^{\mathbf{Ex}}(\mathbf{t}) \\ &= (3.511\angle 5.466^\circ)\Delta\mathbf{v}_{\mathbf{abc}}^{\mathbf{Ex}}(\mathbf{t}) \end{aligned}$$

# Appendix I-6 MV/LV Network Modelling System Implementation

Load and generation profiles as described in section Appendix I-3 result in real and reactive power flows through the network connection emulator are illustrated in Figure I-5.

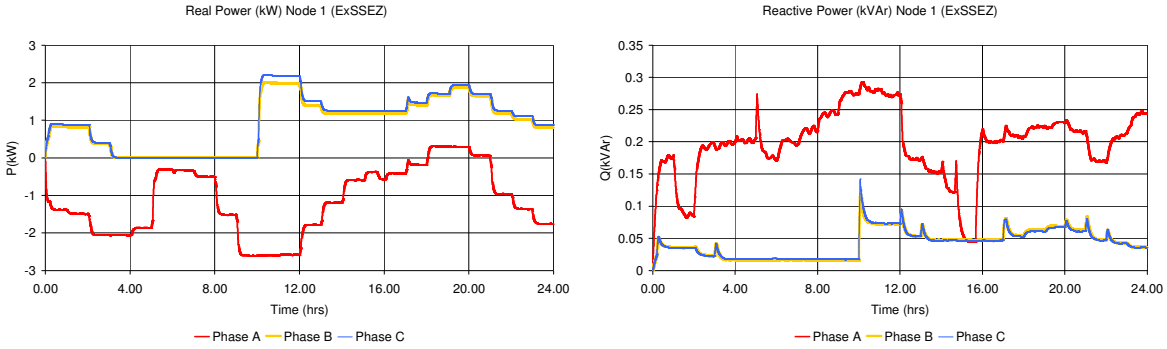


**Figure I-5: Real and reactive power flows through network connection emulator of Experimental SSEZ**

Following application of the power transformation in PSCAD®/EMTDC™ the estimated LV network real and reactive power flows illustrated in Figure I-6 are injected into the PSCAD®/EMTDC™ LV distribution network model at the busbar of the secondary distribution network transformer (node 10) using the controllable current source inverter models described in Appendix H.

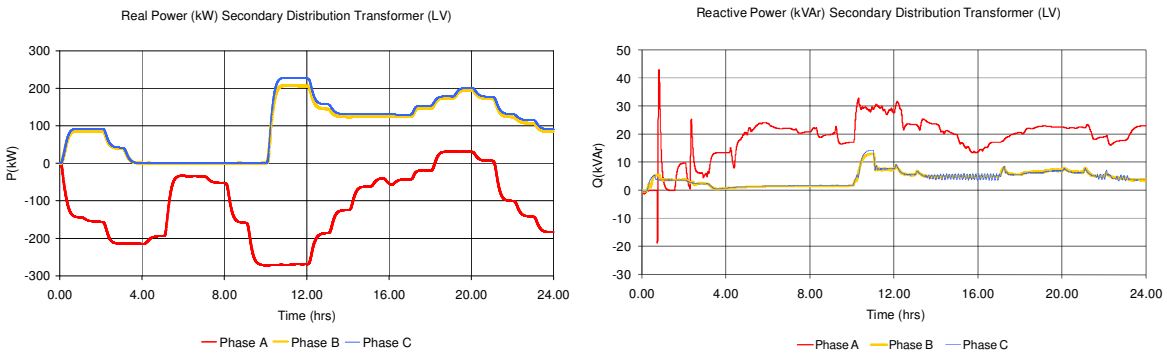


**(a)** **(b)**

**Figure I-6: Real and reactive power flows injected into secondary distribution transformer PSCAD®/EMTDC™ model**

It can be seen that while the profiles of the Experimental SSEZ and the PSCAD®/EMTDC™ secondary distribution transformer model are similar especially the active power profiles some differences do exist due to the operation of the current source inverter models. The active and reactive power flows depicted in Figure I-6 result in magnitude and phase displacements of the voltages at the terminals of the secondary distribution transformer as shown in Figure I-7. These displacements are dependent on the transformer self and mutual impedances, turns ratio, design and tap position. The phase displacements at the transformer terminals due to real and reactive power flows are not large and the phase displacements between the phases remain at about 120° during the test sequence. The phase-neutral voltages at the busbar of the secondary distribution transformer under zero load and generation conditions are approximately 250V. This is not uncommon as distribution network operators tend to keep these voltages high to ensure that remote end phase-neutral voltages do not fall below the statutory limits [29, 42] under heavy loading conditions.

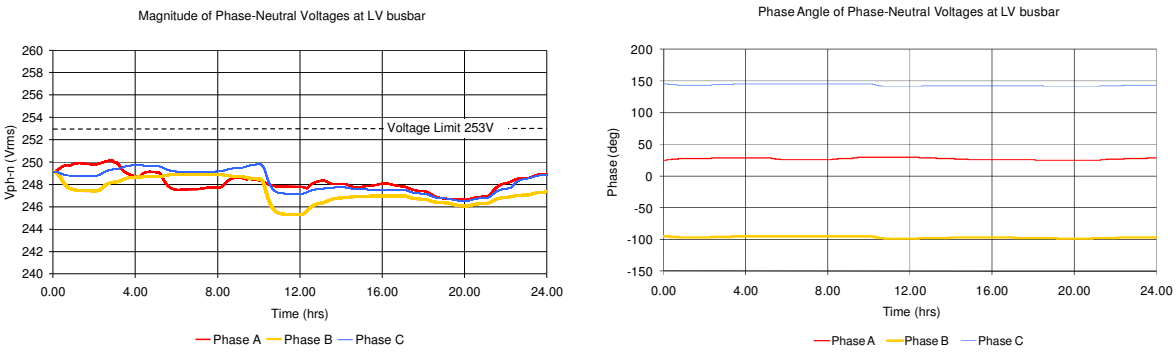


**(a)** **(b)**

**Figure I-7: Phase-neutral voltages at the busbar of secondary distribution network transformer of PSCAD®/EMTDC™ model**

Due to the effect of reactive and unbalanced current flow in LV distribution networks, the phase-neutral voltage drops are generally out of phase with the phase-neutral voltages.

The estimated voltage differences from the LV busbar of the MV/LV distribution network transformer to the remote end of the case study network, as a result of the application of the transformation to the difference in voltages from the network connection emulator to the end node of the Experimental SSEZ, are illustrated in Figure I-8. The phase calculations assume a voltage drop convention from the LV busbar to the remote end of the LV network. This implies that an SSEG generating at unity power factor will result in a voltage change along the phase conductor which will be 180° out of phase with the phase voltage if the conductor is purely resistive.

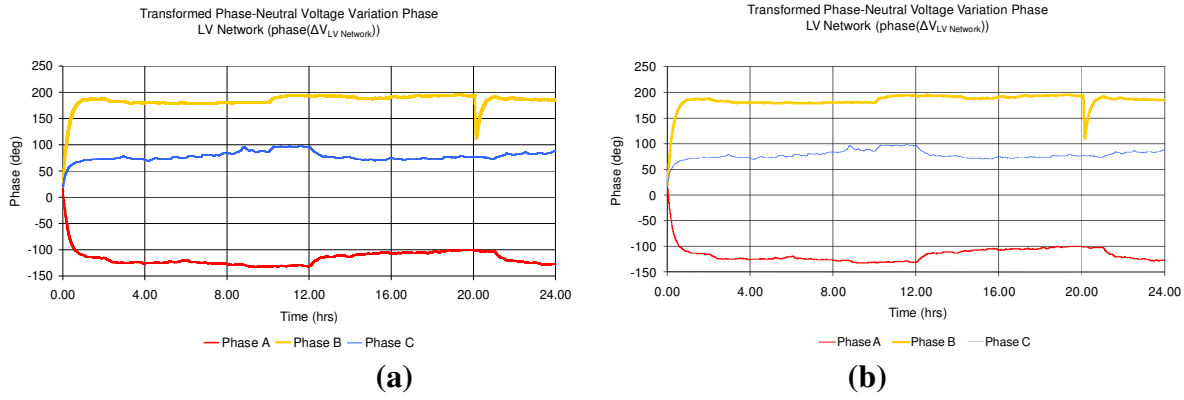


**Figure I-8: Transformation estimates of voltage variations from LV busbar to remote end of case study network**

*N.B. It should be noted that the magnitude of the voltage variation is not the same as voltage regulation which refers to the difference in magnitudes between the phase-neutral voltages at the LV busbar and nodes on the LV network.*

## Appendix I-7 Voltage Variation and Regulation

As stated in chapter two, voltage rise has been identified as the most limiting constraint to the installation of large numbers of SSEGs in LV networks [41]. The statutory limits in the UK are +/- 10% based on a nominal voltage of 230V [29]. These are the limits used for the investigation of voltage variation in this chapter.

Voltage regulation statutory limits differ between countries and DNOs, however in the UK most DNOs allow a maximum of 5-8% voltage regulation [187-189]. For the purposes of this research, 5% is defined as the statutory voltage regulation limit allowed.

## Appendix I-7-1 Dynamic Results

The complex voltage variation quantities, illustrated in Figure I-8, are added to the complex LV busbar voltages. This enables estimation of the remote end voltages of the LV network as illustrated in Figure I-9.

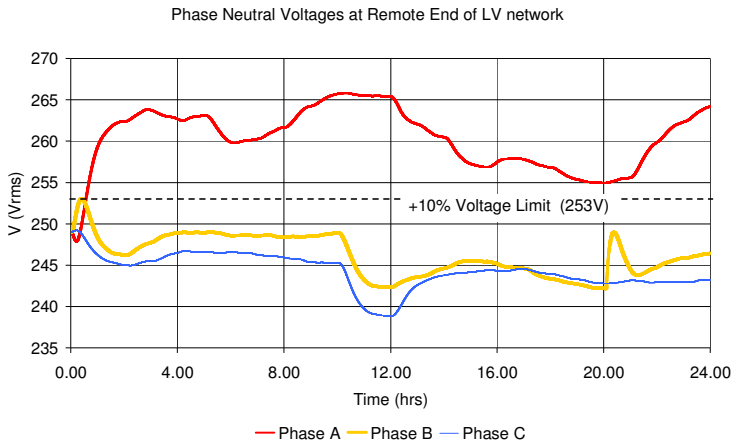


**Figure I-9: Magnitude of phase-neutral voltages at remote end of LV network**

It can be seen from Figure I-9 that the large quantity of generation on phase A of the LV network results in violations of the statutory voltage limits on this phase for almost the duration of the test. Larger amounts of generation on the LV network result in changes to the voltages of the phases with no generation also. This is due to the neutral voltage displacement and the changes in the voltages at the terminals of the secondary distribution transformer during unbalanced conditions. The neutral voltage displacement, as in the case of the impact studies in chapter seven, is due to the neutral current flow which results from unbalanced loading/generating conditions in the system.

It can be seen from Figure I-10, that the transformation estimates that voltage regulation limits will be violated on phase A for more that 40% of the load and generation scenario under investigation.

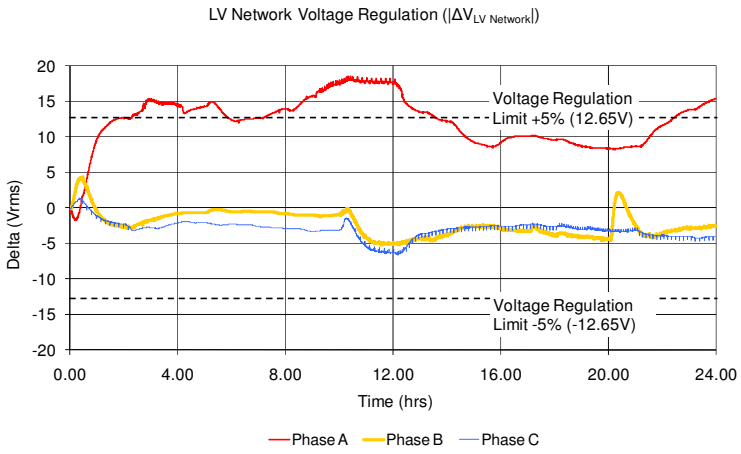


**Figure I-10: Phase-neutral voltage regulation estimate from PSCAD®/EMTDC™ transformation system**

## Appendix I-7-2 Steady-state validation

The model of the UK generic model developed previously [8-9] is used to validate the behaviour of the transformation. The models are steady-state PSCAD®/EMTDC™ models and three scenarios are selected which result in the Experimental SSEZ and transformation operating near or at their limit conditions. The scenarios investigated are detailed in Table I-2.

| **Time** | **Experimental SSEZ component status** | | | | |
|---|---|---|---|---|---|
| | Load Phase A | Load Phase B | Load Phase C | WTGE Output | PV Output |
| 07:30 | Maximum load | Zero load | Zero load | Max power | Max power |
| 09:30 | Zero load | Zero load | Zero load | Max power | Max power |
| 11:00 | Zero load | Maximum load | Maximum load | Max power | Max power |

**Table I-2: Validation scenarios**

The results of the phase-neutral voltage validation are detailed in Table I-3. It can be seen that the impacts of generation on the steady-state voltage rise on phase A are lower in the transformation results than in the PSCAD®/EMTDC™ model. This can be explained in part by the assumption in the derivation of the impedance transformation. This assumed that the ratio of neutral to phase impedances is the same in an LV network as in the Experimental SSEZ. In the case study LV network, the impedances of the neutral and phase conductors are almost identical. Another source of error is the accuracy of the phase of the voltage variation measurements from the Experimental SSEZ. Moreover, the distribution of the load and generation in the systems is also different.

| **Time** | **Transformation Remote End Phase Neutral Voltage (V)** | | | **PSCAD®/EMTDC™ Network Model Remote End Phase Neutral Voltage (V)** | | | **Error (%)** | | |
|---|---|---|---|---|---|---|---|---|---|
| | A | B | C | A | B | C | A | B | C |
| 07:30 | 261.07 | 248.62 | 246.09 | 258.25 | 246.79 | 247.19 | 1.09 | 0.74 | 0.45 |
| 09:30 | 265.13 | 248.72 | 245.32 | 271.99 | 244.43 | 244.67 | 2.52 | 1.76 | 0.27 |
| 11:00 | 265.52 | 243.19 | 239.72 | 274.03 | 237.57 | 238.38 | 3.11 | 2.37 | 0.56 |

**Table I-3: Validation results for remote end voltages**

## Appendix I-8 Voltage Unbalance

The %VUF has a statutory limit of 1.3% in the UK [44], although short-term deviations (less than 1 minute) may be allowed up to 2%, which is the standard limit used for the maximum steady-state %VUF allowed in European networks [42].

It can be seen from Figure I-11, that under the conditions of this study, the transformation indicates that the UK generic LV network will violate UK %VUF limits for extended periods at both the remote ends and to a lesser extent at the LV busbars of the secondary distribution substation. In addition, the European 2% limit is also violated but for shorter periods on both the LV busbar and the remote end of the LV network. The differences in %VUF between the LV busbar and the remote end of the network are relatively small which suggests that the phase change at the transformer terminals as a result of the unbalanced current flow through the transformer has a large influence on the negative sequence voltages. As expected the lowest %VUF was estimated at 7.30 when load and generation on phase A were closely matched and load on phase B and phase C were at a minimum. Again, as in the case of the voltage variation, this scenario designed for the purpose of investigating the operation of the transformation system, results in highly unbalanced conditions which would not be likely to occur in a real LV distribution network.

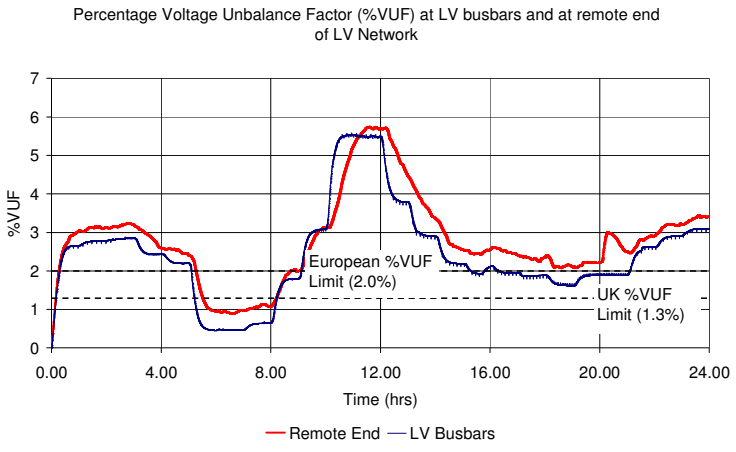


**Figure I-11: Percentage Voltage Unbalance Factor (%VUF) at LV busbars of secondary distribution substation and at remote end of LV network**

### Appendix I-8-2 Steady-state validation

As in the case of voltage variation the results were compared with steady-state results from the PSCAD®/EMTDC™ model [9] and the same set of scenarios as in Table I-4. The results are relatively consistent but errors are again apparent as in the case of the voltage variation validation investigation. The errors in %VUF error are due in part to the same reasons outlined in the voltage validation investigation and also due to changes to the phase difference between phases in the Experimental SSEZ and errors in these measurements. It can be seen that as the voltage unbalance increases the relative accuracy of the result increases. Improvements in the accuracy of the phase measurements from the Experimental SSEZ would increase the accuracy of the results.

| **Time** | **Transformation Remote End %VUF** | **PSCAD®/EMTDC™ Network Model Remote End %VUF** | **Error (%)** |
|---|---|---|---|
| 07:30 | 0.629 | 0.82 | 23.01 |
| 09:30 | 3.004 | 3.72 | 19.20 |
| 11:00 | 5.529 | 6.50 | 14.92 |

**Table I-4: Validation results for % voltage unbalance factor (%VUF)**

## Appendix I-9 Thermal Limits

Transformers and network line components, such as overhead lines and underground cables, have a thermal rating determined by the maximum current carrying capacity of that component. As stated in chapter two, presence of SSEGs may cause an increase in the overall current flowing in the network, bringing system equipment closer to their thermal limits. Therefore, a constraint to the capacity of SSEGs that may be accommodated by LV distribution networks exists due to component thermal limits. In

this section, the MVA rating of the secondary distribution transformer and the section of LV cable nearest to the transformer are investigated. Previous research has indicated that a thermal limit violation is most likely to occur on this cable [21]. The ratings for the transformer and the cable section in this work are as per [41]. Reduced reverse power flow limits are not considered as the MVA ratings of the secondary distribution transformers are symmetrical as they do not feature an On-Load Tap-Changer (OLTC) [6].

## Appendix I-10 Dynamic results

Figure I-12 illustrates the unbalanced current flow in the first 185mm$^2$ section (node 11 to node 12) of underground cable in the LV network. The transformation system predicts that only the neutral conductor is operated above its rating for extended periods of time. This corresponds as expected with the periods of largest %VUF.

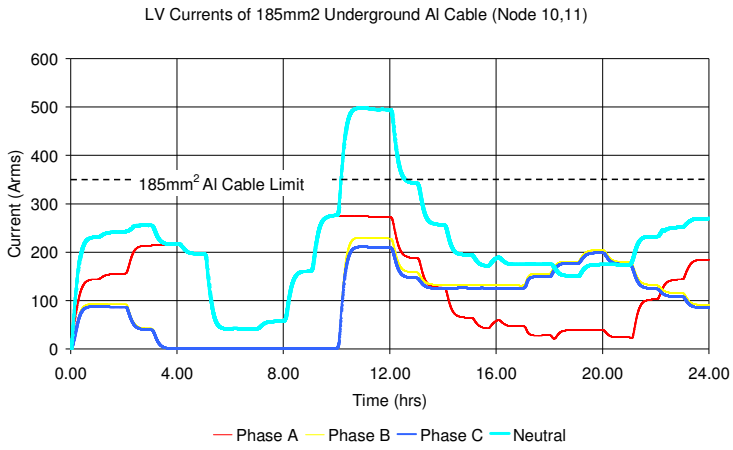


**Figure I-12: Current flow between nodes 10 and 11 (185mm$^2$ section)**

The rating of the secondary distribution transformer is 500kVA at a nominal voltage of 230V. These ratings are not exceeded under the loading and generation scenario of the case study as illustrated by Figure I-13. This is due in part to the comparatively high voltages at the LV busbars of the MV/LV substation. It is possible that the three-phase measurement may be somewhat misleading in terms of damage or ohmic heating effects

in the transformer. This is because the net power flow may not be indicative of the ohmic heating effects in the transformer. For example at 12.00 the net power flow through the three-phase transformer is a 0.2MVA load. However if individual winding are considered there is a load of 0.2MVA on phase B and phase C and 0.3MVA is being generated by the LV network on phase A. This results in 0.7MVA of power flowing through the transformer.

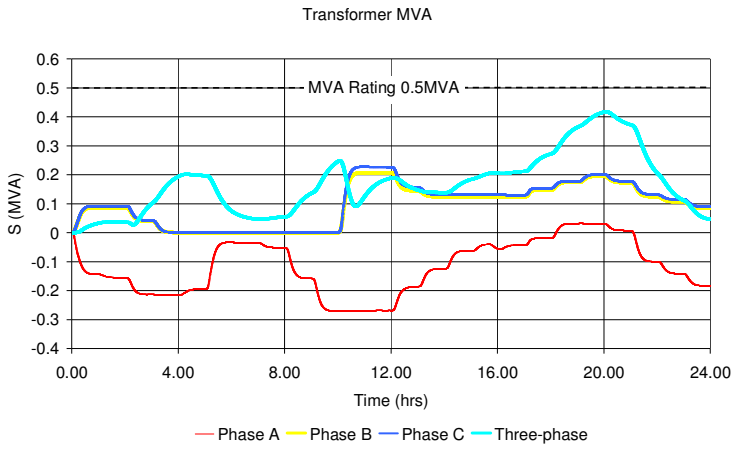


**Figure I-13: Apparent power flow through the LV windings of the secondary distribution network transformer**

## Appendix I-11 Conclusion

The transformation system was used to evaluate the impact of extreme conditions of LV network operation on a case study distribution network. The case-study was based on the UK generic network. The statutory limits for voltage rise and %VUF were found to be violated for almost the duration of the scenario under investigation. A major factor in voltage rise in this investigation was the low tap position of the secondary distribution transformer which resulted in phase-neutral voltages close to 250V under zero load conditions. The main factor in the persistent %VUF violations was due to the highly unbalanced nature of load and SSEG on the network but the system dropped below the statutory limit when load and generation were equal on phase A and the load on phase B

and phase C was at a minimum. Thermal limit and voltage regulation violations were less frequent. Moreover, thermal limit violations on the neutral conductor were more likely than in the phase conductors due to the unbalanced distribution of load and generation. In addition, the thermal limit violations on the neutral was closely related to the %VUF in the system as expected.

The results from this impact study were compared and evaluated with results from validated steady-state models in PSCAD®/EMTDC™. The transformation has been proven to be reasonably accurate in assessment of voltage variation and regulation and therefore can be used as an enabler for LV network impact studies. The error at low levels of voltage unbalance were quite high but an improvement of the measurement systems detecting phase and changes to the ratio of the impedances between the phase and neutral conductors would improve the results.

As the Experimental SSEZ is a non-uniform network with a limited degree of flexibility, case-study networks need to be chosen which facilitate comparison with the Experimental SSEZ in terms of load and generation distribution to enable more accurate results. The transformation also assumes that there are no harmonics in the currents flowing in the LV network under investigation. Finally, the transformation system is inflexible about the ratio phase and neutral impedances in the case-study network as this is dictated by the relationship in the Experimental SSEZ.

The validated transformation, in spite of the shortcomings outlined previously, can therefore be used to evaluate the operation of active network management techniques that are developed in this work especially in the investigation of voltage rise and regulation. This is likely to be the first constraint to be exceeded in any LV distribution network with large penetrations of SSEG.

# Appendix J SAMPLE LABVIEW™ DIAGRAMS

## *Centrallised Voltage Controller*

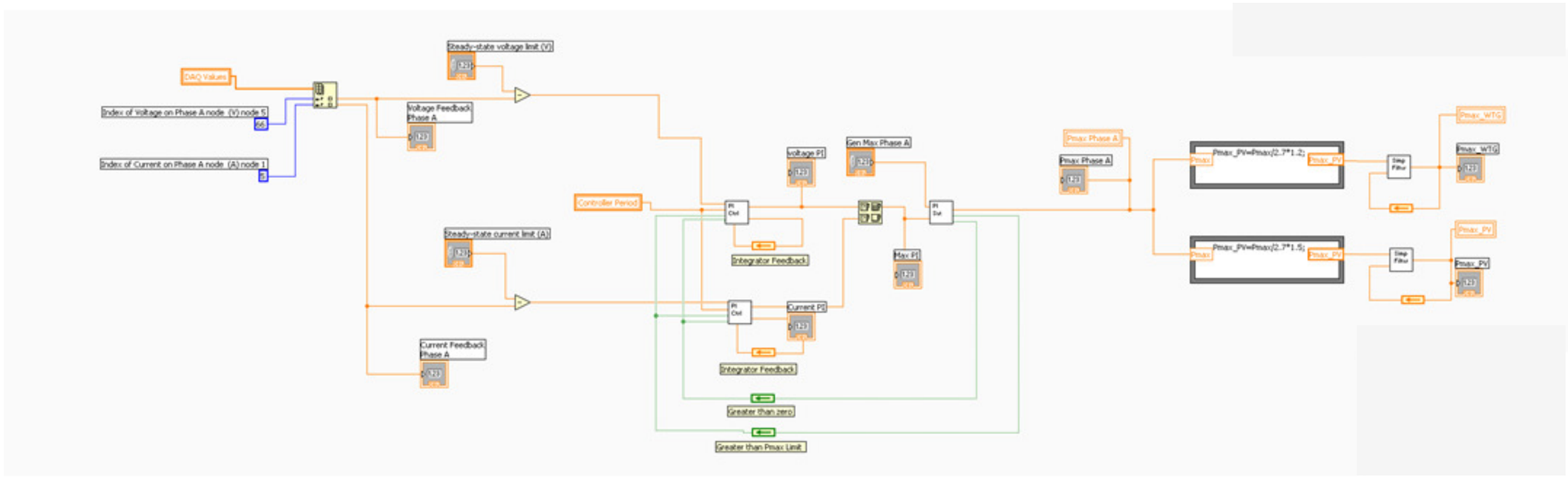

***Wind Turbine Generator Direct Agent (WGA)***